

Diagnostic and Prognostic Analysis
Tools for Monitoring Degradation in
Aged Structures

Yasmine Zaina Rosunally

A thesis submitted in partial fulfillment of the
requirements of the University of Greenwich for the
Degree of Doctor of Philosophy

This research programme was carried out in
collaboration with Cutty Sark Trust

February 2012

DECLARATION

I certify that this work has not been accepted in substance for any degree, and is not concurrently being submitted for any degree other than that of Doctor of Philosophy being studied at the University of Greenwich. I also declare that this work is the result of my own investigations except where otherwise identified by references and that I have not plagiarized the work of others.

Student

.....

Yasmine Zaina Rosunally

1st Supervisor

.....

Professor Chris Bailey

2nd Supervisor

.....

Dr Stoyan Stoyanov

ACKNOWLEDGEMENTS

First, I would like to express my sincere gratitude to my supervisor Prof. Chris Bailey for his guidance and trust throughout my research. Secondly, I would like to thank Dr Stoyan Stoyanov for his help and advice on various aspects of my research over the years.

I would like to acknowledge the collaboration with Cutty Sark Trust, especially the contribution of Peter Mason whose technical discussions were often key to exploring different solutions. I am also grateful to late Dr Sheelagh Campbell for her suggestions and help in reviewing my work. Thanks to George Monger and Ian Bell for their help in understanding the various tricky aspects of the research project and contribution in the laboratory experiments. I am grateful to Cutty Sark Trust for the funding of my PhD research project.

I am grateful to all of those with whom I had the pleasure to work during my time at University of Greenwich. Their sincere friendship and willingness to help made my PhD journey a very fulfilling and entertaining one. The daily tea breaks were always a happy and welcome occasion. A big thank you to Yasmina, Steve, Nitish, Ying Kit, Claudia, Aoife, Madeleine, Maria, Carl, Tim, Thamo and Yek.

I thank all my friends for their invaluable support and encouragement. I am thankful to Bhavna, for understanding me, believing in me and cheering me up when needed. I also thank Vandana for all the advice and support while we both undertook our PhD journeys. I would also like to thank Eleftheria for the inspiration and reassurance she provided during challenging moments.

Finally, I am forever indebted to my parents, Siddique and Asmahan Rosunally, for the constant moral support and encouragement without which I would not be where I am today. I also thank my sister, Dilshaad, for her encouragement and patience throughout my journey.

ABSTRACT

This research addresses the problem of prolonging the life of aged structures of historical value that have already outlived their original designed lives many times. While a lot of research has been carried out in the field of structural monitoring, diagnostics and prognostics for high tech industries, this is not the case for historical aged structures. Currently most maintenance projects for aged structures have focused on the instrumentation and diagnostic techniques required to detect any damage with a certain degree of success. This research project involved the development of diagnostic and prognostic tools to be used for monitoring and predicting the ‘health’ of aged structures. The diagnostic and prognostic tools have been developed for the monitoring of Cutty Sark iron structures as a first application.

The concept of canary and parrot sensor devices are developed where canary devices are small, accelerated devices, which will fail according to similar failure mechanisms occurring in an aged structures and parrot devices are designed to fail at the same rate as the structure, thus mimicking the structure. The model-driven prognostic tool uses a Physics-of-Failure (PoF) model to predict remaining life of a structure. It uses a corrosion model based on the decrease in corrosion rate over time to predict remaining life of an aged iron structures. The data-driven diagnostic tool developed uses Mahalanobis Distance analysis to detect anomalies in the behaviour of a structure. Bayesian Network models are then used as a fusion method, integrating remaining life predictions from the model-driven prognostic tool with information of possible anomalies from data-driven diagnostic tool to provide a probability distribution of predicted remaining life. The diagnostics and prognostic tools are validated and tested through demonstration example and experimental tests.

This research primarily looks at applying diagnostic and prognostic technologies used in high-tech industries to aged iron structures. In order to achieve this, the model-driven and data-driven techniques commonly used had to be adapted taking into consideration the particular constraints of monitoring and maintaining aged structures. The fusion technique developed is a novel approach for prognostics for aged structures and provides the flexibility often needed for diagnostic and prognostic tools.

LIST OF PUBLICATIONS

The research work carried out during the course of this PhD programme has been published in three conference papers and two journal papers:

- Rosunally, Y., Stoyanov, S., Bailey, C., Mason, P., Campbell, S., Monger, G. & Bell, I., 2009, 'Development of a Prognostic Framework for the Iron Structural Material of the s.v. Cutty Sark' 6th International Conference on Condition Monitoring and Machinery Failure Prevention Technologies 2009, Dublin, Vol. 1, pp 674-685.
- Rosunally, Y., Stoyanov, S., Bailey, C., Mason, P., Campbell, S., Monger, G., 2009, 'Prognostic Framework for Remaining Life Prediction of Cutty Sark Iron Structures' Annual Conference of the Prognostic and Health Management Society 2009, San Diego. Proceedings available online at <http://www.phmsociety.org>
- Rosunally, Y., Stoyanov, S., Bailey, C., Mason, P., Campbell, S., Monger, G. & Bell, I., 2010, 'Fusion Approach for Predictive Maintenance of Heritage Structures' Prognostic and Health Management Conference 2010, Macau, Proceedings on USB, pp. 1-6.
- Rosunally, Y., Stoyanov, S., Bailey, C., Mason, P., Campbell, S., Monger, G. & Bell, I. 2010, 'Bayesian Networks for Predicting Remaining Life' Special Issue on PHM for International Journal of Performability Engineering, Vol. 6, No. 5, pp. 499 – 512.
- Rosunally, Y., Stoyanov, S., 2011, 'Fusion Approach for Prognostic Framework of Heritage Structures' IEEE Transactions in Reliability, Vol. 60, Issue 1, pp. 3-13.

NOMENCLATURE

PHM	Prognostic and Health Management
PoF	Physics of Failure
MD	Mahalanobis Distance
C_PoF_RUL	node for probability distribution of remaining life prediction obtain from PoF model for canary device
P_PoF_RUL	node for probability distribution of remaining life prediction obtain from PoF model for parrot device
C_MDValues	node for probability distribution of Mahalanobis Distance values for canary device
P_MDValues	node for probability distribution of Mahalanobis Distance values for parrot
Visual_Inspection	node for probability distribution of damage level detected through visual inspections
Canary_PredictedRUL	node for probability distribution of predicted remaining life for canary device
Parrot_PredictedRUL	node for probability distribution of predicted remaining life for parrot device
ShipStructure_PredictedRUL	node for probability distribution of predicted remaining life for ship structure
C_Time_Period	node representing time for the canary device related input of Bayesian network model
P_Time_Period	node representing time for the parrot device related input of Bayesian network model
Salt125_PoF_RUL	node for probability distribution of remaining life prediction obtain from PoF model for the 0.125mm test device in salt environment

Salt250_PoF_RUL	node for probability distribution of remaining life prediction obtain from PoF model for the 0.25mm test device in salt environment
Salt500_PoF_RUL	node for probability distribution of remaining life prediction obtain from PoF model for the 0.5mm test device in salt environment
Salt125_MDValues	node for probability distribution of Mahalanobis Distance values for the 0.125mm test device in salt environment
Salt250_MDValues	node for probability distribution of Mahalanobis Distance values for the 0.25mm test device in salt environment
Salt500_MDValues	node for probability distribution of Mahalanobis Distance values for the 0.5mm test device in salt environment
Salt125_PredictedRUL	node for probability distribution of predicted remaining life for the 0.125mm test device in salt environment
Salt250_PredictedRUL	node for probability distribution of predicted remaining life for the 0.25mm test device in salt environment
Salt500_PredictedRUL	node for probability distribution of predicted remaining life for the 0.5mm test device in salt environment

CONTENTS

1. INTRODUCTION	1
1.1. Overview	1
1.2. Motivation	3
1.3. Cutty Sark Ship	4
1.4. Challenges in Maintaining Aged Structures	6
1.5. Aims and objectives of the research	8
1.6. General Methodology	9
1.7. Contribution	11
1.8. Thesis Structure	11
2. LITERATURE REVIEW	13
2.1. Prognostics and Health Management	13
2.2. Canary and Parrot Devices Approach	23
2.3. Data Driven Methods	26
2.4. Model Driven Methods	32
2.5. Fusion Methods	39
2.6. Traditional Maintenance Strategies	46
2.7. Applications for Aged Structures	50
2.8. Chapter Summary	58
3. CORROSION DEGRADATION MECHANISMS	60
3.1. Introduction	60
3.2. Age-Related Structural Degradation	60
3.3. Electrochemistry of Corrosion	61
3.4. Types of Corrosion	64

3.5.	Deterioration Models for Corrosion -----	66
3.6.	Consequences of Corrosion-----	69
3.7.	Summary-----	70
4.	DEVELOPING A PHM METHODOLOGY FOR AGED STRUCTURES -----	71
4.1.	Overview-----	71
4.2.	Use of Canary and Parrot Devices -----	73
4.3.	Model Driven Prognostic Tool: Remaining Life Prediction using PoF Model -----	78
4.4.	Data Driven Diagnostic Tool: Anomaly Detection using Mahalanobis Distance Analysis-----	80
4.5.	Fusion Approach: Bayesian Network Models -----	84
4.6.	Summary-----	98
5.	DEMONSTRATION EXAMPLE -----	100
5.1.	Demonstration Setup -----	101
5.2.	Scenarios Investigated for Demonstration Example -----	108
5.3.	Analysis of PHM Methodologies -----	115
5.4.	Summary-----	142
6.	EXPERIMENTAL TRIALS -----	143
6.1.	Experimental Setup-----	143
6.2.	Analysis of Experimental Data-----	147
6.3.	Summary-----	173
7.	CONCLUSION AND FUTURE WORK-----	175
7.1.	Summary of Research -----	175
7.2.	Research Contributions and Impact-----	177
7.3.	Recommendations for Diagnostic and Prognostic tools for Cutty Sark iron structures -----	178
7.4.	Areas for Future Research -----	179
8.	REFERENCES-----	182

9. APPENDIX	191
9.1. Additional PHM Framework Information	191
9.2. Demonstrator Example	193
9.3. Additional Experimental Trials Information	194

FIGURES

Figure 1-1: the composite built vessel (a) and examples of severe corrosion and material deterioration (b and c) that are present in the original fabric of the ship. -----	4
Figure 2-1: Types of Prognostic Algorithms -----	19
Figure 2-2: Advanced warning of failure using canary devices -----	23
Figure 2-3: MSET Process -----	29
Figure 2-4: FMMEA Process used in PoF based PHM -----	33
Figure 2-5: CALCE Life Consumption Monitoring Methodology (SANDBORN, P, 2005) -	36
Figure 2-6: A layered probabilistic graphical model for diagnosis and prognosis -----	41
Figure 2-7: BN for prognosis consisting of a single component, usage and health observation -----	42
Figure 3-1: Anodic and Cathodic Reactions -----	61
Figure 4-1: Use of Deterministic and Probabilistic Approaches within PHM -----	71
Figure 4-2: PHM Framework for Cutty Sark Iron Structures -----	72
Figure 4-3: Material Loss Prediction Using Canary and Parrot devices -----	74
Figure 4-4: Parrot and Canary Device Pairs (a) -----	78
Figure 4-5: Canary and Parrot Device Pairs (a) -----	78
Figure 4-6: Mahalanobis Distance Analysis Methodology -----	84
Figure 4-7: Development process used to build a Bayesian network model -----	88
Figure 4-8: Small BN model for corrosion damage -----	88
Figure 4-9: Bayesian Network with no evidence input -----	90
Figure 4-10: Bayesian network with evidence input on Humidity and Age nodes -----	90
Figure 4-11: Bayesian network with different evidence input on Age node -----	90
Figure 4-12: Conceptual Bayesian Network for Cutty Sark -----	92
Figure 4-13: BN Network -----	93
Figure 4-14 : Reasoning on Evidence -----	97
Figure 5-1: Using generated "Real" Corrosion Data to test PHM Framework -----	101
Figure 5-2: Typical Temperature and RH for Scenario 1 -----	109
Figure 5-3: Corrosion Rates for Scenarios 1 -----	109
Figure 5-4: Typical Temperature and RH for Scenario 2 -----	111
Figure 5-5: Corrosion Rates for Scenarios 2 -----	111
Figure 5-6: Typical Temperature and RH for Scenario 3 -----	112
Figure 5-7: Corrosion Rates for Scenarios 3 -----	112
Figure 5-8: Typical Temperature and RH for Scenario 4 -----	113
Figure 5-9: Corrosion Rates for Scenarios 4 -----	113
Figure 5-10: Typical Temperature and RH for Scenario 5 -----	115
Figure 5-11: Corrosion Rates for Scenarios 5 -----	115
Figure 5-12: Predicting Remaining Life using PoF model based on Linear Bi-logarithmic Law -----	116
Figure 5-13: PoF-based Prediction of Remaining Life for Canary Device -----	117
Figure 5-14: PoF-based Prediction of Remaining Life for Parrot Device -----	118
Figure 5-15: Using MD analysis to detect anomalies in scenarios 2-5 -----	122
Figure 5-16: MD Analysis of Real Data for Scenarios 2 & 3 for Canary -----	123
Figure 5-17: MD Analysis of Real Data for Scenarios 4 & 5 for Canary -----	123
Figure 5-18: MD Analysis of Average Data for Scenarios 2 & 3 for Canary -----	124
Figure 5-19: MD Analysis of Average Data for Scenarios 4 & 5 for Canary -----	124
Figure 5-20: MD Analysis of Real Data for Scenarios 2 & 3 for Parrot -----	125
Figure 5-21: MD Analysis of Real Data for Scenarios 4 & 5 for Parrot -----	125

Figure 5-22: MD Analysis of Average Data for Scenarios 2 & 3 for Parrot -----	126
Figure 5-23: MD Analysis of Average Data for Scenarios 4 & 5 for Parrot -----	126
Figure 5-24: Flowchart Diagram of use Bayesian Network Model-----	127
Figure 5-25: Bayesian Network Model for Demonstrator example -----	128
Figure 5-26: CPT for Canary_PoF_RUL Node in Hugin -----	129
Figure 5-27: CPT for C_Time_Period Node in Hugin -----	129
Figure 5-28: CPT for Canary_MDValues in Hugin-----	130
Figure 5-29: CPT for Canary_PredictedRUL in Hugin -----	131
Figure 5-30: CPT for Parrot_PredictedRUL in Hugin-----	131
Figure 5-31: CPT for ShipStructure_PredictedRUL in Hugin -----	132
Figure 5-32: Probability Distribution of Predicted Remaining Life for Ship Structure (Scenario 1) -----	136
Figure 5-33: Probability Distribution of Predicted Remaining Life for Parrot Device (Scenario 1)-----	136
Figure 5-34: Probability Distribution of Predicted Remaining Life for Canary Device (Scenario 1) -----	137
Figure 6-1: 3 sensor devices of diameter dimensions (0.125mm, 0.25mm and 0.5mm) -----	144
Figure 6-2: Experimental Setup of the 3 Desiccators -----	145
Figure 6-3: Temperature Readings for Desiccators 1, 2 & 3 -----	146
Figure 6-4: Relative Humidity Readings for Desiccators 1, 2 & 3 -----	147
Figure 6-5: Electrical Resistance Readings for 0.125mm iron wires -----	148
Figure 6-6: Electrical Resistance Readings for 0.25mm iron wires -----	148
Figure 6-7: Electrical Resistance Readings for 0.5mm iron wires -----	149
Figure 6-8: Overlay of Temperature and Resistance (0.125mm) -Salt Environment -----	150
Figure 6-9: Overlay of Temperature and Resistance (0.25mm) -Salt Environment-----	150
Figure 6-10: Overlay of Temperature and Resistance (0.5mm) -Salt Environment-----	150
Figure 6-11: Flowchart of noise reduction of electrical resistance readings -----	152
Figure 6-12: Resistance Difference before and after adjustment for temperature effect (0.125mm wire in salt environment) -----	153
Figure 6-13: Electrical Resistance Difference before and after adjustment for temperature effect (0.25mm wire in salt environment) -----	153
Figure 6-14: Electrical Resistance Difference before and after adjustment for temperature effect (0.5mm wire in salt environment)-----	154
Figure 6-15: Comparison of using Moving Average and Median as smoothing technique for 0.125mm iron wire (salt environment)-----	155
Figure 6-16: Comparison of using Moving Average and Median as smoothing technique for 0.25mm iron wire (salt environment) -----	155
Figure 6-17: Comparison of using Moving Average and Median as smoothing technique for 0.5mm iron wire (salt environment)-----	155
Figure 6-18: Flowchart - Predicting remaining life using PoF -----	157
Figure 6-19: Flowchart - Anomaly Detection using MD analysis -----	159
Figure 6-20: Comparing of MD values (0.125mm iron wire - salt) and threshold MD values -----	161
Figure 6-21: Comparing of MD values (0.25mm iron wire - salt) and threshold MD values	162
Figure 6-22: Comparing of MD values (0.5mm iron wire - salt) and threshold MD values -	162
Figure 6-23: Comparing of MD values (0.125mm iron wire - dry) and threshold MD values -----	163
Figure 6-24: Comparing of MD values (0.25mm iron wire - dry) and threshold MD values	164
Figure 6-25: Comparing of MD values (0.5mm iron wire - dry) and threshold MD values -	164
Figure 6-26: Network for Salt Environment Lab Experiments-----	165

Figure 6-27: Network for Dry Environment Lab Experiments-----	165
Figure 6-28: Network for Water Environment Lab Experiments -----	165
Figure 6-29: CPT for Salt125_PoF_RUL Node in Hugin-----	167
Figure 6-30: CPT for Salt125_MDValues in Hugin -----	168
Figure 6-31: CPT for Salt125_PredictedRUL in Hugin -----	168
Figure 6-32: CPT for Salt250_PredictedRUL in Hugin -----	169
Figure 9-1: Parrot Device Designs (a) -----	191
Figure 9-2: Parrot Device Designs (b) -----	191
Figure 9-3: Canary Device Designs (a) -----	192
Figure 9-4: Canary Device Designs (b) -----	192
Figure 9-5: Canary Device Designs (c) -----	192
Figure 9-6: MD Analysis of Max Data for Scenarios 2 & 3 for Canary -----	193
Figure 9-7: MD Analysis of Min Data for Scenarios 2 & 3 for Canary-----	193
Figure 9-8: MD Analysis of Min Data for Scenarios 4 & 5 for Canary-----	193
Figure 9-9: MD Analysis of Max Data for Scenarios 4 & 5 for Canary -----	193
Figure 9-10: MD Analysis of Max Data for Scenarios 2 & 3 for Parrot -----	193
Figure 9-11: MD Analysis of Max Data for Scenarios 2 & 3 for Parrot-----	193
Figure 9-12: MD Analysis of Max Data for Scenarios 4 & 5 for Parrot -----	194
Figure 9-13: MD Analysis of Max Data for Scenarios 4 & 5 for Parrot -----	194
Figure 9-14: Temperature readings for experiment -----	194
Figure 9-15: Relative Humidity readings for experiment. -----	195
Figure 9-16: Overlay of Temperature and Resistance (0.125mm) -Water Environment -----	195
Figure 9-17: Overlay of Temperature and Resistance (0.25mm) -Water Environment-----	196
Figure 9-18: of Temperature and Resistance (0.5mm) -Water Environment-----	196
Figure 9-19: of Temperature and Resistance (0.125mm) -Dry Environment -----	196
Figure 9-20: of Temperature and Resistance (0.25mm) -Dry Environment-----	197
Figure 9-21: of Temperature and Resistance (0.5mm) -Dry Environment -----	197
Figure 9-22: Resistance Difference before and after adjustment for temperature effect (0.125mm wire in water environment)-----	197
Figure 9-23: Resistance Difference before and after adjustment for temperature effect (0.25mm wire in water environment) -----	198
Figure 9-24: Resistance Difference before and after adjustment for temperature effect (0.5mm wire in water environment) -----	198
Figure 9-25: Resistance Difference before and after adjustment for temperature effect (0.125mm wire in dry environment) -----	198
Figure 9-26: Resistance Difference before and after adjustment for temperature effect (0.25mm wire in dry environment)-----	199
Figure 9-27: Resistance Difference before and after adjustment for temperature effect (0.5mm wire in dry environment)-----	199
Figure 9-28: MD Values for experiment on Water - 0.125mm -----	199
Figure 9-29: MD Values for experiment on Water - 0.25mm -----	200
Figure 9-30: MD Values for experiment on Water - 0.5mm -----	200
Figure 9-31: Probability Distributions of Predicted Remaining Life for Dry-0.125 device--	201
Figure 9-32: Probability Distributions of Predicted Remaining Life for Dry-0.25 device ---	202
Figure 9-33: Probability Distributions of Predicted Remaining Life for Dry-0.5 device----	202
Figure 9-34: Probability Distributions of Predicted Remaining Life for Water-0.125 device -----	203
Figure 9-35: Probability Distributions of Predicted Remaining Life for Water-0.25 device	203
Figure 9-36: Probability Distributions of Predicted Remaining Life for Water-0.5 device --	204
Figure 9-37: Probability Distributions of Predicted Remaining Life for Salt-0.125 device--	204

Figure 9-38: Probability Distributions of Predicted Remaining Life for Salt-0.25 device ---205
Figure 9-39: Probability Distributions of Predicted Remaining Life for Salt-0.5 device-----205

TABLES

Table 2-1: Benefits of PHM -----	18
Table 2-2: Summary of Traditional Maintenance Approaches -----	50
Table 4-1: Canary and Parrot Design Characteristics -----	77
Table 4-2: Conditional Probability Table for Variable A -----	86
Table 4-3: CPT for Corrosion node -----	89
Table 5-1: Corrosion rates of steel after 1 year test (GASCOIGNE, A and Bottomley, D, 1995) -----	102
Table 5-2: Average corrosion rate of steel (GASCOIGNE, A and Bottomley, D, 1995) ----	102
Table 5-3: Estimated corrosion rates for temperature and relative humidity pairs after 1st year -----	104
Table 5-4: Estimated corrosion rates for temperature and relative humidity pairs after 5th year -----	104
Table 5-5: Estimated corrosion rates for temperature and relative humidity pairs after 10th year -----	104
Table 5-6: Estimated corrosion rates for temperature and relative humidity pairs after 20th year -----	104
Table 5-7: Coefficients values of the multi-quadratic model (the corrosion rate generator)-	107
Table 5-8: Dataset of min and max monthly temperature and relative humidity (WEATHER, BBC, 2006) -----	107
Table 5-9: Dataset of min and max monthly temperature and relative humidity for harsher conditions -----	110
Table 5-10: Dataset of min and max monthly temperature and relative humidity for harsh alternate conditions -----	114
Table 5-11: Input data required for inference using BN model -----	128
Table 5-12: PoF model-based input data -----	133
Table 5-13: Input data for Parrot Device from MD Analysis Results -----	133
Table 5-14: Input data for Canary Device from MD Analysis Results -----	133
Table 5-15: Demonstrator Timeline for Scenario 1 -----	139
Table 5-16: Demonstrator Timeline for Scenario 2 -----	140
Table 5-17: Demonstrator Timeline for Scenario 3 -----	141
Table 6-1: Standard Deviation of Electrical Resistance Deviation -----	154
Table 6-2: Prediction of Remaining life of iron wires -----	158
Table 6-3: PoF model-based input data -----	169
Table 6-4: Input data from MD Analysis Results for 0.125mm salt device -----	169
Table 6-5: Input data from MD Analysis Results for 0.25mm salt device -----	170
Table 6-6: Input data from MD Analysis Results for 0.5mm salt device -----	170
Table 6-7: Experiment Timeline -----	171
Table 6-8: Updated Probability Distributions for Predicted Remaining Life for all three salt devices. -----	173
Table 9-1: PoF model-based input data -----	200
Table 9-2: Input data from MD Analysis Results -----	200
Table 9-3: Input data from MD Analysis Results -----	201
Table 9-4: Input data from MD Analysis Results -----	201

1. Introduction

1.1. Overview

This research project involves the development of diagnostics and prognostic tools to be used for monitoring and predicting the ‘health’ of aged structures of great historical value. Such activities present particular challenges when applied to aged structures. This chapter introduces the diagnostics, prognostics and structural health monitoring research field, which are then detailed further in the following chapter. This chapter also describes the types of structures considered for this research project. A few examples of aged structures are presented along with the Cutty Sark, which is used as the demonstration application of the diagnostic and prognostic tools developed. The challenges in maintaining such structures and in particular the Cutty Sark ship are discussed. The motivations for undertaking this research work is presented along with the aims and objectives. The chapter ends with an outline of the general methodology for the diagnostic and prognostic tools developed and the contribution made towards the research field of health monitoring, diagnostics and prognostics for aged structures.

Aged structures encompass a broad range of civil and engineering structures that have been built and used for a long period. Any structure in service is affected by age-related deterioration that can lead to failure of the structure. The deterioration occurring is caused by many factors related to the material composition, the architecture, the usage and the environment of the structure. Structural deterioration comes in many forms: coating damage, corrosion, cracking, deformation, stress, fatigue and wear and tear. These factors can act individually or in combination, and their effects are hard to quantify. Corrosion and fatigue are the predominant modes of failure that affect aged iron structures. Fatigue is due to the fluctuating nature of load and corrosion, and is primarily due to environmental effects. A detailed analysis of failure modes and mechanisms of aged structures is provided in chapter 3.

1.1.1. Use of diagnostics and prognostics technology

The prognostics and diagnostics terminologies are used to describe the broad range of processes, which aim to determine material condition at present time and predict material condition at a later predetermined time. Diagnostics is the process of determining the current “health” of a structure while prognostic is the process of predicting the future “health” of a

structure. Structural health monitoring is a term used to describe the sensor system and diagnostics and prognostics technologies used to monitor systems and structures.

Monitoring of aged structures is essential as most of these structures have exceeded their original design life, but are expected to operate reliably and safely over their extended operational lives. The maintenance of these structures would usually be carried out on an ad hoc basis as and when required and little documentation of such repair work is available. The most common form of monitoring the degradation of such structures is visual inspection, which is carried out at varying intervals depending on the usage and age of the structure and the funding available. Visual inspection is a labour intensive and subjective approach to monitoring aged structures and more cost-effective and reliable monitoring strategy is required. Additionally, standard visual inspection techniques do not necessarily detect insidious deterioration that can lead to substantial damage but only detect defects that are clearly visible and most likely easily controllable.

With diagnostic and prognostic tools in place, monitoring of a structure would provide better understanding of the response of the structure under real operational and environmental conditions. Knowledge of where to inspect a structure should damage start to develop would be available, thus reducing inspection time and maintenance costs. Additionally, monitoring can be carried in inaccessible areas. Maintenance decisions can then be taken based on monitoring and prediction results well ahead of time in order to prevent catastrophic failures.

For new structures, diagnostics has been successfully implemented up to a certain extent in many diverse fields such as manufacturing, civil structures, electronics, aerospace, etc. However, this is not the case for prognostics, which has higher requirements compared to diagnostic analysis. For prognostic purposes, assessment of performance of a structure is required, which involves matching the performance and behaviour signatures from recent data with data representing normal performance and behavior. Using these assessment results, prediction algorithms are then used requiring correct interpretation of the data and insightful understanding of degradation processes of the structure monitored. This development of accurate prediction algorithms is usually the most challenging part.

Typically a diagnostic analysis for new structures would involve data collection, signal processing, feature extraction and selection. Additionally, a knowledge base of failure modes

and mechanisms would be available from expert knowledge, physical models and historical data. However, for aged structures, the knowledge base available for use in diagnostic and prognostic analysis is minimal if not completely nonexistent. This may be due to lack of original documentation of the architectural structure, lack of maintenance logs and lack of understanding of properties of materials used at the time and lack of physical models. Thus, very often, the history of the operational and environmental load experienced by an aged structure is unknown. This further complicates the already challenging task of diagnostic and prognostic analysis.

1.2. Motivation

Aged structures play an important role in heritage tourism and thus have a positive economic and social impact. In 2010, the heritage tourism industry's annual contribution to UK's gross domestic product was worth almost £21 billion (HERITAGE LOTTERY FUND, 2011), which is a bigger contribution than car manufacturing or advertising and film industries to the UK industry. Tourism continued to increase while the wider economy was shrinking. Thus, the preservation and maintenance of heritage structures is of utmost importance in order to preserve our historical and cultural heritage and provide identity to the local community as heritage structures raise pride in the local area and create a distinct sense of belonging. Additionally, with heritage being one of the biggest drivers of tourism in the UK, maintaining heritage structures is a vital part in order to continue to grow the tourism industry as it helps to attract new businesses and residents to an area.

Heritage structures usually have different degrees of degradation depending on the techniques used to build them as well as the length of time they have been exposed to their environmental conditions. There is major motivation in the heritage community to modernise maintenance operations to reduce costs as well as to ensure the structures are preserved for future generations (ANASTASI, G. et al., 2009) (GARZIERA, R. et al., 2007). Ideally, the structural integrity of heritage structures should be preserved for as long as possible such that they can serve their original or new purposes as well as preserving a cultural legacy.

Heritage structures such as the Cutty Sark are a great cultural inheritance from the past and need to be preserved. The conservation work being carried out on the ship is "state of the art", but there is no evidence at present for predictions of the effectiveness of the conservation work over the next 50 years. The main motivation for this PhD project is to develop

prognostic and diagnostic tools to help in maintenance decisions for heritage structures such as the Cutty Sark. This has the potential to make huge savings in terms of cost of maintenance while increasing safety and reliability as well as safeguarding a national treasure. For the scope of this project, only the iron structures are considered for the diagnostic and prognostic tools.

1.3. Cutty Sark Ship

The Cutty Sark is a composite-built vessel, built 140 years ago with a wrought iron frame skeleton and teak and rock elm strakes fastened to it. Conservation work is currently being carried out because of extensive deterioration of the wrought iron frames and timber planking (CAMPBELL, Sheelagh A et al., 2005). The main cause of damage of the wrought iron framework is corrosion with various forms of corrosion prevalent in different parts of the ship. The conservation aims to minimize the potential for degradation by removing some agents of deterioration. The strategy is to ensure that dissimilar metals and materials are not in contact and to use surface coatings, which should form a barrier between the iron and agents of deterioration. Figure 1-1 illustrates examples of severe corrosion and material deterioration that are present in the original fabric of the ship.

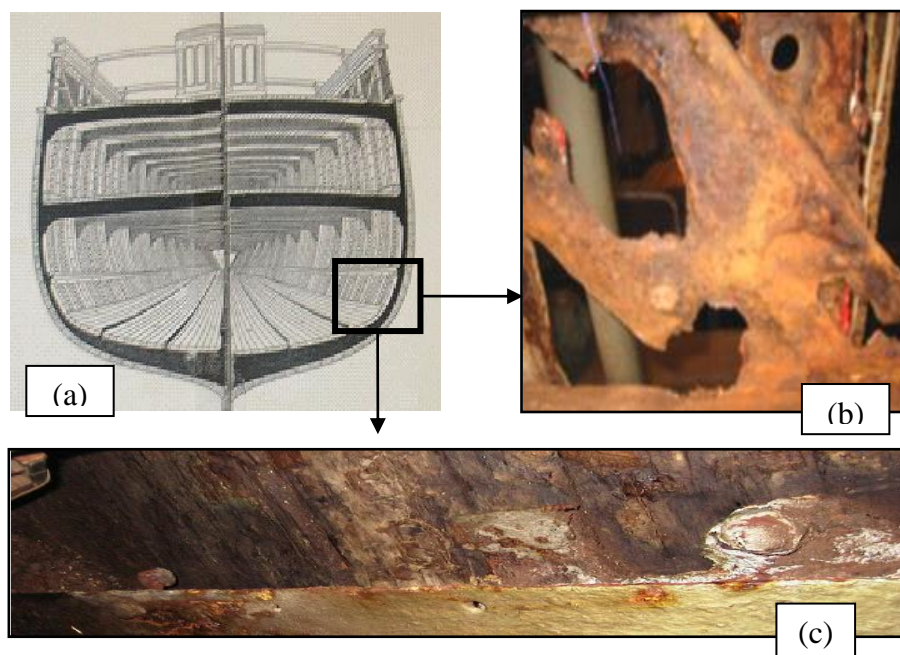


Figure 1-1: the composite built vessel (a) and examples of severe corrosion and material deterioration (b and c) that are present in the original fabric of the ship.

The diagnostic and prognostic tools developed within this research project will be used to predict the current and future “health” of Cutty Sark iron structures. Research and implementation of these tools are a necessary continuation of these conservation works to ensure that the original aim of a 50-year life with only minor and acceptable deterioration (in conservation terms) can be met.

The fastenings used in Cutty Sark are made of Muntz metal (alloy of copper and zinc). Iron and wood are two different types of materials that behave differently under different loads in similar environments. Thus, structures made from these two different materials should be monitored in both parts that use metal or wood. The areas where the iron and wood are in contact are also of importance. For example, iron structures under a particular stress might experience deformation and affect the wood structures (by applying an indirect stress on the wood structures) and thus although the wood structures are not affected by the original applied stress, the structures might still undergo deformation.

The Cutty Sark being around 140 years of age, creep and fatigue would be failures of major concern for the ship. Corrosion is also one of the main aspects of failure to consider as corrosion accelerates creep and fatigue in various different ways for metals, woods and alloys. Since its launch in 1869, the Cutty Sark has been sailing for around 70-80 years until it was dry-docked in 1954. The types of creep, fatigue and corrosion, which the Cutty Sark has been experiencing, would be different types during these two periods because the ship has been used for carrying goods at sea and later converted into a museum in a dry dock.

The development of diagnostic and prognostic tools, which will later be incorporated into a maintenance decision support system, requires input and collaboration of technology and knowledge from different disciplines. Such an inter-disciplinary effort has not yet been developed for heritage structures such as the Cutty Sark. Similar endeavours can be found in the building and maintenance of iron and steel bridges across the world where long-term monitoring systems of bridges is necessary in order to secure structural and operational safety as well as issue early warning on deterioration of structures. The main difficulties here again lie in the technological fusion of different disciplines, which include distributed and embedded sensing, data management and storage, data mining and knowledge discovery, diagnostic and prognostic methods and decision support systems (KO, J. M. and Ni, Y. Q., 2005).

1.4. Challenges in Maintaining Aged Structures

In order to detect and predict faults and failures, it is essential to understand the structures and their behavior. The lack of documentation explaining the design and construction of aged structures makes structural assessment difficult. Intrusive measurement techniques common in monitoring cannot be applied as these have high risk of damaging the structure. The challenges described are commonly observed in aged structures where the lack of technical details of the structures hinder the maintenance process to a great extent (MANDENO, W. L., 2008).

For example, in reference to (GARZIERA, R. et al., 2007), a new technique is presented which involves the use of a laser Doppler vibrometer to measure displacement with great accuracy and reliability. In this project, the aim is to identify the dynamic characteristics of a building, which then help to locate damaged zones, cracks due to structural degradation in historical churches, bells and masonry towers. Wireless sensor networks are also being investigated for the monitoring of historical buildings to facilitate monitoring of appropriate physical characteristics from sensors placed in hard-to-access areas (ANASTASI, G. et al., 2009). Reference (GLISIC, B. and al, 2007) provides more examples of structural monitoring of historic buildings, which have undergone extensive repair and the conservation program where both conventional sensors as well as optical fibre sensors have been used. Such monitoring systems for aged structures have mainly diagnostic capabilities with little or no prognostic capabilities.

The iron structures of the Cutty Sark are made of wrought iron. While considerable attention and a lot of research continues to be directed towards corrosion of iron and steel structures, no comprehensive study has been carried out to date on corrosion models for wrought iron structures (SOARES, C G and al., et, 2008) (SOARES, C. G. and al., et, 2008) (YUANTAI, 2008) (MELCHERS, R. E., 1999) (MELCHERS, R. E. and Jeffrey, R. J., 2008). Information is scarce on corrosion models for prediction of corrosion rates with respect to different influencing factors such as relative humidity, temperature, time of wetness, surface area, chloride concentration and other contaminants. Therefore, uncertainties in quantitative corrosion models are quite high. Straub (STRAUB, Daniel, 2004) reports that physical models of corrosion processes are hard to build, as these require knowledge of the

concentration of oxygen in the environment, the diffusion coefficient in the corrosion products and many other factors, which are not generally available. Additionally, purely empirical models have little value, as the extrapolation of the models outside the calibration range is not possible.

Furthermore, the environmental conditions on a ship such as the Cutty Sark will be different in the future once the restoration work is complete. Added to that, the iron structures would have been treated to decrease corrosion and to protect them from any further corrosion. Therefore, extrapolation of data and information from historic behaviour cannot be carried out and processed in a straightforward manner to provide predictions of future degradation for the ship. Conventional inspections approaches, such as inspect and repair, are not viable options for the ship, as any harmful effects must be detected well in advance of any significant damage on the structures.

Due to the complexity of the corrosion processes, measuring and predicting future corrosion rates for iron structures is a challenge. Corrosion encompasses complex electrochemical reactions for which corrosion rates vary significantly depending on the composition of the materials, the shape of the structures and the surrounding environmental conditions. As mentioned above, many corrosion processes are little understood to date making it difficult to predict corrosion rates of particular structures of particular material within a specific and/or changing environment. The specific challenges for Cutty Sark can be listed as the following:

- Understanding to what extent corrosion affects iron structures.
- Determining the corrosion rates for wrought iron structures as well as composite structures made of wrought iron and timber
- The corrosion rates will be different throughout the ship due to difference in shapes of structures and different environmental conditions
- Finding out to what extent will corrosion affect already aged material
- Developing a correlation between environmental factors and actual corrosion occurring

1.5. Aims and objectives of the research

1.5.1. Aims

There are four main aims for this research. The first is to summarise the major areas of research currently being carried out in the field of maintenance of aged structures, structural health monitoring, diagnostics and prognostics. This project being an interdisciplinary effort, a thorough investigation of the state-of-art in the different disciplines involved is essential. The second aim is to investigate the use of sensors to gather environmental and performance data. Due to restrictions in terms of installation of monitoring equipment, bespoke sensors are required to acquire data. The development and implementation of diagnostic and prognostic tools is the third aim of this research. In brief, within this framework, performance data will be processed to determine at diagnostic level whether the structure is ‘healthy’ or experiencing damage. If damage is detected, a trending process is initiated to estimate the remaining useful life of the structure in the prognostic stage. Various methodologies can be used at both diagnostic and prognostic level. Most importantly, the diagnostic and prognostic tools should provide an accurate update on the extent of corrosion damage and its development such that maintenance actions can be planned at convenient times. Finally, the fourth aim is to demonstrate the utility of the tools developed using some notional examples.

1.5.2. Objectives

To achieve the aims set above a list of objectives has been identified and is detailed below:

- Define conservation in terms of primary parameters for which changes over time is measured. Additionally, the likely values of these parameters over a period of 50 years need to be established. This also involves understanding how the restored structures are expected to perform over time. The parameter(s) chosen should be indicative of the state of the corrosion of that structure, easily measured and provide a continuous update of the state of the structure.
- Damage detection: Design sensors to use around the structure and determine optimal placement of those sensors to detect with high probability and reliability, any damage before it becomes critical. The number of sensor should be kept to a minimum due to operational cost issues.

- PHM Framework: The objective is to investigate model driven and data driven algorithms for diagnostic and prognostic purposes. An appropriate fusion technique should then be used to combine all the diagnostic and prognostic analysis into a PHM framework that will also provide the ability to manage uncertainty
- Diagnostics: The diagnostic tool will compare the 50 years predicted value for a parameter with threshold values that have been chosen to represent a lower bound of acceptable deterioration with time. If any predicted parameter exceeds its threshold value, this should be detected early enough for remedial action to take place. Data trending algorithms will be developed to detect anomalies in chosen parameter measurements that would indicate possible failure in the near future.
- Prognostics: While faults are identified at diagnosis level, usually immediate action will not be required at that stage. The development of a fault is tracked and maintenance is scheduled at the most appropriate time. The prognostic system is expected to have low predictive accuracy at the beginning (which is acceptable and unavoidable) and maximum accuracy towards the end of the life of the structure (which is too late to be useful). Hence, one main objective is to achieve adequate accuracy of predictions of remaining life (for a 50-year period ahead for Cutty Sark example) in the next five to ten years.

1.6. General Methodology

Prognostics and health management (PHM) techniques combine sensing, recording, and interpretation of environmental, operational, and performance-related parameters, which are indicative of a system's health. Prognostics and health management can be implemented using various techniques to sense and interpret the parameters indicative of:

- performance degradation, such as deviation of operating parameters from their expected values
- physical or electrical degradation, such as material cracking, corrosion, interfacial delamination, or increases in electrical resistance or threshold voltage
- changes in a life-cycle environment, such as usage duration and frequency, ambient temperature and humidity, vibration, and shock.

Different approaches can be used individually or combined together to predict failure in terms of a distribution of remaining life and/or level of degradation.

A set of diagnostic and prognostic tools have been developed and a new sensor system has been devised as part of a prognostics and health management system. The diagnostic tool performs anomaly detection using Mahalanobis distance (TAGUCHI, Genichi et al., 2000) as the reasoning algorithm. Mahalanobis distance (MD) is a distance measure based on correlation between two or more variables from which patterns can be identified and analysed. It produces a single metric from multiple sensor data to represent anomalies in the system.

The first prognostic tool is based on the Physics-of-Failure approach, which consists of predicting remaining life of a structure using deterioration models based on environmental factors and any other relevant factors that can lead to deterioration of a structure. This generally involves a physical/empirical model best fit to predict the future state of a structure. Here, a temporal model is used to predict the amount of corrosion at a specified point in time and the evolution of corrosion penetration with time.

The second prognostic tool developed uses a fusion approach that is implemented using Bayesian networks. Bayesian Network models are developed to predict remaining life of a structure by integrating predictions of remaining life (using PoF) with real-time information of possible anomalies in the system (using MD analysis). This fusion approach has been adopted with the aim of developing a prognostic tool that can accommodate the initial lack of information and knowledge regarding the corrosion processes on the Cutty Sark iron structures and handling data uncertainty.

The new sensor system devised consists of two types of devices: Canary and Parrot devices. Canary devices are small-accelerated devices, which will fail according to similar failure mechanisms occurring on Cutty Sark. Canary devices will fail faster than the actual system thus giving advance warning of impending failure. Parrot devices are similar to canary devices but fail at the same rate as Cutty Sark structures. These devices will be placed around the ship for monitoring purposes.

1.7. Contribution

The key contributions of this thesis are highlighted below:

1. Development of a sensor monitoring system comprising of canary and parrot devices in order to measure environmental and performance variables for the iron structures.
2. Development of a prognostic tool that incorporates a PoF model for remaining life prediction of iron structures through the adaptation of the linear-bilogarithmic law.
3. Development of a data-driven diagnostic tool that uses Mahalanobis Distance analysis for anomaly detection.
4. Development of a prognostic tools based using fusion approach to integrate information obtained from the PoF model and anomaly detection to provide updated remaining life prediction using Bayesian Networks.

The diagnostic and prognostic tools developed in this thesis are expected to have a broader impact to the heritage industry as their applications can be extended to aged structures where historical data is scarce, appropriate sensor monitoring techniques are few and understanding of complex failure mechanisms is still incomplete. The results of the research work have been presented at three international conferences and have been published in two journal papers.

1.8. Thesis Structure

The thesis is organised in seven chapters including this chapter. The general layout of the thesis and the topics discussed in each chapter are as follows:

Chapter 2 reviews the Prognostics and Health Management approach on which the PHM framework is based. The following areas are covered in more details: Use of Canary devices, Model-driven methods, Data-driven methods and Fusion methods. A brief overview of maintenance strategies used in the field is also provided. Additionally PHM and SHM efforts for historic structures are reviewed.

Chapter 3 provides background information regarding structure degradation of other maritime heritage structures, failure modes and mechanisms experienced by historic structures such as the Cutty Sark.

In chapter 4, the diagnostic and prognostic tools developed for aged structures are described using the Cutty Sark as example. The use of canary and parrot devices is also detailed. The model-driven method used to predict corrosion rates of iron structures as well as the data-driven method using precursor monitoring and anomaly detection are presented. Then the use of Bayesian networks as a fusion approach for updated remaining life probability distribution is detailed.

Chapter 5 illustrates a demonstration example setup to test the diagnostic and prognostic tool framework. The background information used to develop the demonstration example is presented along with the results from the diagnostic and prognostic tools.

Chapter 6 describes the laboratory experiment carried out to evaluate the methodologies presented within the PHM framework. The results are also detailed and discussed.

Chapter 7 concludes the thesis with a summary of research work carried out, its scientific contribution, the recommendations for diagnostic and prognostic tools and future research areas.

2. Literature Review

2.1. Prognostics and Health Management

2.1.1. Introduction

Prognostics and health management (PHM) is an approach that is used to evaluate the reliability of a system in its actual life-cycle conditions, to determine the initiation of failure, and to mitigate the system risks (MATTHEW, S et al., 2008). The prognostics and diagnostics terminologies are used to describe the broad range of processes, which aim to determine material condition at present time and at a later predetermined time. Diagnostics is as described in (HESS, A. et al., 2005) is the process of determining the state of a component to perform its functions, high degree of fault detection and fault isolation capability with very low false alarm rate. In (GREITZER, F. and al, 2001), Prognostics is described as the process of predicting the future state of a system based on current state and predicted future usage. Diagnostics is carried out to investigate any current failure in a component whereas prognostics will give warning of possible failure in the future and/or predict remaining life of a system such that there is enough time for any preventive measure to be taken to extend life of the system.

Diagnostic methods of PHM systems for fault detection and isolation have achieved good levels of effectiveness depending on the field of application. However, prognostic abilities of PHM systems are still at infancy levels in many application areas as the requirements are often more challenging than those for diagnostic methods. The performance of the prognostic part of a PHM system is dependent on the quality of the diagnostic part. A PHM system can provide many different kinds of predictions. These could be the probability associated with a particular system event occurring or the probability of failure of a system within a set period of time or determining the remaining lifetime of the system under set conditions.

Development of PHM systems depends on the specific requirements of the application. Amongst the main requirements is the amount of time in advance that faults should be detected and how far in future is the prediction of failure required for. In fulfilling these requirements, several factors need to be taken into consideration: the capabilities of the sensors, the logistics available, the current technology shortfalls and the level of safety and reliability that needs to be attained. Additionally, the following factors are critical to perform

prognostics: current health state, historical health state, past maintenance history, and expected future usage (GOH, K M et al., 2006).

There are four general methods for conducting prognostics and health management of systems, which are:

- Fuses and Canaries - also called prognostic cell approach. The prognostic cells are integrated into a specific component or device; these cells incorporate the same failure mechanisms as the embedded device, but fail faster than the actual product by means of scaling.
- Model Driven Methods - such as Physics-of-Failure (PoF) methodology, which is founded on the premise that failures result from fundamental mechanical, chemical, electrical, thermal and radiation processes. It consist of four steps: (1) Failure mode and effect analysis, (2) Life cycle loading monitoring, (3) data reduction and load feature extraction and (4) Damage assessment and remaining life calculation.
- Data Driven Methods - These methods are typically derived from machine learning techniques such as (i) models that establish a set of interconnection relationships between input and output where the parameters of the relationship are adjusted with more information and (ii) detection algorithms that learn a model of the nominal behaviour of a system and then indicate an anomaly when new data fails to match that model (SCHWABACHER, M and Goebel, Kai, 2007).
- Fusion Methods - The aim of fusion/hybrid methods is to integrate both model-based and data-driven methods in order to benefit from the merits of both approaches.

The term Structural Health Monitoring is used also to describe diagnostic and prognostic technologies used to monitor systems and structures. In reference (SPECKMANN, Holger and Roesner, Henrik, 2006), Structural Health Monitoring is described as the continuous, autonomous in-service monitoring of a structure by means of embedded or attached sensors requiring minimal manual intervention to monitor the structural integrity of a structure. This typically involves a large number of sensors used at the front-end to gather data on the condition of the structure. This data is then used in structural analysis and failure models to assess the state of a structure and to predict the remaining useful life (ACHENBACH, J D, 2009).

Structural health monitoring is usually carried in fields such as the electronics industry, aviation industry, civil industry and many others. Boeing is currently looking at implementing a structural health monitoring system focusing on detection and prediction of the corrosion of metallic structures in ageing aircrafts (COLE, I, 2008). In the civil engineering sector, the focus is on the maintenance of increasingly ageing civil infrastructures, especially bridges and high-rise buildings (AUWERAER, H. V.D., 2003). For example, in Japan, there is major concern for the integrity of civil structures with respect to damage caused by earthquakes. Furthermore, it is anticipated that investments in new buildings and infrastructure will decrease while maintenance and renovation of existing structures will increase.

The main motivations for SHM are the optimal use of a structure, minimized downtime and the avoidance of catastrophic failures (BALAGEAS, Daniel, 2010). SHM also aims to minimise human involvement thus reducing labour, downtime and human error, which leads to improved safety and reliability. Additionally, the economic benefits are also considerable in that constant maintenance costs would be expected instead of increasing maintenance costs for classical maintenance approaches. Some of the features usually associated with SHM are (SPECKMANN, Holger and Roesner, Henrik, 2006):

- Sensors permanently attached to the structure
- No physical access to inspection area necessary (safe inspection of hazardous areas)
- Automated inspection without manual operation in the inspection area required
- Questioning several locations at the same time

The transition from research to practice of SHM however is reported to be quite slow. There are many technical challenges still to overcome particularly with regard to sensor development and data transmission (ACHENBACH, J D, 2009). Sensors need to be small and ideally with suitable wireless transmission capabilities to the central station.

The purpose of this chapter is to provide an overview of the diagnostics and prognostic methodologies currently in development and/or in use for aged structures such as ships, bridges and historical buildings as well as aircrafts and electronics. The first section describes the different categories of diagnostic/prognostic methods in PHM. The second section describes the use of canaries as advance warning devices. The third section describes the

model-driven methodologies for prediction of corrosion rates in varied structures. In the fourth section, an overview of data-driven techniques is provided with focus on technologies used for precursor monitoring and anomaly detection. The fifth section describes research carried out on using fusion approaches for prognostics and especially Bayesian Networks, which is, used the fusion prognostic tool developed. The penultimate section provides an overview of current SHM and PHM efforts for historic buildings and ships. The last section summarizes the information provided in this chapter.

2.1.2. Challenges & Issues

The challenges of PHM systems are varied and depend on the application field. While most likely scenarios and future events and behavior can be quantified to a certain extent, the future is not known at the time of prediction. Thus, prediction needs to be treated as a probabilistic process where the predicted remaining time is represented by a probability density function. As a result, we cannot eliminate the inaccuracy and uncertainty (precision and confidence) of the predicted remaining life but only minimize it (HESS, A. et al., 2005).

A common paradox associated with PHM due to the use of Probability Density Functions (PDFs) to represent predicted remaining life is the more precise the remaining life estimate, the less probable this estimate will be correct. In reference (ENGEL, S J et al., 2000), Engel et al demonstrates the distinction between four idealized Probability Density Functions (PDFs) for remaining life. Prognostic methods need to be able to handle real world uncertainties that lead to inaccurate predictions. These uncertainties are grouped into three categories (SUN, Bo et al., 2010):

- Model uncertainty caused by model simplification and model parameters
- Measurements and forecast uncertainty induced by environmental and operational loads
- Uncertainties associated with the characteristics of parameters of a system caused by the production and implementation process of that system.

Thus prognostic accuracy assessment technologies with methods that impartially evaluate the effectiveness and accuracy of a PHM system are required for quantifying the confidence level of the PHM system. Often prognostic methods cannot be used due to lack of empirical data or experience knowledge required to develop and test the methods. This occurs mainly due to the

lack of failure data for systems, as they get safer and more reliable. Additionally some legacy systems lack the necessary documentations (HADDEN, G D et al., 2000).

Sun et al, also discuss the difficulty of determining the Return on Invest (ROI) of a PHM system as it is difficult to quantify the benefits of PHM results. ROI is a process based on cost avoidances associated using PHM and the costs associated with the implementation of PHM. Thus performance measures for PHM need to be well defined in order to assess the anticipated ROI and these would include the overall logistics system, supply chain management and other related resources required for the implementation and running of a PHM system. Finally, maintenance applications tend to be complex (in both volume and substance) which overwhelms users. This leads to users developing mistrust in the system whenever a false alarm occurs or prediction of a failure is missed (KOTHAMASU, Ranganath et al., 2006).

2.1.3. Benefits of PHM

The use of a prognostics health management approach for maintenance of systems provides many advantages in terms of reliability, safety, maintainability and other aspects (SUN, Bo et al., 2010). These are summarised below in Table 2-1.

Criteria	Benefits
Reliability (SUN, Bo et al., 2010)	With monitoring of environmental and usage loads, it is possible to take active control actions increase the lifetime of a system through changes to environmental and/or usage conditions. Collection of data enables PHM to assess the actual condition of a system and predict remaining life which in turn is used to replace components of a system as and when required resulting in improved reliability.
Safety (SUN, Bo et al., 2010)	PHM provides the ability to anticipate incipient faults prior to their progressing to final system failure and time to fix problems before the faults cause a catastrophic failure.
Maintainability (SUN, Bo et al., 2010) (NIU, Gang et al., 2010)	PHM helps eliminate redundant inspections, minimise unscheduled maintenance, extend maintenance cycle, decrease test equipment requirements and ultimately reduce maintenance costs.
Logistics (NIU, Gang et al., 2010) (SUN, Bo et al., 2010)	PHM improves and assists the logistical support system by integrating reliable real time information on current and future status of systems which aid planning maintenance and the logistics associated with maintenance such as transportation and supply chains for spare parts.

System design and Analysis (NIU, Gang et al., 2010)	Through investigation of failure modes, mechanisms, and effects of systems, potential design flaws can be found. This helps in improving design and qualifications processes for systems.
Risk Management (HESS, A et al., 2006)	Some level of risk is inevitable with maintenance decisions where the balance is required between removing a faulty component while it still possesses useful capabilities and achieving the limit of 100% failure avoidance. PHM enables the user to make maintenance decisions by providing the necessary information to evaluate and manage the risks associated with the actions to be taken.

Table 2-1: Benefits of PHM

2.1.4. Overview of Prognostics Techniques

From the literature, many research groups have presented a typical PHM system, which would take sensor values as inputs and ideally perform the following (HADDEN, G D et al., 2000), (SCHWABACHER, M and Goebel, Kai, 2007), (PATNAIK, A R et al., 2006):

- System Monitoring using Sensors - sensors located at critical points
- Fault detection - detecting that something is wrong (diagnostics)
- Fault isolation - determining the location of the fault (diagnostics)
- Fault identification - determining what is wrong, i.e. determine the fault mode (diagnostics)
- Fault prediction - determining when a failure will occur based conditionally on anticipated future usage (prognostics)
- Maintenance Scheduling - determining the appropriate times for maintenance activities based on a cost-benefit analysis

Many PHM algorithms exist whose applicability is highly dependent on the available knowledge of the monitored system. These algorithms can be classified into three main categories: (1) Model-driven, (2) Data-driven and (3) Fusion, which can be further classified as shown in Figure 2-1 which is based on similar representations in (SCHWABACHER, M and Goebel, Kai, 2007) (ZHANG, Huiguo et al., 2009).

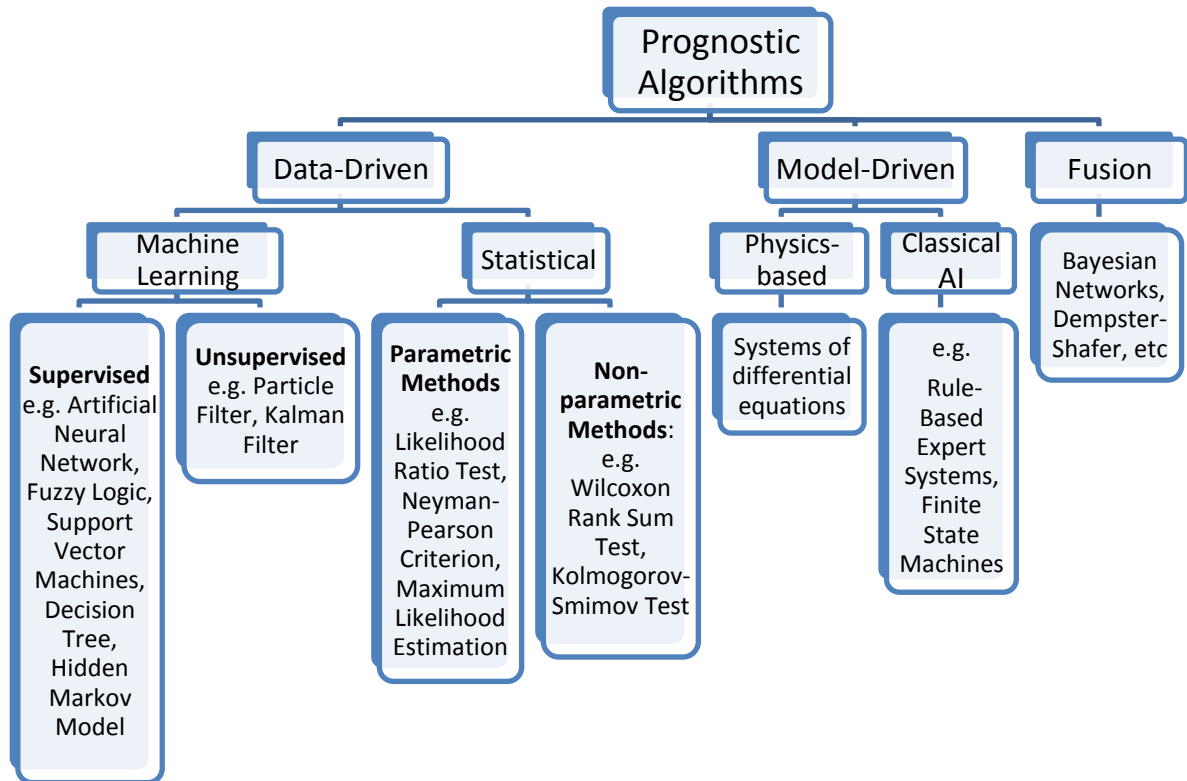


Figure 2-1: Types of Prognostic Algorithms

Model-driven algorithms are hand-coded representation of the system. These can be either physics-based or Artificial Intelligence-based. Physics-based models involve accurate mathematical models encapsulating first principles knowledge of the system. Such models are highly desirable but often difficult to build for complex systems (PATNAIK, A R et al., 2006). Thus, most physics-based models do not capture every details of the system, but capture the essentials features with minimum complexity. AI-based algorithms include rule-based expert systems and finite state machines amongst others.

Schwabacher et al, define data-driven approaches as methods that automatically fit a model of system behavior to historical data rather than hand coding a model (SCHWABACHER, M and Goebel, Kai, 2007). Data-driven methods use real data to approximate and track features revealing the degradation of systems and to forecast the behavior of a system. As a result, data-driven approaches are highly dependent on the quantity and quality of data. As such, data-driven models can be applied immediately in situations for which appropriate physics-based models do not exist or are too expensive and/or complicated to develop. Data-driven approaches are further categorized into machine learning approaches (such as neural networks, fuzzy systems, decision trees, etc.) and statistical approaches. Machine learning

techniques are usually very flexible and can easily adapt to changes resulting from changes in the system itself, in its operating environment or expectations (ZHANG, Huiguo et al., 2009). Further review of data-driven methods used in Prognostics and Health management is provided section 2.3.2.

More recently fusion or hybrid approaches to perform diagnostics and prognostics have emerged with the aim of combining the advantages of PoF models and data-driven methods to provide a more reliable prediction of remaining useful life (ZHANG, Huiguo et al., 2009) (CHENG, Shunfeng and Pecht, Michael, 2009). In reference (ZHANG, Huiguo et al., 2009), the data-driven method is used to “calibrate” the PoF model. Meanwhile, the PoF model is used to define failure criteria and thresholds for the data-driven method and provide an estimate of remaining life based on data-driven results.

2.1.5. Prognostics in application

Prognostics and Diagnostic systems have recently gained strong interest from diverse fields (mechanical and electrical systems, logistics, and construction, medical). Prognostic tools are now researched widely under industrial, government and academia projects. An overview of some projects in various sectors is provided in the following subsections.

2.1.5.1. GE Aviation

GE Aviation is engaged in developing prognostics health management applications for mechanical and electronics systems in the avionics industry. In (SMITHS AEROSPACE, 2004), the ProDAPS project application is described as providing intelligent tools to facilitate the following tasks:

- Extraction of new knowledge and information from system health data
- Reasoning with this knowledge and information to diagnose system state
- Anomaly detection and trending for prognostics
- Determine the optimum actions to meet system management goals.

The ProDAPS application consists of a number of components (Probabilistic High Level Reasoning Engine, Decision Support, Network Editor, Causal Network Editor, Data Mining & Knowledge Discovery, and Reasoning Function) as detailed in (SMITHS AEROSPACE, 2004).

2.1.5.2. PHM for Energetic Materials

Niu et al, are looking into the development of a PHM-based system to ensure the unique and demanding reliability and safety requirements of energetic material systems are met to enable widespread use in both military and civilian applications (NIU, Gang et al., 2010). Energetic materials are a class of materials with a high amount of stored chemical energy that can be released (e.g. hydrogen fuel cells). Traditionally the predicted remaining life of energetic materials was based on an assumed rate of deterioration, which did not account for usage and environmental stresses encountered in real life.

The PHM-based technology would be implemented from initial stage with embedded sensors installed on the actual system for future data collection and health assessment. Investigation into the use of canary materials that exhibit similar behaviours to the energetic material itself are also being carried out. The physicochemical properties and parameters often define how the performance degradation of energetic materials will occur. Currently assessing the material's energy consumption, predicting the remaining useful life, and enhancing the reliability of the energetic material are concerns. A fusion approach combining both the PoF and data-driven approaches are being investigated for energetic material with the aim of benefitting from the merits of both approaches.

2.1.5.3. Integrated Vehicle Health Management in the Auto Industry

Holland presents the Integrated Vehicle Health Management (IVHM) as an active management system of the automotive vehicle's health to guarantee performance of key functions to ensure the requirements for safe and reliable transportation are met (HOLLAND, Steven W, 2008). The aim is to port integrated vehicles health management concepts originally developed for aerospace into automotive industry.

The need for IVHM is motivated by the need for car manufacturers to deliver high value at an affordable price while remaining highly customer-focused. Currently depending on the frequency and severity of faults, different approaches are used to deal with them. The strategy

of “operate till failure” is used for fault with very low frequency and severity. For faults of very high frequency and severity, the product or process is redesigned to eliminate the problem at the source. IVHM is mostly concerned with the strategies to employ in between these extremes. Mathematical models can be used to exploit information available from existing sensors to predict future faults and/or remaining life. Currently condition-based approaches while effective are currently considered too costly due to the need to install additional sensors and the need of considerable engineering effort.

2.1.5.4. Condition-Based Maintenance for Naval Ships

This project supported by the Office of Naval Research of the U.S. Department of defence aims to develop the MPROS architecture (Machinery Prognostics and Diagnostics System) which hosted multiple online diagnostic and prognostic algorithms that can efficiently undertake real time analysis from appropriately instrumented machinery aboard naval ships. Feedback to users regarding the status of the machinery would then be provided to aid in maintenance decisions before embarking on their next mission. MPROS had two phases: the first phase was installed and running in a lab and the second phase was installed on the Navy hospital ship Mercy in San Diego.

One prototype contained four sets of algorithms developed by four different teams. Data concentrators (devices with embedded computers for processing the diagnostic and prognostic algorithms) were placed near the ship’s machinery. The information processed from the data concentrators were then sent over the ship’s networks to a centrally located machine containing the Prognostic/Diagnostic/Monitoring Engine (PDME). The PDME implement a subsystem called Knowledge Fusion (KF) using Dempster-Shafer belief, which combines the information processed from all the data concentrators to form a prioritized list of maintenance tasks. The PDME also serves as a repository for the diagnostic/prognostic conclusions from the data concentrators and the KF processing. Currently the set of algorithms being implemented still needs to be validated in large parts as well as optimized for various purposes.

2.2. Canary and Parrot Devices Approach

2.2.1. Origin of Canary Devices

The word “canary” is derived from one of the coal mining’s earliest systems for warning of the presence of hazardous gas using the canary bird. Because the canary is more sensitive to hazardous gases than humans, the death or sickening of the canary was an indication to the miners to get out of the shaft. The canary thus provided an effective early warning of catastrophic failure that was easy to interpret (VICHARE, N and Pecht, M, 2006).

In prognostics and health management, the same idea is adapted such that canary devices are used in the actual systems and thus providing advance warning of failures. This technique is widely used in the electronics industry to sense excessive current drain and to disconnect power from the concerned part for example (VICHARE, N and Pecht, M, 2006). Canary devices are accelerated devices, which will fail according to similar failure mechanisms, which could possibly occur in actual system being monitored. Canary devices are designed to fail faster than the actual system as an early warning of failure. Canary devices are also used to learn about the effect of several factors, which could lead to failure in the system. Additionally, as shown in Figure 2-2, the canaries can then be calibrated to provide advance warning of failure (the prognostic distance) to allow appropriate maintenance operations (PECHT, Michael, 2006).

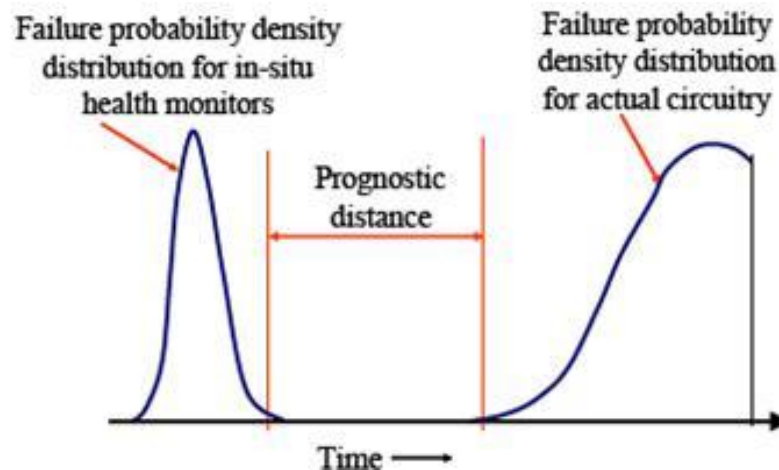


Figure 2-2: Advanced warning of failure using canary devices

2.2.2. Canary Devices: Current State of the Art

2.2.2.1. Use of canary devices in electronics industry

Fuses and canary devices have been used for a while as a means of detecting and preventing failure in the electronics. Vichare (VICHARE, N and Pecht, M, 2006) describes various uses of fuses and canaries, which include circuit breakers to sense excessive current drain and disconnect power from the concerned part and thermostats to sense critical temperature limiting conditions and shut down part of the structure until the temperature returns to normal. Ridgetop Group have commercialized prognostic cells for semiconductor failure mechanisms such as electrostatic discharge, hot carrier, metal migration, dielectric breakdown and radiation effects for which time to failure with respect to the actual product can be pre-calibrated (RIGETOP SEMICONDUCTOR-SENTINEL SILICON LIBRARY, 2004).

2.2.2.2. Corrosion sensors in Structural Health Monitoring of Aircrafts

CSIRO, in conjunction with Boeing Phantom Works and Australia's Defence Science and Technology Organisation (DSTO), has developed structural health monitoring system, which is based on an agent-based system that uses sensor microclimate, and corrosion data to diagnose corrosion and infer the presence of corrosion in locations such as crevices where it cannot be sensed directly (COLE, I, 2008). Clusters of sensors in small local regions of the aircraft measure local microclimate factors, including temperature, humidity, surface wetness and conductivity of surface moisture. The sensor cluster also includes a galvanic corrosion sensor, fabricated from mated strips of copper and aluminum alloy. Each agent forms an autonomous sensing unit by including data acquisition, processing and communications capability with each sensor cluster.

Sensors can however only monitor a small percentage of the aircraft structure and it is not possible to install sensors in some of the areas of high corrosion risk, such as crevices and fastener holes. Thus, the structural health monitoring system also needs a reliable way of inferring the likely progression of corrosion damage at "unsensed" points in the aircraft. The galvanic corrosion sensors (damage sensors) used in the system measure the rate of degradation of the material of the sensor itself, rather than that of the structure to which it is attached.

Correlation relationships between the actual component damage and the sensor damage have been developed through experiments run in environmental chamber tests (MUSTER, T et al., 2005). A model is derived from data streams of the microclimate and damage sensors by an optimization procedure that establishes the best-fit “relationship” between the damage data streams and the microclimate data streams. The model is then used to predict the future progression of damage over immediate time spans (up to 6 months). The model is continuously modified while the system is in use. One of the features of this system is its capability to predict corrosion damage for unsensed points that do not have a sensor array attached by matching the materials, geometry and local microclimate to those at sensed points and making modifications to allow for specific features such as fastener holes.

2.2.3. Use of canary devices for corrosion monitoring

Garnett classifies corrosion detection methods into two major categories (GARNETT, E S, 2005). First, there are corrosion detection devices and techniques used to supplement visual inspection at routine maintenance intervals. Those techniques include Visual, Eddy Current, and Ultrasonic, Electrochemical Impedance Spectroscopy (EIS), Colour Visual Imaging (CVI), Radiography and Infrared imaging. Most of those techniques required skilled operators with knowledge of where to focus the detection. Additionally these devices are only used at maintenance intervals, so damage arising between routine service intervals is problematic.

The second group of corrosion and crack monitoring tools is sensors and/or actuators integrated into automated SHM systems. The sensors subgroup passively measures at discrete predetermined locations: acceleration, ph, humidity, acoustic emission, ion concentration, linear polarization resistance, and chemical potential detectors. The self-sensing actuator subgroup uses the properties of piezoelectric smart materials to actively generate high frequency nondestructive vibrations to inspect a structure for cracks and/or corrosion using Lamb Wave or impedance methods. The advantage of the second group of corrosion and crack detectors is the ability to do real-time monitoring and alert maintenance technicians as the structure changes. A listing of the corrosion and crack detection methods and how they work can be found in (GARNETT, E S, 2005).

Each of the corrosion detection methods listed above has unique properties that make them useful for detecting certain types of corrosion. As of yet, no one method can detect and quantify all types and forms of corrosion in all types of joints, fasteners, and materials. Thus,

it requires multiple techniques to detect corrosion. The advantages and disadvantages of each method are described in (GARNETT, E S, 2005).

The PHM framework being developed here adopts the use of canary devices for monitoring purposes. Intrusive measurement methods cannot be used due to the risk of damaging structures of great historical value within Cutty Sark. The canary devices are smaller versions of the iron structures found on Cutty Sark. The canary devices are designed as such with the aim of accelerating the impact of the factors that cause failure based on the same failure mechanisms as those on the actual structures. The canary devices also undergo treatments such as being soaked in chlorine concentration solution for a predetermined period and/or placed in harsher environments to accelerate corrosion of the structures hence accelerating failure of the structures.

2.3. Data Driven Methods

2.3.1. Overview

Data-driven methods encompass algorithms that learn models directly from the data rather than using a hand-built model based on human expertise (SCHWABACHER, Mark, 2005). Such methods are particularly useful when understanding of first principles of a system is not comprehensive or when developing an accurate model to represent a complex system is too expensive. The two main strategies of data-driven methods are: (1) model cumulative damage and then extrapolate out to obtain a damage threshold and (2) learn the remaining useful life directly from data. Some of the common approaches taken are: (i) variants of neural networks, (ii) fuzzy logic, (iii) Bayesian networks, (iv) Case Based Reasoning and (v) various types of anomaly detection algorithms.

Application of data-driven approach to PHM in industry has been successful to a certain extent for diagnostic purposes whereas implementation of these approaches for prognostic purposes is still very much at an exploratory stage. The efficacy of data-driven approaches depends on the quantity as well as the quality of training data.

Artificial neural networks is one of the most popular machine-learning approaches to prognostics where a model that establishes a set of interconnected functional relationships between input data and desired output is created (SCHWABACHER, M and Goebel, Kai,

2007). The parameters of the functional relationship are adjusted for optimal performance using various techniques. Fuzzy logic is another AI technique that is frequently used for prognostic purposes. Fuzzy logic provides a language (with syntax and local semantics) into which one can translate qualitative knowledge about the problem to be solved thus allowing the use of linguistic variables to model dynamic systems (SCHWABACHER, M and Goebel, Kai, 2007). Case based reasoning is also used to look up a best match in a database of diagnostic cases containing typical problems and solutions encountered while diagnosing a system (PRZYTULA, Wojtek and Thompson, Don, 2000).

2.3.2. Precursor Monitoring and Anomaly Detection

A failure precursor is defined as an event or series of events that is indicative of impending failure (MATTHEW, S et al., 2008). For example, an increased electrical resistance and/or material loss would suggest impending structural failure due to corrosion leading to decreased strength of a metallic component. Precursor monitoring is the continuous measuring of selected parameter(s) for which a change in its value can be associated with a subsequent failure (anomaly detection). Failures can then be predicted using a causal relationship between a measure parameter that can be correlated to a failure. Usually parameters monitored are those that are essential for the reliability of the system and critical for safety. Knowledge of such parameters can be gathered through experience and using historical data of failures.

Precursor monitoring and anomaly detection is useful in situations where the physic-of-failure models for a system are too expensive to build and run due to complexity and insufficient knowledge of the application environment. A generic approach to carrying out precursor monitoring and anomaly detection can be described as follows:

- Through analysis of trends within data, precursors are derived from one or more parameters that show measurable changes based as a result of changes in performance of the system.
- Feature extraction from the selected precursors is carried out to provide better explanation of the current and possible future state of a system.
- To perform anomaly detection, data trend analysis algorithm is developed to detect changes in the values of the measurement variables and to correlate these changes with impending failure of the system.

2.3.2.1. Anomaly Detection Techniques

2.3.2.1.1. MSET

Multivariate State Estimation Technique (MSET) is used to monitor the current state of a system and provide information to make a remaining useful life (RUL). MSET monitors multiple parameters of a system such as temperature, humidity and vibration, and calculate the residuals between the actual and the expected values of these parameters based on the healthy historic data. MSET uses pattern recognition from healthy product data to generate an estimate of current health. The historic data is assumed to cover and provide data for the entire healthy range of the system. The results of MSET are residuals that describe the actual monitored data in terms of the expected healthy values and can thus detect faults by comparing the residuals with the threshold.

Figure 2-3 shows the MSET process as described in reference (CHENG, Shunfeng and Pecht, Michael, 2007). New observations (X_{obs}) are acquired for the monitoring parameters selected. Training data (T) is built using healthy data from historic or current acquired data. Then special data from the training data is picked to create memory matrix D, after which MSET will go through two processes to calculate (1) the actual residuals and (2) the healthy residuals. To calculate the actual residuals, R_x , the new observations, X_{obs} , is subtracted from the estimate of the observation, X_{est} , (i.e. the expected value calculated from the healthy data). To calculate the healthy residuals, R_L , the estimates, L_{est} , of all the remaining training data, L is calculated first, then the residuals between the estimates and remaining training data L is calculated. The fault detection process then compares actual residuals with healthy residuals to decide whether the current product is healthy or not. The common method is to employ a hypothesis test, such as the Sequential Probability Ratio Test (SPRT), to produce alerting patterns. A detailed description of the MSET process can be found in (CHENG, Shunfeng and Pecht, Michael, 2007).

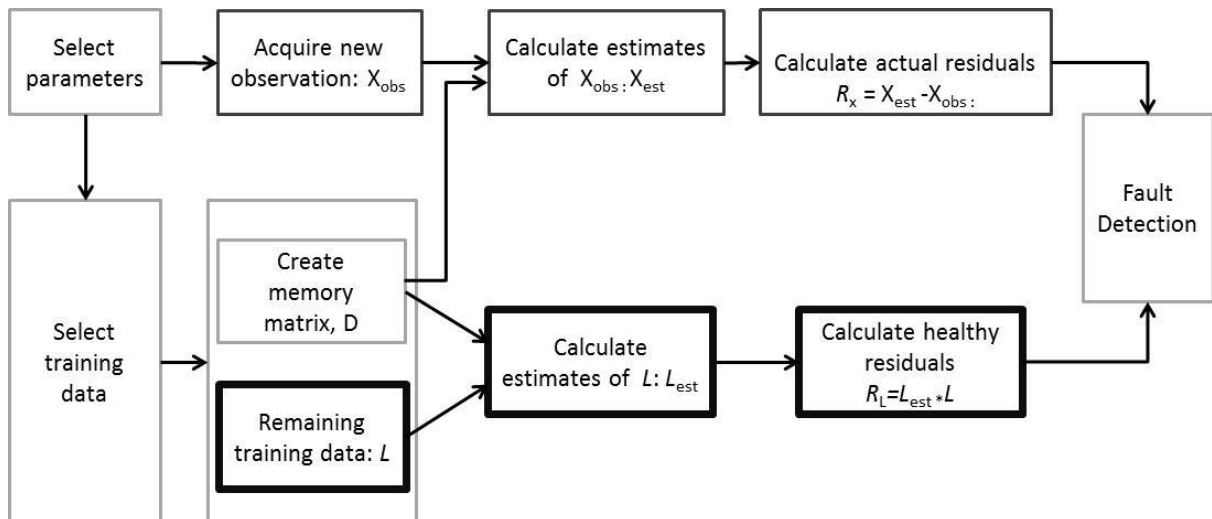


Figure 2-3: MSET Process

2.3.2.1.2. Mahalanobis Distance

Mahalanobis Distance (MD) is a statistical tool developed by Mahalanobis in 1930, to distinguish of a certain group from other groups (akin to the process by which a doctor determines the degree of health of a patient during an examination and classified the health of the patient within a range from healthy to severely ill) (NIE, L et al., 2007). MD is used to find the “nearness” of an unknown point from the mean point of a group (PINJALA, K K et al., 2003). Thus the nearer the unknown point to the mean point of the group (assumed as the “healthy” group), the more likely that point represents a “healthy” state. MD is used mostly to reduce a multivariate system to a univariate system by considering correlation among the parameters. MD is often preferred to other distance measures such as the Euclidean distance, which does not capture correlation between variables and needs to be scaled to reflect differences in variances. The general steps employed for MD analysis are as follows (NIE, L et al., 2007):

- Generation of the Mahalanobis (Normal) Space
 - Define the “Normal” group (the healthy group)
 - Define the y system variables (the performance parameters of a system, e.g. vibration)
 - Gather data for the normal group with sample size $N \gg y$
 - Calculate the Mahalanobis distance MD) for each sample from the defined centre of the normal group.

- Determine the MD threshold value distinguishing the normal group
- Evaluation of system data (outside the normal group)
 - Gather data on the y defined system variables for samples outside the normal group (data from real system being diagnosed)
 - Calculate MD for each sample
 - Compare MD values with MD threshold values to determine whether sample belongs to normal group (healthy) or other groups (unhealthy, faults present)

MD has been applied with a varying degree of success in many applications such as medical diagnostics, fire alarms, automotive, business forecasting and fault detection (CUDNEY, Elizabeth A et al., 2007) (KUMAR, S et al., 2008) (CUDNEY, Elizabeth A et al., 2006).

2.3.2.2. Application Examples

Nie et al (NIE, L et al., 2007), present a prognostics approach using the MD method to predict the reliability of multilayer ceramic capacitors (MLCC) in temperature-humidity bias (THB) conditions. Capacitance, dissipation factor and insulation resistance were the three parameters for which data was collected. A Mahalanobis space (MS) was formed from the MD values of a set of the three identified parameters for non-failed MLCCs. In constructing the Mahalanobis space, the values for the initial period (first 50 data points) were not used due to unusually high MD values at the beginning attributed to transient phenomena. The modified Mahalanobis space had less variation and provided better sensitivity for detection of anomalies. They also suggested an alternative, which was to construct a separate Mahalanobis space for the initial test period with a different MD threshold value.

The MD values for the remaining MLCCs were compared with an MD threshold value. Data for MLCCs, which exceeded the threshold, were examined using the failure criteria for the individual electrical parameters to identify failures and precursors to failure. Although the detection rate was not perfect, the MD method was able to detect failures of the capacitors and identify precursors to failure. They found that for discontinuous or intermittent failures, MD was not successful in identifying these failures as anomalies. The quantity of historical data required is identified as enough data to capture at least the whole life cycle of the system. Additionally, if there is a change in the conditions defining “normal” data, then Mahalanobis space should be updated accordingly. They deduced that the quality and construction of the

MS, together with the choice of the MD threshold, were the critical factors determining the sensitivity of the MD method.

D'Silva et al, use the MD distance metric in the development of a vehicle stability indicator to correlate the various current vehicle chassis sensors (e.g. hand wheel angle, yaw rate and lateral acceleration) (D'SILVA, Siddharth H et al., 2007). This endeavour had the aim of developing a single metric that represents the performance of the vehicle as whole to complement the individual subsystems that quantify the level of vehicle stability enhancement in their domain through measurement of key vehicle signals. MD analysis was used to assess the degree of correlation of the sensor signal, as in general there is a correlation between various pairs of sensor signals when the vehicle operation is linear and stable and a lack of correlation when the vehicle is becoming unstable or operates in a nonlinear region. Currently MD analysis treats unstable and nonlinear operation as unwanted operation and flags their presence with a high scalar metric. They report that preliminary simulation results indicate that the scalar MD metric compares favourably with the traditional multi-metric approach.

2.3.3. Data-Driven methods for Corrosion-Related failures

Dawotola et al (DAWOTOLA, Alex W et al., 2011), use a data-driven approach to find the optimal inspection interval for a petroleum pipeline that is subject to long-term corrosion. This approach takes into consideration both the failure frequency and the consequences of failure due to three forms of corrosion: uniform corrosion, pitting corrosion and stress corrosion. The failure frequency is estimated by fitting historical failure data into either a homogeneous Poisson process or power law while the consequences of corrosion is calculated in terms of economic loss and environmental damage caused by small and large leaks and rupture of pipeline. Both failure frequency and consequences are then used to estimate the total loss due to pipeline operation.

Gu et al (GU, Jinwei et al., 2006), developed the Space-Time Appearance Factorisation model (STAF) that factors space and time-varying effects to monitor the process of corrosion of steel structures by analysing the changes of surface appearance over time. The data driven model separated temporally varying effects from spatial variation, estimating a “temporal characteristic curve” in appearance that depends only on the physical process as well as static spatial textures than remain constant over time. Added to that, they developed the facility to estimate rates and offsets that control different rates at which different spatial locations

evolve, causing spatial patterns on the surface over time such that the speed of evolution can be controlled by separately modifying space and time-varying effects.

2.4. Model Driven Methods

2.4.1. Physics-of-Failure Approach

Physics of Failure is an approach where an accurate mathematical model (with an acceptable degree of uncertainty) can be built from first principles representing the physical processes within the system. Thus, knowledge of specific failure mechanisms and life cycle loading is required to assess product reliability (PECHT, Michael G, 2008). The PoF methodology aims to do prognostics by first calculating the cumulative damage accumulation due to various failure mechanisms within a particular environment of a system and then analyses this information to give predictions of remaining service life of the system. PoF approaches integrate sensor data with prediction models (based on future estimated loads) to predict the future “health” of a system.

Various approaches are presented in literature for carrying on PoF-based prognostics. Failure Modes, Mechanisms and Effect Analysis (FMMEA) is one methodology that is widely adopted to carry out PoF-based prognostics (MATTHEW, S et al., 2008), (PECHT, Michael G, 2008). The FMMEA process is shown in Figure 2-4 (ZHANG, Huiguo et al., 2009).

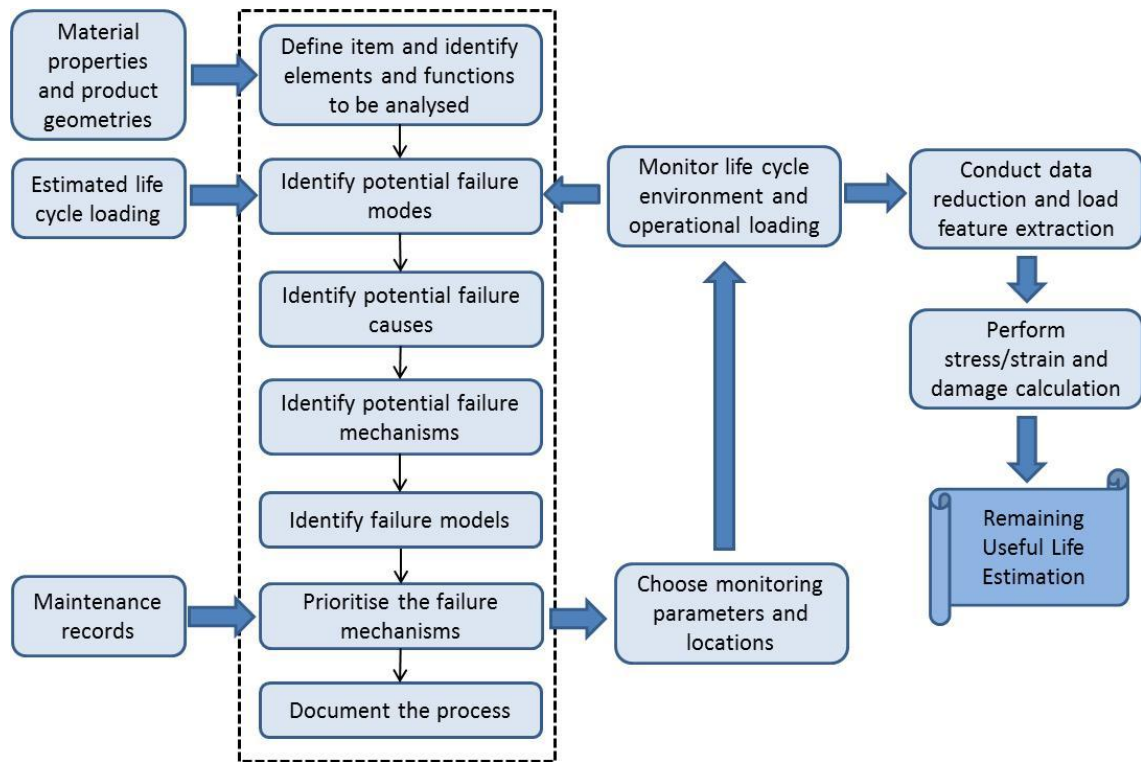


Figure 2-4: FMMEA Process used in PoF based PHM

FMMEA is a systematic methodology to identify potential failure mechanisms and models for all potential failure modes and to prioritise failure mechanisms (PECHT, Michael G, 2008). The failure modes and mechanisms to be monitored are then prioritized according to their severity and likelihood of occurrence. Monitoring parameters and sensor locations can then be determined. Using operational and environmental data, the amount of damage can be calculated from PoF models, which is then used to estimate the remaining life. Further detailed description of the FMMEA process can be found in (ZHANG, Huiguo et al., 2009). Matthew et al, describes a PHM methodology that incorporates FMMEA and PoF models through the following steps (MATTHEW, S et al., 2008):

1. *Life cycle loading monitoring* – the lifecycle of a system is the manufacturing, operating and non-operating loads which individually or in various combinations accumulate damage that can lead to degradation of the system.
2. *Data reduction and load feature extraction* – storage space and CPU load are important factors to consider and it is essential to be able to condense load histories without losing important damage characteristics. Prioritisation of failure mechanisms leads to effective utilization of resources as usually only a few operational and environmental parameters cause the majority of failures.

3. *Damage assessment and remaining life calculation* – PoF models can be used to calculate damage caused by temperature and vibration loading which are common load conditions that accelerate failure.
4. *Uncertainty implementation and assessment* – While PoF models can be used to calculate remaining life, it is still necessary to identify the uncertainties and assess the impact of those uncertainties on the remaining life distributions in order to make risk-informed decisions.

PoF models would generally use as inputs the following: stress level and severity, the architecture or geometry, the material properties and life-cycle profile of a system to calculate the time to failure for a particular failure mechanism of the system. For example, Coffin Manson's model can be used to calculate damage caused by cyclic loading (e.g. temperature). Additionally as life cycle loads are collected in real time, PoF models are generally expected to be able to update predictions continuously. Damage can be calculated from various stresses caused by environmental and/or operational loads. Then damage accumulation is performed for a set period and the remaining life is calculated based on the accumulated damage. (PECHT, Michael G, 2008)

2.4.2. Physics-of-Failure Models for Corrosion-Related failures

Failures in a system are usually due to the processes occurring within and around the system (e.g. mechanical, chemical, electrical, thermal, etc.) as well as the different types of loads the system is subjected to. For example in the case of Cutty Sark, the iron structures present have experienced over the vessel's lifetime various types of corrosion in different locations within the ship. Corrosion models for certain materials have been developed that can predict failure progression in laboratory with set environmental conditions and usage profiles. However, the variation of test conditions such as the use of different metals and environmental conditions in the various corrosion studies means no generic corrosion model to predict corrosion rate has been developed to date.

For the scope of this research project, the corrosion rate of atmospheric corrosion has been studied, as it is one of the main corrosion types the Cutty Sark is subjected to. Atmospheric corrosion is an electrochemical process, with the necessary electrolyte provided by condensation from the atmosphere (TULLMIN, Martin and Roberge, Pierre R., 1995).

Atmospheric corrosion can occur both indoors and outdoors. The main factors that have the most influence on the corrosiveness of the atmosphere at a given site are:

- *time of wetness* – increased time of wetness generally increases corrosion rates.
- *chloride concentration* – presence of chloride ion accelerates corrosion.
- *amount of industrial pollutants* – in presence of moisture, sulphur dioxide is oxidized to form corrosion sulphuric acid.
- *temperature* – rates of corrosion usually increase with high temperature.
- *relative humidity* – as the relative humidity level increases, the thickness of the moisture film increases.
- *Dust* – presence of dust on the surface can increase the surface moisture at a given relative humidity.

Corrosion models are typically based on explicit mathematical models of corrosion rates. Examples of this type of models include the Eyring-Peck model (HALL, P L and Strutt, J E, 2003) and Linear-Bilogarithmic law model (POURBAIX, M, 1982). The Eyring-Peck model is an empirical model based on temperature and humidity of the environment. The Linear-Bilogarithmic law is also an explicit model for the corrosion process controlled by time of exposure and two coefficients, which depend on the exposure conditions. It is expressed as follows in equation (1).

$$P = At^B \quad (1)$$

Where P is the corrosion penetration at exposure time t . A is corrosion rate during the first year of measurement and B is a constant representing a measure of long-term decrease in corrosion rate.

2.4.3. Model-driven approaches applied in the field

2.4.3.1. Using Life Cycle Consumption Methodology to assess remaining life of electronic products

Vichare and Pecht investigated the effect of thermal loads on the reliability of electronic products (VICHARE, N and Pecht, M, 2006). The aim is to continuously monitor the thermal

loads, in-situ and use the data together with precursor reasoning algorithms and stress-and-damage models to do prognostics. They applied the Life Cycle Consumption (LCM) methodology to achieve this aim. At CALCE, Ramakrishnan et al, (RAMAKRISHMAN, A and Pecht, M, 2003) developed LCM where a history of environmental stresses is used in conjunction with physics of failure models to compute damage accumulated and thereby forecast life remaining. Figure 2-5 (SANDBORN, P, 2005) shows the six main steps involved in the LCM Methodology.

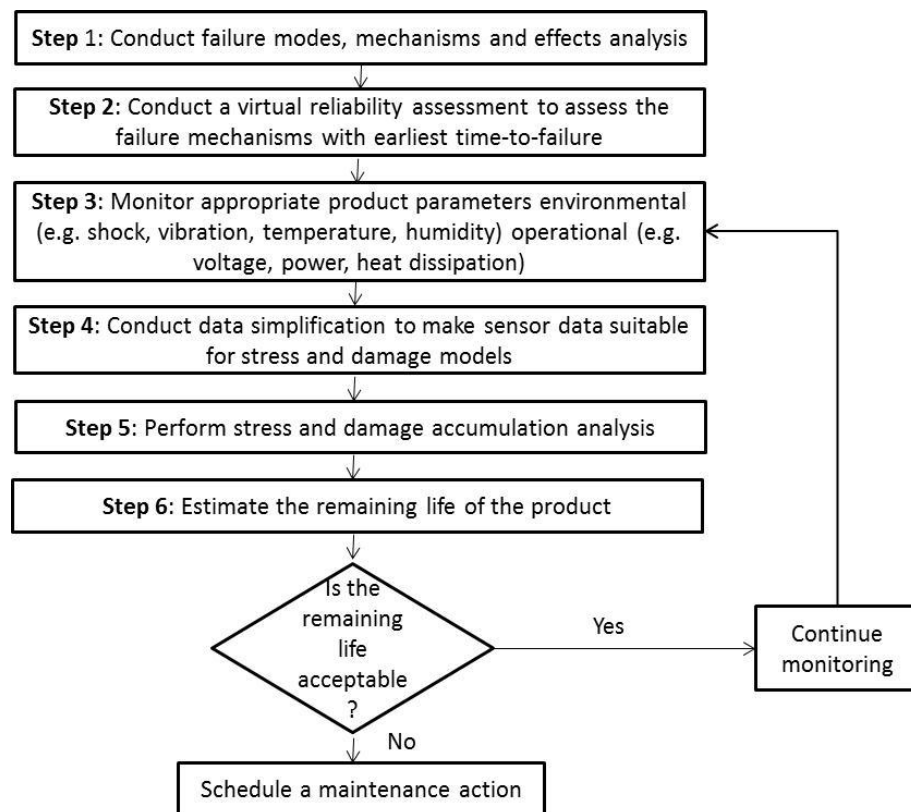


Figure 2-5: CALCE Life Consumption Monitoring Methodology (SANDBORN, P, 2005)

Temperature and vibrations measurements were taken in-situ on the board in the application environment and were used to develop stress and damage models to estimate consumed life. The LCM methodology was then used to predict remaining life. Data reduction and load parameter extraction algorithms were embedded into the sensor module to reduce onboard storage space, power consumption and permit uninterrupted data collection over longer durations. They monitored and statistically analysed the temperatures inside of a notebook computer, including those experienced during usage, storage, and transportation, and discussed the need to collect such data both to improve the thermal design of the product and to monitor prognostics health. After the data was collected, it could be used to estimate the

distributions of the load parameters. The usage history was used for damage accumulation and remaining life prediction.

2.4.3.2. Engine Bearing Prognostics

Orsagh et al (ORSAGH, Rolf et al., 2004) have developed an engine bearing prognostics approach that utilizes available sensor information on-board the aircraft such as rotor speed, vibration, lube system information and aircraft maneuvers to calculate remaining useful life of the engine bearings. Sensed data is linked to fatigue-based damage accumulation models (based on a stochastic version of bearing life equations) and projected engine operation conditions to implement remaining useful life assessment. Model-based estimates can be used when no diagnostic indicators are present and using monitored features at later stages when failure indications are detectable, thus reducing the uncertainty in model-based predictions. Prediction is carried out through a fusion of diagnostic features and physics-based modeling. They perform assessment of remaining life through three functional steps:

- *Sensed data* – signals indicative of bearing health (vibration, oil debris, temperature, etc) are monitored to determine the current bearing conditions.
- *Current bearing health* – engine speed and maneuver induced loading are used as inputs for bearing health models.
- *Future bearing health* – a rolling contact fatigue model utilizing information from sensed data is used to calculate the cumulative damage sustained by the bearing since it is first installed. The model output is then combined with extracted features and future operation conditions to give prediction of remaining useful life.

To achieve a comprehensive diagnostic/prognostic capability throughout the life of critical engine components, model-based information is used to predict the initiation of a fault. In most cases, the predictions will prompt “just in time” maintenance actions to prevent the fault from developing. However due to modeling uncertainties, incipient faults may occasionally develop earlier than predicted. In these situations, sensor-based diagnostics complement the model-based prediction by updating the model to reflect the fact that fault initiation has occurred.

2.4.3.3. Prognostic tool for single spur gear tooth and helical gear

Kacprzyński et al, developed a prognostic tool where predictions are made through the fusion of stochastic physics-of-failure models, relevant system health monitoring data and various inspection results (KACPRZYŃSKI, G J et al., 2002). The inherent uncertainties and variability in material capacity and localized environmental conditions as well as the realization that complex physics-of-failure understanding will always possess some uncertainty, all contribute to the stochastic nature of prognostic modeling. However, accuracy can be improved by creating a prognostics architecture instilled with the ability to account for unexpected damage events, fuse with diagnostic results, and statistically calibrate predictions based on inspection information and real-time system level features.

The approach involves using an integrated mathematical (probabilistic) framework that uses material-level fatigue models, system-level feature models and raw health monitoring measurements. Two prognostic models were developed:

- For a single spur gear tooth – aim was to correlate a 2-D finite element fracture mechanism models and associated crack initiation and propagation algorithms to tooth stiffness and acoustic emission changes. This was achieved by updating/adapting material property distributions or choice of algorithms during damage progressions based on measured or inferred conditions.
- For a helical gear – aim was to predict current and future material level damage as a function of torque from system level vibration using a high fidelity model (built upon contact element and 3-D fracture mechanics FE models of the gear).

2.4.4. Advantage of using PoF models for prognostic purposes

PoF based methodologies can provide information that can be used for advance warning of failures, which helps, minimize unscheduled maintenance and decreasing inspection costs and downtime. Data-driven approaches require data for training the algorithm. In legacy and new systems, very often little data is available initially whereas PoF models can be used if the material properties and structure geometries are available. In addition, many data-driven approaches tend to only detect failure close to the failure point, thus making it difficult to assess remaining life at the beginning.

2.5. Fusion Methods

The fusion approach, also referred to as hybrid approach, is a mixture of the techniques mentioned above. Fusion approaches are generally driven by the need to overcome the lacking of PoF models and data-driven approaches in terms of their diagnostic and prognostic capabilities. Data-driven techniques usually cannot distinguish different failure modes and mechanisms in a system. Additionally there is heavy reliance on a reasonably large training dataset that will explore the necessary loading and environmental conditions that will cause faults and failures. PoF models are developed based on knowledge of specific material properties, geometry and loading conditions and any deviation in those parameters in the actual system will result in erroneous diagnosis and prognosis that is amplified over time. Added to that, PoF models usually find it challenging to deal with complex failure mechanisms.

By fusing the output of both methods, more robust and accurate diagnostics and prognostics will result. Fusion approaches are also being investigated for their capability of fusing data from different predictors where some will yield numeric values, while others will use symbolic ones (BARAJAS, Leandro G and Srinivasa, Narayan, 2008). There are several approaches to perform fusion prognostics. The following section provides an overview of various approaches and their applications.

2.5.1. Bayesian Networks

Bayesian network is another popular method used for fusion prognostics. The following subsections provide an overview of use of Bayesian networks for diagnostic and prognostics purposes and briefly describe some example applications.

2.5.1.1. Overview of Bayesian Networks in diagnostics and prognostics

A Bayesian network is a probabilistic graphical model that represents a set of variables and their probabilistic independencies. Bayesian networks are usually used to represent the probabilistic relationships between causes and effects. Nodes represent the various variables of the system (defined over all its possible states) and the connecting arrows indicate the causality between these variables. Bayesian Networks are based on the Bayes' Rule (equation (2)):

$$P(A|B) = \frac{P(B|A)P(A)}{P(B)} \quad (2)$$

Where for events A and B (provided $P(B) \neq 0$), $P(A)$ is the prior belief (i.e. initial uncertainty in A), $P(A|B)$ is the posterior belief (i.e. the uncertainty having accounted for evidence B), $P(B|A)$ is the likelihood and $P(B)$ is the marginal likelihood.

Bayesian networks are used to represent domains containing some degree of uncertainty as a result of inadequate knowledge of the state of the domain and/or randomness in the mechanisms that control the behaviour of the domain. One unique feature of Bayesian Networks is that results are presented in the form of probability distributions rather than single values. Thus, uncertainty of processed results and impact of various decisions is represented explicitly. Moreover, Bayesian Networks are particularly useful in situations where a large number of interlinked factors need to be taken into consideration.

Przytula et al (PRZYTULA, Wojtek and Choi, Arthur, 2007), have carried out extensive research in the field of diagnostics and prognostics using Bayesian networks with the development and implementation of Bayesian Networks for diagnostics of complex transportation and prognostic of electromechanical and electronic subsystems in aviation systems. Initially the focus was on developing a systematic procedure for the efficient creation of Bayesian networks for diagnostics (PRZYTULA, Wojtek and Thompson, Don, 2000). This process was divided into several phases:

- Problem decomposition – decompose the initial system into simple subsystems
- Sub-problem definition
- Design and testing of a Bayesian network models for each subsystem.
- Integration into a complete Bayesian network.

The main principle in the development was starting with the simplest form of Bayesian networks and increasing their complexity as required while balancing model accuracy and knowledge acquisition cost. Further details on the method developed can be found in (PRZYTULA, Wojtek and Thompson, Don, 2000).

In a subsequent paper (PRZYTULA, Wojtek and Choi, Arthur, 2007), Przytula et al, describe a general purpose probabilistic framework for reasoning in diagnostics and prognostics which coherently integrates multiple sources of evidence, including system usage, environmental conditions of operation as well as system health and health trends. The framework uses a novel form for structure Bayesian networks based on layered, directed graphs. Only essential aspects of system operation for diagnosis and prognosis are represented. Thus, there is a layer of nodes representing the health of systems, a layer or diagnostic and prognostic observations, a layer of usage observations and one or more layers of subsystems as shown in Figure 2-6, (PRZYTULA, Wojtek and Choi, Arthur, 2007). To obtain reliable health prognosis, the information contained in the average usage statistics is combined with the information provided by one or more health observations, which characterize the health of the individual component. Our solution to fusion of the usage and health information relies on a graphical probabilistic framework. It is application independent, very rigorous mathematically and accurate.

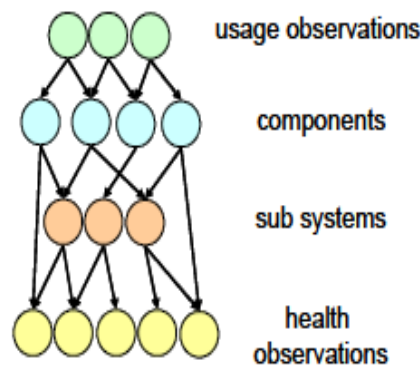


Figure 2-6: A layered probabilistic graphical model for diagnosis and prognosis

Figure 2-7 depicts an example of the model for a simple system consisting of a single component with one usage and one health observation. In this model, the reasoning for diagnosis and prognosis is performed in two steps. First, the reasoning engine accepts the present values for all usage and health observations as specified by the model, producing the diagnosis for all modeled components. The future usage nodes, which indicate the time interval we are interested in predicting health for, are simply set to the present usage values. Next, for prognosis, the future usage values are set as required by a mission, and health trends are used as future health observations. The trends are computed externally by an appropriate trending algorithm which, given the available history of health values, projects to a future

usage value. The prognosis results take the form of the probability of completing the mission, which is specified in terms of the future usage. However, they may be also easily expressed in terms of remaining useful life of the component or system.

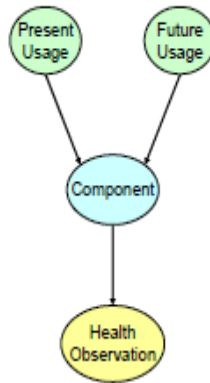


Figure 2-7: BN for prognosis consisting of a single component, usage and health observation

The Bayesian network model developed was then extended further into layered dynamic network model, as the previous static model did not intrinsically account for historical values of health observations, and employed health observation trends that were computing outside of the model (PRZYTULA, Wojtek and Choi, Arthur, 2008). Thus, the temporal structure of the extended model allows the incorporation of all available health history directly in the model. The dynamic networks can accept all available component health histories at once, which the reasoner can fuse together to produce the health diagnosis.

In reference (PRZYTULA, Wojtek et al., 2003), Przytula et al present the methods they employed for Bayesian network evaluation which consist of use of Monte Carlo simulation and efficient visualization of simulation results. Evaluation of Bayesian network models is necessary as the quality of a model determines the quality of diagnostic recommendations obtained using the model. Using evaluation techniques, the critical elements of the model that are responsible for incorrect diagnosis can be identified. Monte Carlo simulation is used to automatically generate diagnostic cases that uniformly cover all the parts of the BN model. The results are presented in the form of sample graphs and matrices that pinpoint which components and observations are responsible for incorrect diagnosis.

2.5.2. Fusion-based prognostics examples

Orsagh et al, (ORSAGH, Rolf et al., 2004) , present an engine bearing prognostics approach, which consists of fusion of diagnostic features and physics-based modelling. Model-based information on damage accumulation is used to predict the initiation of a fault to provide “just in time” maintenance actions to prevent the fault from developing. Additionally sensor-based diagnostics update the model-based prediction where faults might have occurred earlier and was not predicted using model-based techniques. The sensed data is linked with fatigue-based accumulation models based on a stochastic version of the Yu-Harris bearing life equations with projected engine conditions to assess remaining useful life.

In (GOEBEL, Kai and Bonissone, Piero, 2005), Goebel and Bonissone describe a feature level prognostics fusion approach aggregating different information sources to give a continuous output that is ideally amended by a confidence value. First preprocessing occurs using appropriate principal component analysis, filtering, smoothing, normalisation and transformation techniques. Then an adaptive network based fuzzy inference system (ANFIS) is used at the prognostic model that fuses different information sources and produces a remaining life prediction. ANFIS is a representative hybrid system in which neural networks are used to tune a fuzzy logic rule base. The rule set determines the topology of the net (model structure), while dedicated nodes in the corresponding layers of the net (model parameters) define the terms and the polynomial coefficients. Post-processing then follows where the prediction is recursively confirmed through trend analysis. They applied this approach to estimate the time-to-breakage for web breaks in the wet-end part of paper machines in paper mills.

Kumar et al, (KUMAR, Sachin et al., 2008), developed a hybrid prognostics methodology for electronic products utilising both data-driven and PoF techniques. First failure mode, mechanism, and effect analysis (FMMEA) is performed to identify the failure mechanism, critical component and parameters to be monitored. Then continuous monitoring of the identified parameters (providing information on the system’s performance, current health, usage and environmental conditions) is carried out. The data stream is preprocessed using data-driven techniques to extract features that determine system health. The extracted features are used to characterize system health and define baseline performance, which is then used to identify performance deviation of the system and detect anomalies. Trending performance

deviation and anomalies gives an indication of incoming faults or failures. The component causing system degradation is identified using parameter isolation techniques and is matched with the PoF database, which contains information regarding components, their failure mechanism and their damage models. The monitored system parameters obtained from the data-driven analysis are then used in the PoF models to estimate remaining useful life of the system.

A similar approach is taken by Cheng and Pecht, (CHENG, Shunfeng and Pecht, Michael, 2009). Here they additionally propose that if failure models for potential failure mechanisms cannot be identified, the failure can be defined from the historical database where the failed data in the database is classified based on the identified failure mechanisms. Furthermore if the failure mechanisms cannot be identified (for example where a failure is due to complex reactions between different failure mechanisms), the fusion method will use only the data-driven method to predict remaining useful life based on monitored data.

Goebel et al (GOEBEL, Kai et al., 2006) (GOEBEL, Kai et al., 2007), describe an approach to fuse two prediction algorithms for prognostics:

- using first principles to model fault propagation using knowledge of the physics of the system
- using data from experiments at known conditions and component damage level to estimate the fault propagation rate to build an empirical model

They use Dempster-Shafer regression as the fusion method and present results from a case study using rig tests where a bearing was run under mission typical flight profiles. The Dempster-Shafer regression provides a prediction of the output in form of a fuzzy belief assignment. Apart from obtaining more accurate and robust results, the Dempster-Shafer regression helps to quantify the uncertainty of the estimates.

Wang and Jiang, (YANNIAN, Wang and Zhuangde, Jiang, 2005), present a decision fusion algorithm using the Dempster-Shafer theory for diagnostic and prognostic assessment of long distance oil pipeline. It is used to identify and locate leakage and external damage by integrating the real-time signals from sensors with the information about the historic maintenance status records of the pipe, the geological condition and the pipe wall health condition.

Flores-Quintanilla et al use a combination of probabilistic modeling and machine learning techniques to diagnose faults in electrical systems (FLORES-QUINTANILLA, J L et al., 2005). The framework developed consists of two phases: fault detection using Dynamic Bayesian Network that generates a subset of most likely faulty components in the first phase and fault diagnosis using a Particle Filter algorithm to monitor suspicious components and extract the fault components in the second phase. The electrical system concerned is the production line in a factory, which consists of a set of interconnected electrical machines made up of several components. The feasibility of the framework was tested in a simulation environment using several interconnected electrical machines. The Dynamic Bayesian Network chose the electric machines with the highest probability of failure and the particle-filtering algorithm continuously monitored those machines to detect if a component's parameter values had changed. Additionally the Bayesian network was updated periodically based on evidence to evaluate the failure probabilities of each machine.

2.5.2.1. Sensor Validation using Bayesian Networks

Mengshoel et al used Bayesian networks to perform sensor validation within aerospace vehicles. Given a vector of sensor readings, the framework detects whether one or more sensors have failed and are therefore producing bad data (MENGSHOEL, O. J. et al., 2008). The Bayesian network models developed represent the health modes of sensors explicitly, and contain random variables for capturing other aspects of the system (including the health status of other system components). Once input is provided to the Bayesian Network models using sensor readings and commands for the variables capturing other aspect of the system, a MAP (maximum a posteriori hypothesis) query is run over the health of the sensor variables. As a demonstration example, the failed mission of the Mars Polar Lander is discussed. While the cause of the loss of the Mars Polar Lander is not known with certainty, it had enough instrumentation onboard to enable robust state estimation. The radar altimeter as well as the touchdown (contact sensors) provides readings for height above surface which was a critical state variable for the Mars Polar Lander and both had provided conflicting readings with one indicating touchdown and the other not indicating touchdown.

Mengshoel et al advocate that had a Bayesian Network model been used to fuse the two readings, a better estimate of the height above surface could have been provided (MENGSHOEL, O. J. et al., 2008) . Additionally the Bayesian network model could have

been used to find conflicts and causes of conflicts in sensor readings, which can help in deciding which sensor readings to trust.

2.5.2.2. Decision Support for Maintenance Management Using Bayesian Networks

Yan and Shi-Qi developed a decision support system for the Maintenance Management of mechanical systems using Bayesian Networks (YAN, Liu and Shi-qi, Li, 2007). The contents of lubricant oil used in mechanical systems are usually monitored (using spectral analysis, Ferro graph analysis, oil physics and chemical performance analysis, etc) to determine the wear condition of the system. The analysis of wear particle concentration and sizes can determine the severity of wear while analysis of wear particle component, wear particle colour and wear debris can determine the wear site, wear type and reasons of wearing.

Using knowledge of relationships between the fault symptoms and oil monitoring data, a Bayesian diagnosis network was constructed with the topological structure expressing the qualitative knowledge and the probability distributions of the nodes expressing the uncertainties. In addition, a forecasting formula for the condition prediction of the system was introduced in the Bayesian network model. The decision support system thus would estimate and forecast of the system and assist maintenance decision making.

2.6. Traditional Maintenance Strategies

2.6.1. Standard Maintenance Strategies

Various maintenance strategies have been developed and used over the years in different fields. Although equipment needed to be maintained since the beginning of time, the earliest effort on formalizing maintenance is attributed to a book on maintenance of railways published in 1886 (DHILLON, B S, 2006). The term preventive maintenance was coined in the 1950s and a handbook on maintenance of railways was published in 1957. Additionally, various efforts were initiated between World War II and in the 1950s, in the aviation and military fields. Maintenance is the set of processes employed to restore a system or structure to full working order or to the best state possible such that it can perform as intended (STARR, a. and Ball, A., 2000). The following subsections briefly describe the various maintenance approaches used in different fields.

2.6.1.1. Corrective/Reactive Maintenance

Corrective maintenance is a legacy practice that involves repair carried out on a system only once failure has occurred, thus often requiring urgent actions (KOTHAMASU, Ranganath et al., 2006). Corrective maintenance may involve repairing a failed component, servicing and/or rebuilding a component to its original state. This means disruption of operation of a system can occur at any time causing unexpected downtime of the system.

2.6.1.2. Preventive Maintenance

Preventive maintenance is scheduled maintenance carried out to keep a system in a satisfactory operational state by providing for systematic inspection, detection and correction of incipient failures either before their development into major failures or before their occurrence (DHILLON, B S, 2006). The U.S. Navy pioneered preventive maintenance as a means to increase the reliability of their vessels. This proved to be a more cost effective approach compared to reactive maintenance. Studies indicate that savings of as much as 12% to 18% on average can be made (O&M Best Practices Guide, Release 2.0). The main benefits of preventive maintenance are reduced downtime and improved safety as maintenance tasks can be planned to balance workload. There are however several disadvantages to take into account: initial costs might be expensive, unnecessary downtimes and wasted resources to carry out unneeded maintenance and failures might still occur.

2.6.1.3. Reliability-Centred Maintenance

Reliability-Centered Maintenance (RCM) originated from the U.S aviation industry in the late 1960s and was applied by the U.S military services from the middle of 1970s. Because its economic benefit and cost effectiveness were believed significant, since the beginning of 1990s, RCM has been applied to many fields, such as aviation industry, military industry, energy industry, offshore oil production, and so on. (BLISCHKE, Wallace R and Murthy, D.N. Prabhakar, 2003).

RCM is considered as both a preventive and predictive maintenance technique. In Reliability-Centered maintenance, the components of a system are assessed using performance and safety criteria to determine when maintenance is required on the particular components. Fault Tree Analysis (FTA) and Failure Modes and Effects Analysis (FMEA) are carried out to determine which parts of a system are most critical to the system (KOTHAMASU, Ranganath et al.,

2006). Once the critical processes and components of a system are determined, a maintenance strategy is developed which concentrates on ensuring the critical parts are inspected and maintained more frequently than other parts of the system. Also reliability-centered maintenance aims to give feedback on how the original design of a system is performing, thus helping in improving future products (DHILLON, B, 2006).

2.6.1.4. Condition Based Maintenance

Starr. A. and Ball. A. (STARR, a. and Ball, A., 2000), define condition based maintenance (CBM) as maintenance carried out based on the degradation of a parameter indicative of system health.. The aim of CBM is to shift the focus from maintaining a system to sustaining the ability of that system to perform. The parameter monitored is a performance indicator, which gives an early warning of deterioration when there is a change in the readings for that parameter. Various techniques depending on the field of application have been developed to carry out such measurements (e.g. vibration analysis, thermography, visual inspection) (SMITH, R and Mobley, K, 2006). Once the possible presence of a fault is detect, inspection of the system is carried out and maintenance is performed depending on the results of the inspection. CBM can also be described as a predictive maintenance approach.

Predictive maintenance is carried out according to the actual condition of a system (SMITH, R and Mobley, K, 2006). The main aims of a predictive maintenance strategy are to increase the life of a system, reduce the amount of downtime, minimize cost for parts and labour as well as find small problems before they turn into big ones. To achieve those usually more investing in inspection equipment is required along with increased amount of staff training. RCM, Structural Health Monitoring and PHM are all based on the predictive maintenance principle, which is to monitor current condition of a system and perform maintenance only when required.

2.6.1.5. Comparison of Traditional Maintenance Strategies

In references, (DHILLON, B S, 2006) & (DHILLON, B, 2006), Dhillon describes typical corrective, preventive and RCM maintenance programs that can be performed and these are summarised in the table x. Amari (AMARI, S, 2006) also provides a typical maintenance programme that can be applied for condition-based maintenance which is summarized in Table 2-2.

Maintenance Approach	Maintenance Steps
Corrective	<ul style="list-style-type: none"> • Failure recognition • Localising the failure within the system to a specific piece of equipment • Diagnosis within equipment to identify specific failed part of component • Failure part replacement or repair • Checking out and returning the system back to service.
Preventive	<ul style="list-style-type: none"> • Identify components of a system requiring maintenance • Identify what type of preventive maintenance to be performed on these components • Determine the frequency of the maintenance tasks to be performed • Maintenance tasks are then scheduled and carried out • Preventive maintenance tasks and schedules are analysed and improved based on feedback received and information gathered from previous maintenance tasks carried out.
RCM	<ul style="list-style-type: none"> • Identify high priority components with respect to maintenance. • Collect all necessary system failure data. • Perform fault tree analysis. • Apply decision logic to identify failures modes, which are critical. • Formulate maintenance requirements and implement maintenance decisions.

Condition-Based	<ul style="list-style-type: none"> • Identification of failure mechanisms, causes and detection and prevention methods • Identification of the deterioration model associated with the system. • Determination of the costs and effect of various types of failures and maintenance actions • Development of optimal CBM policy for inspection schedules for condition monitoring and optimal maintenance tasks.
------------------------	--

Table 2-2: Summary of Traditional Maintenance Approaches

Contemporary maintenance strategies focus on a predictive approach rather than time-based approach. While the efforts in structural health monitoring concentrate more on the optimum utilization of sensors for structure monitoring and fault detection, the PHM approach takes a more holistic approach to maintenance with a wide variety of techniques used for sensing, diagnosis, prognosis as well as logistics performance. Military, aircraft and electronics industries have so far lead research initiatives in PHM, but other industries have started investigating and implementing PHM practices as well.

Apart from endeavouring to use the latest technologies in sensing, diagnosis and prognosis, PHM encourages solutions that implement a continuous and seamless flow of information throughout the entire process such that maximum use of data obtained through sophisticated sensors is achieved to deliver the most accurate predictive information to help in maintenance decision making. The PHM framework developed for aged structures draw a lot of the structure and techniques from the PHM approach to maintenance.

2.7. Applications for Aged Structures

The maintenance of aged structures is usually conducted through manual inspection of the components according to a set maintenance schedule. This type of maintenance is inefficient and unsafe as faults develop in between inspections are not detected until the next inspection is scheduled. Additionally, very often components are removed for fault repair are still fully functional wasting labour and resources in the process.

The use of sensors within aged structures is spreading slowly across different types of aged structures. However, efficient usage of the data provided by these sensors in developing maintenance plans is still poor. The maintenance of salvaged historic structures brings additional challenges in that knowledge of the structures and materials used for building those ships is scarce and very often, many of the standard type of sensors cannot be used. The next sub-section presents an overview of maintenance efforts for aged structures of various kinds. The following sub-section outlines the restoration and maintenance strategies of three historic ships (SS Great Britain, Vasa and Mary Rose) which have been salvaged and transformed into museums.

2.7.1. SHM and PHM efforts for Historic Structures

Structural health monitoring systems are currently being developed and implemented to serve diverse applications. Most projects involving monitoring the health condition of heritage structures aim to do so using non-destructive and non-invasive sensors as much as possible. There is also often the need for continuous monitoring for real-time assessment of a structure's health as well evolution of any detected anomaly or fault. Additionally, the majority of systems for structural health monitoring often require an integrated approach.

Inaudi and Walder, (INAUDI, D and Walder, R, 2009) describe the various technologies and sensors that a structural monitoring system should have. For example, a building would require fibre optics sensors for strain monitoring, a corrosion monitoring system consisting of concrete corrosion and humidity sensors used for concrete pylon, vibrating pressure cells for measuring the pile loads in the foundations and a laser distance meter to observe the global deformations. The data from these systems are then fused such that correlations between the measurements can be found. The following section provides an overview of technologies and example applications of SHM and PHM in historic structures, as well as buildings and ships in general.

2.7.1.1. Examples

Lubowiecka et al, (LUBOWIECKA, Izabela et al., 2009), developed a methodology integrating laser scanning, ground penetrating radar (GPR) and finite element analysis (FEM) to evaluate the condition of historical bridges for which the geometry is complex and the material properties are unknown and cannot be directly assessed. Using terrestrial laser

scanners (TLS), the geometry of the structure is prepared and a 3D model of the bridge is built. GPR techniques are used to estimate the homogeneity of the structure. The information obtained is used to define a finite element-based structural model, which is then used to model the structural behavior of the bridge.

Inaudi et al, (INAUDI, Daniele et al., 2001), investigated the use of fibre optic sensors for long-term monitoring to help increase the knowledge of the real behavior of historic structures and plan maintenance. Fibre optic sensors were chosen as they can be mounted on the surface of concrete, mortars, bricks, timber, steel and other construction materials. They are also durable, stable and insensitive to external influences (such as temperature variations, corrosion and humidity), thus making them good candidates for long-term health assessment of structures.

They demonstrated the use of fibre optic sensors in the monitoring of a cracked church vault where relatively short sensors with a measurement base of 30-50cm were mounted at different locations along a longitudinal crack that appeared in a small church in Gandria(Spain). Measurements for the crack openings were recorded and their daily and seasonal variations were analysed with respect to ambient temperatures and so far the findings show that crack-opening variations correlate with ambient temperature variations and there is no occurrence of long-term evolution of damage.

Tse et al, (TSE, C Y et al., 2010), developed an integrated SHM system to monitor the structural stability of Alexander Grantham, a historic fireboat harboured in Hong Kong. The aim is to assess the prevailing condition of the fireboat and predict the likelihood of any structural failures before they develop into significant issues that would cause serious threat to the integrity of the structure. The core activities of the integrated SHM program for the fireboat include: (1) Risk assessment and setting monitoring scopes, (2) Identifying representative monitoring parameters, (3) Designing integrated monitoring systems and the sensor network and (4) Data acquisition and processing and interpretation of the data. The current system setup divides into three sub-systems:

- *Continuous monitoring system* — vibrating wire strain gauges, anemometer, accelerometer, tilt meter

- *Periodic monitoring system* — reference points for tape-extensometer, settlement markers
- *Data acquisition system* — devices for continuous logging of data from sensors.

The setup monitors the following parameters: load pattern of the fireboat, deformation of the hull structure, tilting and acceleration, foundation settlement and wind speed and direction. So far, only an observational approach has been used to determine the thresholds of the readings that give an early warning regarding possible degradation. No diagnostic and prognostic capabilities have been developed yet. Additionally the future works identified include statistical models to differentiate undamaged features from damaged structures as well as use of sensor systems that would provide measurement that is more sensitive.

Solis et al, (SOLIS, M et al., 2009) deployed an application for monitoring and detection of structural damage techniques for “La Giralda” sculpture, which is placed on top of Seville cathedral’s tower bell. The sculpture is supported with an internal bar structure, which is fitted over the axis about which it rotates according to the wind direction, allowing it to function as a weathervane. The sculpture was demounted and underwent extensive restoration process between 1999 and 2005 and an instrumentation system consisting of different types of sensors was installed as well.

Most of the sensors were installed in the support shaft, which is the most critical part for the sculpture’s stability. The sensors installed are: 8 strain gauges, 6 accelerometers, 4 inclinometers, 1 anemometer and vane, 2 temperature and humidity probes and 2 corrosion probes using samples of different materials in contact together. The data recorded from the sensors was used to study the dynamic behavior of the sculpture. Additionally accelerations, inclinations, forces, humidity, temperature, galvanic potentials, wind direction and wind velocity data are used in damage detection.

Analysis of corrosion data from corrosion probes revealed that a correlation exists between humidity and galvanic potential does exist where ambient humidity conditions may accelerate corrosion process but no modeling of this correlation was carried out. Results obtained in the first two years of system operation, showed that there was no increasing or decreasing trends in damage detection parameters. This was expected, as two years is a short period compared

to expected lifespan of such structures (previously major damage repairs have been carried out every two hundred years).

The system put in place for monitoring and diagnosis of the sculpture is expected to become more effective with time as more data is acquired. Currently only detection and location of damage can be carried out. There is still a need to quantify the damage through numerical simulation. Even though it is anticipated that the sculpture will not deteriorate over short periods, the authors recommend inspection of the sculpture as well as the instrumentation system every five years as the sensors have short lifespan especially under severe climatic conditions.

Another example of using monitoring techniques is for the maintenance of the wooden structures of The Royal Villa in Monza (built in 1777-1779) which has degraded significantly and experienced cracks as a result (INAUDI, D and Walder, R, 2009). The monitoring was carried out during the restoration as well due to the uncertainties related to the structural behavior and the complex static system. Both conventional and optical fibre sensors with optical fibre sensors being used mainly as extensometers installed between the walls and shorter sensors for crack monitoring. The data was then interpreted and analysed using statistical means. The monitoring data was used heavily in planning and structuring the restoration works.

Bogdan et al, (BOGDAN, B A et al., 2005) (MUFTI, A A, 2003), implemented an SHM system for Manitoba's Golden Boy statue placed on top of the Manitoba Legislative Building. Restoration was carried out on the statue as the steel supporting shaft had deteriorated significantly due to corrosion. A stronger, stainless steel shaft replaced the worn shaft and sensors including electrical strain gauges, accelerometers, fibre optic sensors and thermocouples were installed. Additionally, a web camera and wind meter was installed on the roof of the building.

Data from the sensors and video feed are available through internet to facilitate web-based SHM in real-time. Wind and acceleration data are used to estimate strain experienced by the shaft and these are then correlated with the actual strain record by the strain sensors. This empirical relationship is used to detect faults in the sensors or deterioration of the structure. The data collected within the first year is used as the baseline and everything beyond the first

year will be compared to the baseline. Further damage detection methods are being developed as more data is collected over time with particular focus on dealing with measurement errors and eliminating correlations within measurement data in order to improved monitoring and diagnostics of the structure.

Salvino et al, (SALVINO, Liming W et al., 2009), present a potential SHM architecture for future shipboard application involving use of low cost and dense sensor arrays wireless communications in selected areas of the ship hull as well as conventional sensors measuring global structural response of the ship. The architecture is multi-tiered where on the global level, a real-time, onboard sensor network combined with dynamic based damage detection algorithm can pinpoint possible problems and identify their approximate locations. Then further evaluations are carried out using localised techniques as well as using sensor and inspection information into fatigue based models to evaluate the details of the suspected faults. Future works include embedding data interrogation and processing algorithms at sensors level to enable near real time SHM.

2.7.2. Maintenance Strategies of Historic Ships

2.7.2.1. SS Great Britain

The SS Great Britain was the first ocean going liner with wrought iron hull as well as being the biggest ship in the world in its time. In 1970, SS Great Britain was salvaged from the Falkland Islands and placed in the Great Western Dockyard in Bristol (WATKINSON, David and Lewis, Mark, 2010). In order to preserve the hull, the fabric of the ship and the dockyard structures, a complex preservation project involving innovative use of desiccation was undertaken.

The hull of SS Great Britain contained a range of iron corrosion products that include βFeOOH (Akageneite), Fe_3O_4 (Magnetite) and other chloride infested iron (WATKINSON, David and Lewis, Mark, 2010). Results of experiments showed that to ensure that these iron products do not corrode iron in contact with them, the relative humidity should be 12% or less (WATKINSON, David et al., 2010). However desiccating the hull of the SS Great Britain to 12% relative humidity was deemed too costly and technically challenging with potentially high maintenance costs. Further experiments carried out on the influence of $\text{FeCl}_2 \cdot 4\text{H}_2\text{O}$ and βFeOOH on the rate of iron corrosion showed that corrosion is many times lower at 20%

relative humidity as compared to 25% or 30% relative humidity (WATKINSON, David et al., 2010).

Due to the condition of the iron and length of the hull, conservation methods such as employing stripping or traditional surface treatments were not attempted for fear of further damaging the already badly corroded hull. Additionally, treatments involving removing and/or inhibiting the action of chlorides was not carried out as these were unpredictable and had technical challenge on such a large scale effort (WATKINSON, David and Lewis, Mark, 2010). The main approach to conserve the iron hull was to control the humidity around the ship, which is a major factor in corrosion processes. Thus, a preventive maintenance strategy is employed where desiccation is the adopted method for preserving the ss Great Britain it was assessed to be the least interceptive and least unpredictable method available.

2.7.2.2. Vasa

The Vasa is a battle galleon that sank within one nautical mile of the start of her maiden voyage in 1628 (MAYOL, Dottie E., 1996). Various woods were used with 90% of it being northern oak and various other types of wood making up the rest. The Vasa was salvaged in 1961 and it is claimed that 95% of the ship is still original (MAYOL, Dottie E., 1996). The recovered waterlogged timber hull of the Vasa is the largest of its kind (more than 700 cubic metres of wood weighing around 1500 tons when wet) and it has been underwater for over 300 years. Over such a long time, bacteria had attacked the wood and rust had spread throughout the hull from all the iron objects that had corroded (Preservation and Research - The Vasa Museum, 2010). If the waterlogged wood were allowed to dry out after salvage, the wood would split and collapse. Conservation of waterlogged wood is not easy since new chemical processes are initiated when wood is exposed to oxygen in the air.

The current efforts in maintaining the ship's structure are aimed at controlling the environmental condition around and within the ship (Preservation and Research - The Vasa Museum, 2010). The temperature and humidity are maintained at even levels. High humidity helps bacterial colonies and mold to develop while the conservation agent used to preserve the ships become sticky and attracts dust. If the humidity is too low, there wood might crack and shrink. Currently the relative humidity around the ship is maintained around 51-59% and the temperature is maintained around 18°C-20°C. The light levels are kept below 100 lux and

daylight is not allowed to fall on the ship as organic materials can be broken down by high and intense light levels.

To keep the wood wet, it was treated with polyethylene glycol (PEG) which penetrated degraded cells of waterlogged wood replacing the water, which hinders shrinkage when the wood dries (MAYOL, Dottie E., 1996). Added to that, research is currently being carried out on extraction of iron content from the wood as iron speeds up the deterioration of both wood cellulose and the conservation agent, PEG (MAYOL, Dottie E., 1996). A special cradle was constructed to support and help distribute the Vasa's weight better. It also facilitates conservation treatments that require partial dismantling (The construction and salvage of the Vasa). An advanced laser positioning system is also used to monitor the tiniest movements in the hull of the Vasa. This system is useful in revealing subsiding if the mechanical strength of the wood gradually decreases.

Further complications in the conservation of the Vasa have developed recently. In 2000, an increasing number of white and yellowish salts started to precipitate inside the ship and on the artifacts in the magazine (The construction and salvage of the Vasa). This is been caused by a significant build-up of sulphuric acid within the wood. Additionally, the "new" iron bolts (coated with epoxy or zinc) that were inserted into empty holes after the salvage in the 1960s have severely corroded and the iron compounds formed further accelerates the degradation of wood cellulose. Thus until current research confirm the failure mechanisms affecting the Vasa, a preventive maintenance strategy is adopted whereby the environmental conditions within and around the ship are controlled.

2.7.2.3. Mary Rose

The Mary Rose is a 16th century warship, which was built in Portsmouth and launched in 1511. She sank during an engagement with the French invasion fleet in 1545 and lay buried in the seabed off the south coast of England until she was salvaged in 1982 (ESRF, 2005). The Mary Rose is currently undergoing a conservation spray treatment, which started 10 years ago to wash away sulphuric acid that forms. Large amounts of iron are present in the wood from completed corrosion iron bolts, nails and other objects. Accumulated sulphur compounds within the ship oxidises when in contact with iron which corrodes in presence of oxygen to form sulphuric acid. As uncontrolled atmospheric surroundings can accelerate this process, a

stable climate (constant relative humidity and temperature) around the ship will be created once the spray treatment and drying is completed (ESRF, 2005).

Additionally, researchers are currently using synchrotron x-rays to analyse wood samples to determine the quantities and location of sulphur and iron and their chemical state. This is used to keep a record of the state of deterioration and improve methods of conservation in the future. Currently, research is still undergoing with aims of understanding the failure mechanisms and developing methods to stop or slow down the deterioration of the ship's material and again a preventive maintenance strategy is adopted where environmental conditions are controlled to provide a stable climate for the ship (constant relative humidity and temperature).

2.8. Chapter Summary

The majority of published research involving PHM systems refers either to a single component or to a single aspect of a system. Very few comprehensive research efforts are currently taking a holistic approach when developing a PHM system. As such, diagnostics, prognostics and sensor network remain an area of active research. Many techniques developed so far have demonstrated their effectiveness in laboratory environments but their performance in real-world applications remains uncertain as only a few have been deployed on actual structures.

A complete PHM system would encompass the layout of sensors, the capturing and processing of data from those sensors, the diagnostic and prognostic algorithms used to provide current health status as well as estimate future health status and finally a maintenance decision-making tool, which would act on the processed diagnostic and prognostic information provided.

The number and type of sensors as well as the location of those sensors should be determined with the aim of providing maximum useful data without overloading the system with unnecessary data. The data captured requires pre-processing to remove possible noise and extract performance features that are not readily recognizable in raw data, before passing on to diagnosis and prognosis phases. The diagnostic stages involve detection and reporting of anomalies in the system. This should be achieved with as low false alarm rate as possible to build trust in the end-user.

The prognostic stage in a PHM system is still the most difficult challenge. In order to determine the health status of a system, previous data representing healthy and unhealthy/degraded systems should be ideally be available for comparison. This is often hard to obtain or inexistent for legacy systems or aged structures which have been built at a time when such requirements were not deemed necessary.

In addition to identifying faulty behaviour from normal behavior, the PHM system expects to predict when the system will fail which requires clear understanding of how the system faults develop. Such information is hard to acquire for many systems, as the operation of those systems would stop long before they fail thus preventing collection of data on faulty behaviour.

Remaining lifetime estimate depends on future usage, thus future loads and environments need to be determined in one way or another before remaining life estimation is calculated. Furthermore, uncertainty arising from experiment errors as well as modeling inaccuracies, need to be handled appropriately when performing prognostics and diagnostics. Finally, prognostics and health management of aged structures have their particular limitations to take into consideration such as, lack of structural design, construction and material information, inability to conduct experiments on the structures to learn about their behavior and many more. Currently most aged structure maintenance projects have focused on the instrumentation and diagnostic techniques required to detect any damage with a certain degree of success. However, very little research has been undertaken regarding the prognostic aspect.

This chapter has covered a variety of PHM techniques that are currently being researched in high tech applications. The concept of canary devices was introduced as accelerated sensor devices used to provide warning of impending failure. PoF-based and data-driven prognostic approaches were reviewed with emphasis on anomaly detection algorithms and corrosion-related failure algorithms. Another approach to doing prognostics is fusion prognostics where remaining useful life distribution using data-driven methods and PoF-based method are predicted individually and then fused using a probabilistic method to obtain a new remaining useful life prediction distribution. Examples of fusion prognostics techniques have been reviewed, in particular Bayesian networks. The last section provided an overview of diagnostic and prognostic endeavours for historic structures. The next chapter will detail the particular PHM techniques used to build the PHM framework for Cutty Sark iron structures.

3. Corrosion Degradation Mechanisms

3.1. Introduction

Several degradation mechanisms affect aged iron structures. The main cause of deterioration in aged iron structures is corrosion. The formation of corrosion usually plays a major role in the long-term maintenance of metallic structures. Corrosion consists of complex processes that can occur in different forms. The following subsections provide a brief overview of the causes of age-related structural degradation, degradation mechanisms affecting aged structures, the electrochemistry of corrosion, factors influencing corrosion rate, the different forms of corrosion, corrosion models and finally the consequences of corrosion.

3.2. Age-Related Structural Degradation

Aging of ship structures is defined as the progressive deterioration of structures as a result of normal operational use and environmental influences. The structural deterioration comes in the following forms (WANG, G and Boon, B, 2009) (PAIK, J K and Brenman, F, 2006):

- *Coating damage* - This can take the form of coating cracking, blistering, rust and flaking.
- *Corrosion* – Corrosion occurs due to the chemical reaction between metal and the environment. Further detailed description of corrosion processes is provided in the next section.
- *Cracking* – Cracks originate from defects in structures and accidental overload that leads to initiation of cracks.
- *Mechanical Wear and Tear* – this can be in the form of sliding wear and friction, low and high-stress abrasion etc. Such mechanical damage can result in denting, cracking and coating damage. Local dents often initiate crack, which under repeated loading continue to increase in size.
- *Interaction of different degradation mechanisms* - Corrosion and crack propagation can take place simultaneously. In corroded structures, crack propagation can be accelerated as the stress in the structure increases with material loss due to corrosion.

3.2.1. Degradation Mechanisms of Aged Structures

The main degradation mechanisms identified for aged iron structures are corrosion and fatigue cracking. Fatigue is due to the fluctuating nature of load and corrosion is primarily due to the environmental effects (DISSANAYAKE, P B and Karunananda, P A, 2008). Fatigue cracks can initiate in areas of stress concentration under repeated loading. Initial defects formed during construction of a structure can remain undetected for a long time and cracks may initiate from such defects, and propagate. Fatigue damage at a crack initiation site is influenced by many factors: (i) material properties, (ii) high local stresses, (iii) size of components, (iv) nature of stress variation and (v) environmental and operational factors (PAIK, J K and Brenman, F, 2006). Corrosion is the degradation mechanism that affects aged iron structures the most. The following sections detail the corrosion processes and models, which have been developed so far for remaining life prediction of iron structures.

3.3. Electrochemistry of Corrosion

Understanding how and why corrosion affects structures requires knowledge of electrochemistry of corrosion. This is beyond the scope of this thesis, but an overview of corrosion formation is presented. Corrosion is the deterioration of a material due to chemical interaction of the material with its environment. Corrosion reactions are electrochemical reactions. The corrosion process consists of an anodic and a cathodic reaction as described in (ROBERGE, P R, 2000). At the anode, iron loses electrons and goes into the electrolyte solutions as ferrous ions. At the cathode, the electrons released react with some reducible component of the electrolyte as shown in Figure 3-1. The anodic reaction takes the form of equation (3) and the cathodic reaction takes the form of equation (4).

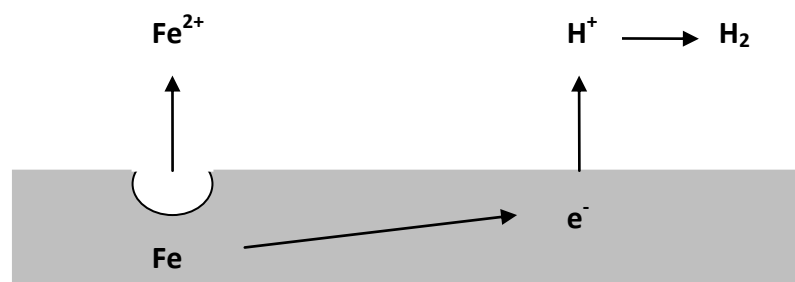


Figure 3-1: Anodic and Cathodic Reactions



The rates of anodic and cathodic reactions are equivalent according to Faradays' Laws and the rate is determined by the total electron flow from anode to cathode (AHMAD, Z, 2006).

3.3.1. Corrosion Rates

The corrosion rate (or rate of material loss) is expressed in equation (5) as the thickness loss of material per unit time. The equation takes the form

$$CPR = \frac{KW}{\rho At} \quad (5)$$

Where, CPR is the corrosion penetration rate, K is a constant (depending on system of units used), W is weight loss, ρ is density, A is the exposed area and t is the exposure time. Corrosion rate can also be defined as weight loss per unit time per unit area represented by equation (6).

$$w = \frac{IM}{nF} \quad (6)$$

Where, w is the weight loss per unit time per unit area, I is the current density, M is the molecular weight of reaction species, n is the number of electrons transferred and F is Faraday's constant.

3.3.2. Factors Affecting Corrosion Rate

Factors causing corrosion and affecting corrosion rate are numerous with some factors being more important in determining corrosion rates for particular types of corrosion. Some of the main factors are illustrated below:

- *Addition of acids* - Usually corrosion of a metal occurs in the presence of an electrolyte where positively and negatively charged ions move thus creating an electric

current. For some solutions, addition of acids or bases that can dissociate into ions can increase the current –carrying capability of the solution.

- *Variation in concentration of solutions* - Small variations affect the corrosion rate of metals.
- *Oxide layer* -The presence of an oxide layer will slow down corrosion rate as the oxide layer prevents the metal and the solution to be in contact. The uniformity and tenacity of the oxide layer matters as well.
- *Pressure* - Pressure can influence the solubility of oxygen, carbon dioxide, chloride and hydroxides in the solution such that more or less positively and negatively charged ions are available for flow of electric current.
- *Temperature* - Corrosion rate increases with increase in temperature. As a rule, reaction rate will double when the temperature rise doubles.
- *Relative humidity* - Corrosion rate usually increases with increase in relative humidity.
- *pH level* - Ph. level of solution can influence the corrosion rate of metals. For example, for pH values below four, ferrous oxide dissolves as it is formed rather than forming a layer on the metal and thus iron is in direct contact with the solution and thus corrosion rates are higher.
- *Surface of material* - The surface of a metal can affect corrosion rate in that non-uniform surfaces promotes initiation of local corrosion and the corrosion rate at these particular points is usually faster than the general corrosion rate.
- *Stimulation of anodic or cathodic reaction* - Ions such as chlorides will prevent the formation of protective oxide films on the metal surface thus increasing corrosion. Sulphur dioxide present in the atmosphere can dissolve in the thin film of moisture present on metal surfaces and the acidic electrolyte formed can stimulate both anodic and cathodic reactions.
- *Flow rate of water* - An increase in flow of water will increase the amount of oxygen available to the surface of the metal. Also increasing flow rate means any protective films will be removed faster, thus putting the metal in direct contact with any corrosive environment.
- *Oxygen content* - The higher the oxygen content the greater the corrosion rate.

- *Chloride content* - Corrosion rate can increase rapidly with present of chloride ions.
- *Pollution level* - Pollutant gases such as sulphur dioxides reacts with water to form sulphuric acid that is highly corrosive to iron.
- *Footfall* - More footfall could lead to increase in relative humidity.

3.4. Types of Corrosion

There are various forms of corrosion that can occur in metal structures as described in (AHMAD, Z, 2006) (BARDAL, E, 2003) (ROBERGE, P R, 2000) (SCHWEITZER, Philip A, 2007) (TRETHERWEY, K. and Chamberlain, J., 1995). The main forms of corrosion of concern for Cutty Sark structures are described below.

3.4.1. Uniform/General

Uniform corrosion is the most common form of corrosion with corrosion attack evenly distributed over the surface leading to relative uniform thickness reduction (BARDAL, E, 2003). As the electrochemical reaction occurs with equivalent intensity over the entire exposed surface, the rate of corrosion can be equated to the electron current flow between the anode and the cathode. While being the most common form of corrosion, it is not the most dangerous form of corrosion as the rate of uniform corrosion is more easily measurable than other more complex forms of corrosion.

3.4.2. Atmospheric

In atmospheric corrosion, a complex electrochemical process taking place in corrosion cells consisting of base metal, metallic corrosion products, surface electrolyte and the atmosphere (SCHWEITZER, Philip A, 2007). It depends on the following factors: relative humidity, temperature, sulphur dioxide content, chloride content, amount of rainfall as well as geographical location. Depending on the specific contaminants present and the material in consideration, all types of corrosion can occur. Atmospheric corrosion is considered a discontinuous process, as an electrolyte (usually water from rain, fog, dew or high humidity) is not always present. Thus, atmospheric corrosion only takes place during time of wetness (SCHWEITZER, Philip A, 2007). The corrosion rate is determined by the time of wetting, the frequency and duration of dry periods, relative humidity, temperature and temperature variation.

3.4.3. Galvanic

Galvanic corrosion occurs when two metals with different electrochemical potentials are in metal-to-metal contact in an electrolyte (AHMAD, Z, 2006). Due to the difference in potentials, current will flow from the anode to the cathode such that the less noble metal (the anode) will corrode faster than the more noble metal (the cathode). The galvanic series is used to determine which metal will corrode faster than the other, that is, which metal will behave as the anode and which metal as the cathode. Galvanic corrosion is present on the ship as part of the metal structures is made of both iron and muntz components.

3.4.4. Crevice

Crevice corrosion is defined in (TRETHERWEY, K. and Chamberlain, J., 1995) as corrosion attack which occurs because part of a metal surface is in a shielded or restricted environment, compared to the rest of the metal which is exposed to a large volume of electrolyte. This is likely to occur on the ship when the protection coating on the iron structures cracks and crevices form.

3.4.5. Pitting

Pitting corrosion is a form of localised corrosion in which small pits are formed. These pits usually penetrate from the top of a horizontal surface downward in a nearly vertical direction, thus preventing pitting being detected often until failure occurs (BARDAL, E, 2003). The extent and intensity of pitting corrosion is difficult to measure because the number and size of pits (diameter and depth) vary from region to region and within each region. Serious damage can be caused with even small loss of materials. The surface of a metal can affect corrosion rate in that non-uniform surfaces promotes initiation of local corrosion and the corrosion rate at these particular points is usually faster than the general corrosion rate. Thus, damage in small areas is more pronounced and has more serious effects on the overall strength of the material at these particular places.

3.4.6. Microbiologically Influenced (MIC)

MIC is corrosion promoted by microorganisms that can be found in both metals and non-metals. Microorganisms are living organism found almost everywhere in the environment and they can be divided into four main types, namely, fungi, algae, diatoms and bacteria

(TRETHERWEY, K. and Chamberlain, J., 1995). Microorganisms can affect corrosion behaviour in many ways as described in (ROTHWELL GP, 2006):

- By production slimes and deposits which give rise to crevice corrosion
- By creating corrosion conditions through their metabolic products or by destroying materials added to the system to provide corrosion inhibition
- By directly influencing the corrosion reactions

Given the right condition such as the appropriate temperature, pH level, water and food, the microorganisms will develop and grow in numbers. In general, microorganisms release chemicals in the environment of the metal concerned, thus changing the environment surroundings and creating optimum conditions for corrosion of the metal.

3.4.7. Corrosion of metal by Wood

Wood can release corrosive substances such as acetic acids, which are volatile leading to corrosion of metal near the wood. Different types of wood have different acetic acid content as illustrated in (NPL, 2006). The rate of formation of acetic acid depends on the temperature and moisture content of the wood while the rate of emission of the acetic acid depends of the shape of the wood structure concerned. The chlorine content of wood can also affect corrosion rate of metal. Wood structures near or within a marine environment will absorb a higher quantity of chloride that will accelerate of corrosion of metal parts in contact with the wood.

3.5. Deterioration Models for Corrosion

The thermodynamics and kinetics of corrosion control corrosion reactions. Thermodynamics gives an indication of the tendency of electrode reactions to occurs whereas corrosion kinetics addresses the rates of such reactions (AHMAD, Z, 2006).

3.5.1. Thermodynamics of Corrosion

Thermodynamics laws provide information on feasibility of a particular reaction, i.e. whether a metal will oxidize into its ions if the ions are of lower energy state than the pure metal. For the corrosion reaction to occur, the metal must surmount the energy barrier, which is also called the free energy of activation, which is represented by equation (7) (BARDAL, E, 2003):

$$\Delta G^{\circ} = -RT \ln K \quad (7)$$

Where, ΔG° is the free energy of activation at standard state parameters (i.e. 298K and 1 atm. Pressure), R is the universal gas constant, T is the absolute temperature and K is the equilibrium constant.

Energy changes during corrosion reactions can be measured as electrical potentials and flow of current such that electrical measurements can be used to measure rate of corrosion reaction. Work done is expressed in terms of potential difference and charge transported (Faraday's Law). Several methods are used to study the rate of a reaction involving the determination of the amount of reactants remaining in products after a given time (AHMAD, Z, 2006):

- The Pourbaix diagram shows a qualitative picture of what can happen at a given pH and potential, that is, whether the metal will corrode, form a passivating layer or be stable to corrosion (BARDAL, E, 2003).
- The Nernst equation relates the actual potential of an electrode, E , to the standard potential of an electrode, E_0 as a function of the concentrations of ions taking part in the corrosion reaction.
- The Butler-Volmer equation expresses the fundamental relationship between the current flowing and the applied voltage (JENKINS, T., 2007).

3.5.2. Mathematical Models for Corrosion Related Deterioration

Age related deterioration in aged structures is time-variant in nature. Several mathematical models for predicting time-variant corrosion related deterioration due to aging have been researched and developed (PAIK, J K and Brenman, F, 2006). Most of those models are time-variant empirical models developed through statistical analysis of corrosion measurement data for specific materials, environmental conditions and operational loading. However, corrosion is a complex process that is influenced by many factors and using statistical analysis of corroded structures alone is not enough to identify the key influencing factors.

To obtain prediction of corrosion, models based on corrosion mechanisms are required. Most corrosion models developed so far apply for uniform corrosion. These models are sometimes extended for pitting corrosion where pit depth and width are assumed random variables

following lognormal distributions (SADIQ, R et al., 2004). The most common and generic time-variant corrosion model is the Linear-Bilogarithmic law model (POURBAIX, M, 1982). It is an explicit model for the corrosion process, and is based on the decrease of corrosion rate over time. Several extended models of Linear-Bilogarithmic law model exist for particular metals and environmental conditions

3.5.3. Extended models of Linear-Bilogarithmic Model

The following subsections describe extended versions of the Linear-Bilogarithmic model taking into account various factors that affect corrosion rate.

3.5.3.1. Effect of time wetness, sulphur dioxide concentration and chloride concentration on corrosion

The growing oxide film in dry atmospheres usually protects the underlying metal from further corrosion following a logarithmic/power law. When exposed to rain, the metal may corrode but the rate falls when it dries. Thus, the factor commonly termed “time of wetness” is required as well as average temperature, average relative humidity and so on. In (GONZALEZ, J E and al, et, 2003), a modified version of the Linear-Bilogarithmic law was used for corrosion depth such as equation (8).

$$d(t) = t^a + 10^{(b(SO_2)+c(Cl^-)+d(TOW))} \quad (8)$$

Where a , b , c and d are constants, (SO_2) as concentration of sulphur oxide in mg/ (m² day), (Cl) as the concentration of chlorides in mg/ (m² day), and TOW as time of wetness (h/year). Such an equation is however of limited value due to the difficulties in determining the local conditions precisely.

3.5.3.2. Two phase corrosion model

This model consists of two phase (in the first phase rapid exponential corrosion growth and in the second a slow linear growth) as depicted in equation (9) (SADIQ, Rehan et al., 2004).

$$d(t) = at + b(1 - e^{-ct}) \quad (9)$$

Where a = constant (typical value: 0.009mm/yr), b = corrosion depth scaling constant (typical value: 6.27mm) and c = corrosion rate inhibition factor (typical value: 0.14yr⁻¹)

3.5.3.3. Corrosion Model for Carbon Steel and Copper Samples

Corrosion accelerates in presence of chloride ion such that the rate of deposition of chloride ion affects the rate of corrosion. The chloride deposition rate in turn depends on the cleaning effect of rain. Experiments have been carried out on plain carbon steel and copper samples at two atmospheric test stations in open environment: Havana in Cuba and Medellin in Colombia, which experience different amount and frequency of rain. Further details of the experiment carried out over the period of one year can be found in (CORVO, F. et al., 2005). The model proposed as a result of these experiments is one that extends the Linear-Bilogarithmic law for atmospheric equation. It incorporates the cleaning effect of rain in the determination of the acceleration rate of chloride ions and is represented in equation (10).

$$K = at^b [CL]^c (W/D)^d \quad (10)$$

Where K = mass loss; a , b , c and d = constants; $[CL]$ = chloride deposition rate; W = rainfall (mm); D = rainy days; t = time of exposure. The cleaning effect of rain is represented by the ratio W/D (amount of rain/ frequency of rain).

3.6. Consequences of Corrosion

In general, failure due to corrosion is a result of the electrochemical action of the corrosion on the material causing a loss of the material (in this case, metals) by dissolution or oxidation. Metals will usually react with elements from the environment to change from a high-energy state to a low energy state. Corrosion typically occurs at the surface of the material. In addition, localized attacks can lead to corrosion cracking as wet corrosion attacks metals selectively instead of uniformly. This can lead to failure much more rapidly as one part of a component loses material much faster than another adjacent part leading to cracks propagating steadily under a stress much less than the stress required in standard conditions. Corrosion also increases the rate of growth of fatigue cracks in most metals and alloys. Hence, fatigue strength of a material can be reduced substantially and thus failure will occur at relatively light loads and/or within shorter periods. Therefore, several properties of a structure are affected due to corrosion.

Some of these changes in properties can be monitored to determine corrosion rate for the structure and/or at particular locations for that structure. Some of the main consequences of corrosion on structures are illustrated below:

- *Reduction of metal thickness* - Decrease in metal thickness will lead to decrease in mechanical strength, which may then lead to structural failure. This is particularly dangerous in localized corrosion where only a small amount of metal loss can lead to structural failure of a component.
- *Loss of surface properties of materials* - Properties such as electrical conductivity, surface reflectivity or heat transfer can be affected by change in composition of the surface.
- *Appearance* - Appearance of a structure will change as its metallic surfaces corrode. Thus, the changing aesthetics of the structure will affect its appeal.
- *Safety* - The margin of safety for a system will change as corrosion damages the structure of the system.

3.7. Summary

While several degradation mechanisms affect aged structures, the main cause of deterioration in aged iron structures is corrosion. Thus for the PHM methodology developed, the diagnostic and prognostic tools will take into consideration mainly failures due to corrosion degradation mechanisms which affect the “health” of aged iron structures. For Cutty Sark, the main forms of corrosion affecting its structure are uniform, galvanic and pitting corrosion. The next chapter will detail the particular diagnostic and prognostic tools developed as part of the PHM methodology for aged iron structures using the Cutty Sark as the example application.

4. Developing a PHM Methodology for Aged Structures

4.1. Overview

For the PHM framework developed, one diagnostic tool and two prognostic tools have been developed. The diagnostic tool uses a data-driven method to perform precursor monitoring and anomaly detection. The first prognostic tool is developed using a model-driven method, which consists of a Physics-of-Failure model for corrosion related deterioration. The second prognostic tool, using a fusion approach, takes the information processed from the diagnostic tool and the first prognostic tool and provides updated remaining life predictions. The diagnostic tool and model-driven based prognostic tool are deterministic approaches towards detecting and predicting failure. The fusion based prognostic tool uses a probabilistic approach that incorporates the results from the two former tools as depicted in Figure 4-1.

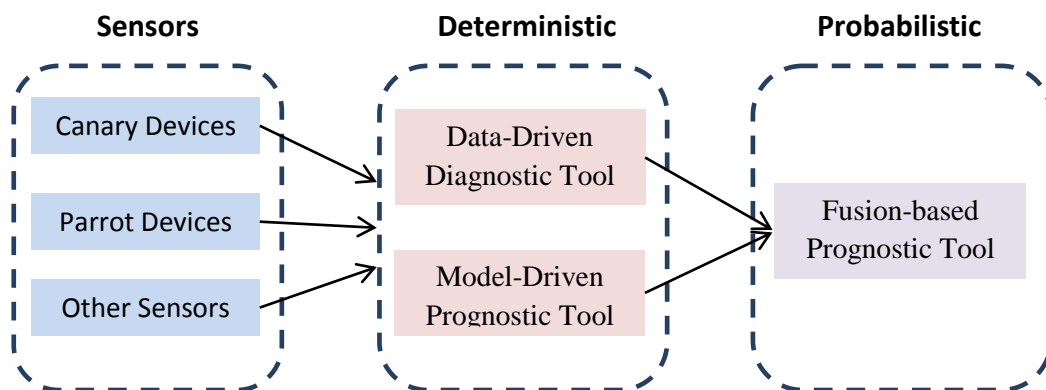


Figure 4-1: Use of Deterministic and Probabilistic Approaches within PHM

The PHM methodology developed combines the use of the diagnostic and prognostic tools as shown in Figure 4-2. The PHM methodology includes the use of canary and parrot devices (similar to canary devices but mimic actual rate of deterioration in a structure instead of developing an accelerated rate of deterioration as in canary devices) as well as other environmental sensors placed around the ship for data gathering. Thus, monitoring of performance, environmental and operational parameters is carried out where appropriate.

The diagnostic tool implements precursor monitoring and anomaly detection on the performance parameters to be carried out at regular intervals. Ideally, those parameters should be monitored throughout the lifetime of the iron structures to understand the status of their

health. Feature extraction is carried out on the monitored parameters of the healthy structure to create a training dataset representing healthy structures. Using Mahalanobis Distance (MD) as the anomaly detection algorithm, the performance parameters of the structure under consideration are then compared with the healthy training dataset for anomaly detection. Simultaneously, the remaining life of the structure is predicted through the model-driven prognostic tool using an appropriate PoF model (provided the failure definition is given). Information from the model-driven prognostic tool and the data-driven diagnostic tool is fed into a Bayesian Network model, which then processes the probability distribution of predicted remaining life of the structure.

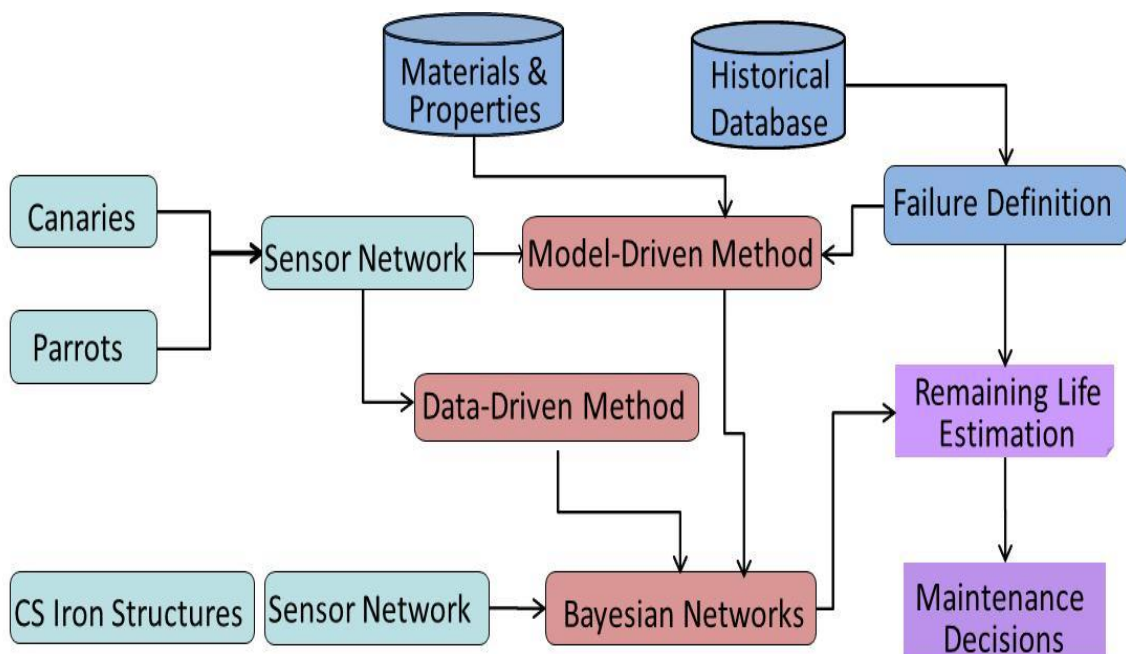


Figure 4-2: PHM Framework for Cutty Sark Iron Structures

Using the model-driven method alone to predict future health of a structure is not sufficient as the PoF models may fail to capture real life conditions which might not been accounted for but are still experienced by the structure during its lifetime. PoF models based on failure mechanisms due to corrosion usually contain a high degree of uncertainty due to the lack of understanding of the complex processes involved in the corrosion of iron structures.

The data-driven diagnostic tool delivers reliable results of anomaly detection when good training data is available but while data-driven algorithms such as Mahalanobis distance perform well in detecting anomalies, such techniques do not provide any prediction capabilities. Hence, a fusion approach using Bayesian Networks has been adopted with the

aim of developing a prognostic tool that can accommodate the initial lack of information and knowledge regarding the corrosion processes on the *Cutty Sark*'s iron structures and handling data uncertainty. The following four sections describe (a) the use of canary and parrot devices, (b) the data-driven diagnostic tool, (c) the model-driven prognostic tool and (d) the fusion-based prognostic tool.

4.2. Use of Canary and Parrot Devices

4.2.1. Overview

The methodology of using canary devices to give warnings to impending failures is adopted for the PHM framework of *Cutty Sark* iron structures, the main purpose of which is to provide an awareness of the onset of degradation mechanisms before any major failure of the iron structures occurs. Canary devices will therefore give advance warning of impending failures in the iron structures. These devices are used as it is difficult to use non-destructive inspection techniques (e.g. ultrasound, acoustic emission, etc) as corrosion-prone areas are often inaccessible or in hidden locations and care needs to be taken in handling the actual fabric of the ship for measurement purposes.

Canary and parrot devices will be used to gain valuable information on the behavior of similar iron structures in various different environmental conditions experienced within the ship. Along with canary devices, parrot devices representing miniature systems of the iron structures with the same mechanisms of failure and within the same environmental conditions are also used. The main reason for using parrot devices as well as canary devices is that it is not possible to carry out direct measurements and monitoring on the actual iron structures due to risk of damaging structures of great historical value within *Cutty Sark*.

4.2.2. Purpose of Canary and Parrot devices

The main objective of the use of canary and parrot devices is to provide an indication of the failure of the structures in the short and long term. To that end, strong correlations between the canary devices, parrot devices and iron structures need to be developed. The acceleration factors between the canary and the parrot devices will be identified in the beginning and these will be updated, as new data on corrosion damage from the devices becomes available. The parrot devices will in turn be calibrated to the actual failure levels of the iron structures. Thus, a sound understanding of the corrosion damage occurring within the canary and parrot devices

and the iron structures is necessary to enable accurate corrosion predictions. An example form of acceleration factor (AF) between a canary and a parrot device is shown in equation (11).

$$AF_{(time=t)} = \frac{(Material_loss_{canary})_{time=t}}{(Material_loss_{parrot})_{time=t}} \quad (11)$$

Figure 4-3 illustrates the initial concept of how canary and parrot devices can be used to perform predictions. A canary device and a parrot device are both monitored for percentage of material loss. Given the acceleration factor between the canary and the parrot is known, when the canary device fails at time t, it can be calculated when parrot device will fail (i.e. when iron structure of ship will fail). One point to be noted is that the predictions and acceleration factors will be updated when new data for canary and parrot device is acquired, thus increasing the accuracy of the predictions as shown by the probability distributions on the graph below.

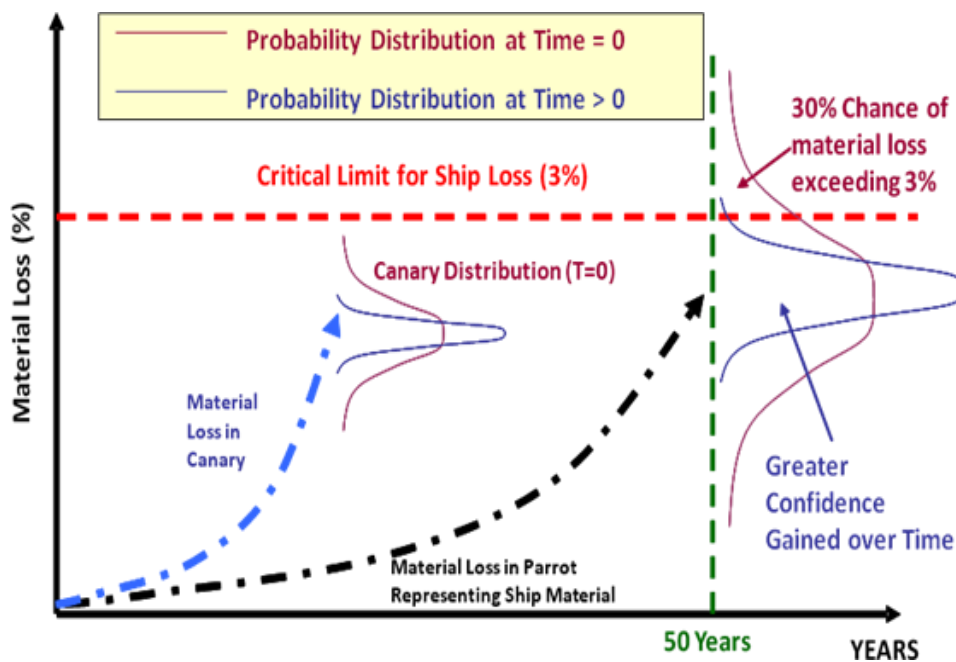


Figure 4-3: Material Loss Prediction Using Canary and Parrot devices

4.2.3. Design of Canary and Parrot Devices

The canary devices will be designed to include the same mechanisms (at an accelerated speed) that can lead to failure in the actual iron structures. Here failure is mainly due to corrosion of iron structures, but the different parts of the iron structures are subjected to different types of corrosion and the environmental conditions for the iron structures differ

within the ship. The degradation of the canary devices will be assessed using accelerated testing and the degradation levels will be calibrated and correlated to the actual failure levels of the iron structures.

Measurement for environmental factors for the canary devices will also be carried out with the aim to understand the effect of changes in environmental conditions on the different degradation mechanisms of the iron structures. Canary devices are designed to fail faster than the actual system, while parrot devices are designed to represent the actual Cutty Sark wrought iron components. In general, the dimensions of the parrot devices are slightly bigger compared to their respective canary devices to ensure a smaller area-to-volume ratio and hence less corrosion penetration. Currently, the design of the canary and parrot devices has not yet been finalised. However, the design characteristics of the devices as well as other factors related to the use of canary and parrot devices within a PHM framework for Cutty Sark have been set out. The different types of canary and parrot devices proposed are for monitoring:

- corrosion of iron structures
- different environmental conditions present within the ship.
- degradation mechanisms due to bacterial attack of iron, abrasion and other degradation of protective coatings

The main factors taken into account for the design of the Canary and Parrot devices are as follows:

- Location within the ship
 - Locations with harshest environments which would create best environment for corrosion
 - Locations that are not easily accessible for visual inspections and other regular monitoring of corrosion damage.
 - Different locations within the ship will experience different varying environmental conditions and therefore should be analysed separately.
- Types of corrosion to be monitored
 - Uniform Corrosion

- Atmospheric Corrosion
- Crevice Corrosion
- Pitting Corrosion
- Types of structures on which canary/parrot devices will be based on
 - Structures which are hidden within other structures thus hard/impossible to reach for any visual inspections or monitoring
 - Frequency of measurements of environmental and performance factors

The main differences between Canary and Parrot devices are as follows:

- Canary devices will be smaller structures and will thus be more reactive than bigger parrot devices
- Parrot should not be new teak or iron and should have undergone a certain amount of corrosion enough to mimic the ship's original fabric.
- Parrots devices will be painted with no moisture allowed whereas canary devices will be painted but will allow moisture in through gaps and flaws
- Canary devices will be immersed in chlorine solution while parrot devices will not undergo such treatment.

Table 4-1 shows a summary of the material and treatment of materials initially envisaged as well as a list of possible corrosion damage parameters and corrosion causes.

Materials/Treatment of materials	Measurements
1 Dry iron filings and salt in a paint system capsule	<ul style="list-style-type: none"> ● Corrosion damage parameters (performance metrics)
2 Pre-corroded and cleaned mild steel samples coated with the paint system	<ul style="list-style-type: none"> ● Weight change ● Electrical Resistance ● Dilation
3. A mild steel bolted joint assembly with variants:	<ul style="list-style-type: none"> ● Dimension changes

<ul style="list-style-type: none"> • Clean interfaces coated with the paint system • Dry salt contaminated interfaces coated with the paint system • Wet salt contaminated surfaces coated with the paint system 	<ul style="list-style-type: none"> • Appearance changes • Surface hardness/roughness • Linear Polarisation Resistance • Corrosion causes (environmental factors) • Relative Humidity • Temperature • Cracking of paint • Chloride concentration
<p>4 Timber to detect:</p> <ul style="list-style-type: none"> • fungal attack • bacterial attack 	
<p>5 Oak and iron sample together and pre-soaked.</p>	

Table 4-1: Canary and Parrot Design Characteristics

4.2.3.1. Preliminary designs of Canary and Parrot Devices

Figure 4-4 and Figure 4-5 show two different pairs of Canary and Parrot devices to be used in experimental trials on Cutty Sark. The canary device is an iron wire secured with plastic bolts and the parrot device is two iron sections bolted together using plastic bolts (Figure 4-4). In Figure 4-5, the iron wire in the canary device is sandwiched between two wood sections and the iron section in the parrot device is bolted to a wood section using plastic bolts. These pairs have been designed with a view of representing the different types of corrosion on the different types of iron structures present on Cutty Sark. These Canary and Parrot pairs can be placed in locations experiencing different environmental conditions within the ship. Measurements will be carried out on a monthly basis for the first set of the Canary and Parrot pairs, every six months for the second set of the Canary and Parrot pairs and after one year for the third set of the Canary and Parrot pairs. Several more Canary and Parrot pairs have been designed for trials on Cutty Sark at a later stage and are shown in appendix section 9.1.

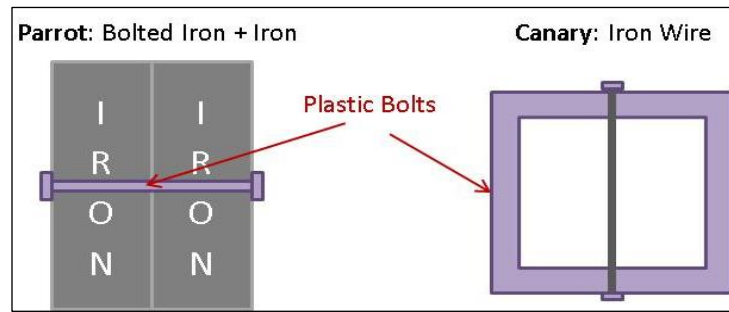


Figure 4-4: Parrot and Canary Device Pairs (a)

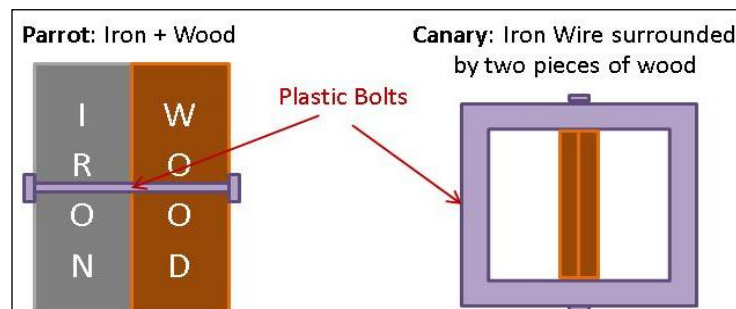


Figure 4-5: Canary and Parrot Device Pairs (a)

4.3. Model Driven Prognostic Tool: Remaining Life Prediction using PoF Model

4.3.1. Failure processes affecting iron structures

The degradation of the iron structures of the ship is mainly due to corrosion. Therefore, the Physics-of-Failure model used for the prognostic is mostly based on corrosion models. Corrosion leads to loss of strength and can ultimately cause structural failure.

The four different types of corrosion occur under different conditions and depend on the following deviations as stated in (BARDAL, E, 2003):

- The design (macro-geometry of the metal surfaces)
- The combination of metal and environment
- The state of the surface (e.g. cleanliness and roughness)
- Other deterioration mechanisms.

4.3.2. Model-Driven Method: Physics of Failure Models for Corroded Iron

Physics of Failure approach (PoF) utilises knowledge of the life-cycle load profile and material properties of a structure and architecture to identify potential future failure mechanisms. The PoF methodology aims to do prognostics by first calculating the cumulative damage accumulation due to various failure mechanisms within a particular environment of a system and then analyses this information to give predictions of remaining service life of the system. The Physics of Failure model used for Cutty Sark iron structures is based on mainly corrosion models.

The following factors can be considered as the input parameters for corrosion based PoF models of Cutty Sark structures:

- Environmental Loads
- Relative Humidity
- Temperature
- Chloride Ion Concentration
- External Support Structure
- Operational Loads
- Footfall
- Material Properties
- Geometry
- Architecture

Ideally, PoF models for Cutty Sark would incorporate most of the environmental and operational loads mentioned. However there are few such models which have been investigated and developed to date for wrought iron structures (STRAUB, Daniel, 2004), (MELCHERS, R. E., 1999), (MELCHERS, R. E. and Jeffrey, R. J., 2008). Hence, the generic “Linear Bi-logarithmic Law” for atmospheric corrosion (POURBAIX, M, 1982) is used as a starting point for the PoF model for Cutty Sark iron structures.

4.3.2.1. PoF model: Linear Bilogarithmic Law

The Linear Bilogarithmic Law represents corrosion rate as a function of time based on the understanding that the build-up of corrosion products tends to reduce the corrosion over time. The law is expressed as shown in equation (12).

$$P = At^B \quad (12)$$

Where P is corrosion penetration, t is exposure time, A is corrosion rate during the first year of measurement and B is a constant representing a measure of long-term decrease in corrosion rate.

A generic approach to implementing the Linear Bi-logarithmic law as a PoF model would involve the following steps:

- Obtain initial values of corrosion penetration from experimental trials (under normal environmental and operational loads) over the 1st year.
- Determine A & B , using linear regression on $\ln(P) = \ln(A) + B\ln(t)$
- Define failure in the test structure as corrosion penetration being more than $x\%$ of initial depth of structure, D .
- Calculate remaining life using $t = e^{(\ln(0.03*D) - \ln A)/B}$
- From 2nd year onwards, the model can be updated as new measurements become available.

According to Pourbaix, this law is valid for extrapolation of up to 20-30 years (POURBAIX, M, 1982). However, for such long periods, environmental conditions are likely to change making the corrosion penetration prediction unreliable with time.

4.4. Data Driven Diagnostic Tool: Anomaly Detection using Mahalanobis Distance Analysis

4.4.1. Overview

Prediction of remaining life using PoF methodology is usually accompanied with uncertainties due to inaccuracy of the model itself, inaccuracy in measurement processes and

varying environmental and operational loads, which might not have been taken into account in the model. During normal operation, all “health” parameters follow a similar pattern, however in presence of a fault that might lead to a failure, these parameters would usually increase in proportion to the magnitude of the fault. Hence, it is important to monitor “health” parameters of the real structure under operation and precursor monitoring becomes an essential tool in determining the current “health” of a system and providing an indication of any change on predicted remaining life.

4.4.2. Precursor Monitoring

As described in chapter 3, the term precursor defines a “health” parameter, which is a measurable variable of which significant changes can be associated with a forthcoming failure. For example, an increased corrosion penetration rate and material loss would suggest impending structural failure due to decreased strength of the component. Failures can then be predicted by using a causal relationship between a measured variable that can be correlated with subsequent failure.

For the scope of this project, the following precursor variables have been identified: weight change, dimension change and electrical resistance. Feature extraction was carried out on the precursor variables; the average value, maximum value and minimum value were computed for a certain amount of readings of the precursor variables at a time. Feature extraction was needed in order to capture changes that are not visible using the real data only. Then an anomaly detection algorithm is developed to correlate the change in the precursor variable with the impending failure. The anomaly detection algorithm developed for the PHM framework developed uses Mahalanobis Distance (MD).

4.4.3. Theory of Mahalanobis Distance

Mahalanobis Distance (MD) is a distance measure based on correlation between two or more variables in multi-dimensional space from which patterns can be identified and analysed. It is used to distinguish the pattern of a certain group from other groups (TAGUCHI, Genichi et al., 2000). Using Mahalanobis Distance, multidimensional data obtained from sensors for various performance factors can be reduced to univariate data to represent anomaly from a system. Here the Mahalanobis distance technique is used to measure the degree of health of

an iron structure by processing all multidimensional measurement data available (i.e. dimension change, weight change, and electrical resistance).

A Mahalanobis space is created which is centred on the typical performance variable values representing a healthy structure. Any deviation in the performance variables is then determined by the distance from the centre point. Threshold values are determined by extensive testing of the system that generates “healthy” performance data. Mahalanobis distance values greater than these threshold values then indicate possible failure in the structure. The Mahalanobis Distance takes the form of equation (13):

$$D^2 = (x - m)^T C^{-1}(x - m) \quad (13)$$

Where D^2 is Mahalanobis distance, x , vector of data from sensors for observed parameters, m , vector of mean values of independent variables from training set and C^{-1} , inverse covariance matrix of independent variables from training set.

The health of an iron structure is defined by several performance parameters. Each parameter in each vector is standardized by subtracting the mean of the parameter and dividing it by the standard deviation. These mean and standard deviation are calculated from the data collected for normal or healthy structure. The MD values are calculated for the healthy group. These MD values define the Mahalanobis space, which is used as a reference set for the MD measurement scale. Then, the MD values for the test structure are calculated after the parameters are standardized using the mean and standard deviation for normal-group. The resulting MD values from test system are compared with the MD values of the healthy system to determine test structure's health.

4.4.4. Mahalanobis Distance Analysis of Precursors for Cutty Sark Iron Structures

The methodology used to carry out MD analysis of precursors for iron structures is depicted in Figure 4-6. The following steps are performed to find the MD value to determine the current health of an iron structure/device:

1. Generate baseline for healthy behavior - experiments are conducted on healthy structures within the range of environmental and operational conditions the structure is assumed to experience.

2. Perform feature extraction on performance parameters to select features providing meaningful data.
3. The data from selected features is normalised with the mean and standard deviation of the data. This is done by reducing the data by its original mean and dividing the data by its original standard deviation respectively.
4. Once normalised values are obtained, two healthy datasets are created: Dataset A and Dataset B. The Matlab mahal function is then used to generate MD values with Dataset A used as the reference sample and Dataset B used as the health observations for which MD values are generated.
5. A MD threshold value is determined based on the MD values obtained for Dataset B.
6. Perform MD analysis on test structures
7. Test structures are subjected to similar tests as for the healthy structures, data from the same performance parameters is collected, and the same features are extracted as in step 1.
8. Each observation in time of the test data is then normalised using the mean and standard deviation of the healthy data.
9. Once normalised values are obtained, the test Dataset C is created from those values. The Matlab mahal function is then used again to generate MD values for Dataset C with Dataset A used as the reference sample again.
10. The MD values of the test dataset are compared with the threshold MD value. MD Values higher than the threshold MD value would indicate an anomaly in the system.

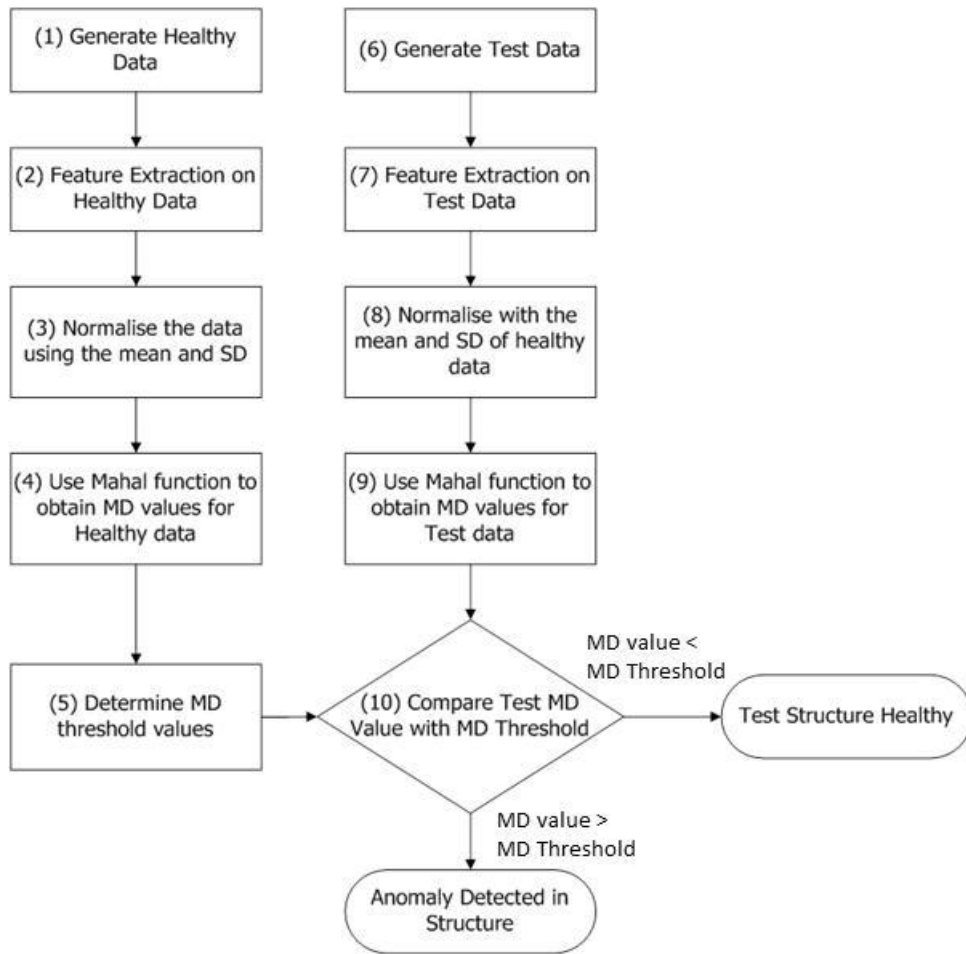


Figure 4-6: Mahalanobis Distance Analysis Methodology

4.5. Fusion Approach: Bayesian Network Models

4.5.1. Introduction

A Bayesian network is a probabilistic graphical model that represents a set of variables and their probabilistic independencies and it is based on an approach of probability theory by Thomas Bayes (BROMLEY, J et al., 2004). A certain degree of uncertainty in the prediction of remaining life from PoF models for corrosion prevails due to the lack of understanding of the complex processes involved in corrosion of iron structures. Calibration of the canary and parrot device pairs is also a challenge while precursor monitoring and anomaly detection require good training data to deliver reliable results of anomaly detection. Bayesian network is used here as a fusion approach within the PHM framework in order to obtain more accurate prediction of remaining life for the iron structures.

Within this framework, prediction of remaining life using PoF models and anomaly detection through precursor monitoring is carried out as described in the previous sections. The

information output from these models is then used as input data to the Bayesian network models developed. Bayesian Network models help to coherently integrate causes leading to a failure as well as the evidence of the effects of that failure and handles uncertainty in prediction of remaining life within a rigorous mathematical approach.

4.5.1.1. Baye’s Rule and Bayesian Networks

A Bayesian network model consists of three elements:

1. A set of nodes - representing the system variables where each node has a finite set of mutually exclusive states.
2. A set of links/arcs – representing the cause and effect relationships between the nodes
3. A set of conditional probability tables - expressing the probability of a node being in a particular state given the states of other connecting nodes.

Bayesian networks operate by propagating beliefs using Bayes’ Rule from equation (15) through the network once some evidence about that state of certain nodes can be asserted. When evidence of a node is confirmed, this belief is propagated upwards in the network by calculating posterior probabilities of the evidence of all other nodes connected to the confirmed node. Thus, the current belief in the evidence of all the nodes in a network can be computed, given knowledge of the evidence of a few of the nodes and the relationships between them.

$$P(A|B) = \frac{P(B|A)P(A)}{P(B)} \tag{15}$$

Where $P(A)$ is the prior belief (i.e. initial uncertainty in A), $P(A/B)$ is the posterior belief (i.e. the uncertainty having accounted for evidence B), $P(B/A)$ is the likelihood and $P(B)$ is the marginal likelihood. Assume A is a variable with n states a_1, a_2, \dots, a_n , then $P(A)$ denotes a probability distribution over these states as shown in equation (16).

$$P(A) = (x_1, x_2, \dots, x_n); x_i \geq 0 \quad (16)$$

Where x_i is the probability of A being in state a_i . This can be written as $P(A = a_i) = x_i$ or $P(a_i) = x_i$, e.g. $P(\text{Age} = \text{new}) = 0.2$.

The Bayesian network treatment of certainties in causal networks makes use of conditional probabilities. If variable B has m states b_1, b_2, \dots, b_n , then $P(a / b) = x$. The probability $P(A/B)$ implies an $n \times m$ table including the probabilities $P(a_i / b_j)$. Table 4-2 shows an example of $P(a_i / b_j)$, where $1 \leq i \leq 2$ and $1 \leq j \leq 3$. The columns sum to one.

	b_1	b_2	b_3
a_1	0.1	0.6	0.2
a_2	0.9	0.4	0.8

Table 4-2: Conditional Probability Table for Variable A

4.5.1.2. Advantages/Reasons for choosing Bayesian Networks

Bayesian statistics has many benefits for decision-making problems as usually decision-making are hard due to lack of knowledge and uncertainty about relevant parameters for a model. Bayesian Statistics allows for the quantification of uncertainties using subjective probability. Predictions can be made based on initial available data (objective and subjective) and are updated as new data is acquired. Bayesian methods use all relevant available information and not just knowledge from data only. Bayesian techniques are used to obtain estimations by combining subjective data and observed data right from the start even with only a small set of observed data available. Additionally, Bayesian networks can incorporate variables of any kind (i.e. physical, economic, social or any other type).

For the case of Cutty Sark, historical data is difficult to obtain and accurate models of corrosion of the iron structures for the current environmental conditions of Cutty Sark is not available. Thus, information from other sources needs to be incorporated to be able to form a data set from which predictions can be made. This information can come from experts in the

field or visual inspections of the structures. Using Bayesian networks, simple causal graphical structures can be built to represent the system under investigation and this can be extended and modified later with relative ease as more knowledge is gathered.

4.5.2. Bayesian Network Model Development Process

The development process followed for Bayesian network models for the PHM framework is shown in Figure 4-7 and can be broken into five general steps:

1. Developing the structure of the model – the model variables, nodes and arcs are specified
2. Parameterising the model (qualitative and quantitative) – the states for the nodes are assigned and the conditional probability table of the nodes are defined and parameterized using a combination of methods
3. Evaluation of the model and testing scenarios – this involves assessing the model to check if the model is representing the right information and producing the expected results
4. Reasoning on the model – this entails propagation of beliefs and updating the probability distribution of remaining nodes
5. Updating the model – this can comprise either updating the model structure or updating the CPTs or both when more learning data and knowledge becomes available

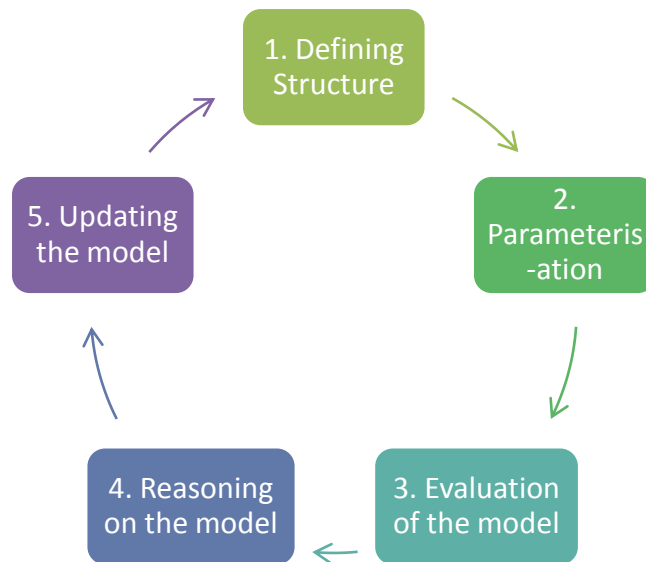


Figure 4-7: Development process used to build a Bayesian network model

4.5.3. Bayesian Network Model for a small structure

This section demonstrates the development of a Bayesian network development for a small structure following the development process described in the previous section. Let us consider building a small Bayesian network model to predict the presence of corrosion in an iron structure. Many factors can be taken into account such as the environmental conditions, the age of the structure, etc. These are represented in a Bayesian Network model connected by directed links based on the cause/effect relationships of the nodes. In Figure 4-8, the variables *humidity* and *age* have an impact on the variable *corrosion*, meaning the presence of *corrosion* can be determined by the states of *humidity* and *age*. The states of each variable can take different types of discrete values. Here the variable *humidity* is represented by intervals (i.e. 0%-30%, 30%-100%). The variable *age* has states that take ordered values *new*, *intermediate*, and *old* and the states of the variable *corrosion* are represented by ordered values *yes* and *no*.

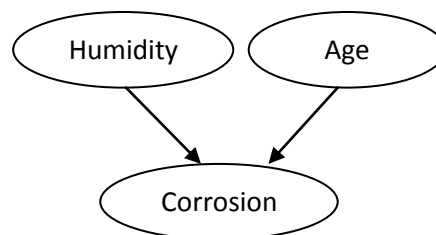


Figure 4-8: Small BN model for corrosion damage

In Figure 4-8, the variable *Corrosion* has two parents: variables *Humidity* and *Age*. The latter two variables do not have any parents. The joint probability distributions for the variables are defined as $P(\text{Corrosion} \mid \text{Age}, \text{Humidity})$, $P(\text{Humidity})$, and $P(\text{Age})$. These probabilities can be either determined by an expert or extracted from a data set. Since the variables *Humidity* and *Age* have no parents, their prior probabilities can be simply specified as follows:

- $P(\text{Humidity} = \text{"0-30"}) = 0.7$ and $P(\text{Humidity} = \text{"30-100"}) = 0.3$
- $P(\text{Age} = \text{new}) = 0.2$, $P(\text{Age} = \text{intermediate}) = 0.6$, and $P(\text{Age} = \text{old}) = 0.2$.

The variable *Corrosion* has two states and two parents, one with two states and one with three states. The conditional probability distribution of variable *Corrosion* can be shown as on Table 4-3. The *yes* and *no* label in the first column are the states of variable *Corrosion*.

Humidity	0% - 30%			30% - 100%		
Age	new	intermediate	Old	new	intermediate	old
yes	0.1	0.4	0.4	0.3	0.5	0.9
No	0.9	0.6	0.6	0.7	0.5	0.1

Table 4-3: CPT for Corrosion node

Bayesian networks can be conditioned on any subset of their variables, supporting any direction of reasoning. Thus, any variable may be query variables or evidence variables. Figure 4-9 shows the Bayesian network at initial stage with no evidence input on any node. Whenever new information is acquired, new beliefs can be calculated. Suppose that humidity is within the 30% to 100% range and the age of the structure is old, then $P(\text{Humidity} = \text{"30-100"}) = 1.0$ and $P(\text{Age} = \text{old}) = 1.0$. They are shown in Figure 4-10 as percentages (100.00 and 00.00) with red colors. This kind of probabilities is referred to as evidence. When new evidence is applied to a Bayesian network, the beliefs on the other variables may change. This is also called belief updating. This is shown in Figure 4-10 and Figure 4-11 where the probability distribution on the *Corrosion* node changes depending on the evidence input on *Humidity* and *Age* nodes.

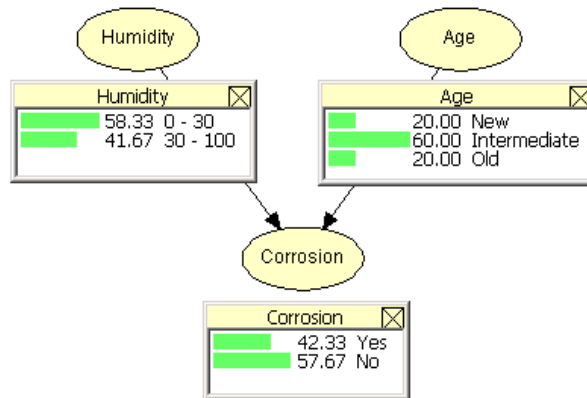


Figure 4-9: Bayesian Network with no evidence input

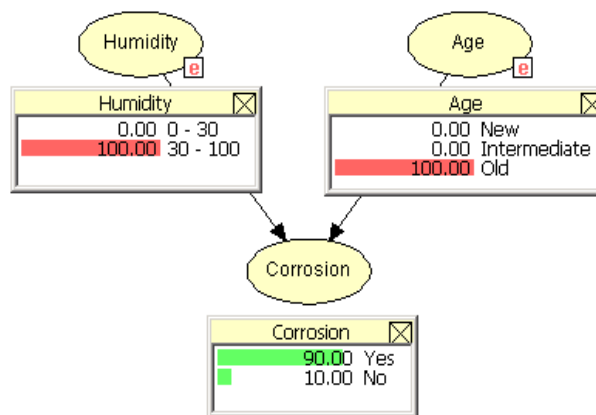


Figure 4-10: Bayesian network with evidence input on Humidity and Age nodes

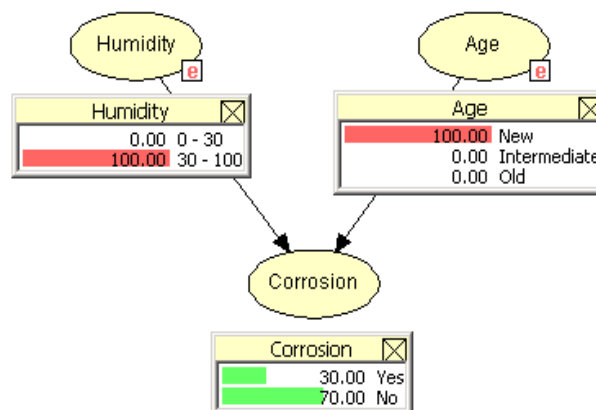


Figure 4-11: Bayesian network with different evidence input on Age node

The evidence that humidity is 30-100 and age is old, increases the belief on corrosion to 90% in Figure 4-10 while the evidence that humidity is 30-100 but age is new in Figure 4-11 decreases the belief on corrosion to 30 %.

4.5.4. Bayesian Network Model for Fusion-based Prognostics tool

4.5.4.1. Development of Bayesian Network Model

Although a lot of research has been carried out on deterioration of iron structures, the results and knowledge from these research projects is not directly applicable to the case of Cutty Sark (YUANTAI, 2008) (MANDENO, W L, 2008) (STRAUB, Daniel, 2004). These research projects are usually carried out using specific materials as example and the knowledge gained is mostly only applicable for particular structures and scenarios. Due to the complexity of corrosion processes, the corrosion rates for different materials differ. The environmental conditions can affect the corrosion rates significantly even for structures made of the same material. Also for various reasons, observation data is often not easily acquired and usually input data from other structures cannot be reused due to the particularities of each structure. Thus for the development of the Bayesian network model for the PHM framework, subjective inputs from industry experts are usually required as well as observation data to be able to run models and simulations for the deterioration of an iron structure for example.

The Bayesian network model developed is organised in a layered structure with the top layer representing the prediction of remaining life of the system under consideration, the middle layer representing the diagnosis and prognosis observations of the structure and the bottom layer representing usage and health observations with the nodes in the different layers connected by causal links. This approach is similar to that described in (PRZYTULA, K W and Choi, A, 2007). Here, Bayesian network's ability to link different types of information whether it is coming from empirical or physical models into a single probabilistic graphical model is used to develop this Bayesian network model.

The initial structure (i.e. the whole Cutty Sark ship) is decomposed into sub-structures and a Bayesian Network model is developed for each substructure. The submodels then integrate to make a complete model. Figure 4-12 shows the initial Bayesian network model, where factors influencing the remaining life prediction and the performance factors indicating current "health" are represented in different layers and arcs are used to represent the relationships.

This initial model while aiming to be as comprehensive as possible with regards to representation of causes and effects of corrosion on iron structures was deemed unfeasible to model due to lack of knowledge and data required to model all the particular nodes.

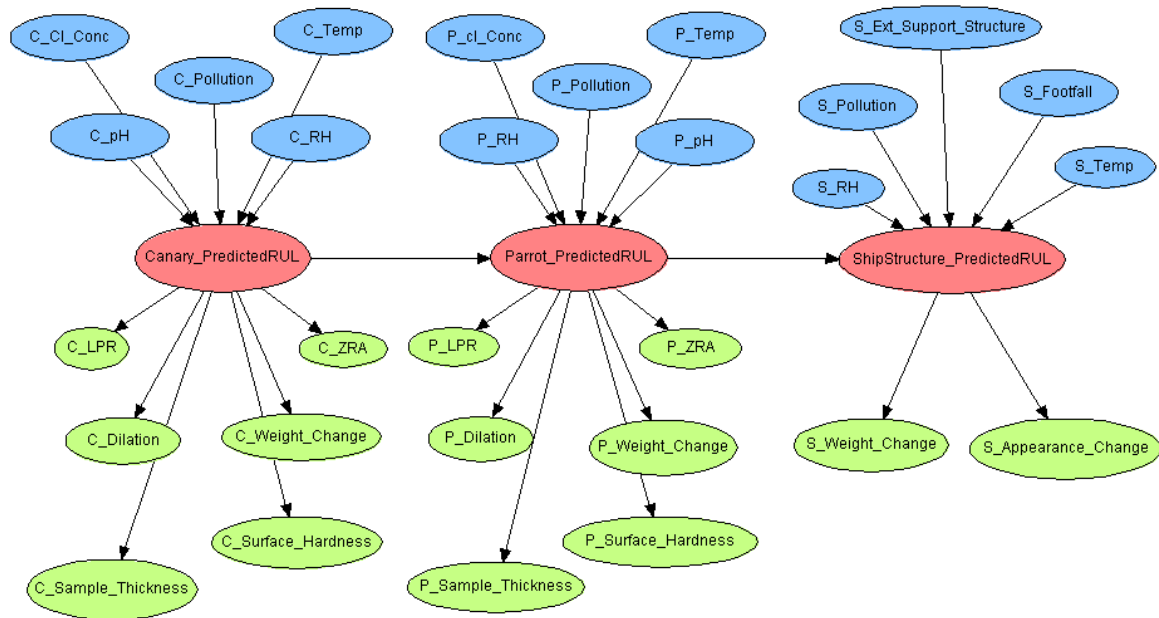


Figure 4-12: Conceptual Bayesian Network for Cutty Sark

Figure 4-13 shows a modified version of the Bayesian network model for Cutty Sark iron structures. Remaining life predictions from PoF models for canary (C_{PoF_RUL}) and parrot (P_{PoF_RUL}) devices provide input for the top layer nodes representing the causes of failure. The bottom layer nodes represent the anomaly detection results for canary ($C_{MDValues}$) and parrot ($P_{MDValues}$) devices using Mahalanobis Distance analysis, thus representing the effects of failure as well as usage and health observations (*Visual Inspection*). The nodes in the middle layer represent the diagnosis and prognosis for the canary ($Canary_PredictedRUL$) and parrot ($Parrot_PredictedRUL$) device as well as that of the ship iron structure ($ShipStructure_PredictedRUL$). Two additional nodes representing time are included into the model to account for the point in time at which the model is run (C_{Time_Period} for the canary and P_{Time_Period} for the parrot devices). Evidence on these two nodes will always be provided when reasoning using the network as such information should always be available. The nodes across the layers are linked together such that evidence recorded for one of the nodes will result in a belief updating of all the nodes connected to it. The links between nodes ' C_{PoF_RUL} ', ' $Canary_PredictedRUL$ ' and ' $C_{MDValues}$ ' mean that the prediction of remaining life of the canary device using PoF models will affect the failure prediction of

the canary device which in turn affects the MD value obtained from the MD analysis of failure precursors of the canary device. The node ‘*Canary_PredictedRUL*’ links to node ‘*Parrot_PredictedRUL*’ that in turn links to node ‘*ShipStructure_PredictedRUL*’. This is to represent the correlation between failure rates in canary device, parrot device and the ship structure under consideration. This approach allows for predictions of health of components for which damage can be observed directly as well as predictions of health that can be made indirectly using information about usage loads and environmental conditions.



Figure 4-13: BN Network

The information required to build the Bayesian network model can be broken into two parts: (1) the structure, which is defined using knowledge of the system and the diagnostic and prognostic observations that can be made and (2) the parameters, which are defined from the data being collected from laboratory experiment, and field use. Data gathering for building Bayesian Networks is very flexible and essentially two main techniques are used to build a Bayesian network model:

- Expert Knowledge - manually build graphical structure of the network, identify, and populate the conditional probability table based on expert’s knowledge of system.
- Learning Analysis - Graphical structure of the network and the conditional probability table are both obtained from experimental data.

For our case, a mixture of both approaches is used. The structure of the Bayesian network was devised after acquiring knowledge from engineers, corrosion experts, preservation experts as well as information obtained from literature. Then the initial set of probability of values is based on existing measurements from sensors, historical information for relevant parameters of appropriate corrosion models and subjective information from the domain experts. The next section details the populating of the conditional probability tables of the nodes in the Bayesian network model described above.

4.5.4.2. Parameterisation: States definition and Populating CPTs

The parameterisation of a Bayesian network model can be broken into two stages: (1) defining the states of each node and (2) populating the Conditional Probability Tables (CPTs) for the node. States of a node can be categorical, continuous or discrete. The states of each node must be mutually exclusive and exhaustive, that means the variable must take on exactly one of these values at a time. The states of all the nodes for the Bayesian Network model built for the PHM framework are defined to be either categorical or discrete. The states for each node are presented in the table below.

Nodes	States
Canary_PoF_RUL	Intervals $([-\infty, 0], [0, 1], \dots, [5, \infty])$ representing the 5 year lifetime of a canary device.
Canary_PredictedRUL	Intervals $([-\infty, 0], [0, 1], \dots, [5, \infty])$ replicating that of node Canary_PoF_RUL.
Parrot_PoF_RUL	Intervals $([-\infty, 0], [0, 1], \dots, [20, \infty])$ representing the 20 year lifetime of a parrot device
Parrot_PredictedRUL	Intervals $([-\infty, 0], [0, 1], \dots, [20, \infty])$ replicating that of node Parrot_PoF_RUL.
ShipStructure_PredictedRUL	Intervals $([-\infty, 0], [0, 1], \dots, [20, \infty])$ replicating that of node Parrot_PredictedRUL
Canary_MDValues	Intervals $([-\infty, 0], [0, 1], \dots, [15, \infty])$ representing the typical MD values expected during operation.
Parrot_MDValues	Intervals $([-\infty, 0], [0, 1], \dots, [15, \infty])$ representing the typical MD values expected during operation.
C_Time_Period	Discrete values [1, 5] representing the period the canary device is expected to be in operation.
P_Time_Period	Discrete values [1, 20] representing the period the parrot device is expected to be in operation.
Visual_Inspection	Order values [1, 5] representing the severity of damage detected on structures during visual inspection.

Once the states of the nodes are defined, the relationship between the nodes is developed. This relationship is defined using conditional probability tables (CPTs). A CPT quantifies the probability of a node/variable being in a particular state, given the states of its parent nodes. The probabilities are derived from (1) direct elicitation of scenarios from expert, (2) data obtained from PoF model and anomaly detection and (2) equations used to describe relationships between the nodes. The CPTs for nodes '*C_PoF_RUL*' and '*P_PoF_RUL*' represent the unconditional probability distribution of predicted remaining life from the PoF models taking into account the factors influencing the remaining life prediction for the canary and parrot devices. Nodes without parents have an unconditional distribution defined for their CPTs. For nodes with parents (child nodes), the probability distribution of their states will depend on the state in which the parent nodes are. For example, the CPT for node '*Ship_Visual_Inspection*' depends on the state of node '*ShipStructure_PredictedRUL*'. The Bayesian network model was built with as few nodes as possible and minimal interaction amongst the nodes in order to reduce the amount of conditional probabilities to be specified.

It should be noted that so far, the preliminary parameters and CPTs have been derived from published literature, current understanding of the system and input from the PoF model and MD analysis. Further development of the model would involve an iterative refinement process, which would include expert elicitation as well as any information available from experimental or field results. As the CPTs of the Bayesian Network models for the demonstrator example and the experimental trial differ slightly, the populating of the CPTs is described in detail in Chapter 5 for the demonstrator example and in Chapter 6 for the experiment trial.

4.5.4.3. Running BN models

There are several software packages for developing Bayesian network models, each with their own strengths and weaknesses:

- Commercial – Hugin Expert A/S (HUGIN, 2011), Netica (NORSYS SOFTWARE CORP.), AgenaRisk (AGENA, 201), Analytica (LUMINA, 2011) and Bayesia (BAYESIA)
- Non-commercial – GeNIe & SMILE (DECISION SYSTEMS LABORATORY, 2007)

Bayesian network software packages include a graphical user interface for building the Bayesian network model and a runtime module that handles the probabilistic calculation and evidence propagation. First, the model structure is constructed by creating the nodes using the graphical user interface. These nodes are then linked to other nodes under the constraint that no directed loops are created in the network. The CPTs are then generated through educated guesses from experts or inferred from data. Most of the software packages support different types of nodes (i.e. chance nodes, utility nodes, etc) and these nodes can be assigned different types of states (i.e. labelled, internal, Boolean, continuous, etc). Additionally some offer the facility to create complex equations using numerous statistical distributions and mathematical operations. Furthermore, parameter and structural learning features are also available as well as sensitivity analysis capabilities.

Hugin software package was selected for the development of the Bayesian network models for the PHM framework, as it possesses the most comprehensive set of features regarding the development, testing and running of Bayesian network models as well as a powerful and intuitive user interface. A large range of built-in statistical distributions and expressions are available for building CPTs. Hugin software also allows mixing of discrete and continuous nodes to model quantitative and qualitative variables. Hugin software uses the Junction Tree algorithm to perform probabilistic inference. This algorithm first transforms the Bayesian network into a tree where each node in the tree corresponds to a subset of variables in the Bayesian networks. The algorithm then exploits several mathematical properties of this tree to perform propagation (i.e. probabilistic inference).

For the Bayesian network model, the reasoning for diagnosis and prognosis is performed in three main steps. First, the reasoning engine reads the model information, which includes the structure of the network as well as the CPTs for all the nodes of the network. It then loads the values for all nodes for which observations are available as shown in Figure 4-14. In a normal scenario, evidence for all the blue and green nodes (i.e. top and bottom layers of nodes) should be available and entered into the network. At present, for the static version of the Bayesian network, two nodes are introduced representing the point in time (for canary and parrot device) at which the network is being run. In the third step, the reasoning engine then performs evidence propagation and produces the update probability distributions for the predicted remaining life of the canary and parrot device as well the ship structure (nodes `Canary_PredictedRUL`, `Parrot_PredictedRUL` and `ShipStructure_PredictedRUL`).

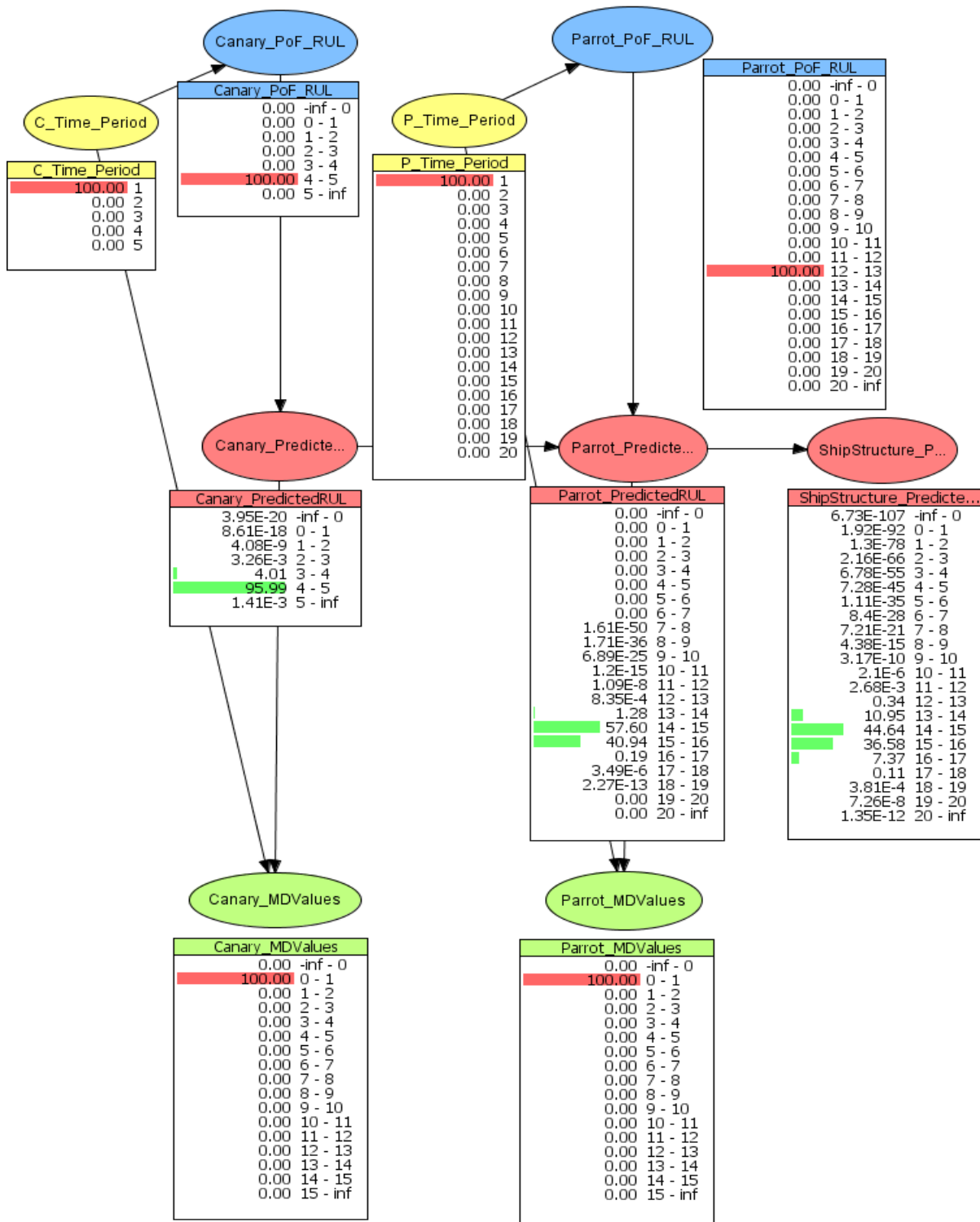


Figure 4-14 : Reasoning on Evidence

4.5.4.4. Evaluation of Bayesian network model

The evaluation of the Bayesian network model is undertaken to determine whether the model is doing the right job (validation) and whether the model is doing the job right (verification). The two types of evaluations applied were qualitative and quantitative. Qualitative evaluation was used to compare different versions of structures of Bayesian networks that were accordingly refined until a satisfactory version was obtained. To validate the model, an appraisal is carried out to determine whether the key variables and their relationships are represented correctly. The appraisal in terms of the structure of the Bayesian network model has thus far been carried out with the help of experts. Quantitative validation of a Bayesian network model involves the following:

- Testing the reasoning accuracy based on the model
- Evaluating the model's performance robustness
- Evaluating the model's tolerance to noises

Sensitivity analysis is often used to investigate the performance robustness and tolerance to noises by studying the effect of small changes of numeric parameters on a Bayesian network's performance. It uses calculation of variance reduction for continuous variables and entropy reduction for discrete variables. It helps in verifying correct initial model structure and parameterization. A number of test case scenarios (in the demonstrator example) were defined which represent real-life cases encountered during the lifetime of an iron structure. Each test case constitutes a set of findings used as inputs to the networks. For evaluation, the goal was to get the Bayesian network model to tell us what we expect to see, that is, to present expert judgment and any initial empirical data on how the system works and behaves. The results from quantitative evaluation of these test case scenarios are presented in the next chapter.

4.6. Summary

A PHM framework based on the use of bespoke sensors, diagnostic and prognostic tools has been presented. The application of this PHM framework is the prediction of remaining life of wrought iron structures of the Cutty Sark, which experiences various complex corrosion processes over time. The concept of use of Canary and Parrot devices is explained where it has been devised in order to obtain sensor data on current state of the ship structures and the surrounding environment without using any direct intrusive measurement techniques.

For the model-driven prognostic tool, a Physics-of-Failure model for prediction of corrosion rate of wrought iron over time is developed. This is a temporal model based on the Linear Bilogarithmic law for corrosion. In the data-driven diagnostic tool, precursor monitoring is carried out to detect anomalies using Mahalanobis distance analysis of failure precursors of canary and parrot devices. This also includes feature extraction on performance parameters to create a training data set representing healthy structures.

Finally, Bayesian networks are used as a fusion approach to perform probability distributions for remaining life predictions. The main aim of integrating the diagnostic tool and the prognostic tools is to harness the strength of each methodology while minimising the impacts of their shortcomings. The Physics-of-Failure model in the model-driven diagnostic tool used for this framework currently does not capture real life conditions in the prediction of remaining life of an iron structure. Within the diagnostic tool, using Mahalanobis distance analysis for precursor monitoring and anomaly detection provides good diagnostic capabilities when good training data is available but does not offer prognostic capabilities. The use of a Bayesian network model as a fusion approach is considered key in bringing this PHM framework together as it can handle different types of input to produce probability distributions of remaining life of the iron structures for the Cutty Sark. The next chapter describes the data gathering carried out to develop and test the diagnostic and prognostic tools discussed.

5. Demonstration Example

An example application has been set up to demonstrate the methods discussed in the previous chapter. The following section describes the setup for the demonstration example, which will be used to test the diagnostic and prognostic tools developed followed by a description of the different scenarios investigated. In section 5.3, the tools developed and tested are:

1. the model-driven prognostic tool using a PoF model to predict the remaining life of the devices used in the demonstrator example
2. the data-driven diagnostic tool using precursor monitoring and anomaly detection and
3. the fusion-based prognostic tool using Bayesian Network models are used to update the predicted remaining life.

The results of the tests are discussed. The final section in this chapter provides a summary of the demonstration example setup, the significance of the results and possible improvements of the current PHM methodologies used.

For this example application, the expected lifetime of a parrot device is 20 years and that of a canary device is 5 years under normal environmental conditions. The expected lifetimes of the devices are described in further detail in section 5.2. The 20 years lifetime for the parrot device was defined to reflect the fact that the Linear-Bilogarithmic law will hold for 20 years or so according to Pourbaix (POURBAIX, M, 1982). There are five scenarios investigated:

- Scenario 1 (Normal “Healthy” conditions): the environmental conditions (relative humidity and temperature) are set such that the canary and parrot device has a life expectancy of 5 years and 20 years respectively.
- Scenario 2 (Mixed conditions): normal environmental conditions for the first 15 years of lifetime of the parrot device and the first 3.75 years of the lifetime of the canary device. The devices experience harsher environmental conditions for the remaining lifetime.
- Scenario 3 (Mixed conditions): normal environmental conditions for the first 5 years of lifetime of the parrot device and for the first 1.25 years of the lifetime of the canary

device. The devices experience harsher environmental conditions for the remaining lifetime.

- Scenario 4 (Harsh conditions): harsh environmental conditions throughout the lifetime of the canary and parrot devices.
- Scenario 5 (Alternate conditions): alternate normal (for four months) and harsh environmental conditions (for two months) throughout the lifetime of the canary and parrot devices

5.1. Demonstration Setup

To be able to demonstrate the methodologies developed in the diagnostic and prognostic tools, a data set of corrosion rate measurements over time is required so that the predictive power of the models can be tested against this data set of corrosion rates. At present time, such a complete set of real data from experimental measurements (i.e. Cutty Sark) is not available. Therefore, the following approach to generate demonstration data sets of corrosion rates (i.e. data to substitute real corrosion measurements and corrosion history over time) required for the prognostic examples is undertaken. This dataset, shown on the left side of Figure 5-1, has been generated to have certain characteristics as would typically be observed in the corrosion of iron structures, and therefore to mimic real corrosion data attributes and trends.

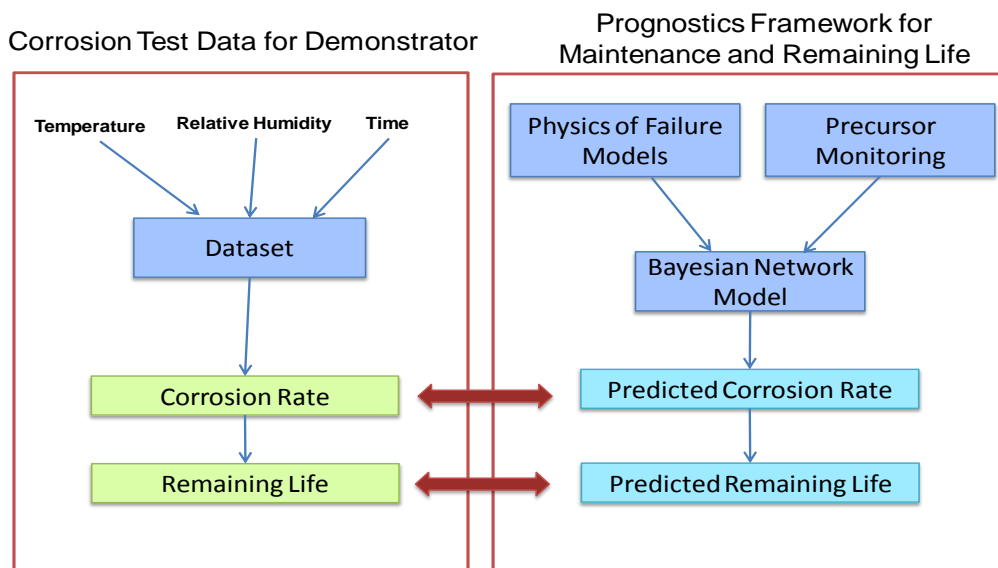


Figure 5-1: Using generated "Real" Corrosion Data to test PHM Framework

Initial first year corrosion rates of steel (Table 5-1 and Table 5-2), as detailed in the report ‘Atmospheric corrosion rates of railway bridge structures’ (GASCOIGNE, A and Bottomley, D, 1995), have been used as a guidance on typical values for corrosion rates of metals and their variation as a result of changes in the environmental conditions. For example, the seasonal variations in weather conditions throughout the year result in slightly higher corrosion rates during the height of summer and winter. Corrosion rates increase as the temperature and/or relative humidity increase. The corrosion rate for wrought iron was adjusted by multiplying the corrosion rate of steel by a factor of 0.7 as recommended by the same report. Baseline initial first year corrosion rate of 35µm/year is assumed at temperature 20°C and relative humidity 60%. This value is in the range reported in the literature (GASCOIGNE, A and Bottomley, D, 1995).

Test Commenced	Corrosion rate (µm/year)
February	28.5
May	29.5
August	34.3
November	33.5

Table 5-1: Corrosion rates of steel after 1 year test (GASCOIGNE, A and Bottomley, D, 1995)

UK data	Average Corrosion Rate (µm/year)	Minimum/Maximum (µm/year)
Rural	36	6 – 64
Urban	71	71
Light Industrial	47	30 – 53
Industrial	77	36 – 173
Industrial/Marine	51	36 – 66
Marine	34	15 – 79

Table 5-2: Average corrosion rate of steel (GASCOIGNE, A and Bottomley, D, 1995)

On this basis, the generated dataset of corrosion rate values to act as a representation of real measured data at different temperature and relative humidity levels is constructed to have the following attributes:

- Environmental Conditions: temperature range is 0°C to 30°C and relative humidity range 30%-90%;
- Corrosion rate values are greater at higher temperature and/or higher relative humidity;
- Corrosion rates are more sensitive to relative humidity changes than the temperature changes;
- Magnitude of values of the corrosion rates that are generated are in the range of the measured data reported in the literature.

The dataset of corrosion rates, with the attributes above, for temperature and relative humidity pairs for the first year is detailed in Table 5-3. The corrosion rates listed are in unit μm per year. This data, although not based on real corrosion values obtained through measurements, is realistic and has the trends of real corrosion rate changes as a function of temperature and relative humidity. Three similar tables (see Table 5-4 to Table 5-6) with datasets for the corrosion rates at times corresponding to the fifth, tenth and the twentieth year are also derived. The data in Tables 5-4 to 5-6 was derived on the basis of the data in Table 5-3 such that the relation between the corrosion rates between the first, fifth, tenth and twentieth year follows a power law relation and captures the effect of time on the corrosion rate.

Equation (18) represents a typical power law equation based on a sample of the data from Tables 5-3 to 5-6, where y is the corrosion rate and t is the time at which the corrosion rate is generated. The power law rule is applied to ensure the generated corrosion rates data follows a known corrosion phenomena that the corrosion rates are usually much higher in the first few years, and then gradually decrease and stabilise after 5-10 years once a protective layer (e.g. rust) has formed (POURBAIX, M, 1982).

$$y = 34.3t^{-0.353} \quad (18)$$

Temp. (°C)/ RH(%)	0	5	10	15	20	25	30
30	4	7	10	13	14	17	23
40	7	10	13	17	18	24	32
50	10	15	17	20	23	28	39
60	15	25	27	28	35	37	49
70	25	32	35	36	46	48	62
80	32	39	42	44	58	60	82
90	40	45	50	57	66	70	90

Table 5-3: Estimated corrosion rates for temperature and relative humidity pairs after 1st year

Temp. (°C)/ RH(%)	0	5	10	15	20	25	30
30	2.0	3.5	5.0	6.5	7.0	8.5	11.5
40	3.5	5.0	6.5	8.5	9.0	12.0	16.0
50	5.0	7.5	8.5	10.0	11.5	14.0	19.5
60	7.5	12.5	13.5	14.0	17.5	18.5	24.5
70	12.5	16.0	17.5	18.0	23.0	24.0	31.0
80	16.0	19.5	21.0	22.0	30.0	29.0	41.0
90	20.0	22.5	25.0	28.5	33.0	35.0	45.0

Table 5-4: Estimated corrosion rates for temperature and relative humidity pairs after 5th year

Temp. (°C)/ RH(%)	0	5	10	15	20	25	30
30	1.6	2.8	4.0	5.2	5.6	6.8	9.2
40	2.8	4.0	5.2	6.8	7.2	9.6	12.8
50	4.0	6.0	6.8	8.0	9.2	11.2	15.6
60	6.0	10.0	10.8	11.2	14.0	14.8	19.6
70	10.0	12.8	14.0	14.4	18.4	19.2	24.8
80	12.8	15.6	16.8	17.6	24.0	23.2	32.8
90	16.0	18.0	20.0	22.8	26.4	28.0	36.0

Table 5-5: Estimated corrosion rates for temperature and relative humidity pairs after 10th year

Temp. (°C)/ RH(%)	0	5	10	15	20	25	30
30	1.44	2.52	3.60	4.68	5.04	6.12	8.28
40	2.52	3.60	4.68	6.12	6.48	8.64	11.50
50	3.60	5.40	6.12	7.20	8.28	10.10	14.00
60	5.40	9.00	9.72	10.10	12.60	13.30	17.60
70	9.00	11.50	12.60	12.90	16.60	17.30	22.30
80	11.50	14.00	15.10	15.80	21.60	20.90	29.50
90	14.40	16.20	18.00	20.50	23.80	25.20	32.40

Table 5-6: Estimated corrosion rates for temperature and relative humidity pairs after 20th year

Tables 5-3 to 5-6 contain discrete test values for corrosion rate as a function of the time, temperature and relative humidity. Based on the principles above used to derive this data, it can be seen as a realistic and possible set of corrosion data that could be obtained in a scenario of real measurements. A corrosion rate generator is now required in order to generate corrosion rate data with respect to any particular set of time, temperature and relative humidity values that will be defined in the study case of validating the developed diagnostic and prognostics methodology. The data generator is developed as a model that interpolates continuously in three-dimensional space (time-temperature-humidity) the data in Table 5-3 to Table 5-6. The corrosion rates that can be generated with this model would then be used for various scenarios of environmental conditions and over time as datasets that are used to represent "real" data against which the diagnostic and prognostic tools are tested. The corrosion rate generator is based on a multi-quadratic model taking the form of equation (19).

$$f(X) = \sum_{i=1}^m a_i \sqrt{|X - \bar{X}^i|^2 + 1} \quad (19)$$

where X is a three-dimensional vector representing the three parameters; time (in years), temperature (in °C) and relative humidity (in %) for evaluation. $f(X)$ returns the value of the corrosion rate that is generated (in unit μm per year). \bar{X}^i is a three-dimensional vector representing a triplet of time, temperature and humidity with the known values from Table 5-3 to Table 5-6, ($i=1, \dots, m$). The triplet data points in the Tables 5-3 to 5-6 are 80, and therefore in the above model $m=80$.

The coefficients, a_i in the multi-quadratic function are computed by requiring the function in equation 5-2 to fit exactly the given set of data (from Table 5-3 to Table 5-6) for the data points ($i=1, \dots, 80$). This requirement results in solving a linear system of m ($m=80$ in this case) equations with the coefficients in the multi-quadratic model a_i ($i=1, \dots, m$) as unknowns. Using the multi-quadratic model ensures that the data generated is in line with the trends for the corrosion rates observed in real life when time, temperature and relative humidity change. It is an interpolation function for the data in Table 5-3 to Table 5-6. That is the model predicts the exact value for the corrosion rate at the triplet (time, temperature, relative humidity) points used in the tables. The coefficients of the model are reported in Table 5-7. For example, this model will generate at arbitrary conditions for time = 17 years, Temperature = 18°C and RH = 65%, a value of the corrosion rate of 13.67 μm per year. Such value is to be viewed as an experimentally measured value under this condition.

i	a_i	i	a_i	I	a_i	I	a_i
1	0.45753	21	0.24037	41	-0.08505	61	0.19556
2	-0.31168	22	0.46009	42	-0.32661	62	-0.06578
3	-0.10663	23	0.79331	43	-0.35930	63	0.03957
4	-1.40685	24	1.96285	44	-0.21628	64	0.20639
5	0.06605	25	0.26066	45	-0.28671	65	-0.02451
6	-0.43313	26	0.62047	46	-0.39429	66	-0.08846
7	-0.17816	27	0.96064	47	-0.49274	67	-0.00099
8	-1.82370	28	2.17804	48	-0.56476	68	-0.09419
9	0.15597	29	0.65134	49	-0.21290	69	0.11856
10	-1.10261	30	1.20598	50	-0.53286	70	-0.15412
11	-0.98147	31	1.66168	51	-0.66712	71	-0.08174
12	-2.19659	32	2.84622	52	-0.58649	72	-0.02259
13	-0.78706	33	1.15913	53	-0.53619	73	-0.13025
14	-1.24245	34	1.63121	54	-0.74405	74	-0.19153
15	-1.29924	35	2.30209	55	-0.92549	75	-0.14376
16	-2.75690	36	3.72977	56	-0.76187	76	-0.04643

17	-1.03482	37	1.91464	57	-0.22864	77	0.25241
18	-1.48422	38	2.35611	58	-0.54534	78	0.05574
19	-2.73816	39	3.56277	59	-0.79182	79	-0.09579
20	-5.51639	40	5.43862	60	-0.53770	80	-0.00801

Table 5-7: Coefficients values of the multi-quadratic model (the corrosion rate generator)

Values for the monthly temperature and relative humidity range in London, UK, from the BBC weather web site [(WEATHER, BBC, 2006), see Table 5-8], is used in this study to generate artificial histories for both the temperature and relative humidity over a period of 20 years. The values for a temperature/ relative humidity scenario are obtained by randomly generating values in the min-max range for the respective month.

Month	Average Minimum Temperature (°C)	Average Maximum Temperature (°C)	Average Minimum Relative Humidity (%)	Average Maximum Relative Humidity (%)
January	2	6	77	86
February	2	7	72	85
March	3	10	64	81
April	6	13	56	71
May	8	17	57	70
June	12	20	58	70
July	14	22	59	71
August	13	21	62	76
September	12	19	65	80
October	8	14	70	85
November	5	10	78	85
December	4	7	81	87

Table 5-8: Dataset of min and max monthly temperature and relative humidity (WEATHER, BBC, 2006)

The approach detailed above for the simulation of corrosion data for this demonstration example was deemed necessary as to the author's knowledge there is not such dataset set for corrosion available for analysis. Additionally simulation of corrosion data allowed for the

testing of scenarios, which are usually experienced in the real world. Furthermore, data with well-defined characteristics can be used to test particular aspects of PHM methodologies developed. The simulated corrosion data was also vital in developing the training dataset for the data-driven diagnostic tool.

5.2. Scenarios Investigated for Demonstration Example

The diagnostic and prognostic tools are tested for a parrot device assumed to be made of wrought iron material with the following dimensions: length $L = 2$ cm, width $W = 1$ cm, depth $D = 1.2$ cm. The canary device, also assumed to be made of wrought iron material has smaller dimensions than the respective parrot device providing larger area-to-volume ratio (length $L = 2$ cm, width $W = 1$ cm, depth $D = 0.6$ cm). Therefore, the rate of relative material loss in the canary device is higher compared to the respective parrot device.

The expected lifetime of a parrot device is 20 years and that of a canary device is 5 years under normal conditions. The 20 years lifetime was chosen to reflect the fact that the Linear-Bilogarithmic law will hold for 20 years or so according to Pourbaix (POURBAIX, M, 1982). Using the corrosion generator described in the previous section, the corrosion rates under normal environmental conditions were generated and the cumulative corrosion for time, $t = 5$ years and $t = 20$ years were calculated. The average cumulative corrosion after 5 years was 174mm, which is approximately 3% of the original depth of the canary device. The average cumulative corrosion after 20 years was 353mm, which is approximately 3% of the original depth of the parrot device. Therefore, for this demonstration, a failure in a canary or parrot device is defined as the corrosion penetration being more than 3% of the initial depth of the device. The diagnostic and prognostic tools are tested under the following five scenarios.

5.2.1. Scenario 1 (Normal “healthy” conditions)

Normal relative humidity and temperature for which the parrot device has life expectancy of 20 years while the canary device has a life expectancy of 5 years. The relative humidity and temperature in scenario 1 for normal healthy conditions are in the range detailed in Table 5-8 . Such conditions will generate the normal corrosion rate expected throughout the lifetime of the canary/parrot devices (i.e. these are the conditions a “healthy” canary/parrot would experience throughout their lifetime).

Figure 5-2 shows an example of randomly generated profile of the temperature and relative humidity values (derived from the BBC weather data shown in Table 5-8) used to represent scenario 1 over a 20-year period. The fluctuation in the temperature and relative humidity values arise from the season changes throughout one year. Once this scenario is assumed, the corrosion rate history over the 20 years can also be generated using the multi-quadratic model described above for corrosion rate generation. An example of such generated corrosion rate measurements is shown in Figure 5-3. As already discussed, this data is used as corrosion measurements over time, and it is generated using equation (5-2) to test the diagnostic and prognostic tools discussed in the previous chapter.

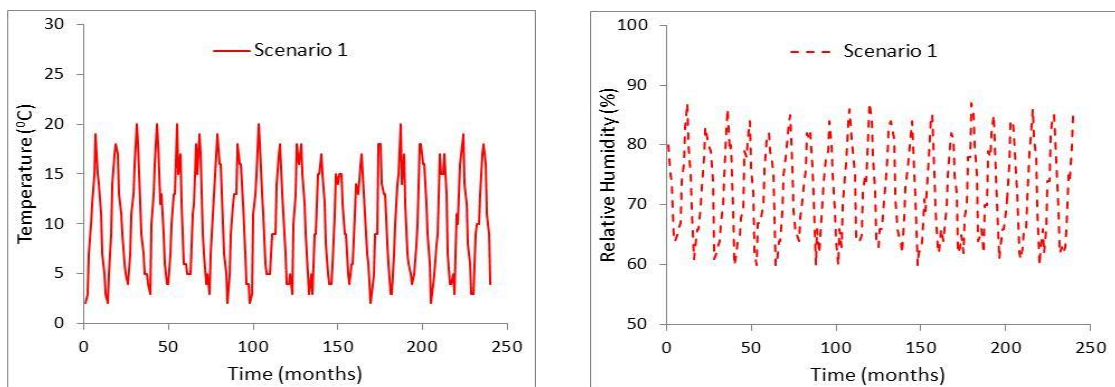


Figure 5-2: Typical Temperature and RH for Scenario 1

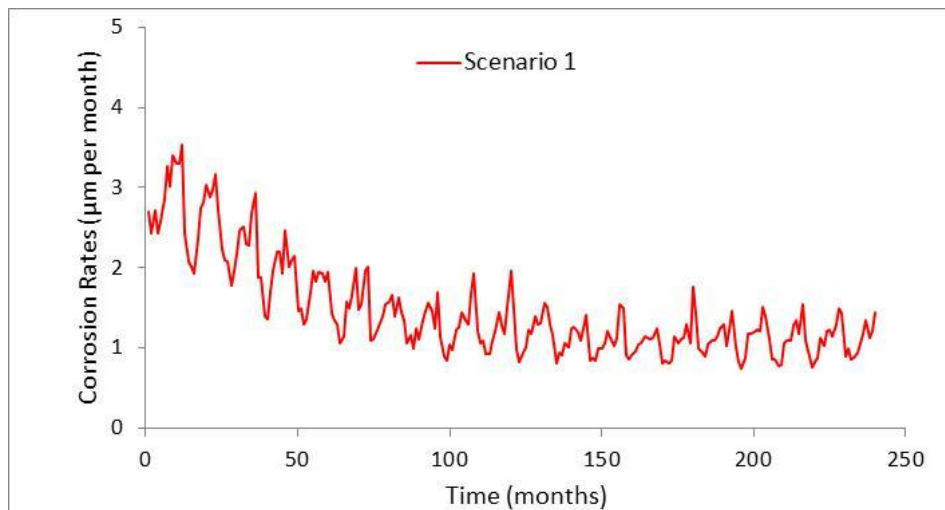


Figure 5-3: Corrosion Rates for Scenarios 1

5.2.2. Scenario 2 (Mixed conditions)

The parrot device experiences normal conditions during the first 15 years of its life and harsher conditions (i.e. higher temperature and relative humidity compared with the normal case) afterwards for the remaining of its life. Similarly, the canary device experiences normal conditions during the first 3.75 years of its life and harsher conditions afterwards for the remaining of its life. This scenario has been devised with the aim of demonstrating that the PHM framework can detect anomalies that can occur in healthy canary/parrot devices thus requiring inspection and maintenance. Here the amount of time after which the canary and parrot device experience higher corrosion rates has been chosen arbitrarily for demonstration.

Figure 5-4 shows the temperature and relative humidity values (derived from the BBC weather data shown in Table 5-8) used to represent scenario 2 over a 20-year period for the parrot device. For the first 15 years, the temperature and relative humidity ranges are similar to that of scenario 1. For the remaining life, the temperature and relative humidity ranges are slightly higher than that of scenario 1 to represent harsh environmental conditions where the temperature is increased by 3°C and the relative humidity is increased by 5% as shown in Table 5-9. An example of such generated corrosion rates measurements for scenario 2 is shown in Figure 5-5.

Month	Average Minimum Temperature (°C)	Average Maximum Temperature (°C)	Average Minimum Relative Humidity (%)	Average Maximum Relative Humidity (%)
January	5	9	82	91
February	5	10	77	90
March	6	13	69	86
April	9	16	61	76
May	11	20	62	75
June	15	23	63	75
July	17	25	64	76
August	16	24	65	81
September	15	22	70	85
October	11	17	75	90
November	8	13	83	90
December	7	10	86	92

Table 5-9: Dataset of min and max monthly temperature and relative humidity for harsher conditions

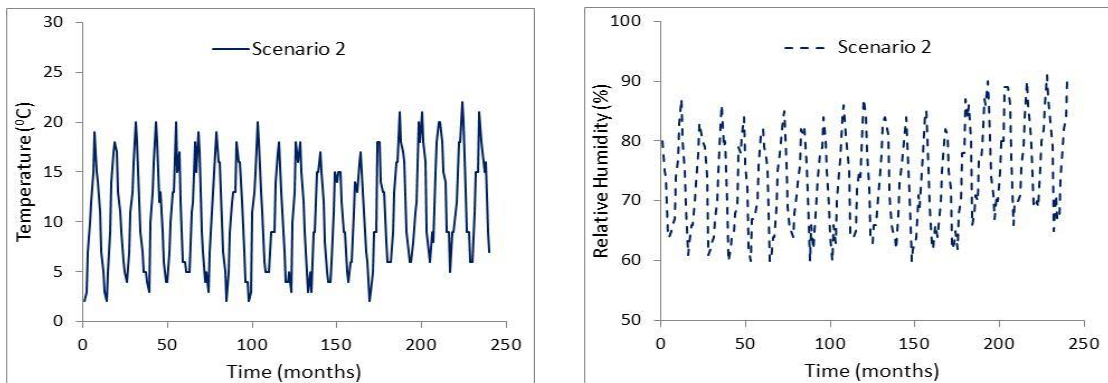


Figure 5-4: Typical Temperature and RH for Scenario 2

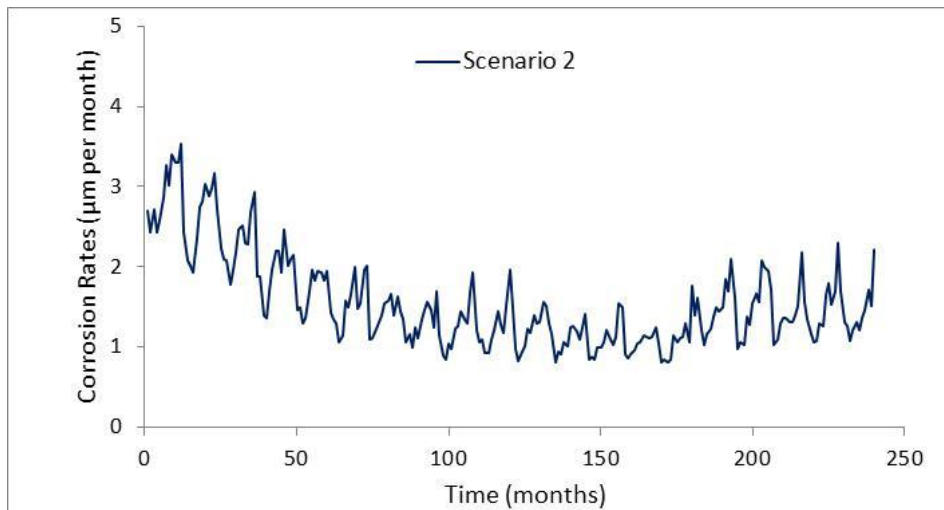


Figure 5-5: Corrosion Rates for Scenarios 2

5.2.3. Scenario 3 (Mixed conditions)

The parrot device experiences normal conditions during the first quarter of its life and harsher conditions (i.e. higher temperature and relative humidity compared with the normal case) afterwards for the remaining of its life. The canary device also experiences normal conditions during the first quarter of its life and harsher conditions afterwards for the remaining of its life. This is a variation on scenario 2 again to demonstrate that the PHM framework can detect anomalies that can occur later in initially healthy canary/parrot devices thus requiring inspection and maintenance.

Figure 5-6 shows the temperature and relative humidity values used to represent scenario 3 over a 20-year period for the parrot device. For the first 5 years, the temperature and relative humidity ranges are similar to that of scenario 1 (as shown in Table 5-8). For the remaining life, the temperature and relative humidity ranges used are from Table 5-9 to represent harsh environmental conditions. An example of such generated corrosion rate measurements for scenario 3 is shown in Figure 5-7.

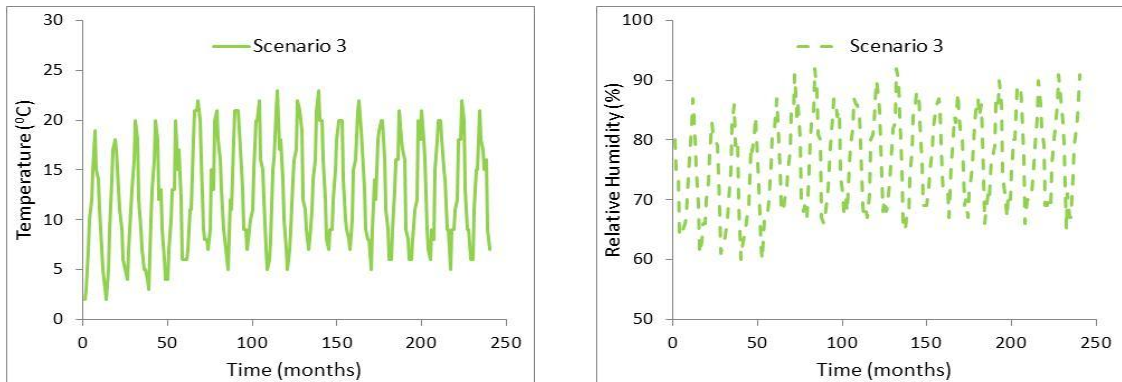


Figure 5-6: Typical Temperature and RH for Scenario 3

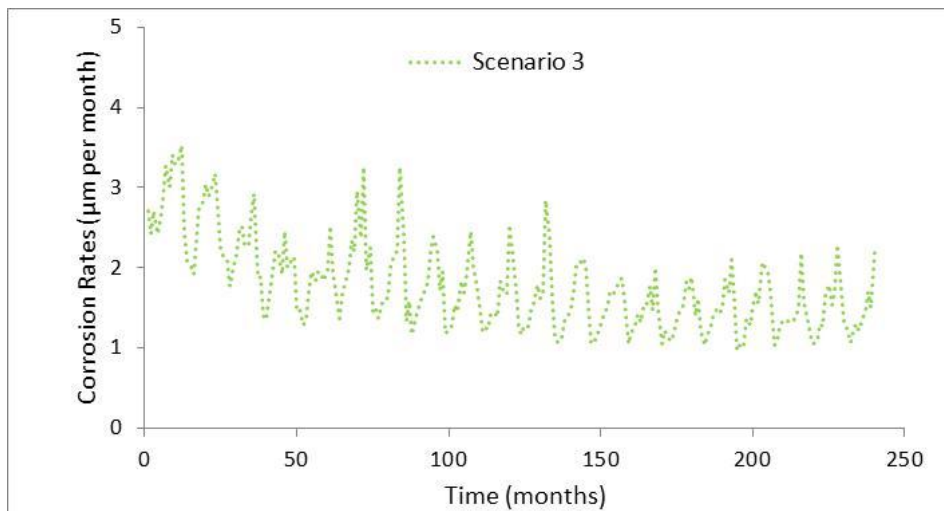


Figure 5-7: Corrosion Rates for Scenarios 3

5.2.4. Scenario 4 (Harsh conditions)

The parrot device experiences harsh environmental conditions from the beginning throughout its life (i.e. higher temperature and relative humidity compared with the normal case). The canary device experiences similar harsh conditions throughout its life. This scenario is used to demonstrate that the PHM framework can detect anomalies in canary/parrot devices right from the beginning should such a situation arise. It should be noted that in real life, one would

expect that once such anomalies are detected, the system would be inspected and any imminent failure dealt with in an appropriate manner while here this scenario just continues showing with the same high corrosion rates.

Figure 5-8 shows the slightly higher temperature and relative humidity values used from Table 5-9 represent scenario 4 over a 20-year period for the parrot device. The same temperature and relative humidity ranges are used for the canary device. An example of such generated corrosion rate measurements for scenario 4 is shown in Figure 5-9.

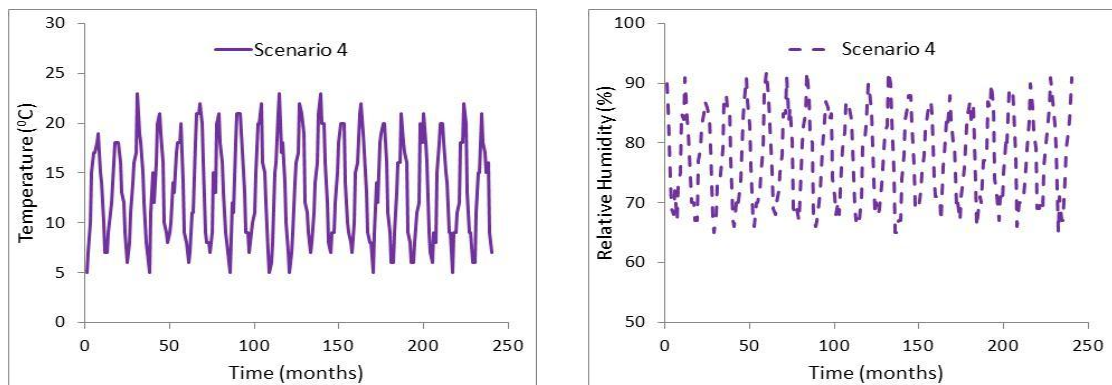


Figure 5-8: Typical Temperature and RH for Scenario 4

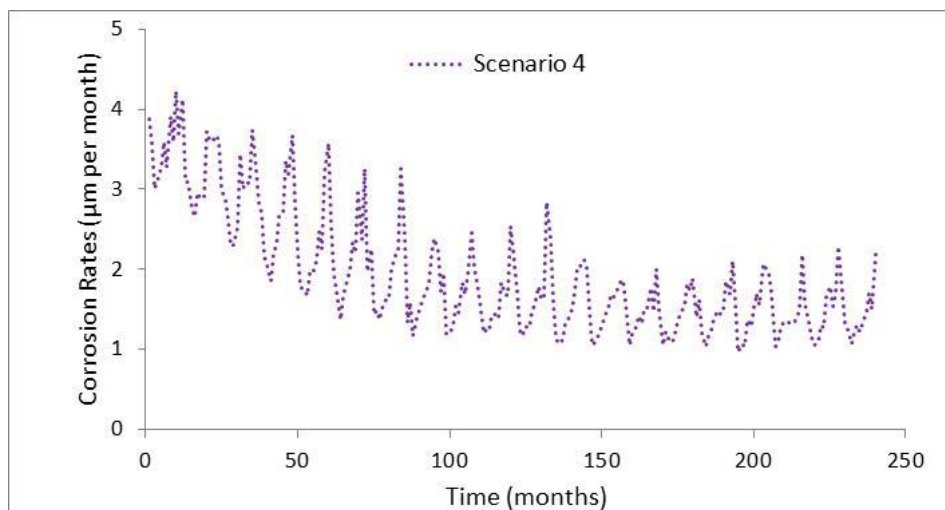


Figure 5-9: Corrosion Rates for Scenarios 4

5.2.5. Scenario 5 (Alternate conditions)

The parrot device alternately experiences normal and harsh environmental conditions from the beginning throughout its life. The canary device also alternately experiences normal and harsh conditions throughout its life. This scenario is used to demonstrate that the PHM framework

can detect anomalies in canary/parrot devices caused by varying conditions over time, which mirrors the situation where corrosion occurs during periods where the structure might be exposed to harsher conditions for only a short periods followed by similar periods of normal conditions.

Table 5-10 shows the temperature and relative humidity ranges used for the harsh environmental conditions where the temperature is increased by 5°C and the relative humidity is increased by 8%. Here the temperature and relative humidity ranges are set at normal (i.e. same as scenario 1) for four months and then increased to the harsh conditions as shown in Table 5-10 for two months then set back to normal conditions for another four months and so on. This cycle is repeated throughout the lifetime of both devices. An example of such generated corrosion rate measurements for scenario 5 is shown in Figure 5-11.

Month	Average Minimum Temperature (°C)	Average Maximum Temperature (°C)	Average Minimum Relative Humidity (%)	Average Maximum Relative Humidity (%)
January	7	11	85	94
February	7	12	80	93
March	8	15	72	89
April	11	18	64	79
May	13	22	65	78
June	17	25	66	78
July	19	27	67	79
August	18	26	68	84
September	17	24	73	88
October	13	19	78	93
November	10	15	86	93
December	9	12	89	95

Table 5-10: Dataset of min and max monthly temperature and relative humidity for harsh alternate conditions

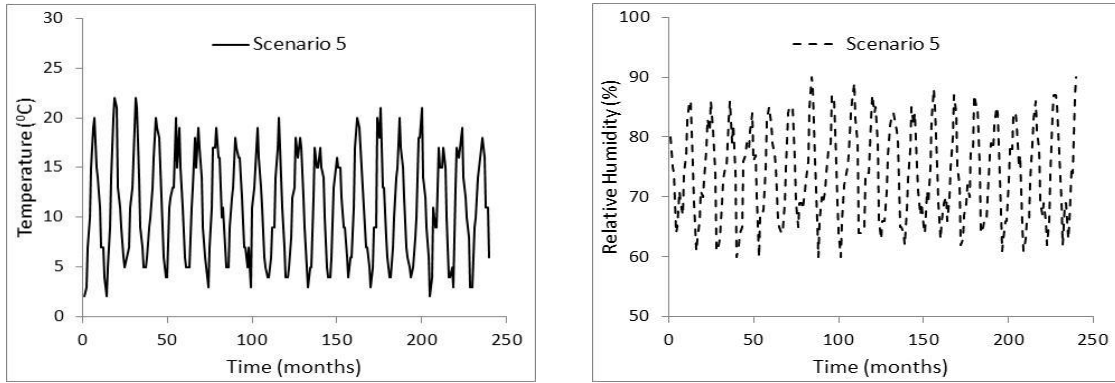


Figure 5-10: Typical Temperature and RH for Scenario 5

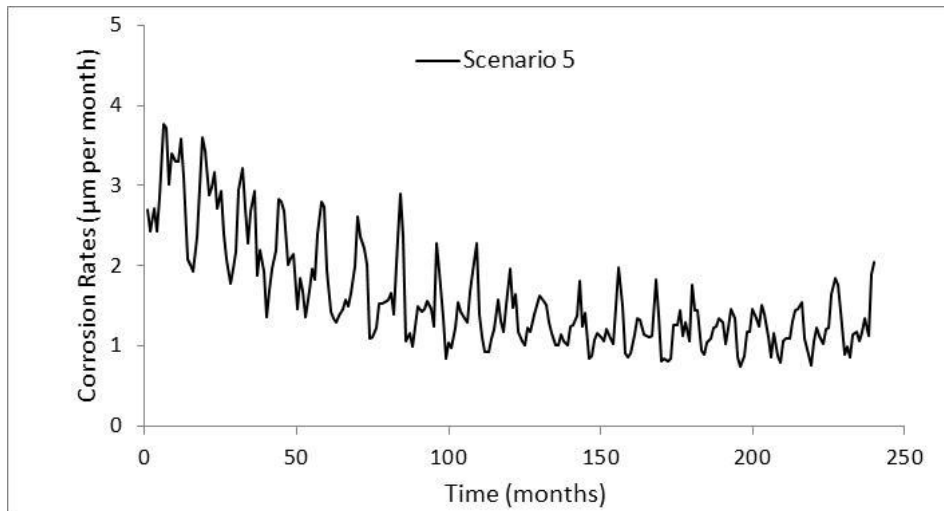


Figure 5-11: Corrosion Rates for Scenarios 5

5.3. Analysis of PHM Methodologies

5.3.1. Predicting remaining life using PoF Approach (Model Driven)

In this demonstration, the Linear Bilogarithmic Law for atmospheric corrosion is used as the PoF model to predict the remaining life of a canary and parrot device pair (for scenarios 1-5). Figure 5-12 shows the steps carried out to predict remaining life of the canary and parrot devices:

- Step (1) – Calculate Penetration Depth P_t at time t : Using the available corrosion rate data up to time t for a particular scenario (as discussed in section 5.2), the cumulative penetration, P_t , over the time, t is calculated using equation (19).

$$P = P_1 + P_2 + \dots + P_t \quad (19)$$

- Step (2) – Determine A and B from the linear bi-logarithm equation. This is achieved using linear regression where three sets of data obtained from step (1) are used to fit

the equation. For example, in this case we have used P_t data at time points representing 10%, 15% and 30% of the history up to the current point in time. A and B are derived from the regression line taking the form of equation (20).

$$\ln(P) = \ln(A) + B\ln(t) \quad (20)$$

- Step (3) – Calculate remaining life, t_{rul} : Using equation (21) with the failure criteria $P_t = 3\%$ of original depth, the remaining life is calculated.

$$t_{rul} = e^{\frac{\ln(P_t) - \ln(A)}{B}} \quad (21)$$

The predicted remaining life of the devices is updated each year by repeating the above steps.

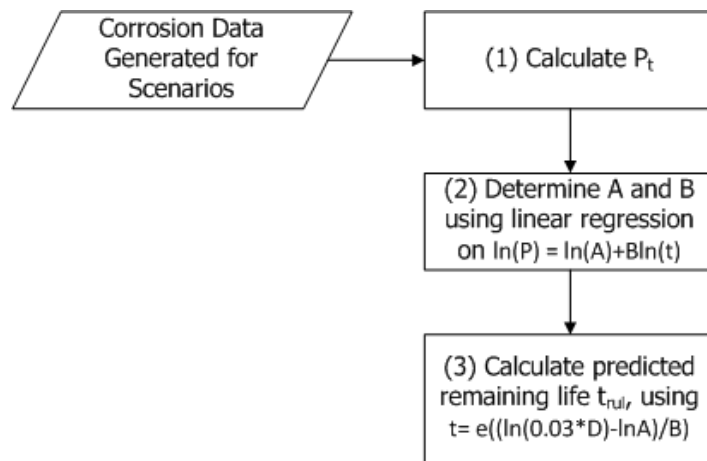


Figure 5-12: Predicting Remaining Life using PoF model based on Linear Bi-logarithmic Law

5.3.1.1. Results and Discussion

Figure 5-13 shows the lifetime prediction of the PoF model for a canary device over time (for scenarios 1-5) and compares this with the expected remaining life under normal environmental conditions for that canary device (approximately 5 years in this case as described earlier in section 5.2). The remaining life predictions in Figure 5-13 show the instance for which the last 10% of the lifetime of the current life of the canary device is used to recalculate and update the constants A and B . For a parrot device, data from the last 15% of the lifetime is used to recalculate and update the constants A and B in the lifetime model. As canary devices have shorter lives than parrot devices, the lifetime model uses less historical data to calculate constants A and B in order to capture recent changes that might affect the

structure more significantly. Currently, the ratio of lifetime to be used to get the most accurate predictions is still under investigation. The amount of historical data required will be defined from data of experiment trials once these are available.

In Figure 5-13, for scenario 1, the predicted remaining life is close to the approximated expected lifetime of 5 years thus reflecting the normal environmental conditions set for generating the corrosion rates for this scenario. In scenario 2, the predicted remaining life is similar to Scenario 1 in the beginning but later, a shorter remaining life is predicted. This is in agreement with what is expected as for the first 3.75 years of the canary's life, normal environmental conditions was experienced and harsher environmental conditions was experienced for the remaining life. As for Scenario 3, the predicted remaining life is much lower as harsher environmental conditions were experienced after first 1.25 years of its lifetime.

In scenario 4, the predicted remaining life is much lower from the beginning as harsh environmental conditions were applied to the canary device right from the beginning. In scenario 5, the environmental conditions were altered continuously from normal to harsh. This results in shorter remaining life than expected for the canary device as shown in the graph. It should be noted that scenarios 2-5 have been devised for testing purposes only as in real life if the expected remaining life was much lower than the expected remaining life, inspection of the structure under consideration would be carried out and repairs would be made if required.

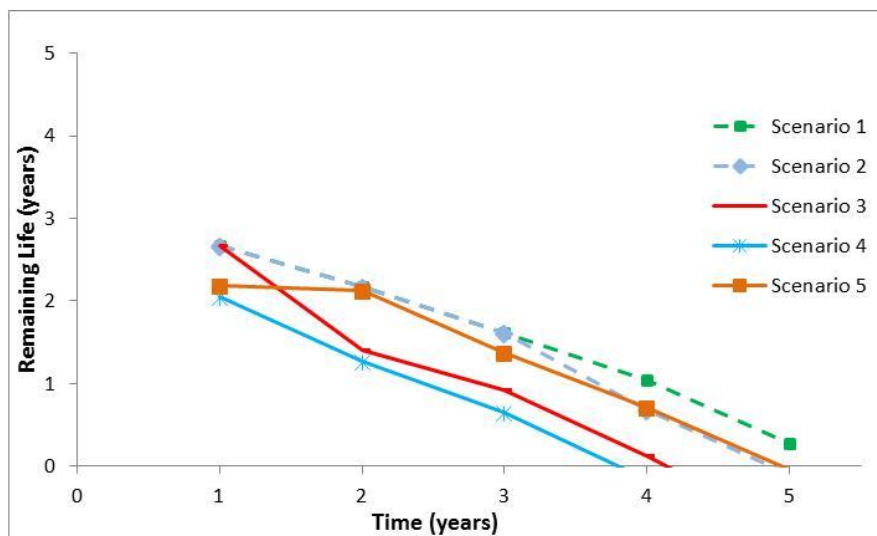


Figure 5-13: PoF-based Prediction of Remaining Life for Canary Device

Figure 5-14 shows the lifetime prediction of the PoF model over time (for scenarios 1-5) and compares this prediction with the expected remaining life under normal environmental conditions for the parrot device (approximately 20 years in this case as described earlier in section 5.2). Predictions of remaining life for scenario 1 is considerably lower than expected due to the higher rates of corrosion occurring in the first few years, thus predicting a shorter remaining life. Later on, as the corrosion rate stabilises, the predicted remaining life is very close to that expected as shown in the graph for scenario 1.

In scenario 2, the predicted remaining life is similar to Scenario 1 in the beginning but later, a shorter remaining life is predicted thus reflecting the change to harsher environmental conditions after the first 15 years of life. As for scenario 3, the trend for the predicted remaining life changes after the first 5 years of the lifetime, thus reflecting the change to harsher environmental conditions (as simulated in the corrosion datasets) causing earlier failure in the parrot device and shortening the remaining life to 16 years.

In scenario 4, the predicted remaining life is much lower from the beginning reflecting the harsh environmental conditions applied to the parrot device right from the beginning. In scenario 5, the environmental conditions are altered continuously from normal to harsh resulting in shortening the remaining life to 18 years. Here again, it should be noted that scenarios 2-5 have been devised for testing purposes only and a structure would be inspected and repaired if needed should the predicted remaining life be shorter than expected.

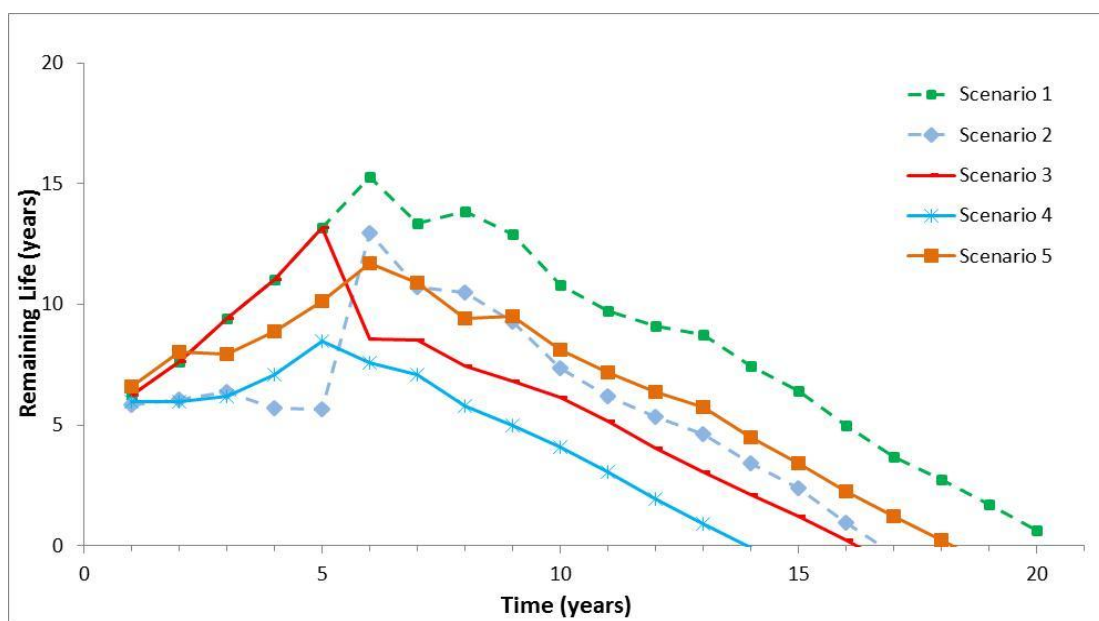


Figure 5-14: PoF-based Prediction of Remaining Life for Parrot Device

5.3.2. Data Driven Diagnostic Tool: Using Mahalanobis distance analysis for anomaly detection

In this example, MD analysis is carried out to assess the corrosion of the devices assuming environmental conditions under scenarios 2-5. Scenario 1 is used as the training data as normal environmental conditions are assumed to represent a healthy device (5 years for canaries and 20 years for parrots). The following subsections will detail the setup for performing the MD analysis as well as an analysis of the results obtained.

5.3.2.1. Feature Extraction

Three precursor variables are monitored that represent corrosion rate in the canary and parrot device: weight change rate, dimension change rate and electrical resistance change rate. Data features from the three precursor variables were additionally processed such that average, maximum and minimum values over a certain period were computed (for the demonstration, these computations were carried out for every four readings taken over a four month period). The use of basic feature extraction techniques here aims to capture changes that cannot be observed using raw data only. For example, for weight change rate, apart from the original (raw) data of the weight change rate (weight change per month), three sets of data were generated using feature extraction that was performed for every four readings of weight change rate: (i) average weight change rate, (ii) maximum weight change rate and (iii) minimum weight change rate. The average feature was computed to even out small fluctuations in corrosion rate such that when anomaly detection is performed using MD analysis, the results would not be biased due to small fluctuations. Computation of the maximum value over a certain period was carried out such that if corrosion did occur at a higher rate than usual during that time, this information would be captured and used afterwards. The computation of minimum value over a certain period is also carried with a view to possibly detect any further unforeseen patterns.

5.3.2.2. Setup for Anomaly Detection

For this demonstration, three precursors are monitored for both canary and parrot devices: (i) dimension change rate, (ii) weight change rate and (iii) electrical resistance change rate. Figure 5-15 shows the steps carried out to perform MD analysis for the canary and parrot devices:

- Step 1 - Generate corrosion penetration (dimension change), weight change and electrical change

Corrosion penetration (dimension change) over the lifetime of the device is simulated using A and B values obtained from Step 2 in the PoF model for scenario 1. P_t , the corrosion penetration for each time step is calculated using equation (20). Then the weight change and electrical resistance change is derived using equations (22) and (23) respectively. Several datasets consisting of dimension change rate, weight change rate and electrical resistance change rate with slight arbitrarily defined variations (2%-5% randomness) are generated to build the healthy data.

$$\Delta W_t = \frac{\Delta P_t * E * \rho}{K} \quad (22)$$

where, ΔW_t is the weight change rate at time t , ΔP_t is the corrosion penetration at time t , E is the exposed area, ρ is the metal density and K , a constant for unit conversion

$$\Delta R_t = \frac{\rho * L}{w * P_t} \quad (23)$$

where, ΔR_t is the corrosion penetration at time t , P_t is the corrosion penetration at time t , ρ is the electrical resistivity, L , length of the device and w , the width of the device.

- Step 2 - *Feature Extraction*: This is carried out on the data generated from Step 1 such that the average, maximum and minimum (over a period time, $t=t$ to time, $t=t+4$) is calculated.
- Step 3 – *Normalisation of data*: The data for each performance parameters (real, average, maximum and minimum) is then normalised using the mean and standard deviation to remove scaling effects as dimension change, weight change and electrical resistance all have different units. This now constitutes the Mahalanobis space (i.e. the training dataset).
- Step 4 – *Compute healthy MD values*: Using the Mahal function from Matlab, Mahalanobis distance analysis is carried out to obtain the MD values for healthy data. If new healthy data is available, this step is repeated to obtain new MD values.

- Step 5 – *Determine MD threshold value*: The MD threshold values are determined using the average and standard deviation of the MD values for healthy data obtained from Step 4 as well as expert knowledge. Currently the MD threshold is set as average of MD values plus one standard deviation of the MD values.
- Step 6 – *Generate Test data*: Test data is generated in the same manner as in step 1 but for scenarios (2-5).
- Step 7 - *Feature Extraction*: Feature extraction is carried out to obtain average, maximum and minimum is performed on test data in a similar manner as in Step 2.
- Step 8 – *Normalisation of data*: This is carried out using the mean and standard deviation of health data from step 3.
- Step 9 – *Compute MD Values*: Using the Mahal () function from Matlab, the MD values is obtained for test data.
- Step 10 - Compare MD value for test data with MD threshold value

The MD values will also be used in the Bayesian Network models developed as shown in the next section.

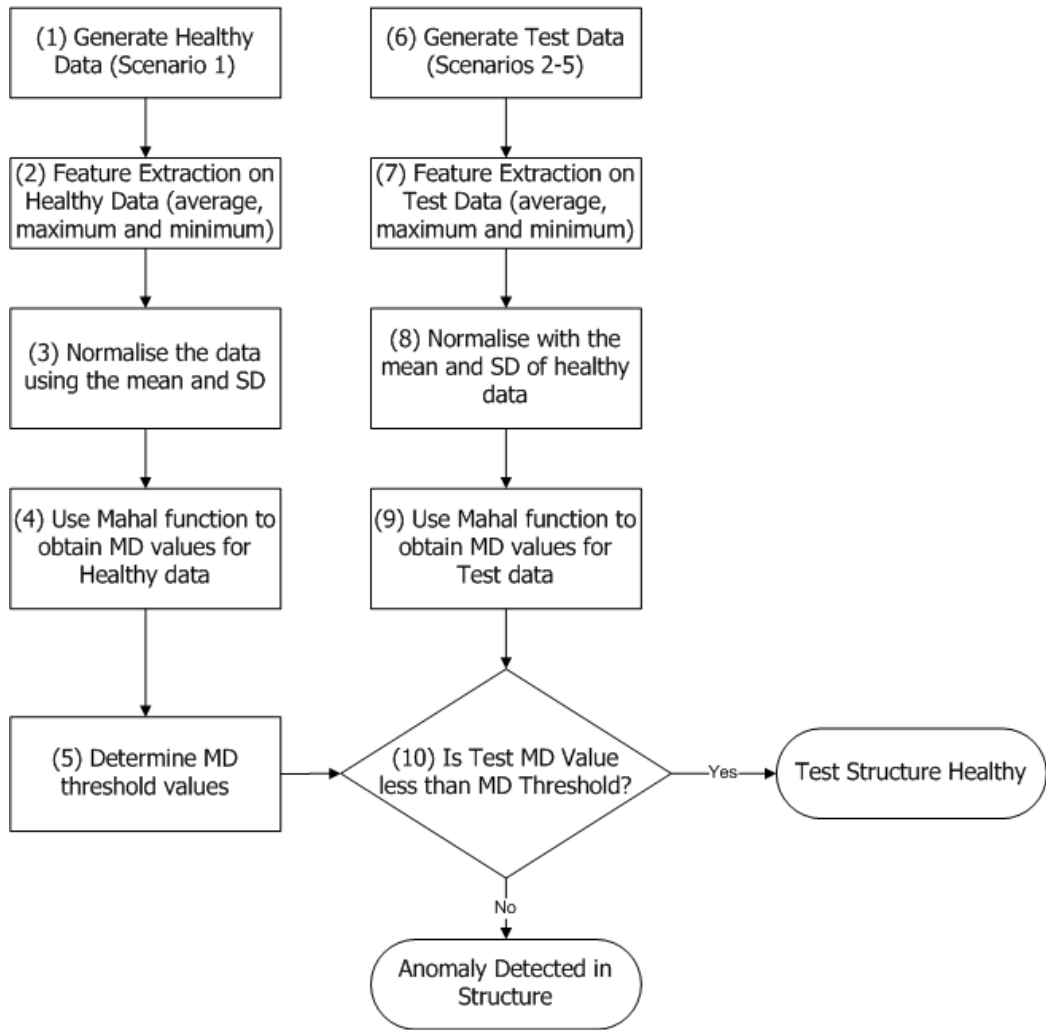


Figure 5-15: Using MD analysis to detect anomalies in scenarios 2-5

5.3.2.3. Results and Discussions

The Mahalanobis distance values obtained are plotted against each data point. Here a data point represents a period of one month as measurements are taken on a monthly basis. Figure 5-16 shows the MD value history for scenarios (1-3) for the real data, i.e. dimension change rate, electrical resistance change rate and weight change rate for the canary device (without any feature extraction performed). An MD threshold value of 5.5 is used to distinguish between anomalies in the device being detected or not, which represents the average of MD values (for the cases of normal healthy conditions) plus one standard deviation of the MD values. Expert knowledge can also be used to define the MD threshold value. The MD threshold can be further tuned if required to obtain desired sensitivity. The MD value history for scenario 2 reflects the harsher environmental conditions inflicted after the first 3.75 years of the lifetime of the canary device. For scenario 3, the effect of the harsher environmental

conditions inflicted after the first 1.25 years of the lifetime is visible through the higher MD value history obtained.

Figure 5-17 shows the MD value history for scenarios (1, 4, and 5) for the original data for the canary device. As expected, the MD values for scenario 4 are above the MD threshold throughout almost the whole lifetime of the canary device due to harsh environmental conditions experienced by the canary device throughout its lifetime. As for scenario 5, the MD values go above and below the MD threshold value periodically as expected following the harsh and normal environmental conditions inflicted on the canary device alternately.

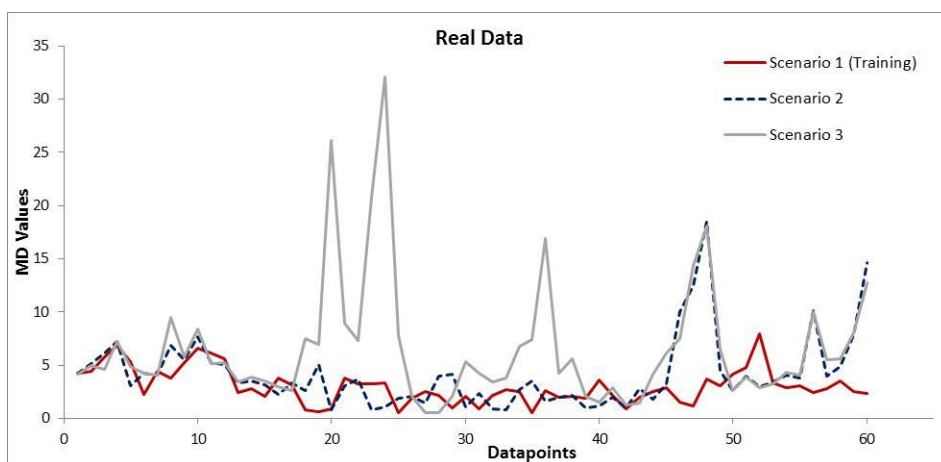


Figure 5-16: MD Analysis of Real Data for Scenarios 2 & 3 for Canary

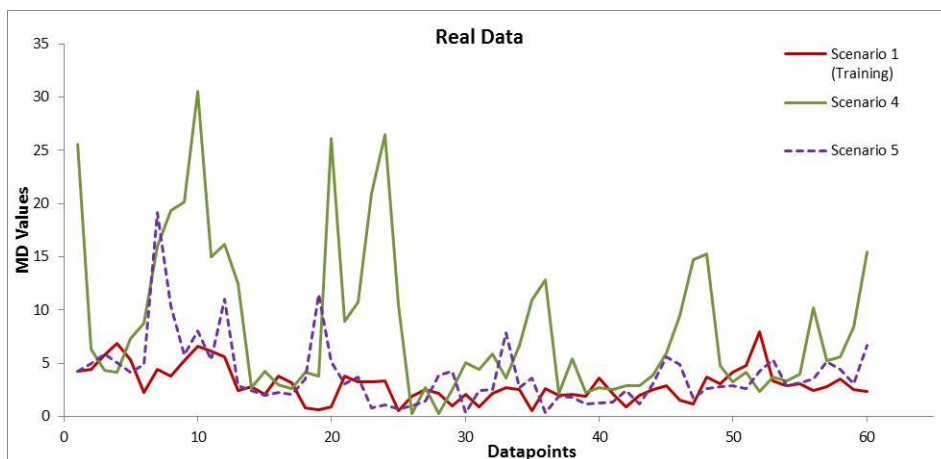


Figure 5-17: MD Analysis of Real Data for Scenarios 4 & 5 for Canary

Figure 5-18 and Figure 5-19 show the MD value history for scenarios 1-5 for the average of real data (i.e. the average of dimension change rate over a 4-months period, the average of

electrical resistance change rate over a 4-months period and the average of weight change rate over a 4-months period) for the canary device. Here a data point represents a period of four months as the average is calculated for four measurements are taken on a monthly basis. Again, here, the MD threshold value of 5.7 is used representing the average of MD values plus one standard deviation of the MD values. The results observed for scenarios 2-4 are similar to that of the MD analysis of the original data. However, the MD values for scenario 5 do not alternate above and below the MD threshold value as much as observed for the original data.

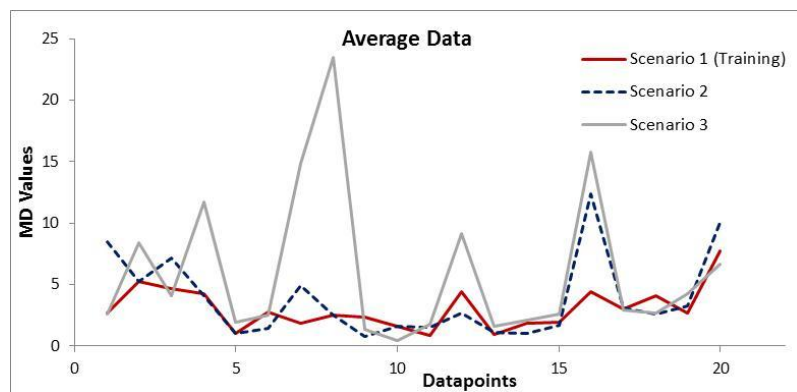


Figure 5-18: MD Analysis of Average Data for Scenarios 2 & 3 for Canary

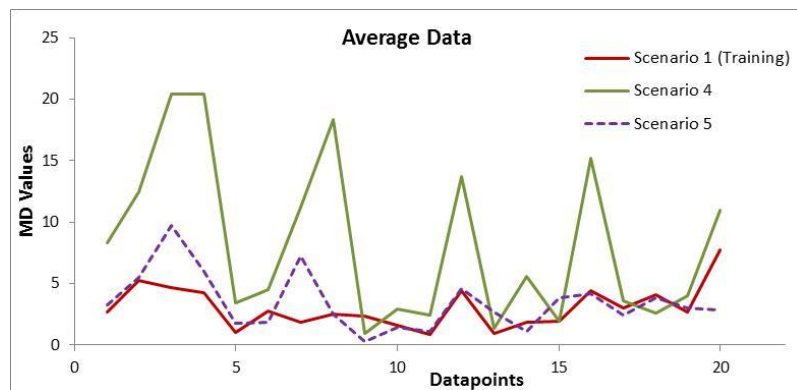


Figure 5-19: MD Analysis of Average Data for Scenarios 4 & 5 for Canary

In a similar manner, MD analysis is carried out on the parrot device. As the parrot device experiences higher corrosion rates in the first few years, two different MD threshold values for the lifetime life of the parrot device are considered. Once the corrosion rate stabilises after the first few years, the long-term threshold MD value is used to compare the long-term performance of the parrot device. In this case, MD value of 4.7 is used for original, average and minimum data and an MD value of 4.9 is used for maximum data.

Figure 5-20 and Figure 5-21 show the MD value history for real data for scenarios (1-3) and scenarios (1, 4, 5) respectively. Figure 5-22 and Figure 5-23 show the MD value history for the average of real data for the parrot device for scenarios (1-3) and scenarios (1, 4, 5) respectively. Similar trends as the ones from the MD analysis of the canary device are observed when analysis of the MD values for the last 80% of the lifetime for scenarios 2-5 is considered.

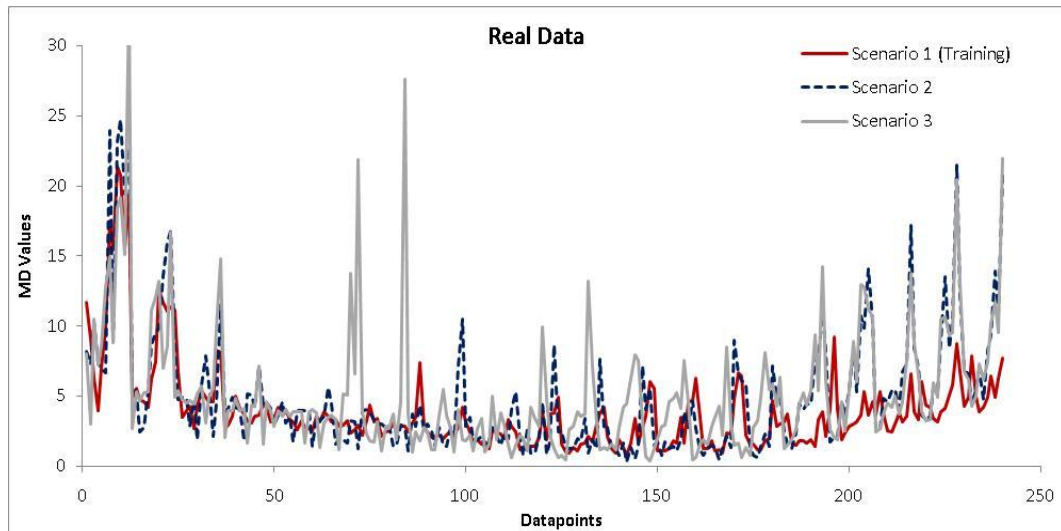


Figure 5-20: MD Analysis of Real Data for Scenarios 2 & 3 for Parrot

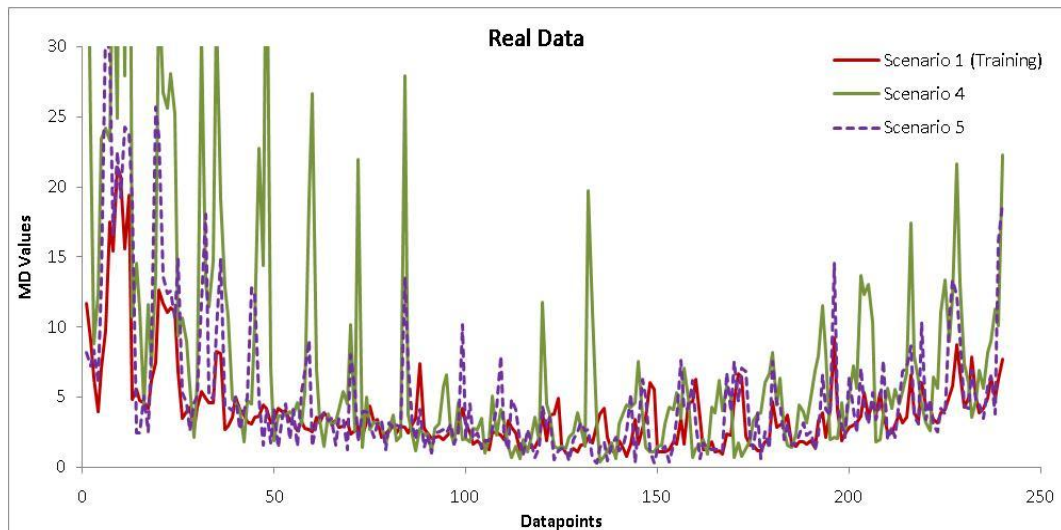


Figure 5-21: MD Analysis of Real Data for Scenarios 4 & 5 for Parrot

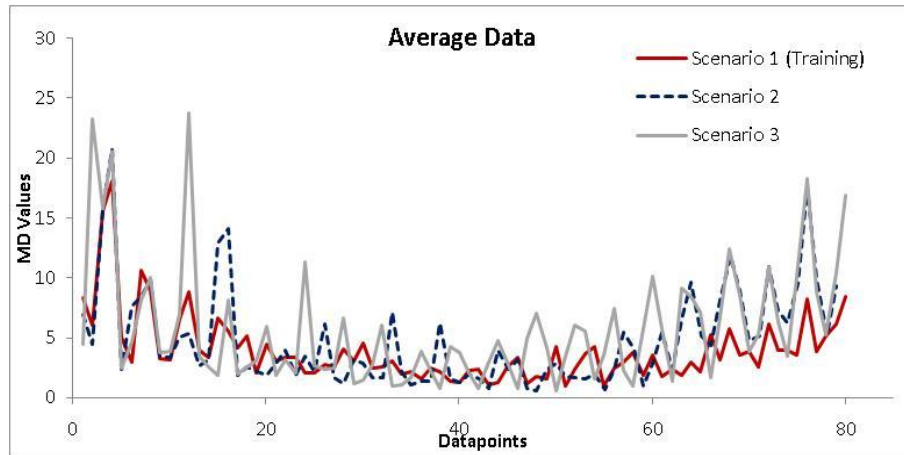


Figure 5-22: MD Analysis of Average Data for Scenarios 2 & 3 for Parrot

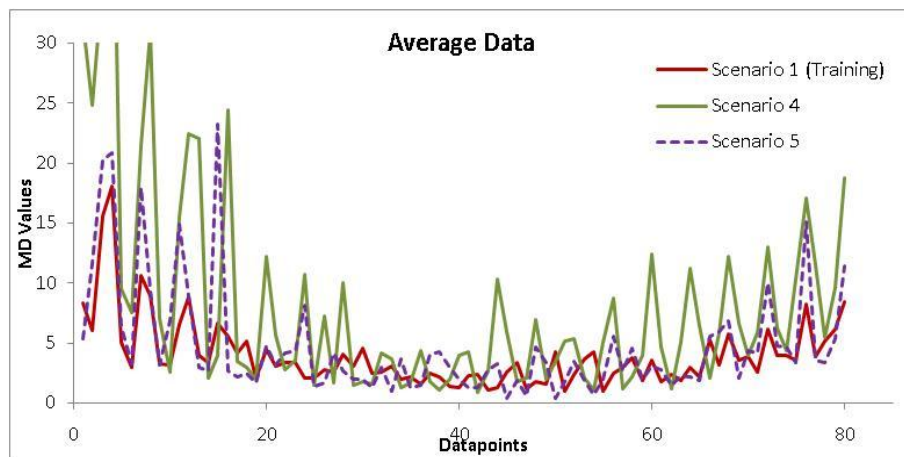


Figure 5-23: MD Analysis of Average Data for Scenarios 4 & 5 for Parrot

In appendix section 9.2.1 , the MD value histories for the MD analysis of maximum and minimum data over a three months period for the canary and parrot devices is shown. The observed results reflect similar trends as for MD analysis of the average data for the three performance parameters.

5.3.3. Results and discussion of fusion based prognostics tool

5.3.3.1. Developing the Bayesian Network model

The flowchart diagram in Figure 5-24 shows the steps taken to build and use the Bayesian network model for prognostic purposes using the demonstrator example detailed in the previous sections. Steps 1-3 involve building the model:

- Step 1 - the variables and relationships between the variables are represented using nodes and arcs to build the structure of the Bayesian network model.

- Step 2 - the states of each node are defined.
- Step 3 - involves defining the conditional probability table for each node.
- Step 4 - evidence propagation is performed every time monitoring data is available (i.e. data from PoF model, MD Analysis and other measurements) to obtain an updated probability distribution for predicted remaining life.
- Step 5 – Recommend inspection of structure if predicted remaining life is below acceptable level.

Steps 1-3 are repeated if the model needs updating with new training data.

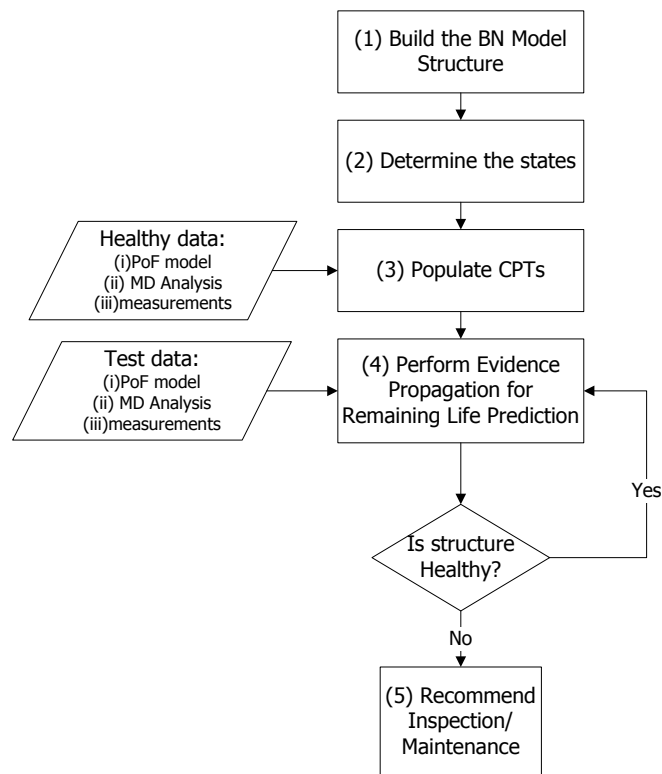


Figure 5-24: Flowchart Diagram of use Bayesian Network Model

The Bayesian network model used is shown in Figure 5-25. It is similar to the Bayesian network model shown in Figure 4-13 except for the lack of the ‘*Visual_Inspection*’ node. At the time of development of this example, information was not available regarding visual inspection and its relation to corrosion related damage of iron structures and thus for this example, this variable is not represented in the model.

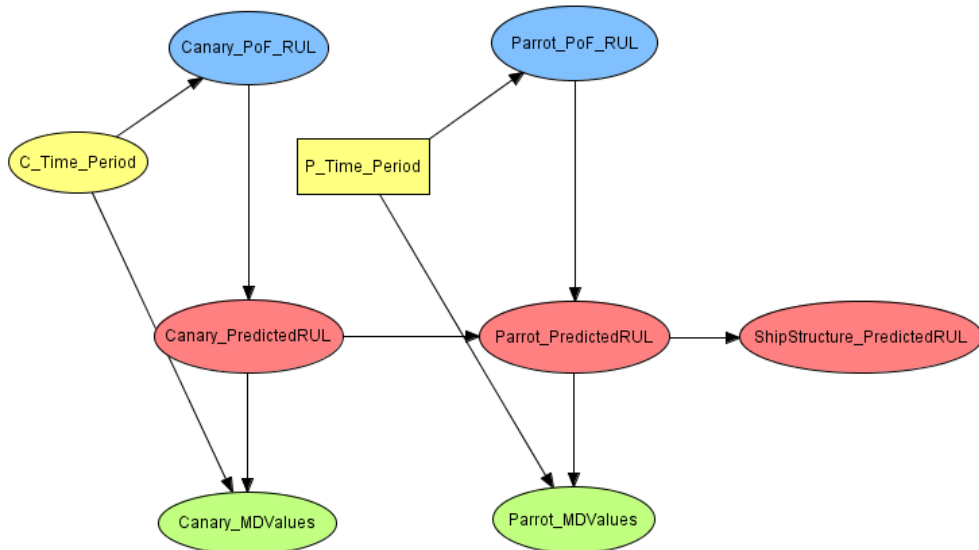


Figure 5-25: Bayesian Network Model for Demonstrator example

Table 5-11 illustrates what data is required to input in the model for probability inference of predicted remaining life of canary, parrot and ship structure. The values for the time variables $T_{c,i}$ and $T_{p,i}$ are set according to the current lifetime value of the canary and parrot devices respectively. $m_{c,i}$ and $m_{p,i}$ are the MD values for canary and parrot devices. $L_{c,i}$ and $L_{p,i}$ are the predicted remaining life using the PoF model.

Canary			Parrot		
Time	MD Values	PoF-based Predicted RUL	Time	MD Values	PoF-based Predicted RUL
$T_{c,1}$	$m_{c,1}$	$L_{c,1}$	$T_{p,1}$	$m_{p,1}$	$L_{p,1}$
$T_{c,2}$	$m_{c,2}$	$L_{c,2}$	$T_{p,2}$	$m_{p,2}$	$L_{p,2}$
$T_{c,3}$	$m_{c,3}$	$L_{c,3}$	$T_{p,3}$	$m_{p,3}$	$L_{p,3}$
...

Table 5-11: Input data required for inference using BN model

5.3.3.2. Populating the Conditional Probability Tables (CPTs)

This section provides detailed description of the populating of the CPTs for each node in the BN mode structure. The CPT describes the probability of a node being within a state given a combination of values of its parents' states. If a node has no parents, it is described by a marginal probability distribution. The values for the CPTs in this model are hypothetical and are intended for illustrative purposes only. The conditional probability tables for each node are devised as follows:

- *Canary_PoF_RUL* – the states for this variable are continuous and have been discretised into seven finite states represented by intervals ($-\infty - 0$, $0 - 1$, ..., $5 - \infty$) to reflect the 5 year lifetime of a canary device. This node has one parent node, *C_Time_Period*. Thus, the probabilities of the states of this node are conditional on the states of its parent nodes. For each state of node *C_Time_Period*, the probability distribution for node *Canary_PoF_RUL* follows a normal distribution with mean and variance from Table 5-12 representing the predicted remaining life from PoF model used in section 5.3.1 and is input in Hugin as shown in Figure 5-26.

Canary_PoF_RUL					
C_Time_Per...	1	2	3	4	5
Expression	Normal(2.59, 0.11)	Normal(2.1, 0.1)	Normal(1.8, 0.24)	Normal(1.1, 0.1)	Normal(0.31, 0.05)
C_Time_Per...	1	2	3	4	5
-inf - 0	2.878889E-15	1.560099E-11	0.000119	0.000252	0.082818
0 - 1	8.173177E-7	0.000252	0.051116	0.375663	0.916167
1 - 2	0.037626	0.375663	0.607219	0.621872	0.001015
2 - 3	0.854181	0.621872	0.334393	0.002213	2.047989E-14
3 - 4	0.108182	0.002213	0.007149	9.372337E-10	1.23512E-33
4 - 5	1.06262E-5	9.372337E-10	3.54892E-6	2.351849E-20	1.769359E-61
5 - inf	1.845649E-13	2.351849E-20	3.24545E-11	3.012589E-35	5.628488E-98

Figure 5-26: CPT for Canary_PoF_RUL Node in Hugin

- *Parrot_PoF_RUL* – the states for this variable are also continuous and have been discretized into 22 finite states represented by intervals ($-\infty - 0$, $0 - 1$, ..., $20 - \infty$) to represent the 20 year lifetime of a canary device. Similar to node *Canary_PoF_RUL*, the CPT for this node is populated using mean values and variance (from Table 5-12) of predicted remaining life from PoF model used in section 5.3.1.
- *C_Time_Period* – the states of this variable are discrete taking the values 1 to 5. This represents the number of years these devices are expected to be in operation. For demonstration purpose, the evidence is propagated in the network every year, hence the range of values for the states of this node being 1 to 5. The CPT is populated in Hugin as shown in Figure 5-27.

C_Time_Period	
1	0.2
2	0.2
3	0.2
4	0.2
5	0.2

Figure 5-27: CPT for C_Time_Period Node in Hugin

- *P_Time_Period* – similar to *C_Time_Period* node, the states of this variable are discrete but take the values 1 to 20.
- *Canary_MDValues* – The states here are continuous and have been discretised into 17 finite states represented by intervals ($-\infty - 0$, $0 - 1$, ..., $15 - \infty$) to represent the typical MD values expected during operation. This node has two parent nodes: *C_Time_Period* and *Canary_PredictedRUL*. The probabilities of the states of this node are conditional on how the state of its parent nodes combine and follows a normal distribution based on MD threshold values (Table 5-13) from MD analysis of precursors in section 5.3.2. The CPT is populated using the Expression Builder feature in Hugin shown in Figure 5-28.

Canary_MDValues																								
C_Time_Per...	1								2															
Canary_Pre...	-inf - 0	0 - 1	4 - 5	5 - inf	-inf - 0	0 - 1	4 - 5	5 - inf	-inf - 0	0 - 1								
Expression	Normal(6.268*(1+...				Normal(6.268*(1-...				Normal(6.268*(1+0				Normal(3.13*(1+2...				Normal(3.13*(1-2							
C_Time_Per...	1								2								3							
Canary_Pre...	-inf - 0	0 - 1	1 - 2	2 - 3	3 - 4	4 - 5	5 - inf	-inf - 0	0 - 1	5 - inf	-inf - 0	0 - 1								
-inf - 0	0	7.2944E-8	4.01913...	0.004326	0.039839	0.190439	7.19464...	0	2.9987E...	0	1.81541...	0.299265	0	1.20426...						
0 - 1	1	5.8193E-7	0.000172	0.009363	0.051402	0.133442	4.68985...	1	1.04028...	1	2.40302...	0.607469	1	6.5934E...						
1 - 2	0	4.3062E-6	0.000741	0.023306	0.089184	0.161175	2.89436...	0	6.25256...	0	1.12589...	0.0925	0	6.19751...						
2 - 3	0	2.67829...	0.002673	0.048776	0.130108	0.16369	0.00015	0	6.60596...	0	0.001975	0.000766	0	1.03264...						
3 - 4	0	0.00014	0.008111	0.08583	0.159601	0.139787	0.000655	0	0.001257	0	0.148462	2.64129...	0	0.00328						
4 - 5	0	0.000615	0.020693	0.126992	0.164621	0.100376	0.0024	0	0.044852	0	0.641414	3.36735...	0	0.241903						
5 - 6	0	0.002273	0.044386	0.15799	0.142776	0.060604	0.007397	0	0.318015	0	0.204244	1.5114E...	0	0.664511						
6 - 7	0	0.007061	0.080052	0.165273	0.104122	0.030766	0.019167	0	0.474505	0	0.00039	2.33201...	0	0.089926						
7 - 8	0	0.018437	0.121396	0.145377	0.063846	0.013132	0.041755	0	0.151333	0	3.27644...	1.22082...	0	0.000379						
8 - 9	0	0.040477	0.154791	0.107524	0.032918	0.004713	0.076481	0	0.009906	0	1.04123...	2.15136...	0	3.4056E...						
9 - 10	0	0.074717	0.165962	0.066869	0.01427	0.001422	0.117791	0	0.000125	0	1.17665...	1.26965...	0	5.65249...						
10 - 11	0	0.115969	0.149621	0.034966	0.005201	0.000361	0.152539	0	2.89843...	0	4.59442...	2.50061...	0	1.64179...						
11 - 12	0	0.151346	0.113421	0.015373	0.001594	7.68939...	0.166099	0	1.19363...	0	6.10461...	1.63952...	0	8.13446...						
12 - 13	0	0.166082	0.072294	0.005683	0.000411	1.37816...	0.152081	0	8.57309...	0	2.73537...	3.57185...	0	6.78081...						
13 - 14	0	0.153247	0.038746	0.001766	8.89023...	2.07619...	0.117085	0	1.06171...	0	4.10971...	2.5821E...	0	9.43189...						
14 - 15	0	0.1189	0.017459	0.000461	1.61832...	2.62883...	0.075795	0	2.25086...	0	2.06236...	6.18706...	0	2.1776E...						
15 - inf	0	0.150704	0.009441	0.000123	2.83234...	3.06765...	0.07057	0	8.12991...	0	3.44738...	4.90971...	0	8.31486...						

Figure 5-28: CPT for Canary_MDValues in Hugin

- *Parrot_MDValues* – the states are assigned the same as for the node *Canary_MDValues* and the CPT is populated using the same procedure as for that node using the values from Table 5-14.
- *Canary_PredictedRUL* – the states are similar to that of node *Canary_PoF_RUL*. However, this node has two parent nodes: *C_Time_Period* and *Canary_PoF_RUL*. Currently the probability distribution of predicted remaining life from node *Canary_PoF_RUL* is assumed to represent the probability distribution of predicted remaining life from node *Canary_Predicted_RUL*. Thus, the probability

distribution follows a normal distribution with the mean value being the current value of node *Canary_PoF_RUL* that is input in Hugin as shown in Figure 5-29.

Canary_PredictedRUL							
Expression	Normal (Canary_PoF_RUL, 0.2)						
Canary_Po...	-inf - 0	0 - 1	1 - 2	2 - 3	3 - 4	4 - 5	5 - inf
-inf - 0	0.987326	0.176386	0.001966	3.53006E-7	6.20433E-13	8.89159E-21	2.24337E-29
0 - 1	0.01267	0.647228	0.17442	0.001966	3.53005E-7	6.20433E-13	1.69173E-19
1 - 2	3.8721E-6	0.17442	0.647228	0.17442	0.001966	3.53005E-7	9.1247E-12
2 - 3	9.85172E-12	0.001966	0.17442	0.647228	0.17442	0.001966	3.67458E-6
3 - 4	1.87205E-19	3.53005E-7	0.001966	0.17442	0.647228	0.17442	0.012308
4 - 5	2.54473E-29	6.20433E-13	3.53005E-7	0.001966	0.17442	0.647228	0.483228
5 - inf	2.42321E-41	8.89159E-21	6.20433E-13	3.53006E-7	0.001966	0.176386	0.50446

Figure 5-29: CPT for Canary_PredictedRUL in Hugin

- *Parrot_PredictedRUL* – the states are similar to that of node *Parrot_PoF_RUL* and the CPT are similar to that of node *Canary_PoF_RUL*. However, this node has three parents’ nodes instead of two nodes: *P_Time_Period*, *Parrot_PoF_RUL* and *Canary_PredictedRUL*. The probability distribution for this node is assigned in same manner as for node *Canary_PredictedRUL* and is then adjusted to account for effect of node *Canary_PredictedRUL*. Here the correlation factor between predicted remaining lives of canary and parrot devices is assumed 0.2. Thus mean for the normal distribution is adjusted using the expression builder in Hugin as shown in Figure 5-30.

Parrot_PredictedRUL														
Expression	Normal (Parrot_PoF_RUL + Canary_PredictedRUL * 0.2, 0.2)													
Canary_Pre...	-inf - 0													
Parrot_PoF...	-inf - 0	0 - 1	1 - 2	...	18 - 19	19 - 20	20 - inf	-inf - 0	0 - 1	1 - 2	...	18 - 19	19 - 20	20 - inf
-inf - 0	0.996	0.289	0.007	...	0	0	0	0.977	0.133	0.001	...	0	0	0
0 - 1	0.004	0.615	0.283	...	0	0	0	0.023	0.636	0.132	...	0	0	0
1 - 2	4.342E-7	0.095	0.615	...	8.765E...	0	0	1.252E-5	0.227	0.636	...	0	0	0
2 - 3	4.171E...	4.99E-4	0.095	...	1.747E...	8.765E...	0	6.202E...	0.004	0.227	...	0	0	0
3 - 4	2.958E...	3.64E-8	4.99E-4	...	2.362E...	1.747E...	2.099E...	2.444E...	1.21E-6	0.004	...	0	0	0
4 - 5	1.493E...	2.469E...	3.64E-8	...	2.169E...	2.362E...	4.143E...	7.226E...	4.092E...	1.21E-6	...	0	0	0
5 - 6	5.261E...	1.337E...	2.469E...	...	1.355E...	2.169E...	5.535E...	1.551E...	1.207E...	4.092E...	...	0	0	0
6 - 7	1.282E...	5.406E...	1.337E...	...	5.771E...	1.355E...	5.008E...	2.369E...	2.823E...	1.207E...	...	0	0	0
7 - 8	2.145E...	1.575E...	5.406E...	...	1.68E...	5.771E...	3.072E...	2.54E-69	4.966E...	2.823E...	...	0	0	0
8 - 9	2.454E...	3.243E...	1.575E...	...	3.354E...	1.68E...	1.279E...	1.894E...	6.367E...	4.966E...	...	0	0	0
9 - 10	1.914E...	4.656E...	3.243E...	...	4.615E...	3.354E...	3.616E...	9.758E...	5.83E-71	6.367E...	...	0	0	0
10 - 11	1.016E...	4.624E...	4.656E...	...	4.406E...	4.615E...	6.963E...	3.457E...	3.76E-69	5.83E-71	...	0	0	0
11 - 12	3.66E...	3.158E...	4.624E...	...	2.947E...	4.406E...	9.15E-69	8.392E...	1.692E...	3.76E-69	...	0	0	0
12 - 13	8.947E...	1.477E...	3.158E...	...	1.402E...	2.947E...	8.234E...	1.392E...	5.272E...	1.692E...	...	0	0	0
13 - 14	1.482E...	4.717E...	1.477E...	...	4.862E...	1.402E...	5.099E...	1.575E...	1.132E...	5.272E...	...	0	0	0
14 - 15	1.662E...	1.026E...	4.717E...	...	1.286E...	4.862E...	2.19E-27	1.213E...	1.669E...	1.132E...	...	0	0	0
15 - 16	1.262E...	1.517E...	1.026E...	...	2.842E-6	1.286E...	6.609E...	6.348E...	1.683E...	1.669E...	...	0	0	0
16 - 17	0	1.523E...	1.517E...	...	0.007	2.842E-6	1.434E...	0	1.159E...	1.683E...	...	0	0	0
17 - 18	0	1.037E...	1.523E...	...	0.283	0.007	2.354E-5	0	5.439E...	1.159E...	...	0	0	0
18 - 19	0	0	1.037E...	...	0.615	0.283	0.033	0	0	5.439E...	...	0	0	0
19 - 20	0	0	0	...	0.095	0.615	0.623	0	0	0	...	0	0	0
20 - inf	0	0	0	...	4.99E-4	0.095	0.344	0	0	0	...	0	0	0

Figure 5-30: CPT for Parrot_PredictedRUL in Hugin

- *ShipStructure_PredictedRUL* – the states replicate that of node *Parrot_PredictedRUL*. This node has only one parent node: *Parrot_PredictedRUL*. At the moment, no

15	6.44	0.01		
16	4.99	0.07		
17	3.84	0.03		
18	2.79	0.01		
19	1.73	0.01		
20	0.64	0.01		

Table 5-12: PoF model-based input data

Time (years)	Mean MD	Standard Deviation	MD Threshold	Variance
1	12.72	0.81	13.53	0.97
2	7.77	1.00	8.77	1.51
3	5.10	0.57	5.67	0.48
4	3.68	0.203	3.88	0.06
5	3.27	0.13	3.40	0.02
6	3.19	0.31	3.50	0.15
7	2.83	0.09	2.92	0.01
8	2.78	0.20	2.97	0.06
9	2.41	0.76	3.16	0.86
10	2.20	0.26	2.45	0.10
11	2.15	0.17	2.31	0.04
12	1.97	0.33	2.29	0.16
13	2.51	0.21	2.72	0.07
14	2.62	0.43	3.05	0.28
15	2.96	0.38	3.34	0.22
16	2.39	0.07	2.46	0.01
17	3.89	0.79	4.67	0.92
18	3.90	0.68	4.59	0.70
19	4.58	0.31	4.89	0.14
20	5.52	0.49	6.01	0.37

Table 5-13: Input data for Parrot Device from MD Analysis Results

Time (yrs)	Mean MD	Standard Deviation	MD Threshold	Variance
1	6.26	1.95	8.21	5.69
2	3.13	0.61	3.74	0.56
3	2.29	0.44	2.73	0.29
4	2.67	0.40	3.08	0.24
5	3.78	0.33	4.11	0.17

Table 5-14: Input data for Canary Device from MD Analysis Results

The CPTs for the current model have been constructed with the best information available, which currently is drawn from a mix of expert opinion and relevant sets of data found in literature. As more data or knowledge becomes available, the CPTs will be adjusted to reflect improved learning data sets.

5.3.3.3. Testing the BN models

Once all the CPTs are specified, the BN model can be compiled and ‘run’. Scenarios have been devised and are examined. The predictions of the remaining life using the PoF models and the MD values from Mahalanobis Distance analysis are used as evidence input for nodes (*Canary_PoF_RUL*, *Parrot_PoF_RUL*, *Canary_MDValues* and *Parrot_MDValues*). The state for the nodes, C_Time_Period and P_Time_Period, representing time for canary device and parrot device are selected. The reasoning engine (using Hugin) for this Bayesian network model then performs propagation of probabilities and the scenario can be examined by its effects on the remaining nodes (i.e. hypothesis nodes, *Canary_PredictedRUL*, *Parrot_PredictedRUL* and *ShipStructure_PredictedRUL*) which display updated probability distributions. The scenarios tested for the Bayesian Network model developed are as follows:

- Scenario 1 (Normal “healthy” conditions) - Normal relative humidity and temperature for which the parrot device has life expectancy of 20 years while the canary device has a life expectancy of 5 years. At the end of the first five years, a new canary device with a life expectancy of 5 years is used, while the parrot device remains unchanged. This is repeated at the end of the next 5 years for two more times. Thus in total four canary devices are used (one for each 5-year period).
- Scenario 2 (Harsh conditions) - The parrot device experiences harsh environmental conditions from the beginning throughout its life (i.e. higher temperature and relative humidity compared with the normal case). The canary device experiences similar harsh conditions throughout its life. This scenario is used to demonstrate that the PHM framework can detect anomalies in canary/parrot devices right from the beginning should such a situation arise. Here Bayesian network analysis is carried out up to failure in canary device occurs. This reflects the real world situation where if the canary device were found to be deteriorating at a rate much faster than expected, then the parrot device would also be deteriorating at a faster rate. In such a case, further detailed inspection of the actual iron ship structure would be required.

- Scenario 3 (Mixed conditions): The parrot device experiences normal conditions during the first 10 years of its life and harsher conditions (i.e. higher temperature and relative humidity compared with the normal case) afterwards for the remaining of its life. Here for the first 10 years, the first three canary devices used (one for every 5-year period) experience normal conditions and the last canary device used experiences harsh conditions. This scenario aims to demonstrate that the PHM framework can detect anomalies that can occur later in the iron structures, which is reflected in canary/parrot devices. Here the amount of time after which the canary and parrot device experience higher corrosion rates has been chosen arbitrarily for the purpose of demonstration.

5.3.3.4. Analysis of Results

The graphs in Figure 5-32 provides a visual interpretation of the results of Scenario 1 for node *ShipStructure_PredictedRUL* from the Bayesian Network model built as detailed in section 5.3.3.1. The graph shows the probability distribution of remaining life of a “healthy” ship structure (experiencing normal environmental conditions throughout its life) over time. At year 1, higher probabilities are observed for a predicted remaining life of 6-8 years. The predicted remaining life is low due to high corrosion rates in the beginning but once the corrosion rates slows down over the next few years, the predicted remaining life increases. Thus, the probability distributions shift to the right for the next 8 years. For example at year 5, the probability distribution predicts a remaining life in the range of 11-12 years which reflects closely to what is expected for a prediction made after 5 years lifetime (i.e. 5 years plus predicted 12 years would be an overall possible lifetime of 17 years). After year 9, the probability distribution shift to the left as we enter the second part of the lifetime of the structure and thus predicted remaining life decreases accordingly.

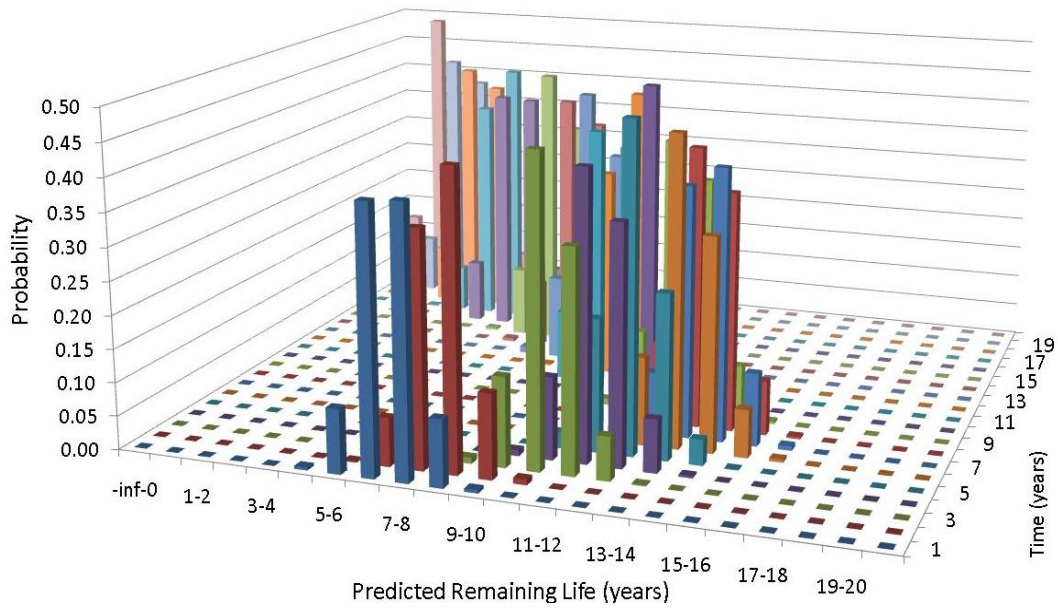


Figure 5-32: Probability Distribution of Predicted Remaining Life for Ship Structure (Scenario 1)

The graph in Figure 5-33 provides a visual interpretation of the results of Scenario 1 for nodes *Parrot_PredictedRUL*. The probability distributions of predicted remaining life follow the same trend as that of the graph for the ship structure. This is because the CPT of the ship structure is based on that of the CPT for the parrot device (as shown in Figure 5-33).

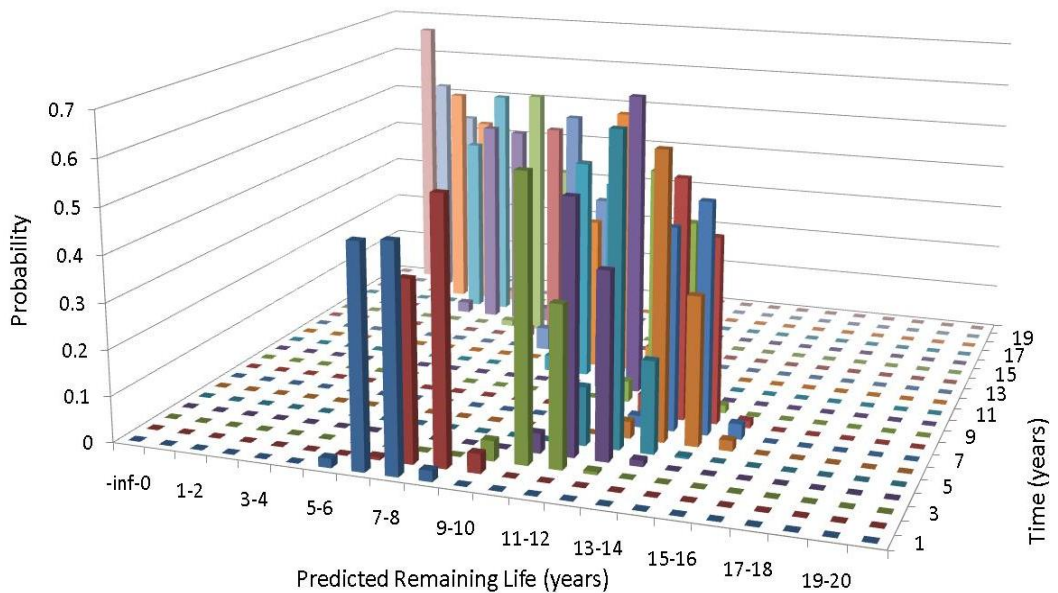


Figure 5-33: Probability Distribution of Predicted Remaining Life for Parrot Device (Scenario 1)

The graph in Figure 5-34 provides a visual interpretation of the results of Scenario 1 for node *Canary_PredictedRUL*. The graph shows the probability distribution of remaining life of the

four “healthy” canary devices over the 20-year period. At year 1, higher probabilities are observed for a predicted remaining life of 2-3 years. The predicted remaining life is less than the expected 4 years due to high corrosion rates in the beginning but once the corrosion rates slows down, the predicted remaining life increases. This cycle is repeated four times for each new canary device used after the 5-year period.

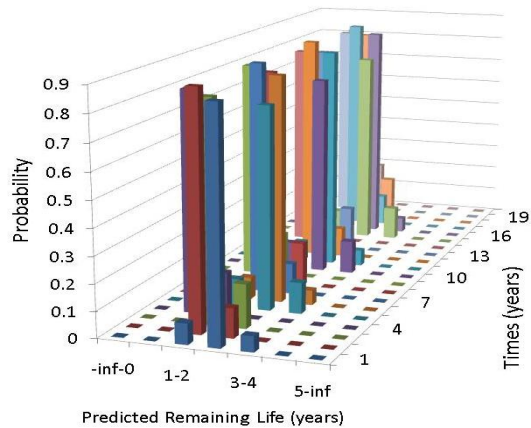


Figure 5-34: Probability Distribution of Predicted Remaining Life for Canary Device (Scenario 1)

The probability distribution graphs in Table 5-15 provide a numerical interpretation of the results of Scenario 1 for nodes *Canary_PredictedRUL*, *Parrot_PredictedRUL* and *ShipStructure_PredictedRUL*. Throughout scenario 1, only one parrot device is used for the 20-year period and four canary devices are used for the 20-year period (one for each 5-year period). Hence, in Table 5-15 at Time 1 and 5 years, the probability distribution for the first canary is shown. At Time 10 years, the probability distribution for the second canary is shown. At time 15 years, the probability distribution for the third canary is shown and at time 20 years, the probability distribution for the fourth canary is shown. At times 1, 5, 10, 15 and 20 years, the probability distribution for the one parrot and corresponding ship structure is shown.

At year 1, higher probabilities are observed for a predicted remaining life of 6-8 years for the Parrot and Ship Structure while for the Canary, higher probabilities are assigned for a predicted remaining life of 2-3 years. This is expected due to higher corrosion rates in the beginning as explained previously. The probability distributions shift as expected with time reflecting healthy structures for scenario 1. For example, at year 15, the probability distributions predict a remaining life in the range of 6-8 years for both the parrot and ship structure, while a remaining life in the range of 0-1 years is predicted for the canary device.

Time (yrs)	Canary	Parrot	Ship Structure																																																																										
1	<table border="1"> <thead> <tr> <th colspan="2">Canary_PredictedRUL</th> </tr> </thead> <tbody> <tr><td>0.00</td><td>-inf - 0</td></tr> <tr><td>9.66E-3</td><td>0 - 1</td></tr> <tr><td>9.96</td><td>1 - 2</td></tr> <tr><td>76.98</td><td>2 - 3</td></tr> <tr><td>13.01</td><td>3 - 4</td></tr> <tr><td>0.04</td><td>4 - 5</td></tr> <tr><td>4.69E-6</td><td>5 - inf</td></tr> </tbody> </table>	Canary_PredictedRUL		0.00	-inf - 0	9.66E-3	0 - 1	9.96	1 - 2	76.98	2 - 3	13.01	3 - 4	0.04	4 - 5	4.69E-6	5 - inf	<table border="1"> <thead> <tr> <th colspan="2">Parrot_PredictedRUL</th> </tr> </thead> <tbody> <tr><td>0.00</td><td>-inf - 0</td></tr> <tr><td>6.81E-78</td><td>0 - 1</td></tr> <tr><td>5.44E-52</td><td>1 - 2</td></tr> <tr><td>2.18E-31</td><td>2 - 3</td></tr> <tr><td>5.1E-16</td><td>3 - 4</td></tr> <tr><td>9.04E-6</td><td>4 - 5</td></tr> <tr><td>1.97</td><td>5 - 6</td></tr> <tr><td>47.49</td><td>6 - 7</td></tr> <tr><td>48.22</td><td>7 - 8</td></tr> <tr><td>2.32</td><td>8 - 9</td></tr> <tr><td>1.46E-3</td><td>9 - 10</td></tr> <tr><td>6.1E-9</td><td>10 - 11</td></tr> <tr><td>1.23E-16</td><td>11 - 12</td></tr> </tbody> </table>	Parrot_PredictedRUL		0.00	-inf - 0	6.81E-78	0 - 1	5.44E-52	1 - 2	2.18E-31	2 - 3	5.1E-16	3 - 4	9.04E-6	4 - 5	1.97	5 - 6	47.49	6 - 7	48.22	7 - 8	2.32	8 - 9	1.46E-3	9 - 10	6.1E-9	10 - 11	1.23E-16	11 - 12	<table border="1"> <thead> <tr> <th colspan="2">ShipStructure_PredictedRUL</th> </tr> </thead> <tbody> <tr><td>8.07E-26</td><td>-inf - 0</td></tr> <tr><td>5.63E-18</td><td>0 - 1</td></tr> <tr><td>4.41E-12</td><td>1 - 2</td></tr> <tr><td>7.13E-7</td><td>2 - 3</td></tr> <tr><td>3.89E-3</td><td>3 - 4</td></tr> <tr><td>0.44</td><td>4 - 5</td></tr> <tr><td>9.65</td><td>5 - 6</td></tr> <tr><td>39.50</td><td>6 - 7</td></tr> <tr><td>39.90</td><td>7 - 8</td></tr> <tr><td>10.01</td><td>8 - 9</td></tr> <tr><td>0.50</td><td>9 - 10</td></tr> <tr><td>4.83E-3</td><td>10 - 11</td></tr> <tr><td>3.69E-6</td><td>11 - 12</td></tr> <tr><td>5.28E-10</td><td>12 - 12</td></tr> </tbody> </table>	ShipStructure_PredictedRUL		8.07E-26	-inf - 0	5.63E-18	0 - 1	4.41E-12	1 - 2	7.13E-7	2 - 3	3.89E-3	3 - 4	0.44	4 - 5	9.65	5 - 6	39.50	6 - 7	39.90	7 - 8	10.01	8 - 9	0.50	9 - 10	4.83E-3	10 - 11	3.69E-6	11 - 12	5.28E-10	12 - 12
Canary_PredictedRUL																																																																													
0.00	-inf - 0																																																																												
9.66E-3	0 - 1																																																																												
9.96	1 - 2																																																																												
76.98	2 - 3																																																																												
13.01	3 - 4																																																																												
0.04	4 - 5																																																																												
4.69E-6	5 - inf																																																																												
Parrot_PredictedRUL																																																																													
0.00	-inf - 0																																																																												
6.81E-78	0 - 1																																																																												
5.44E-52	1 - 2																																																																												
2.18E-31	2 - 3																																																																												
5.1E-16	3 - 4																																																																												
9.04E-6	4 - 5																																																																												
1.97	5 - 6																																																																												
47.49	6 - 7																																																																												
48.22	7 - 8																																																																												
2.32	8 - 9																																																																												
1.46E-3	9 - 10																																																																												
6.1E-9	10 - 11																																																																												
1.23E-16	11 - 12																																																																												
ShipStructure_PredictedRUL																																																																													
8.07E-26	-inf - 0																																																																												
5.63E-18	0 - 1																																																																												
4.41E-12	1 - 2																																																																												
7.13E-7	2 - 3																																																																												
3.89E-3	3 - 4																																																																												
0.44	4 - 5																																																																												
9.65	5 - 6																																																																												
39.50	6 - 7																																																																												
39.90	7 - 8																																																																												
10.01	8 - 9																																																																												
0.50	9 - 10																																																																												
4.83E-3	10 - 11																																																																												
3.69E-6	11 - 12																																																																												
5.28E-10	12 - 12																																																																												
5	<table border="1"> <thead> <tr> <th colspan="2">Canary_PredictedRUL</th> </tr> </thead> <tbody> <tr><td>0.00</td><td>-inf - 0</td></tr> <tr><td>83.43</td><td>0 - 1</td></tr> <tr><td>16.56</td><td>1 - 2</td></tr> <tr><td>0.01</td><td>2 - 3</td></tr> <tr><td>7.82E-9</td><td>3 - 4</td></tr> <tr><td>1.85E-18</td><td>4 - 5</td></tr> <tr><td>8.82E-29</td><td>5 - inf</td></tr> </tbody> </table>	Canary_PredictedRUL		0.00	-inf - 0	83.43	0 - 1	16.56	1 - 2	0.01	2 - 3	7.82E-9	3 - 4	1.85E-18	4 - 5	8.82E-29	5 - inf	<table border="1"> <thead> <tr> <th colspan="2">Parrot_PredictedRUL</th> </tr> </thead> <tbody> <tr><td>4.31E-20</td><td>7 - 8</td></tr> <tr><td>6.8E-12</td><td>8 - 9</td></tr> <tr><td>7.98E-6</td><td>9 - 10</td></tr> <tr><td>0.08</td><td>10 - 11</td></tr> <tr><td>12.68</td><td>11 - 12</td></tr> <tr><td>66.91</td><td>12 - 13</td></tr> <tr><td>19.90</td><td>13 - 14</td></tr> <tr><td>0.42</td><td>14 - 15</td></tr> <tr><td>1.01E-4</td><td>15 - 16</td></tr> <tr><td>2.19E-10</td><td>16 - 17</td></tr> <tr><td>3.27E-18</td><td>17 - 18</td></tr> <tr><td>2.85E-28</td><td>18 - 19</td></tr> <tr><td>1.35E-40</td><td>19 - 20</td></tr> </tbody> </table>	Parrot_PredictedRUL		4.31E-20	7 - 8	6.8E-12	8 - 9	7.98E-6	9 - 10	0.08	10 - 11	12.68	11 - 12	66.91	12 - 13	19.90	13 - 14	0.42	14 - 15	1.01E-4	15 - 16	2.19E-10	16 - 17	3.27E-18	17 - 18	2.85E-28	18 - 19	1.35E-40	19 - 20	<table border="1"> <thead> <tr> <th colspan="2">ShipStructure_PredictedRUL</th> </tr> </thead> <tbody> <tr><td>4.55E-8</td><td>7 - 8</td></tr> <tr><td>1.72E-4</td><td>8 - 9</td></tr> <tr><td>0.04</td><td>9 - 10</td></tr> <tr><td>2.40</td><td>10 - 11</td></tr> <tr><td>19.93</td><td>11 - 12</td></tr> <tr><td>48.99</td><td>12 - 13</td></tr> <tr><td>24.65</td><td>13 - 14</td></tr> <tr><td>3.87</td><td>14 - 15</td></tr> <tr><td>0.11</td><td>15 - 16</td></tr> <tr><td>8.48E-4</td><td>16 - 17</td></tr> <tr><td>3.46E-7</td><td>17 - 18</td></tr> <tr><td>3.63E-11</td><td>18 - 19</td></tr> <tr><td>1.4E-16</td><td>19 - 20</td></tr> <tr><td>1.38E-22</td><td>20 - inf</td></tr> </tbody> </table>	ShipStructure_PredictedRUL		4.55E-8	7 - 8	1.72E-4	8 - 9	0.04	9 - 10	2.40	10 - 11	19.93	11 - 12	48.99	12 - 13	24.65	13 - 14	3.87	14 - 15	0.11	15 - 16	8.48E-4	16 - 17	3.46E-7	17 - 18	3.63E-11	18 - 19	1.4E-16	19 - 20	1.38E-22	20 - inf
Canary_PredictedRUL																																																																													
0.00	-inf - 0																																																																												
83.43	0 - 1																																																																												
16.56	1 - 2																																																																												
0.01	2 - 3																																																																												
7.82E-9	3 - 4																																																																												
1.85E-18	4 - 5																																																																												
8.82E-29	5 - inf																																																																												
Parrot_PredictedRUL																																																																													
4.31E-20	7 - 8																																																																												
6.8E-12	8 - 9																																																																												
7.98E-6	9 - 10																																																																												
0.08	10 - 11																																																																												
12.68	11 - 12																																																																												
66.91	12 - 13																																																																												
19.90	13 - 14																																																																												
0.42	14 - 15																																																																												
1.01E-4	15 - 16																																																																												
2.19E-10	16 - 17																																																																												
3.27E-18	17 - 18																																																																												
2.85E-28	18 - 19																																																																												
1.35E-40	19 - 20																																																																												
ShipStructure_PredictedRUL																																																																													
4.55E-8	7 - 8																																																																												
1.72E-4	8 - 9																																																																												
0.04	9 - 10																																																																												
2.40	10 - 11																																																																												
19.93	11 - 12																																																																												
48.99	12 - 13																																																																												
24.65	13 - 14																																																																												
3.87	14 - 15																																																																												
0.11	15 - 16																																																																												
8.48E-4	16 - 17																																																																												
3.46E-7	17 - 18																																																																												
3.63E-11	18 - 19																																																																												
1.4E-16	19 - 20																																																																												
1.38E-22	20 - inf																																																																												
10	<table border="1"> <thead> <tr> <th colspan="2">Canary_PredictedRUL</th> </tr> </thead> <tbody> <tr><td>0.00</td><td>-inf - 0</td></tr> <tr><td>83.33</td><td>0 - 1</td></tr> <tr><td>16.66</td><td>1 - 2</td></tr> <tr><td>0.01</td><td>2 - 3</td></tr> <tr><td>7.84E-9</td><td>3 - 4</td></tr> <tr><td>1.82E-18</td><td>4 - 5</td></tr> <tr><td>8.52E-29</td><td>5 - inf</td></tr> </tbody> </table>	Canary_PredictedRUL		0.00	-inf - 0	83.33	0 - 1	16.66	1 - 2	0.01	2 - 3	7.84E-9	3 - 4	1.82E-18	4 - 5	8.52E-29	5 - inf	<table border="1"> <thead> <tr> <th colspan="2">Parrot_PredictedRUL</th> </tr> </thead> <tbody> <tr><td>2.57E-12</td><td>7 - 8</td></tr> <tr><td>5.01E-6</td><td>8 - 9</td></tr> <tr><td>0.07</td><td>9 - 10</td></tr> <tr><td>12.10</td><td>10 - 11</td></tr> <tr><td>66.46</td><td>11 - 12</td></tr> <tr><td>21.13</td><td>12 - 13</td></tr> <tr><td>0.24</td><td>13 - 14</td></tr> <tr><td>3.73E-5</td><td>14 - 15</td></tr> <tr><td>4.27E-11</td><td>15 - 16</td></tr> <tr><td>2.66E-19</td><td>16 - 17</td></tr> <tr><td>7.48E-30</td><td>17 - 18</td></tr> <tr><td>8.78E-43</td><td>18 - 19</td></tr> <tr><td>4.32E-58</td><td>19 - 20</td></tr> </tbody> </table>	Parrot_PredictedRUL		2.57E-12	7 - 8	5.01E-6	8 - 9	0.07	9 - 10	12.10	10 - 11	66.46	11 - 12	21.13	12 - 13	0.24	13 - 14	3.73E-5	14 - 15	4.27E-11	15 - 16	2.66E-19	16 - 17	7.48E-30	17 - 18	8.78E-43	18 - 19	4.32E-58	19 - 20	<table border="1"> <thead> <tr> <th colspan="2">ShipStructure_PredictedRUL</th> </tr> </thead> <tbody> <tr><td>1.44E-4</td><td>7 - 8</td></tr> <tr><td>0.04</td><td>8 - 9</td></tr> <tr><td>2.29</td><td>9 - 10</td></tr> <tr><td>19.48</td><td>10 - 11</td></tr> <tr><td>48.81</td><td>11 - 12</td></tr> <tr><td>25.33</td><td>12 - 13</td></tr> <tr><td>3.97</td><td>13 - 14</td></tr> <tr><td>0.08</td><td>14 - 15</td></tr> <tr><td>4.88E-4</td><td>15 - 16</td></tr> <tr><td>1.58E-7</td><td>16 - 17</td></tr> <tr><td>1.34E-11</td><td>17 - 18</td></tr> <tr><td>3.82E-17</td><td>18 - 19</td></tr> <tr><td>2.69E-23</td><td>19 - 20</td></tr> <tr><td>5.45E-31</td><td>20 - inf</td></tr> </tbody> </table>	ShipStructure_PredictedRUL		1.44E-4	7 - 8	0.04	8 - 9	2.29	9 - 10	19.48	10 - 11	48.81	11 - 12	25.33	12 - 13	3.97	13 - 14	0.08	14 - 15	4.88E-4	15 - 16	1.58E-7	16 - 17	1.34E-11	17 - 18	3.82E-17	18 - 19	2.69E-23	19 - 20	5.45E-31	20 - inf
Canary_PredictedRUL																																																																													
0.00	-inf - 0																																																																												
83.33	0 - 1																																																																												
16.66	1 - 2																																																																												
0.01	2 - 3																																																																												
7.84E-9	3 - 4																																																																												
1.82E-18	4 - 5																																																																												
8.52E-29	5 - inf																																																																												
Parrot_PredictedRUL																																																																													
2.57E-12	7 - 8																																																																												
5.01E-6	8 - 9																																																																												
0.07	9 - 10																																																																												
12.10	10 - 11																																																																												
66.46	11 - 12																																																																												
21.13	12 - 13																																																																												
0.24	13 - 14																																																																												
3.73E-5	14 - 15																																																																												
4.27E-11	15 - 16																																																																												
2.66E-19	16 - 17																																																																												
7.48E-30	17 - 18																																																																												
8.78E-43	18 - 19																																																																												
4.32E-58	19 - 20																																																																												
ShipStructure_PredictedRUL																																																																													
1.44E-4	7 - 8																																																																												
0.04	8 - 9																																																																												
2.29	9 - 10																																																																												
19.48	10 - 11																																																																												
48.81	11 - 12																																																																												
25.33	12 - 13																																																																												
3.97	13 - 14																																																																												
0.08	14 - 15																																																																												
4.88E-4	15 - 16																																																																												
1.58E-7	16 - 17																																																																												
1.34E-11	17 - 18																																																																												
3.82E-17	18 - 19																																																																												
2.69E-23	19 - 20																																																																												
5.45E-31	20 - inf																																																																												
15	<table border="1"> <thead> <tr> <th colspan="2">Canary_PredictedRUL</th> </tr> </thead> <tbody> <tr><td>0.00</td><td>-inf - 0</td></tr> <tr><td>80.92</td><td>0 - 1</td></tr> <tr><td>19.06</td><td>1 - 2</td></tr> <tr><td>0.02</td><td>2 - 3</td></tr> <tr><td>1.22E-8</td><td>3 - 4</td></tr> <tr><td>3.3E-18</td><td>4 - 5</td></tr> <tr><td>1.67E-28</td><td>5 - inf</td></tr> </tbody> </table>	Canary_PredictedRUL		0.00	-inf - 0	80.92	0 - 1	19.06	1 - 2	0.02	2 - 3	1.22E-8	3 - 4	3.3E-18	4 - 5	1.67E-28	5 - inf	<table border="1"> <thead> <tr> <th colspan="2">Parrot_PredictedRUL</th> </tr> </thead> <tbody> <tr><td>1.14E-18</td><td>2 - 3</td></tr> <tr><td>3.88E-10</td><td>3 - 4</td></tr> <tr><td>3.45E-4</td><td>4 - 5</td></tr> <tr><td>1.32</td><td>5 - 6</td></tr> <tr><td>57.71</td><td>6 - 7</td></tr> <tr><td>39.77</td><td>7 - 8</td></tr> <tr><td>1.20</td><td>8 - 9</td></tr> <tr><td>6.87E-4</td><td>9 - 10</td></tr> <tr><td>4.47E-9</td><td>10 - 11</td></tr> <tr><td>2.55E-16</td><td>11 - 12</td></tr> <tr><td>1.09E-25</td><td>12 - 13</td></tr> <tr><td>3.21E-37</td><td>13 - 14</td></tr> <tr><td>6.6E-51</td><td>14 - 15</td></tr> </tbody> </table>	Parrot_PredictedRUL		1.14E-18	2 - 3	3.88E-10	3 - 4	3.45E-4	4 - 5	1.32	5 - 6	57.71	6 - 7	39.77	7 - 8	1.20	8 - 9	6.87E-4	9 - 10	4.47E-9	10 - 11	2.55E-16	11 - 12	1.09E-25	12 - 13	3.21E-37	13 - 14	6.6E-51	14 - 15	<table border="1"> <thead> <tr> <th colspan="2">ShipStructure_PredictedRUL</th> </tr> </thead> <tbody> <tr><td>1.23E-10</td><td>1 - 2</td></tr> <tr><td>1.14E-6</td><td>2 - 3</td></tr> <tr><td>2.68E-3</td><td>3 - 4</td></tr> <tr><td>0.34</td><td>4 - 5</td></tr> <tr><td>11.00</td><td>5 - 6</td></tr> <tr><td>44.52</td><td>6 - 7</td></tr> <tr><td>36.02</td><td>7 - 8</td></tr> <tr><td>7.83</td><td>8 - 9</td></tr> <tr><td>0.29</td><td>9 - 10</td></tr> <tr><td>2.5E-3</td><td>10 - 11</td></tr> <tr><td>1.78E-6</td><td>11 - 12</td></tr> <tr><td>2.52E-10</td><td>12 - 13</td></tr> <tr><td>2.01E-15</td><td>13 - 14</td></tr> <tr><td>2.87E-21</td><td>14 - 15</td></tr> </tbody> </table>	ShipStructure_PredictedRUL		1.23E-10	1 - 2	1.14E-6	2 - 3	2.68E-3	3 - 4	0.34	4 - 5	11.00	5 - 6	44.52	6 - 7	36.02	7 - 8	7.83	8 - 9	0.29	9 - 10	2.5E-3	10 - 11	1.78E-6	11 - 12	2.52E-10	12 - 13	2.01E-15	13 - 14	2.87E-21	14 - 15
Canary_PredictedRUL																																																																													
0.00	-inf - 0																																																																												
80.92	0 - 1																																																																												
19.06	1 - 2																																																																												
0.02	2 - 3																																																																												
1.22E-8	3 - 4																																																																												
3.3E-18	4 - 5																																																																												
1.67E-28	5 - inf																																																																												
Parrot_PredictedRUL																																																																													
1.14E-18	2 - 3																																																																												
3.88E-10	3 - 4																																																																												
3.45E-4	4 - 5																																																																												
1.32	5 - 6																																																																												
57.71	6 - 7																																																																												
39.77	7 - 8																																																																												
1.20	8 - 9																																																																												
6.87E-4	9 - 10																																																																												
4.47E-9	10 - 11																																																																												
2.55E-16	11 - 12																																																																												
1.09E-25	12 - 13																																																																												
3.21E-37	13 - 14																																																																												
6.6E-51	14 - 15																																																																												
ShipStructure_PredictedRUL																																																																													
1.23E-10	1 - 2																																																																												
1.14E-6	2 - 3																																																																												
2.68E-3	3 - 4																																																																												
0.34	4 - 5																																																																												
11.00	5 - 6																																																																												
44.52	6 - 7																																																																												
36.02	7 - 8																																																																												
7.83	8 - 9																																																																												
0.29	9 - 10																																																																												
2.5E-3	10 - 11																																																																												
1.78E-6	11 - 12																																																																												
2.52E-10	12 - 13																																																																												
2.01E-15	13 - 14																																																																												
2.87E-21	14 - 15																																																																												

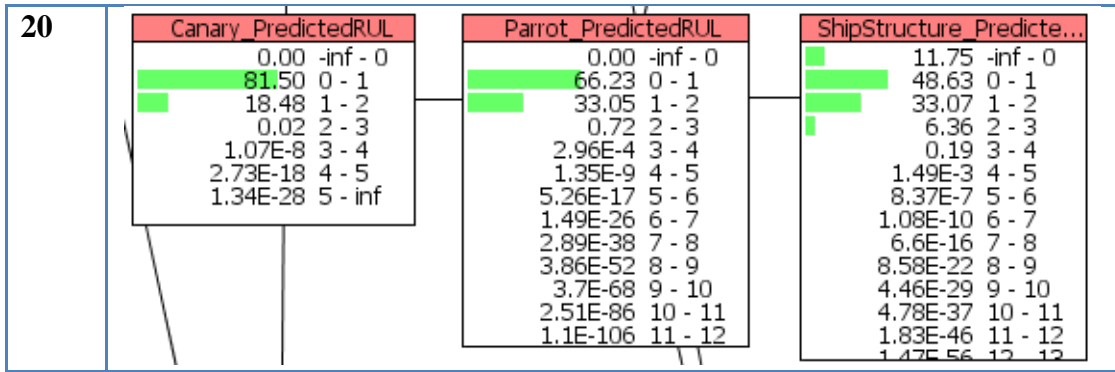


Table 5-15: Demonstrator Timeline for Scenario 1

The probability distribution graphs in Table 5-16 provides a numerical interpretation of the results of Scenario 2 for nodes *Canary_PredictedRUL*, *Parrot_PredictedRUL* and *ShipStructure_PredictedRUL*. At year 1, the probability distributions predict a remaining life in the range of 4-5 years for both the Parrot and Ship Structure while for the Canary; the predicted remaining life is in the range of 1-2 years. The range predicted is lower than that of scenario 1 as both canary and parrot devices as well as the ship structure experience harsher conditions from the beginning and throughout their lifetime. At year 5, the probability distributions predict a remaining life in the range of 5-7 years for both the parrot and ship structure instead of the expect range of 12-13 years as seen in Table 5-15 for year 5 predictions. This again confirms expected predictions for remaining life for scenario 2.

Time (yrs)	Canary	Parrot	Ship Structure																																								
1	<table border="1"> <tr><th colspan="2">Canary_PredictedRUL</th></tr> <tr><td>0.00 -inf - 0</td></tr> <tr><td>10.40 0 - 1</td></tr> <tr><td>84.52 1 - 2</td></tr> <tr><td>5.05 2 - 3</td></tr> <tr><td>0.03 3 - 4</td></tr> <tr><td>3.36E-6 4 - 5</td></tr> <tr><td>1.38E-4 5 - inf</td></tr> </table>	Canary_PredictedRUL		0.00 -inf - 0	10.40 0 - 1	84.52 1 - 2	5.05 2 - 3	0.03 3 - 4	3.36E-6 4 - 5	1.38E-4 5 - inf	<table border="1"> <tr><th colspan="2">Parrot_PredictedRUL</th></tr> <tr><td>0.00 -inf - 0</td></tr> <tr><td>1.59E-19 0 - 1</td></tr> <tr><td>1.78E-11 1 - 2</td></tr> <tr><td>2.04E-5 2 - 3</td></tr> <tr><td>0.29 3 - 4</td></tr> <tr><td>59.85 4 - 5</td></tr> <tr><td>37.52 5 - 6</td></tr> <tr><td>2.26 6 - 7</td></tr> <tr><td>0.08 7 - 8</td></tr> <tr><td>3.21E-6 8 - 9</td></tr> <tr><td>7.6E-13 9 - 10</td></tr> <tr><td>1.01E-21 10 - 11</td></tr> <tr><td>9.83E-33 11 - 12</td></tr> </table>	Parrot_PredictedRUL		0.00 -inf - 0	1.59E-19 0 - 1	1.78E-11 1 - 2	2.04E-5 2 - 3	0.29 3 - 4	59.85 4 - 5	37.52 5 - 6	2.26 6 - 7	0.08 7 - 8	3.21E-6 8 - 9	7.6E-13 9 - 10	1.01E-21 10 - 11	9.83E-33 11 - 12	<table border="1"> <tr><th colspan="2">ShipStructure_PredictedRUL</th></tr> <tr><td>7.42E-12 -inf - 0</td></tr> <tr><td>1.41E-7 0 - 1</td></tr> <tr><td>5.88E-4 1 - 2</td></tr> <tr><td>0.17 2 - 3</td></tr> <tr><td>10.70 3 - 4</td></tr> <tr><td>45.34 4 - 5</td></tr> <tr><td>35.12 5 - 6</td></tr> <tr><td>8.14 6 - 7</td></tr> <tr><td>0.52 7 - 8</td></tr> <tr><td>0.02 8 - 9</td></tr> <tr><td>1.64E-4 9 - 10</td></tr> <tr><td>3.56E-8 10 - 11</td></tr> <tr><td>1.19E-12 11 - 12</td></tr> <tr><td>2.26E-18 12 - 13</td></tr> </table>	ShipStructure_PredictedRUL		7.42E-12 -inf - 0	1.41E-7 0 - 1	5.88E-4 1 - 2	0.17 2 - 3	10.70 3 - 4	45.34 4 - 5	35.12 5 - 6	8.14 6 - 7	0.52 7 - 8	0.02 8 - 9	1.64E-4 9 - 10	3.56E-8 10 - 11	1.19E-12 11 - 12	2.26E-18 12 - 13
Canary_PredictedRUL																																											
0.00 -inf - 0																																											
10.40 0 - 1																																											
84.52 1 - 2																																											
5.05 2 - 3																																											
0.03 3 - 4																																											
3.36E-6 4 - 5																																											
1.38E-4 5 - inf																																											
Parrot_PredictedRUL																																											
0.00 -inf - 0																																											
1.59E-19 0 - 1																																											
1.78E-11 1 - 2																																											
2.04E-5 2 - 3																																											
0.29 3 - 4																																											
59.85 4 - 5																																											
37.52 5 - 6																																											
2.26 6 - 7																																											
0.08 7 - 8																																											
3.21E-6 8 - 9																																											
7.6E-13 9 - 10																																											
1.01E-21 10 - 11																																											
9.83E-33 11 - 12																																											
ShipStructure_PredictedRUL																																											
7.42E-12 -inf - 0																																											
1.41E-7 0 - 1																																											
5.88E-4 1 - 2																																											
0.17 2 - 3																																											
10.70 3 - 4																																											
45.34 4 - 5																																											
35.12 5 - 6																																											
8.14 6 - 7																																											
0.52 7 - 8																																											
0.02 8 - 9																																											
1.64E-4 9 - 10																																											
3.56E-8 10 - 11																																											
1.19E-12 11 - 12																																											
2.26E-18 12 - 13																																											
3	<table border="1"> <tr><th colspan="2">Canary_PredictedRUL</th></tr> <tr><td>0.00 -inf - 0</td></tr> <tr><td>100.00 0 - 1</td></tr> <tr><td>1.19E-5 1 - 2</td></tr> <tr><td>1.16E-10 2 - 3</td></tr> <tr><td>6.04E-18 3 - 4</td></tr> <tr><td>9.85E-28 4 - 5</td></tr> <tr><td>8.35E-38 5 - inf</td></tr> </table>	Canary_PredictedRUL		0.00 -inf - 0	100.00 0 - 1	1.19E-5 1 - 2	1.16E-10 2 - 3	6.04E-18 3 - 4	9.85E-28 4 - 5	8.35E-38 5 - inf	<table border="1"> <tr><th colspan="2">Parrot_PredictedRUL</th></tr> <tr><td>0.00 -inf - 0</td></tr> <tr><td>1.08E-20 0 - 1</td></tr> <tr><td>9.79E-12 1 - 2</td></tr> <tr><td>3.69E-5 2 - 3</td></tr> <tr><td>0.63 3 - 4</td></tr> <tr><td>56.48 4 - 5</td></tr> <tr><td>42.24 5 - 6</td></tr> <tr><td>0.65 6 - 7</td></tr> <tr><td>3.83E-4 7 - 8</td></tr> <tr><td>5.58E-9 8 - 9</td></tr> <tr><td>7.74E-16 9 - 10</td></tr> <tr><td>5.97E-25 10 - 11</td></tr> <tr><td>2.07E-36 11 - 12</td></tr> </table>	Parrot_PredictedRUL		0.00 -inf - 0	1.08E-20 0 - 1	9.79E-12 1 - 2	3.69E-5 2 - 3	0.63 3 - 4	56.48 4 - 5	42.24 5 - 6	0.65 6 - 7	3.83E-4 7 - 8	5.58E-9 8 - 9	7.74E-16 9 - 10	5.97E-25 10 - 11	2.07E-36 11 - 12	<table border="1"> <tr><th colspan="2">ShipStructure_PredictedRUL</th></tr> <tr><td>1.34E-11 -inf - 0</td></tr> <tr><td>2.93E-7 0 - 1</td></tr> <tr><td>1.26E-3 1 - 2</td></tr> <tr><td>0.22 2 - 3</td></tr> <tr><td>10.34 3 - 4</td></tr> <tr><td>44.04 4 - 5</td></tr> <tr><td>37.31 5 - 6</td></tr> <tr><td>7.90 6 - 7</td></tr> <tr><td>0.20 7 - 8</td></tr> <tr><td>1.36E-3 8 - 9</td></tr> <tr><td>9.83E-7 9 - 10</td></tr> <tr><td>1.46E-10 10 - 11</td></tr> <tr><td>2.21E-15 11 - 12</td></tr> <tr><td>2.24E-21 12 - 13</td></tr> </table>	ShipStructure_PredictedRUL		1.34E-11 -inf - 0	2.93E-7 0 - 1	1.26E-3 1 - 2	0.22 2 - 3	10.34 3 - 4	44.04 4 - 5	37.31 5 - 6	7.90 6 - 7	0.20 7 - 8	1.36E-3 8 - 9	9.83E-7 9 - 10	1.46E-10 10 - 11	2.21E-15 11 - 12	2.24E-21 12 - 13
Canary_PredictedRUL																																											
0.00 -inf - 0																																											
100.00 0 - 1																																											
1.19E-5 1 - 2																																											
1.16E-10 2 - 3																																											
6.04E-18 3 - 4																																											
9.85E-28 4 - 5																																											
8.35E-38 5 - inf																																											
Parrot_PredictedRUL																																											
0.00 -inf - 0																																											
1.08E-20 0 - 1																																											
9.79E-12 1 - 2																																											
3.69E-5 2 - 3																																											
0.63 3 - 4																																											
56.48 4 - 5																																											
42.24 5 - 6																																											
0.65 6 - 7																																											
3.83E-4 7 - 8																																											
5.58E-9 8 - 9																																											
7.74E-16 9 - 10																																											
5.97E-25 10 - 11																																											
2.07E-36 11 - 12																																											
ShipStructure_PredictedRUL																																											
1.34E-11 -inf - 0																																											
2.93E-7 0 - 1																																											
1.26E-3 1 - 2																																											
0.22 2 - 3																																											
10.34 3 - 4																																											
44.04 4 - 5																																											
37.31 5 - 6																																											
7.90 6 - 7																																											
0.20 7 - 8																																											
1.36E-3 8 - 9																																											
9.83E-7 9 - 10																																											
1.46E-10 10 - 11																																											
2.21E-15 11 - 12																																											
2.24E-21 12 - 13																																											

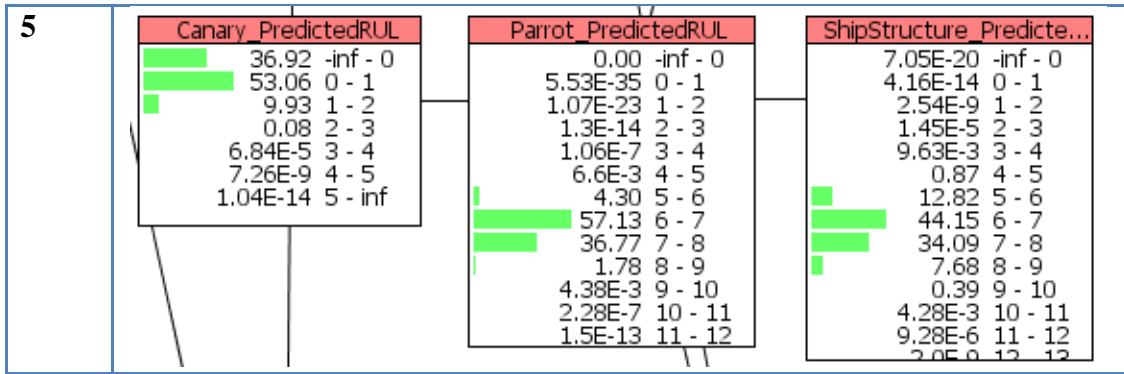


Table 5-16: Demonstrator Timeline for Scenario 2

The probability distribution graphs in Table 5-17 provide a numerical interpretation of the results of Scenario 3. Throughout scenario 3, only one parrot device is used and three canary devices are used (one for each 5-year period). In Table 5-17 at Time 1 and 5 years, the probability distribution for the first canary is shown. At Time 10 years, the probability distribution for the second canary is shown. At time 13 years, the probability distribution for the third canary is shown. At times 1, 5, 10 and 13 years, the probability distribution for the one parrot and corresponding ship structure is shown.

As per the scenario, the third canary device starts to experience harsher conditions from the beginning of its lifetime (from year 11 for the overall period of the scenario). The parrot device also starts to experience harsh conditions after year 10. At year 13, the predicted remaining life for the canary device experiencing harsh conditions is in the range of 0-1 years thus predicted to fail 2 years before expected for a health canary. The probability distributions predict a remaining life in the range of 4-6 years (instead of an expected 8-10 years for a healthy device) for the parrot device and the ship structure reflecting the effect of the probability distribution of the canary device. In a scenario 1, the probability distributions at year 15 would predict remaining life in the range of 6-8 years as shown in Table 5-15. In this case, the correlation factor assigned between the canary and parrot device seems effective to a certain extent in allowing events in the canary device to propagate to probability distributions of the parrot device. The results for scenarios 3 indicate that the CPTs for the nodes *Canary_PredictedRUL* and *Parrot_PredictedRUL* need to be adjusted in terms of correlation factor between the two devices in order to increase sensitivity.

Time (yrs)	Canary	Parrot	Ship Structure																																																																																																															
1	<table border="1"> <thead> <tr> <th colspan="3">Canary_PredictedRUL</th> </tr> </thead> <tbody> <tr><td>0.00</td><td>-inf</td><td>0</td></tr> <tr><td>0.01</td><td>0</td><td>1</td></tr> <tr><td>11.45</td><td>1</td><td>2</td></tr> <tr><td>77.38</td><td>2</td><td>3</td></tr> <tr><td>11.12</td><td>3</td><td>4</td></tr> <tr><td>0.03</td><td>4</td><td>5</td></tr> <tr><td>3.13E-6</td><td>5</td><td>-inf</td></tr> </tbody> </table>	Canary_PredictedRUL			0.00	-inf	0	0.01	0	1	11.45	1	2	77.38	2	3	11.12	3	4	0.03	4	5	3.13E-6	5	-inf	<table border="1"> <thead> <tr> <th colspan="3">Parrot_PredictedRUL</th> </tr> </thead> <tbody> <tr><td>0.00</td><td>-inf</td><td>0</td></tr> <tr><td>2.63E-55</td><td>0</td><td>1</td></tr> <tr><td>7.4E-34</td><td>1</td><td>2</td></tr> <tr><td>1.19E-17</td><td>2</td><td>3</td></tr> <tr><td>1.42E-6</td><td>3</td><td>4</td></tr> <tr><td>1.96</td><td>4</td><td>5</td></tr> <tr><td>76.18</td><td>5</td><td>6</td></tr> <tr><td>20.42</td><td>6</td><td>7</td></tr> <tr><td>1.44</td><td>7</td><td>8</td></tr> <tr><td>3.49E-4</td><td>8</td><td>9</td></tr> <tr><td>5.54E-10</td><td>9</td><td>10</td></tr> <tr><td>4.19E-18</td><td>10</td><td>11</td></tr> <tr><td>1.27E-28</td><td>11</td><td>12</td></tr> </tbody> </table>	Parrot_PredictedRUL			0.00	-inf	0	2.63E-55	0	1	7.4E-34	1	2	1.19E-17	2	3	1.42E-6	3	4	1.96	4	5	76.18	5	6	20.42	6	7	1.44	7	8	3.49E-4	8	9	5.54E-10	9	10	4.19E-18	10	11	1.27E-28	11	12	<table border="1"> <thead> <tr> <th colspan="3">ShipStructure_PredictedRUL</th> </tr> </thead> <tbody> <tr><td>8.99E-19</td><td>-inf</td><td>0</td></tr> <tr><td>1.72E-12</td><td>0</td><td>1</td></tr> <tr><td>6.96E-7</td><td>1</td><td>2</td></tr> <tr><td>3.89E-3</td><td>2</td><td>3</td></tr> <tr><td>0.49</td><td>3</td><td>4</td></tr> <tr><td>14.60</td><td>4</td><td>5</td></tr> <tr><td>53.21</td><td>5</td><td>6</td></tr> <tr><td>26.76</td><td>6</td><td>7</td></tr> <tr><td>4.65</td><td>7</td><td>8</td></tr> <tr><td>0.29</td><td>8</td><td>9</td></tr> <tr><td>2.91E-3</td><td>9</td><td>10</td></tr> <tr><td>1.2E-6</td><td>10</td><td>11</td></tr> <tr><td>1.25E-10</td><td>11</td><td>12</td></tr> <tr><td>4.12E-16</td><td>12</td><td>12</td></tr> </tbody> </table>	ShipStructure_PredictedRUL			8.99E-19	-inf	0	1.72E-12	0	1	6.96E-7	1	2	3.89E-3	2	3	0.49	3	4	14.60	4	5	53.21	5	6	26.76	6	7	4.65	7	8	0.29	8	9	2.91E-3	9	10	1.2E-6	10	11	1.25E-10	11	12	4.12E-16	12	12
Canary_PredictedRUL																																																																																																																		
0.00	-inf	0																																																																																																																
0.01	0	1																																																																																																																
11.45	1	2																																																																																																																
77.38	2	3																																																																																																																
11.12	3	4																																																																																																																
0.03	4	5																																																																																																																
3.13E-6	5	-inf																																																																																																																
Parrot_PredictedRUL																																																																																																																		
0.00	-inf	0																																																																																																																
2.63E-55	0	1																																																																																																																
7.4E-34	1	2																																																																																																																
1.19E-17	2	3																																																																																																																
1.42E-6	3	4																																																																																																																
1.96	4	5																																																																																																																
76.18	5	6																																																																																																																
20.42	6	7																																																																																																																
1.44	7	8																																																																																																																
3.49E-4	8	9																																																																																																																
5.54E-10	9	10																																																																																																																
4.19E-18	10	11																																																																																																																
1.27E-28	11	12																																																																																																																
ShipStructure_PredictedRUL																																																																																																																		
8.99E-19	-inf	0																																																																																																																
1.72E-12	0	1																																																																																																																
6.96E-7	1	2																																																																																																																
3.89E-3	2	3																																																																																																																
0.49	3	4																																																																																																																
14.60	4	5																																																																																																																
53.21	5	6																																																																																																																
26.76	6	7																																																																																																																
4.65	7	8																																																																																																																
0.29	8	9																																																																																																																
2.91E-3	9	10																																																																																																																
1.2E-6	10	11																																																																																																																
1.25E-10	11	12																																																																																																																
4.12E-16	12	12																																																																																																																
5	<table border="1"> <thead> <tr> <th colspan="3">Canary_PredictedRUL</th> </tr> </thead> <tbody> <tr><td>0.00</td><td>-inf</td><td>0</td></tr> <tr><td>80.42</td><td>0</td><td>1</td></tr> <tr><td>19.56</td><td>1</td><td>2</td></tr> <tr><td>0.02</td><td>2</td><td>3</td></tr> <tr><td>1.38E-8</td><td>3</td><td>4</td></tr> <tr><td>3.96E-18</td><td>4</td><td>5</td></tr> <tr><td>2.07E-28</td><td>5</td><td>-inf</td></tr> </tbody> </table>	Canary_PredictedRUL			0.00	-inf	0	80.42	0	1	19.56	1	2	0.02	2	3	1.38E-8	3	4	3.96E-18	4	5	2.07E-28	5	-inf	<table border="1"> <thead> <tr> <th colspan="3">Parrot_PredictedRUL</th> </tr> </thead> <tbody> <tr><td>0.00</td><td>-inf</td><td>0</td></tr> <tr><td>2.06E-22</td><td>0</td><td>1</td></tr> <tr><td>9.13E-14</td><td>1</td><td>2</td></tr> <tr><td>2.97E-7</td><td>2</td><td>3</td></tr> <tr><td>8.6E-3</td><td>3</td><td>4</td></tr> <tr><td>3.48</td><td>4</td><td>5</td></tr> <tr><td>49.06</td><td>5</td><td>6</td></tr> <tr><td>45.50</td><td>6</td><td>7</td></tr> <tr><td>1.95</td><td>7</td><td>8</td></tr> <tr><td>1.65E-3</td><td>8</td><td>9</td></tr> <tr><td>1.65E-8</td><td>9</td><td>10</td></tr> <tr><td>1.5E-15</td><td>10</td><td>11</td></tr> <tr><td>1.07E-24</td><td>11</td><td>12</td></tr> </tbody> </table>	Parrot_PredictedRUL			0.00	-inf	0	2.06E-22	0	1	9.13E-14	1	2	2.97E-7	2	3	8.6E-3	3	4	3.48	4	5	49.06	5	6	45.50	6	7	1.95	7	8	1.65E-3	8	9	1.65E-8	9	10	1.5E-15	10	11	1.07E-24	11	12	<table border="1"> <thead> <tr> <th colspan="3">ShipStructure_PredictedRUL</th> </tr> </thead> <tbody> <tr><td>1.1E-13</td><td>-inf</td><td>0</td></tr> <tr><td>3.62E-9</td><td>0</td><td>1</td></tr> <tr><td>1.82E-5</td><td>1</td><td>2</td></tr> <tr><td>8.37E-3</td><td>2</td><td>3</td></tr> <tr><td>0.71</td><td>3</td><td>4</td></tr> <tr><td>10.90</td><td>4</td><td>5</td></tr> <tr><td>40.30</td><td>5</td><td>6</td></tr> <tr><td>38.35</td><td>6</td><td>7</td></tr> <tr><td>9.30</td><td>7</td><td>8</td></tr> <tr><td>0.43</td><td>8</td><td>9</td></tr> <tr><td>4.14E-3</td><td>9</td><td>10</td></tr> <tr><td>3.94E-6</td><td>10</td><td>11</td></tr> <tr><td>6.16E-10</td><td>11</td><td>12</td></tr> <tr><td>6.84E-15</td><td>12</td><td>12</td></tr> </tbody> </table>	ShipStructure_PredictedRUL			1.1E-13	-inf	0	3.62E-9	0	1	1.82E-5	1	2	8.37E-3	2	3	0.71	3	4	10.90	4	5	40.30	5	6	38.35	6	7	9.30	7	8	0.43	8	9	4.14E-3	9	10	3.94E-6	10	11	6.16E-10	11	12	6.84E-15	12	12
Canary_PredictedRUL																																																																																																																		
0.00	-inf	0																																																																																																																
80.42	0	1																																																																																																																
19.56	1	2																																																																																																																
0.02	2	3																																																																																																																
1.38E-8	3	4																																																																																																																
3.96E-18	4	5																																																																																																																
2.07E-28	5	-inf																																																																																																																
Parrot_PredictedRUL																																																																																																																		
0.00	-inf	0																																																																																																																
2.06E-22	0	1																																																																																																																
9.13E-14	1	2																																																																																																																
2.97E-7	2	3																																																																																																																
8.6E-3	3	4																																																																																																																
3.48	4	5																																																																																																																
49.06	5	6																																																																																																																
45.50	6	7																																																																																																																
1.95	7	8																																																																																																																
1.65E-3	8	9																																																																																																																
1.65E-8	9	10																																																																																																																
1.5E-15	10	11																																																																																																																
1.07E-24	11	12																																																																																																																
ShipStructure_PredictedRUL																																																																																																																		
1.1E-13	-inf	0																																																																																																																
3.62E-9	0	1																																																																																																																
1.82E-5	1	2																																																																																																																
8.37E-3	2	3																																																																																																																
0.71	3	4																																																																																																																
10.90	4	5																																																																																																																
40.30	5	6																																																																																																																
38.35	6	7																																																																																																																
9.30	7	8																																																																																																																
0.43	8	9																																																																																																																
4.14E-3	9	10																																																																																																																
3.94E-6	10	11																																																																																																																
6.16E-10	11	12																																																																																																																
6.84E-15	12	12																																																																																																																
10	<table border="1"> <thead> <tr> <th colspan="3">Canary_PredictedRUL</th> </tr> </thead> <tbody> <tr><td>0.00</td><td>-inf</td><td>0</td></tr> <tr><td>80.19</td><td>0</td><td>1</td></tr> <tr><td>19.79</td><td>1</td><td>2</td></tr> <tr><td>0.02</td><td>2</td><td>3</td></tr> <tr><td>1.41E-8</td><td>3</td><td>4</td></tr> <tr><td>4.0E-18</td><td>4</td><td>5</td></tr> <tr><td>2.08E-28</td><td>5</td><td>-inf</td></tr> </tbody> </table>	Canary_PredictedRUL			0.00	-inf	0	80.19	0	1	19.79	1	2	0.02	2	3	1.41E-8	3	4	4.0E-18	4	5	2.08E-28	5	-inf	<table border="1"> <thead> <tr> <th colspan="3">Parrot_PredictedRUL</th> </tr> </thead> <tbody> <tr><td>0.00</td><td>-inf</td><td>0</td></tr> <tr><td>4.56E-50</td><td>0</td><td>1</td></tr> <tr><td>4.29E-36</td><td>1</td><td>2</td></tr> <tr><td>1.86E-24</td><td>2</td><td>3</td></tr> <tr><td>3.92E-15</td><td>3</td><td>4</td></tr> <tr><td>4.41E-8</td><td>4</td><td>5</td></tr> <tr><td>3.22E-3</td><td>5</td><td>6</td></tr> <tr><td>2.43</td><td>6</td><td>7</td></tr> <tr><td>47.80</td><td>7</td><td>8</td></tr> <tr><td>47.97</td><td>8</td><td>9</td></tr> <tr><td>1.80</td><td>9</td><td>10</td></tr> <tr><td>1.15E-3</td><td>10</td><td>11</td></tr> <tr><td>7.94E-9</td><td>11</td><td>12</td></tr> </tbody> </table>	Parrot_PredictedRUL			0.00	-inf	0	4.56E-50	0	1	4.29E-36	1	2	1.86E-24	2	3	3.92E-15	3	4	4.41E-8	4	5	3.22E-3	5	6	2.43	6	7	47.80	7	8	47.97	8	9	1.80	9	10	1.15E-3	10	11	7.94E-9	11	12	<table border="1"> <thead> <tr> <th colspan="3">ShipStructure_PredictedRUL</th> </tr> </thead> <tbody> <tr><td>2.82E-27</td><td>-inf</td><td>0</td></tr> <tr><td>2.88E-20</td><td>0</td><td>1</td></tr> <tr><td>1.76E-14</td><td>1</td><td>2</td></tr> <tr><td>1.22E-9</td><td>2</td><td>3</td></tr> <tr><td>7.19E-6</td><td>3</td><td>4</td></tr> <tr><td>5.35E-3</td><td>4</td><td>5</td></tr> <tr><td>0.52</td><td>5</td><td>6</td></tr> <tr><td>10.00</td><td>6</td><td>7</td></tr> <tr><td>39.73</td><td>7</td><td>8</td></tr> <tr><td>39.70</td><td>8</td><td>9</td></tr> <tr><td>9.63</td><td>9</td><td>10</td></tr> <tr><td>0.41</td><td>10</td><td>11</td></tr> <tr><td>3.76E-3</td><td>11</td><td>12</td></tr> <tr><td>2.0E-6</td><td>12</td><td>12</td></tr> </tbody> </table>	ShipStructure_PredictedRUL			2.82E-27	-inf	0	2.88E-20	0	1	1.76E-14	1	2	1.22E-9	2	3	7.19E-6	3	4	5.35E-3	4	5	0.52	5	6	10.00	6	7	39.73	7	8	39.70	8	9	9.63	9	10	0.41	10	11	3.76E-3	11	12	2.0E-6	12	12
Canary_PredictedRUL																																																																																																																		
0.00	-inf	0																																																																																																																
80.19	0	1																																																																																																																
19.79	1	2																																																																																																																
0.02	2	3																																																																																																																
1.41E-8	3	4																																																																																																																
4.0E-18	4	5																																																																																																																
2.08E-28	5	-inf																																																																																																																
Parrot_PredictedRUL																																																																																																																		
0.00	-inf	0																																																																																																																
4.56E-50	0	1																																																																																																																
4.29E-36	1	2																																																																																																																
1.86E-24	2	3																																																																																																																
3.92E-15	3	4																																																																																																																
4.41E-8	4	5																																																																																																																
3.22E-3	5	6																																																																																																																
2.43	6	7																																																																																																																
47.80	7	8																																																																																																																
47.97	8	9																																																																																																																
1.80	9	10																																																																																																																
1.15E-3	10	11																																																																																																																
7.94E-9	11	12																																																																																																																
ShipStructure_PredictedRUL																																																																																																																		
2.82E-27	-inf	0																																																																																																																
2.88E-20	0	1																																																																																																																
1.76E-14	1	2																																																																																																																
1.22E-9	2	3																																																																																																																
7.19E-6	3	4																																																																																																																
5.35E-3	4	5																																																																																																																
0.52	5	6																																																																																																																
10.00	6	7																																																																																																																
39.73	7	8																																																																																																																
39.70	8	9																																																																																																																
9.63	9	10																																																																																																																
0.41	10	11																																																																																																																
3.76E-3	11	12																																																																																																																
2.0E-6	12	12																																																																																																																
13	<table border="1"> <thead> <tr> <th colspan="3">Canary_PredictedRUL</th> </tr> </thead> <tbody> <tr><td>0.00</td><td>-inf</td><td>0</td></tr> <tr><td>100.00</td><td>0</td><td>1</td></tr> <tr><td>3.92E-5</td><td>1</td><td>2</td></tr> <tr><td>1.25E-9</td><td>2</td><td>3</td></tr> <tr><td>2.13E-16</td><td>3</td><td>4</td></tr> <tr><td>1.19E-25</td><td>4</td><td>5</td></tr> <tr><td>2.01E-35</td><td>5</td><td>-inf</td></tr> </tbody> </table>	Canary_PredictedRUL			0.00	-inf	0	100.00	0	1	3.92E-5	1	2	1.25E-9	2	3	2.13E-16	3	4	1.19E-25	4	5	2.01E-35	5	-inf	<table border="1"> <thead> <tr> <th colspan="3">Parrot_PredictedRUL</th> </tr> </thead> <tbody> <tr><td>0.00</td><td>-inf</td><td>0</td></tr> <tr><td>7.05E-14</td><td>0</td><td>1</td></tr> <tr><td>2.82E-7</td><td>1</td><td>2</td></tr> <tr><td>9.25E-3</td><td>2</td><td>3</td></tr> <tr><td>3.88</td><td>3</td><td>4</td></tr> <tr><td>52.36</td><td>4</td><td>5</td></tr> <tr><td>42.40</td><td>5</td><td>6</td></tr> <tr><td>1.34</td><td>6</td><td>7</td></tr> <tr><td>6.4E-4</td><td>7</td><td>8</td></tr> <tr><td>2.71E-9</td><td>8</td><td>9</td></tr> <tr><td>8.31E-17</td><td>9</td><td>10</td></tr> <tr><td>1.85E-26</td><td>10</td><td>11</td></tr> <tr><td>2.86E-38</td><td>11</td><td>12</td></tr> </tbody> </table>	Parrot_PredictedRUL			0.00	-inf	0	7.05E-14	0	1	2.82E-7	1	2	9.25E-3	2	3	3.88	3	4	52.36	4	5	42.40	5	6	1.34	6	7	6.4E-4	7	8	2.71E-9	8	9	8.31E-17	9	10	1.85E-26	10	11	2.86E-38	11	12	<table border="1"> <thead> <tr> <th colspan="3">ShipStructure_PredictedRUL</th> </tr> </thead> <tbody> <tr><td>3.82E-9</td><td>-inf</td><td>0</td></tr> <tr><td>1.96E-5</td><td>0</td><td>1</td></tr> <tr><td>9.27E-3</td><td>1</td><td>2</td></tr> <tr><td>0.79</td><td>2</td><td>3</td></tr> <tr><td>11.73</td><td>3</td><td>4</td></tr> <tr><td>41.97</td><td>4</td><td>5</td></tr> <tr><td>36.82</td><td>5</td><td>6</td></tr> <tr><td>8.37</td><td>6</td><td>7</td></tr> <tr><td>0.32</td><td>7</td><td>8</td></tr> <tr><td>2.76E-3</td><td>8</td><td>9</td></tr> <tr><td>1.73E-6</td><td>9</td><td>10</td></tr> <tr><td>2.32E-10</td><td>10</td><td>11</td></tr> <tr><td>1.35E-15</td><td>11</td><td>12</td></tr> <tr><td>1.71E-21</td><td>12</td><td>12</td></tr> </tbody> </table>	ShipStructure_PredictedRUL			3.82E-9	-inf	0	1.96E-5	0	1	9.27E-3	1	2	0.79	2	3	11.73	3	4	41.97	4	5	36.82	5	6	8.37	6	7	0.32	7	8	2.76E-3	8	9	1.73E-6	9	10	2.32E-10	10	11	1.35E-15	11	12	1.71E-21	12	12
Canary_PredictedRUL																																																																																																																		
0.00	-inf	0																																																																																																																
100.00	0	1																																																																																																																
3.92E-5	1	2																																																																																																																
1.25E-9	2	3																																																																																																																
2.13E-16	3	4																																																																																																																
1.19E-25	4	5																																																																																																																
2.01E-35	5	-inf																																																																																																																
Parrot_PredictedRUL																																																																																																																		
0.00	-inf	0																																																																																																																
7.05E-14	0	1																																																																																																																
2.82E-7	1	2																																																																																																																
9.25E-3	2	3																																																																																																																
3.88	3	4																																																																																																																
52.36	4	5																																																																																																																
42.40	5	6																																																																																																																
1.34	6	7																																																																																																																
6.4E-4	7	8																																																																																																																
2.71E-9	8	9																																																																																																																
8.31E-17	9	10																																																																																																																
1.85E-26	10	11																																																																																																																
2.86E-38	11	12																																																																																																																
ShipStructure_PredictedRUL																																																																																																																		
3.82E-9	-inf	0																																																																																																																
1.96E-5	0	1																																																																																																																
9.27E-3	1	2																																																																																																																
0.79	2	3																																																																																																																
11.73	3	4																																																																																																																
41.97	4	5																																																																																																																
36.82	5	6																																																																																																																
8.37	6	7																																																																																																																
0.32	7	8																																																																																																																
2.76E-3	8	9																																																																																																																
1.73E-6	9	10																																																																																																																
2.32E-10	10	11																																																																																																																
1.35E-15	11	12																																																																																																																
1.71E-21	12	12																																																																																																																

Table 5-17: Demonstrator Timeline for Scenario 3

From these preliminary results, the main observation is that the predictions of remaining life reflect the expected results for most scenarios. However, the accuracy of the prediction for the remaining life and the confidence in the predictions is not at the level expected for this PHM

framework. As more knowledge through more experiments and/or expert contribution is available, the CPTs should be revised to include improved and more comprehensive data set.

5.4. Summary

In this chapter, the diagnostic and prognostic tools described in the chapter 4 are evaluated and tested using a demonstration example. This example consisted of a canary and parrot device pair, with the canary device having smaller dimensions than the parrot device. A set of scenarios for canary/parrot pair was devised using simulated corrosion data for evaluation and testing of the tools. The predicted remaining life of the canary and parrot devices was calculated using the PoF model and compared for a set of scenarios. Similarly, anomaly detection was carried out on the devices using Mahalanobis distance analysis for all the scenarios. The results obtained for these two tools were close to that expected for the particular scenarios.

A Bayesian network model was used as a fusion prognostic tool to provide updated remaining life prediction for the canary and parrot devices. Additionally in this model, an iron structure was represented and was assigned similar prior probability distribution for predicted remaining life as that of the parrot device and the posterior probability distribution for the predicted remaining life is calculated. Here again the preliminary results are promising, however as developing Bayesian network model is an iterative process, it is expected that at the next iteration, the nodes the states of the nodes and the associated CPTs will be updated such that better precision can be achieved during prediction of remaining life.

One key element for improving the accuracy and confidence in diagnosis and prognosis is the correlation of damage detection and quantification of the canary/parrot sensor devices and the actual aged structure monitored. While simulation (e.g. simulation of corrosion data as used in the demonstration example in this chapter) is an effective way to enrich the data set, it is imperative to carry out evaluation and testing in the field in order to validate the tools such that reliable diagnosis and prognosis can be obtained. Data obtained from field use can then be used to update the models. Each variant of canary and parrot device pairs designed to monitor different failure mechanism needs to be calibrated with the actual structure to be monitored under varying environmental conditions. The next chapter describes how the diagnostic and prognostic tool were used during an experiment trial carried out on iron wire devices used as canary/parrot devices and discusses the results obtained.

6. Experimental Trials

6.1. Experimental Setup

An experiment was set up to investigate and test the diagnostic and prognostic tools developed. The following chapter describes the aims and the setup of the experiment. Then analysis of the data collected is carried out and the results are discussed. The aims of this experiment were threefold:

- Understand corrosion behavior of iron structures
 - To investigate the ranges of temperature and relative humidity that affects iron structures
 - To determine how much corrosion takes place under set temperature and relative humidity conditions
- Test suitability of canary and parrot sensor devices
 - To test whether the sensor devices designed are corroding at the expected rate within the set time under set environmental conditions.
 - To assess suitability of current corrosion parameters monitored
- Test PHM Framework
 - Test the data-driven diagnostic tool
 - Test the model-driven prognostic tool
 - Test the fusion based prognostic tool

6.1.1. Experimental Description

Prior to deploying a test-bed for experimental trials, the sensor devices to be used were investigated. There are many aspects of the design of the sensor devices to consider:

- The thickness of the sensor devices needed to be small enough to experience corrosion within a certain time limit.
- Protective paint or coating could be applied to the sensor devices to mimic the iron structures in the Cutty Sark.
- The actual shapes of the sensor devices and the interconnection

For the experimental setup, as a starting point, three iron wires of different diameter dimensions (0.125mm, 0.25mm and 0.5mm) and of 1m in length were used as shown in Figure 6-1.

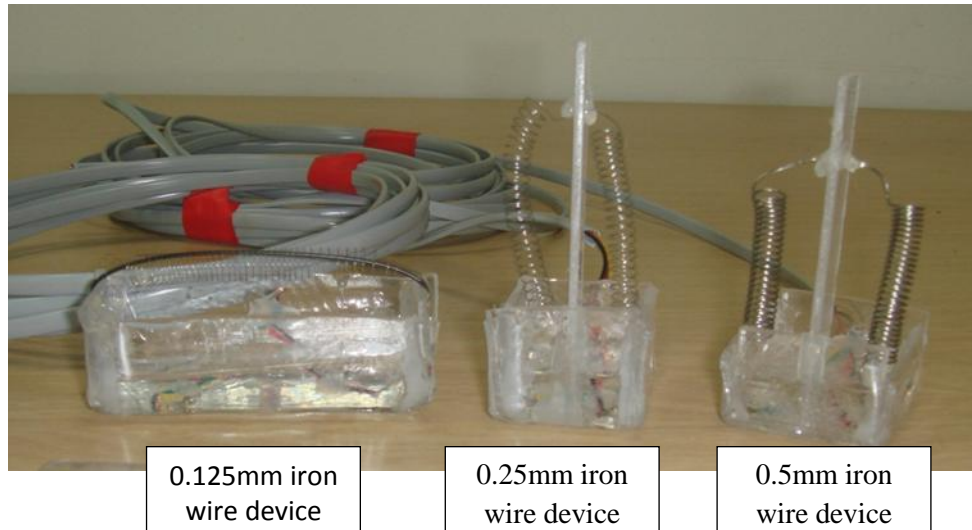


Figure 6-1: 3 sensor devices of diameter dimensions (0.125mm, 0.25mm and 0.5mm)

Three desiccators were used to house the three iron wires of different diameter dimensions. While all 3 desiccators were placed in the same room under normal room temperature, each desiccator had different relative humidity environments. Desiccator 1 had a dry environment. Desiccator 2 had water in the lower tray thus raising the relative humidity compared to Desiccator 1. Desiccator 3 had salt saturated water in the lower tray, thus experiencing the highest relative humidity and harshest environment of the three desiccators. Figure 6-2 shows the setup for the three desiccators.

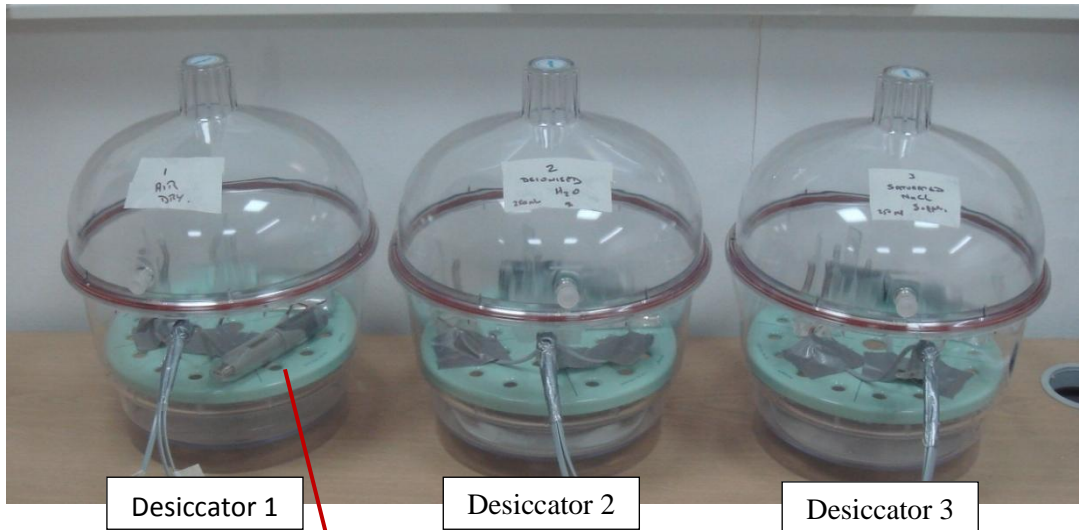


Figure 6-2: Experimental Setup of the 3 Desiccators

One data logger was placed in each desiccator measuring temperature and humidity at a rate of one sample every 15 minutes. The experiments were conducted for a total of 85 days from May to August 2010. Figure 6-3 and Figure 6-4 show the graphs for temperature and relative humidity for all the three desiccators for the month of May. The temperature readings for all the desiccator are within the same range as expected as the three desiccators were placed in the same room experiencing the same temperature throughout the experiment.

The relative humidity readings for desiccator 1 (dry) were in the range of 30%-40%, which is much lower than desiccators 2 and 3 as expected. The relative humidity readings for desiccator 3 (salty) were in the range of 80%-90% as expected. The relative humidity readings dropped to the 30%-40% range for 3 days for desiccator 3 at the end of the month of May, as

the experiment in desiccator 3 had been stopped and the iron wires were removed from that desiccator were subjected to further salt treatment. The data logger in the desiccator continued to record the relative humidity and temperature during that time thus registering the drop in relative humidity readings.

The iron wires connected to a PXI module and a data-logging script developed in Labview was used to record the electrical resistance of the wires every hour. The PXI module used to connect the iron wires to record the electrical resistance readings had only eight connectors available. As there was three sets of three iron wire devices for which the electrical resistance readings needed to be taken, the electrical resistance of the thickest wire (0.5mm) in desiccator 3 (dry environment) was only recorded at certain times. The electrical resistance readings of the other eight iron wire devices were recorded every hour. Once the salt iron devices failed the 0.5mm iron wire in desiccator 3, (dry environmental was then connected permanently to the PXI module and the electrical resistance readings were recorded every hour as well from then on.

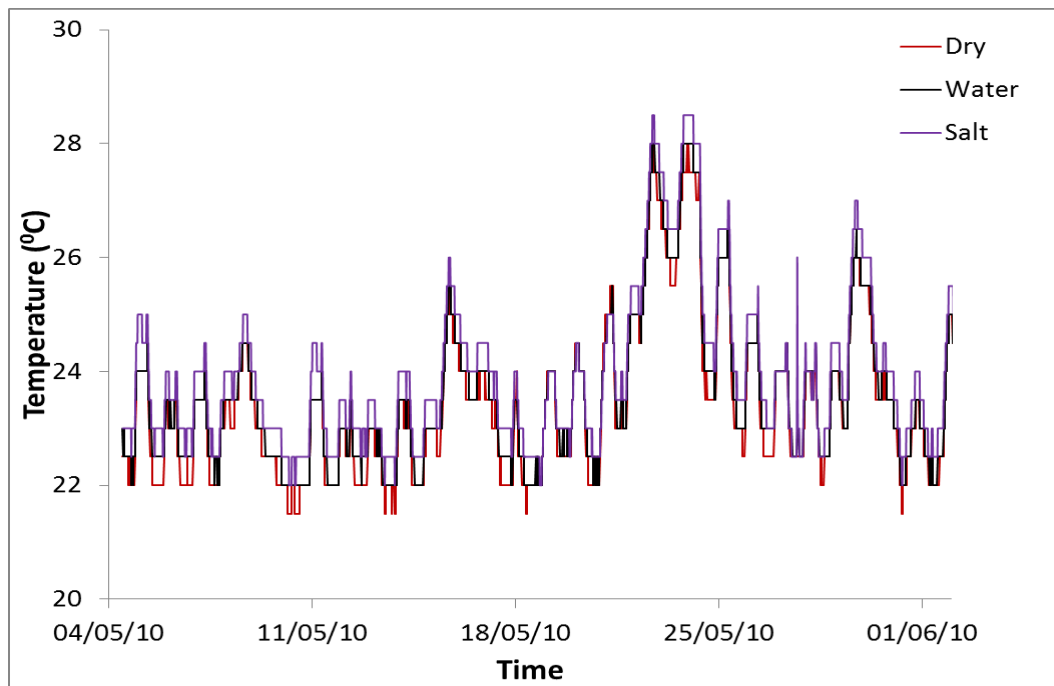


Figure 6-3: Temperature Readings for Desiccators 1, 2 & 3

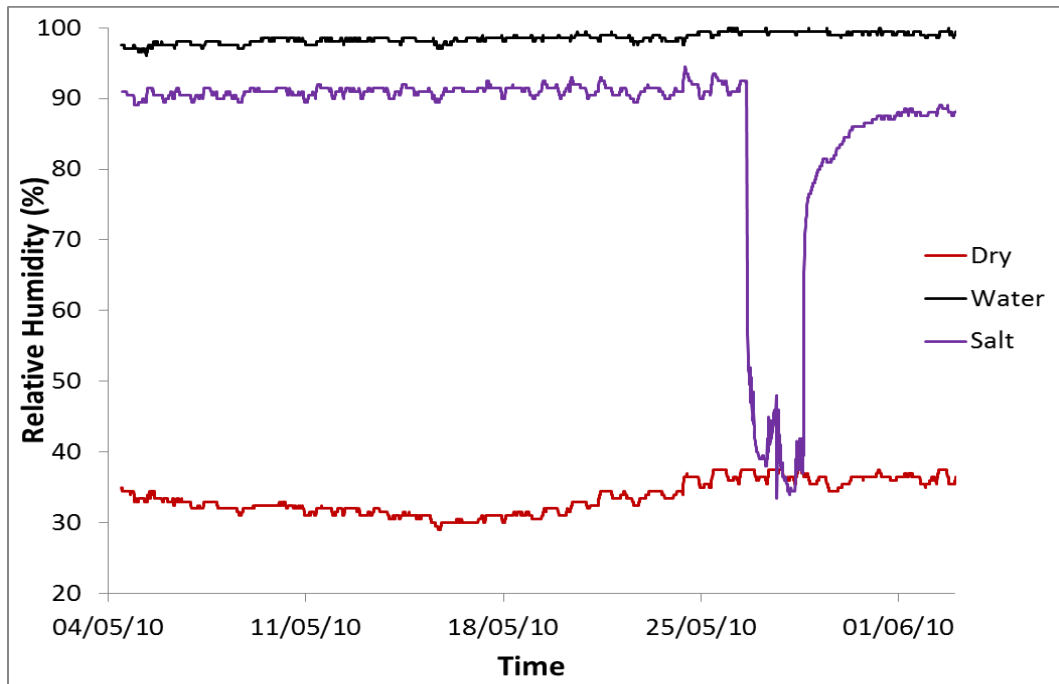


Figure 6-4: Relative Humidity Readings for Desiccators 1, 2 & 3

After running the experiment for 13 days, the electrical resistance readings for the eight iron wires being monitored remained stable indicating that the iron wires were not corroding. The wires in Desiccator 3 (salt water environment) were disconnected and soaked for 1 day in saturated salt water and left to dry for another day before being installed back in Desiccator 3 for further monitoring. The wires in Desiccator 1 and 2 were not treated further and monitoring continued for them as well. The experiment was then run until all the wires in Desiccator 3 (salt-water environment) were corroded. The experiment was run for another 5 days for the iron wires in desiccators 1 and 2. The drop in relative humidity as shown in Figure 6-4 between 26 May 2010 and 29 May 2010 is due to the desiccator being open at the time to remove the corroded 0.125mm and 0.25mm iron wires. The graphs for temperature and relative humidity for all the three desiccators throughout the whole experiment is found in appendix section 9.3.1.

6.2. Analysis of Experimental Data

Figure 6-5 to Figure 6-7 show the electrical resistance readings taken for the three wires (diameters 0.125mm, 0.25mm, 0.5mm) in desiccators 1, 2 and 3 during the whole experimental trial. Missing data points are due to the PXI system being restarted at times as the PXI module was disconnected from the PXI system when other unrelated experiments were loaded and run on the PXI system. In addition, there was no reading taken for 3 days

from 17 May 2010 and 20 May 2010 while the wires in Desiccator 3 were given additional treatment with the aim of accelerating the corrosion process.

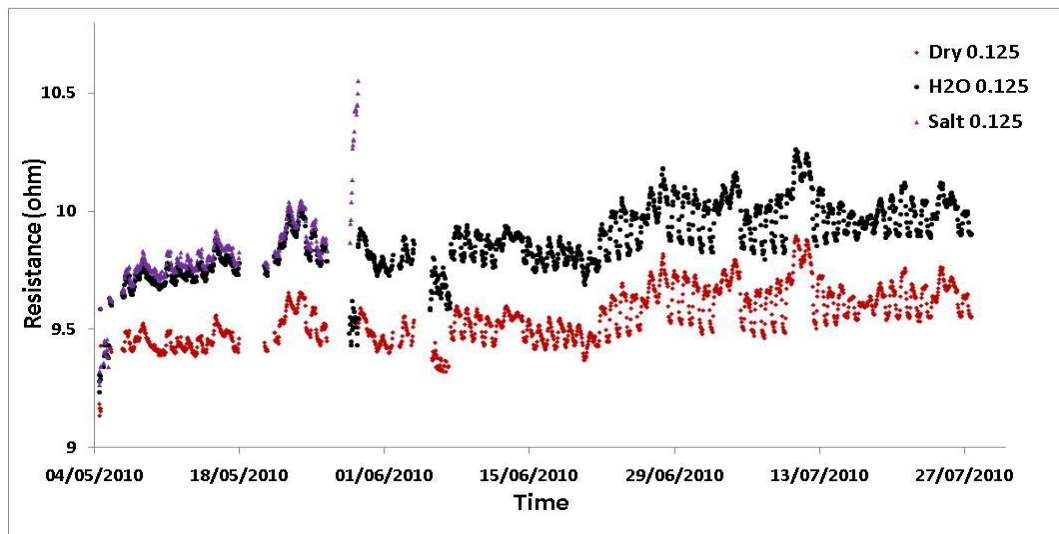


Figure 6-5: Electrical Resistance Readings for 0.125mm iron wires

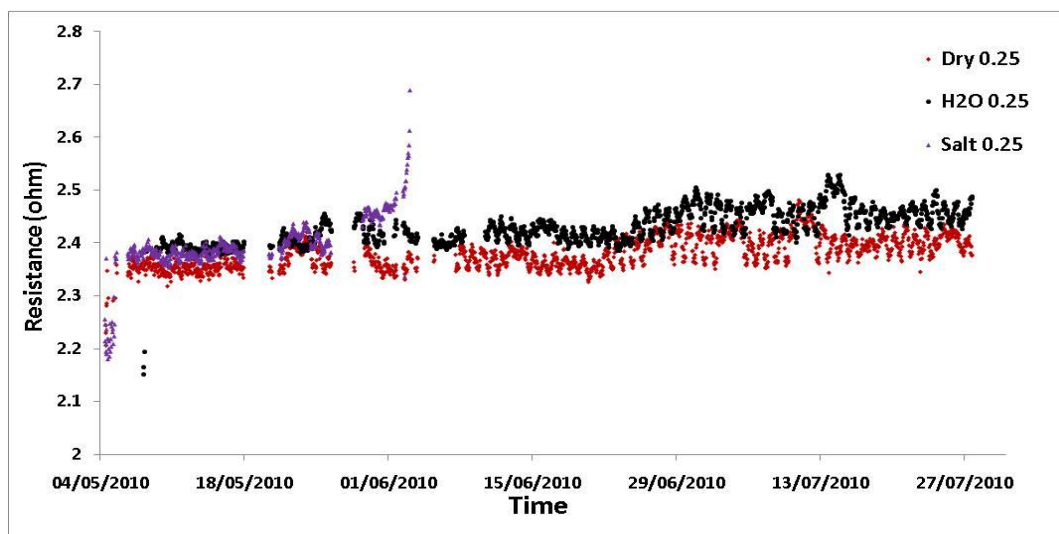


Figure 6-6: Electrical Resistance Readings for 0.25mm iron wires

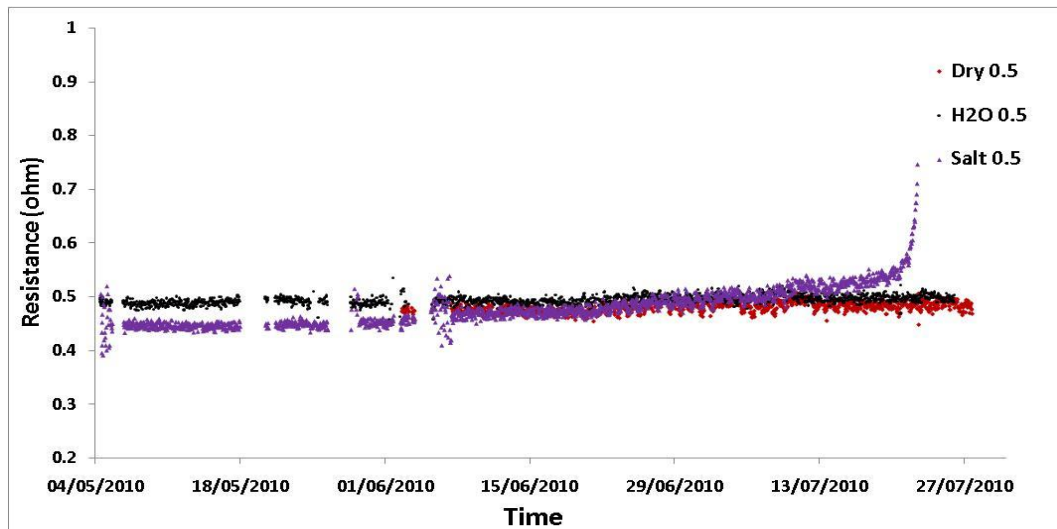


Figure 6-7: Electrical Resistance Readings for 0.5mm iron wires

As the electrical resistance readings for the same diameter, iron wire was plotted against each other, a trend in the readings was observed for 0.125mm and 0.25mm wires. While the 0.125mm wires were placed in different desiccators, they still experience the same trend in change in electrical resistance at the same time, thus implying that the different environments in the desiccators did not have the expected effect on the corrosion of the iron wires. The 0.5mm iron wires did not follow the same trend as observed for the other two types of iron wires.

After further investigation, it was determined that the room temperature was the cause of the noise to the measurement of the electrical resistance readings of the iron wires. Due to the thermal coefficient of the iron wires, the resistivity of the iron wires would change due to changes in temperature as well as corrosion that might occur. Figure 6-8 to Figure 6-10 show an overlay of readings of the temperature inside Desiccator 3 and the electrical resistance of the iron wires. It can be observed that the electrical resistance of 0.125mm iron wire device follows the same trend as the temperature (Figure 6-8). The same occurs for the 0.25mm iron wire device (Figure 6-9). The electrical resistance of the 0.5mm iron wire device however does not follow the same trend as the temperature (Figure 6-10) as the thermal coefficient was not high enough to affect the electrical resistance of the thickest iron wire device. The graphs of overlay of readings of the temperature inside desiccators 1 and 2 can be found in appendix section 9.3.2.

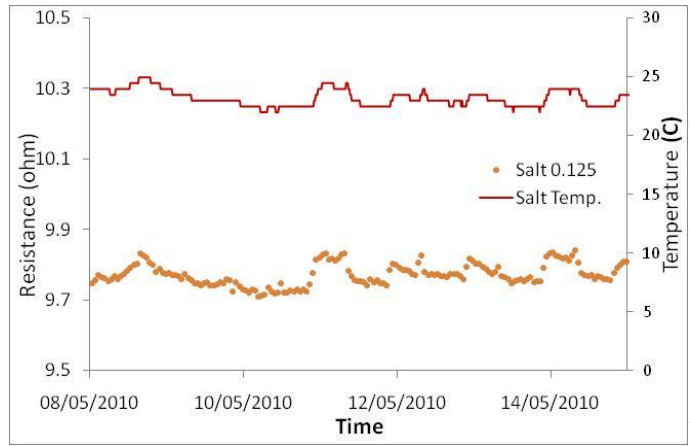


Figure 6-8: Overlay of Temperature and Resistance (0.125mm) -Salt Environment

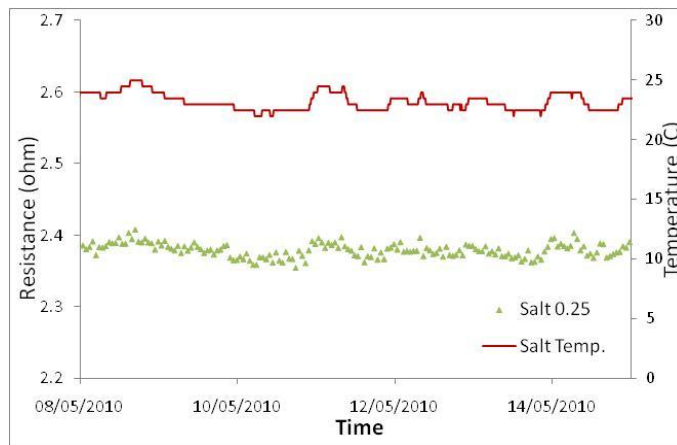


Figure 6-9: Overlay of Temperature and Resistance (0.25mm) -Salt Environment

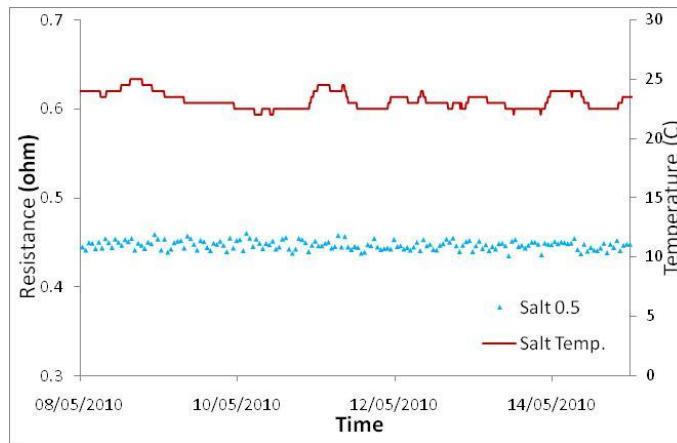


Figure 6-10: Overlay of Temperature and Resistance (0.5mm) -Salt Environment

6.2.1. Noise reduction of electrical resistance data

Figure 6-11 shows the steps carried out to remove the noise caused by the influence of temperature on the resistivity of the iron wires and to filter any additional noise:

1. As the actual resistivity for the iron wires used is unknown, resistivity ρ_{ref} of 9.71×10^{-8} ohm.m at temperature of 20°C (Resistivity and Temperature Coefficient, 2011) was used at the start to calculate ρ_t at temperature, T_t and time, t using equation (24).

$$\rho_t = \rho_{ref}[1 + \alpha(T_t - T_{ref})] \quad (24)$$

where, ρ_t is the resistivity at temperature T_t at time t , ρ_{ref} is the resistivity at reference temperature T_{ref} , α is the temperature coefficient of resistivity for the iron wire, T_t is the temperature at time t (during experiment) and T_{ref} is the reference temperature that α is specified at for the iron wire

2. Every time a new electrical resistance reading is taken, the resistivity ρ_{t+1} is calculated again using equation (25). This is performed, as the actual resistivity for the iron wires is unknown.

$$\rho_{t+1} = \rho_t[1 + \alpha(T_{t+1} - T_t)] \quad (25)$$

where, ρ_{t+1} is the resistivity at temperature T_{t+1} , ρ_t is the resistivity at reference temperature T_t , α is temperature coefficient of resistivity for the iron wire, T_{t+1} is temperature at time, $t+1$ (during experiment) and T_t is temperature for which ρ_t was calculated in step 1.

3. At each electrical resistance reading taken, using ρ obtained in step 2, R_t^{adj} is calculated using equation (26), representing the expected electrical resistance at temperature T_t .

$$R_t^{adj} = \frac{l * \rho_t}{A} \quad (26)$$

Where, ρ_t is the resistivity at temperature T at time t , l is the length of iron wire and A is the cross sectional area of iron wire

4. Finally, the difference in electrical resistance, ΔR_t , can be calculated using equation (27). ΔR_t is due to the corrosion of the iron wires without noise due to temperature effect on resistivity.

$$\Delta R_t = R_t^o - R_t^{adj} \quad (27)$$

Where, R_t^o is the original electrical resistance reading at time t and R_t^{adj} is the adjusted electrical resistance at time t

5. Using moving average (over a window size of 20), filtering of noise of random nature is carried out on ΔR_t
6. The resulting ΔR can then be used either in PoF models and/or for anomaly detection.

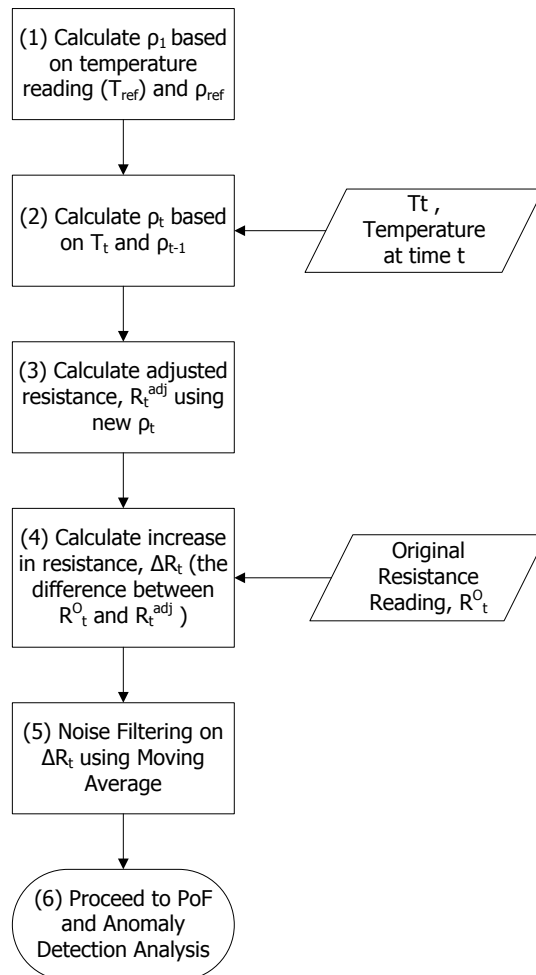


Figure 6-11: Flowchart of noise reduction of electrical resistance readings

The graphs for the 0.125mm (Figure 6-12) and 0.25mm (Figure 6-13) iron wires show the most marked difference between the original difference and adjusted difference of electrical

resistance. The graph for the 0.5 mm iron wires (Figure 6-14) shows almost no difference between the original and adjusted difference. This is believed to be because the temperature coefficient of the resistivity is not high enough to affect the electrical resistance of the 0.5mm iron wire and thus the original electrical resistance difference is used for the 0.5mm iron wire for the rest of the analysis. The graphs for resistance differences before and after the adjustment of temperature effect for iron wires in dry and water environments can be found in appendix section 9.3.3.

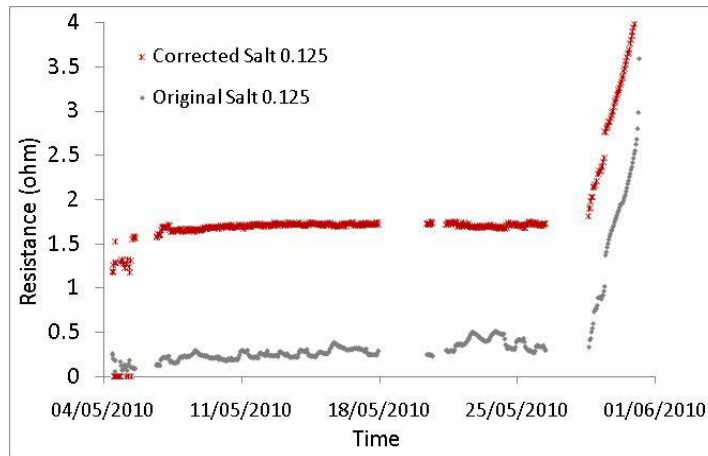


Figure 6-12: Resistance Difference before and after adjustment for temperature effect (0.125mm wire in salt environment)

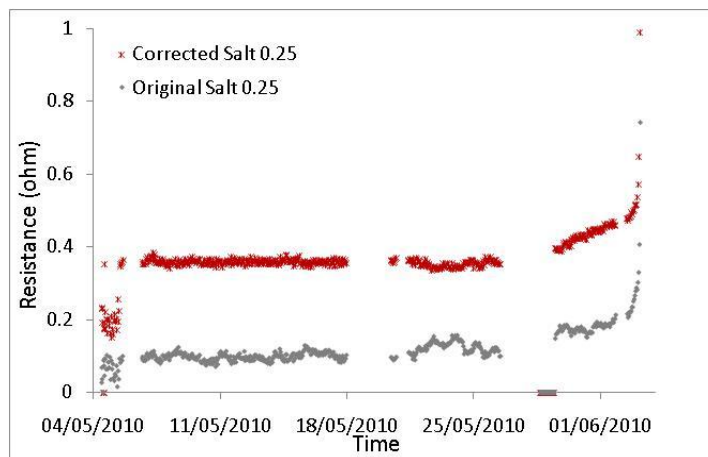


Figure 6-13: Electrical Resistance Difference before and after adjustment for temperature effect (0.25mm wire in salt environment)

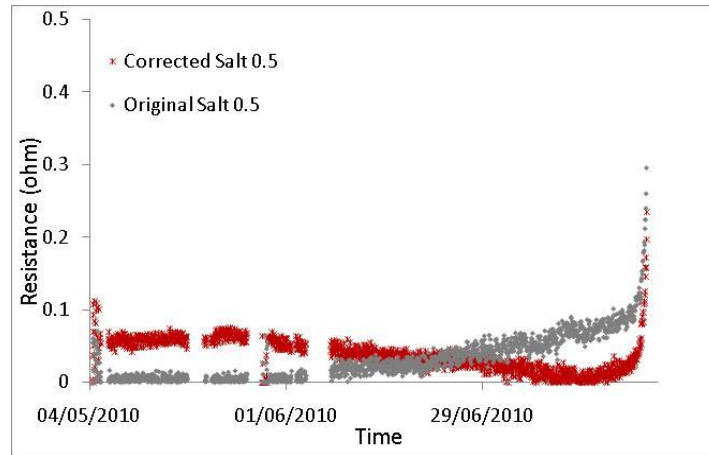


Figure 6-14: Electrical Resistance Difference before and after adjustment for temperature effect (0.5mm wire in salt environment)

The filtering of random noise on the electrical resistance difference was carried out using moving average and median. For both filters, a filtering weight of 20 was used. The results of both filtering techniques were assessed by applying standard deviation on the electrical resistance difference before and after filtering for readings taken in the first 7 days of the experimental trial. Table 6-1 shows the standard deviations for (i) original resistance difference, (ii) moving average filtered resistance difference and (iii) median filtered resistance difference. The standard deviations decrease when either filter is applied with the moving average filter giving slightly smaller standard deviations overall compared to the median filter. Therefore, the electrical resistance difference data that had undergone noise filtering using moving average filter was used from thereon. Figure 6-15 to Figure 6-17 show graphs for comparison of filters and the original data for 0.125mm, 0.25mm and 0.5mm iron wires in Desiccator 3 (salt environment).

	Original	Mov. Avg.	Median
Dry 0.125	0.0336	0.0299	0.0338
Dry 0.25	0.0134	0.0069	0.0088
Dry 0.5	0.0188	0.0255	0.0259
Water 0.125	0.0582	0.0535	0.0559
Water 0.25	0.0134	0.0093	0.0103
Water 0.5	0.0089	0.0050	0.0048
Salt 0.125	0.5243	0.4123	0.4113
Salt 0.25	0.0608	0.0445	0.0453
Salt 0.5	0.0223	0.0187	0.0190

Table 6-1: Standard Deviation of Electrical Resistance Deviation

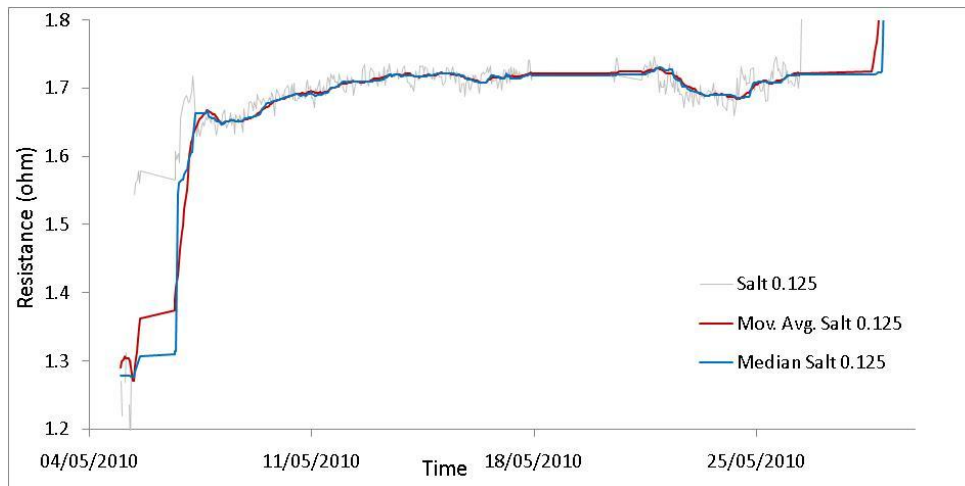


Figure 6-15: Comparison of using Moving Average and Median as smoothing technique for 0.125mm iron wire (salt environment)

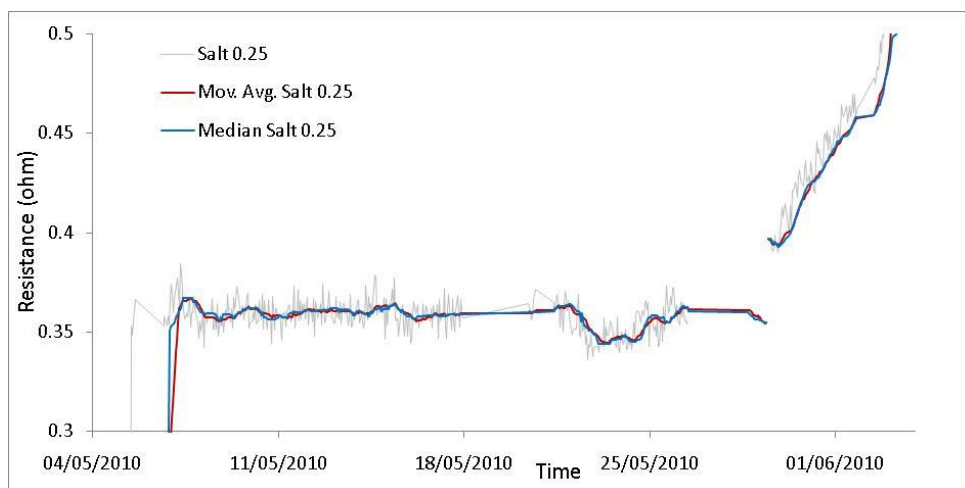


Figure 6-16: Comparison of using Moving Average and Median as smoothing technique for 0.25mm iron wire (salt environment)

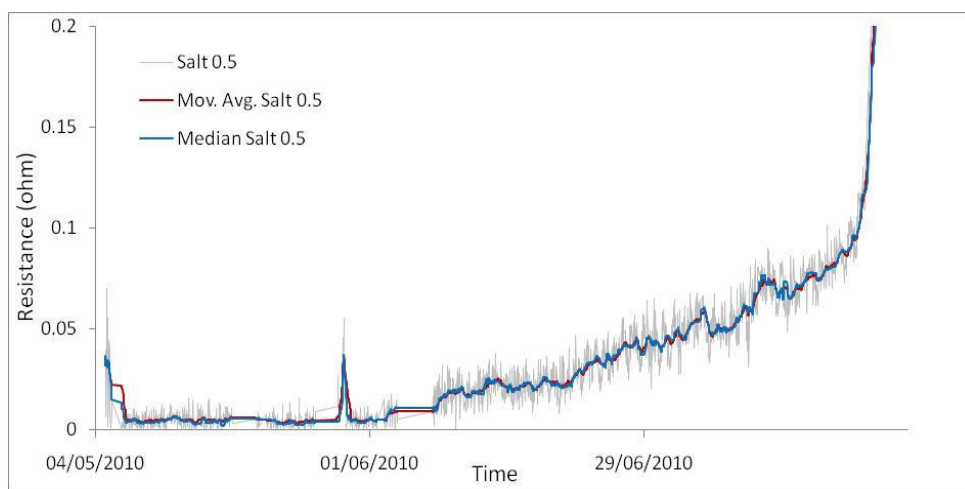


Figure 6-17: Comparison of using Moving Average and Median as smoothing technique for 0.5mm iron wire (salt environment)

6.2.2. Using PoF model to predict remaining life: Results and Discussions

Figure 6-18 shows the steps carried out to predict remaining life of the iron wires using the using the model-driven approach that uses a PoF model:

1. At each electrical resistance reading taken, using ρ of 0.097 ohm. μ m (Resistivity and Temperature Coefficient, 2011), the corresponding diameter is calculated using equation (28) and difference in diameter, ΔD .

$$D_t = \sqrt{\frac{\rho_{ref} * 4 * l * 1000000}{\pi * R_t}} \quad (28)$$

Where, ρ_{ref} is the reference resistivity (Resistivity and Temperature Coefficient, 2011) , l is the length of iron wire and R_t is the measured resistance of the iron wire

2. Plot ΔD against time
3. Use trend-line fitting over ΔD readings over a period of 10 days to obtain logarithmic model. Here due to the short period of time over which the experiment was run, only a short period is used in the trend-line fitting.
4. Estimated the corrosion penetration over 1st year, A , based on logarithmic model obtained (29).

$$P = At^B \quad (29)$$

Where P is corrosion penetration, t is exposure time, A is corrosion rate during the first year of measurement and B is a constant representing a measure of long-term decrease in corrosion rate. A and B are obtained through trend-line fitting, t is assigned to 365 days in order to obtain corrosion penetration over 1st year.

5. Calculate predicted remaining life of iron wires using equation (30). The model-driven approach defined in Chapter 4 has been modified here to accommodate for the lack of corrosion data required for over a year in order to use the Linear Bilogarithmic law for prediction of corrosion penetration over time. An arbitrary value of 0.5 is assigned to B while A is obtained from following the procedure detailed in steps 1-4.

$$t = e^{\frac{\ln(P) - \ln(A)}{B}} \quad (30)$$

Where, P is the loss in diameter (due to corrosion) which will lead to failure of iron wire, A is the corrosion penetration for the 1st year and B is the degree of decrease of corrosion over time (here assigned arbitrarily).

6. The predicted remaining life, t can then be used in the fusion based prognostic tool as input information for the Bayesian Network model.

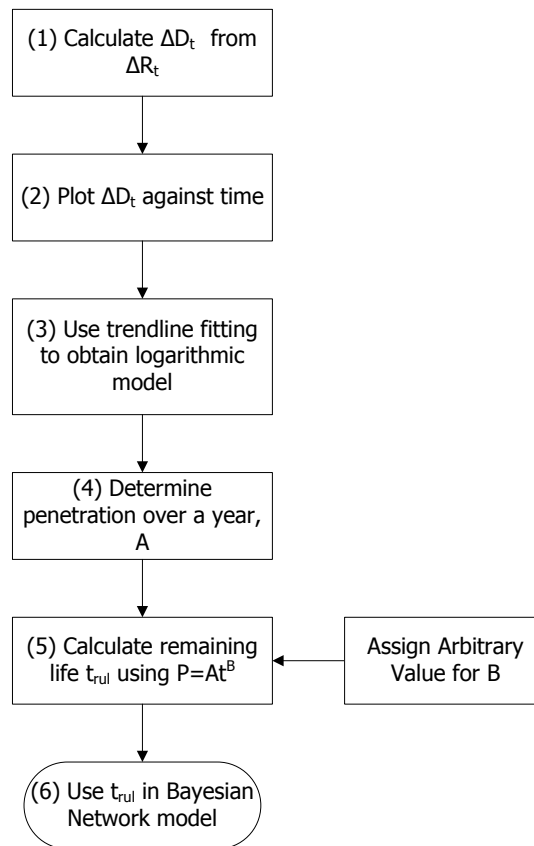


Figure 6-18: Flowchart - Predicting remaining life using PoF

Table 6-2 shows the predicted remaining life of the iron wires using the model-driven approach described above in years (T) and in days (t). A is the estimated corrosion rate over the first year. For all three different environments, the thickest wire (0.5mm) has the longest predicted remaining life as expected. For the water and salt environments, the thinnest wire (0.125mm) has the shortest predicted remaining life, while for the dry environment the 0.25m has the shortest predicted remaining life. Here it is believed that due to errors in measurement

procedures, the predicted remaining life for the iron wires in the dry environment is not as accurate as expected.

It should be noted that when using the Linear-Bilogarithmic law as a PoF model, it is recommended to use data recorded over the first year before making any prediction. As the experiment was run for just under 3 months, the measurement readings were extrapolated first before being used in the PoF model. This could have a significant effect on the values of the predicted remaining life of the iron wires. However, the PoF model developed here is believed to be a good starting prediction model for remaining life of iron wires (with respect to failure being caused by corrosion).

	A (mm/year)	T (years)	t(days)
Dry 0.125	10.59	5.58	2036
Dry 025	22.90	4.77	1740
Dry 0.5	15.78	40.15	14656
Water 0.125	13.84	3.26	1191
Water 0.25	24.58	4.14	1511
Water 0.5	9.44	112.13	40929
Salt 0.125	14.21	3.09	1130
Salt 0.25	20.61	5.88	2147
Salt 0.5	27.07	13.65	4981

Table 6-2: Prediction of Remaining life of iron wires

6.2.3. Data-Driven Approach: Using Mahalanobis Distance Analysis for Anomaly Detection

Figure 6-19 shows the steps carried out to perform anomaly detection on the iron wires in the three different environments using Mahalanobis Distance analysis.

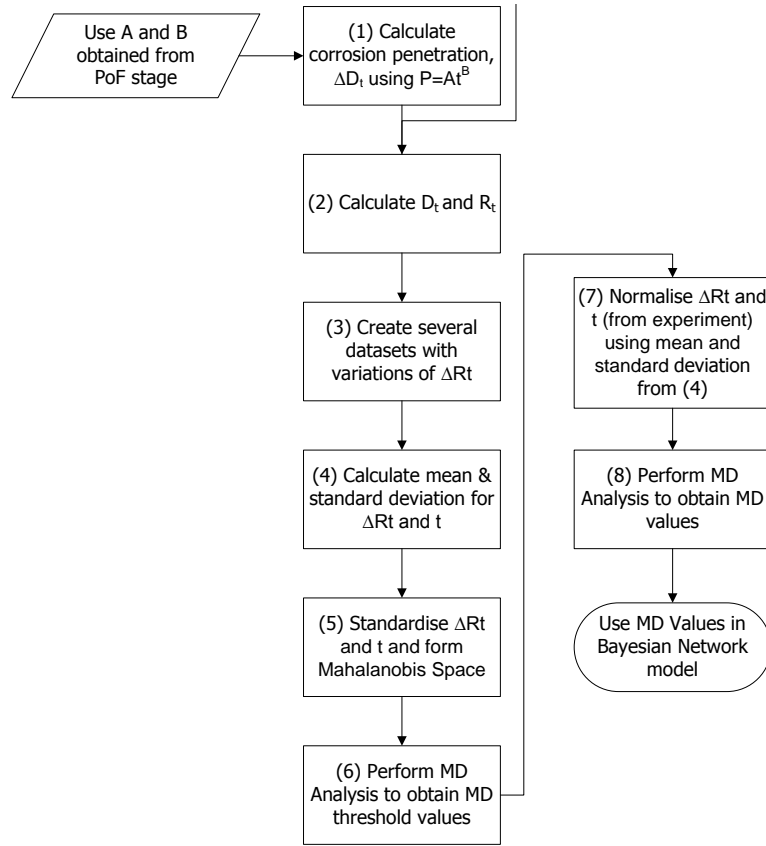


Figure 6-19: Flowchart - Anomaly Detection using MD analysis

The process involves 8 steps, which are detailed below:

1. First, expected corrosion penetration over time needs to be simulated. Using A and B values obtained from step 4 in PoF model used in previous section, penetration, ΔD_t , for each time step (every day) is calculated using equation (31).

$$\Delta D_t = A * t^B \quad (31)$$

Where, ΔD_t is the difference in diameter (i.e. corrosion penetration) at time t , A is the corrosion penetration over the 1st year and B , the decrease of corrosion over time.

2. Calculate D_t which is the difference between original diameter, D_0 and corrosion penetration, ΔD_t and the resulting R_t which is the resistance at time t for corresponding diameter, D_t , using and Rt using equation 32.

$$R_t = \frac{\rho * l}{\pi * (D_t/2)^2} \quad (32)$$

Where, D_t is the diameter of iron wire at time t , l is the length of iron wire, and ρ is the resistivity of the iron wire.

3. ΔR_t , the difference between original resistance, R_0 (at the beginning when no corrosion has yet occurred) and the current resistance, R_t is calculated for every time step. Several datasets consisting of ΔR_t with slight arbitrarily defined variations (2%-5% randomness) are generated to build the training dataset.
4. The mean and standard deviation of ΔR_t and t in the training dataset is calculated.
5. ΔR_t and t are then standardised and used to construct the Mahalanobis space. Once constructed the mahalanobis space will be used each time mahalanobis distance analysis is carried and is only updated if new training dataset becomes available.
6. Using the Mahal function in Matlab, Mahalanobis Distance analysis is carried out to determine the MD threshold values from the training dataset. Thus, the MD threshold values will be used each time until the mahalanobis space is updated and new MD threshold values are determined.
7. The ΔR_t (obtained from step 6 in section 3.2.1) from experiment readings and t are standardized using mean and standard deviation from step 4.
8. Using the Mahal function in Matlab and the mahalanobis space developed in step 5, Mahalanobis Distance analysis is carried out to determine the MD values for ΔR_t . The MD values can then be used in the Bayesian Network models developed.

Two training datasets have been developed for this experiment: one for the iron wires in the Salt environment and one for the iron wires for both Water and Dry environments. The training datasets were developed for $t=90$ days as this was the duration of the experiment.

6.2.3.1. Results Analysis

The Mahalanobis distance values corresponding to each data point (every hour) are plotted as a function of time for each device. Figure 6-20 shows the MD value history for salt-0.125 device (red graph) and the MD value history for a similar healthy device (blue graph). Three different MD thresholds are applied to distinguish between anomaly in the device being

detected or not. The first 25% of the lifetime has MD threshold value of 3.5, the next 50% of the lifetime has MD threshold value of 2 and the last 25% of the lifetime has MD threshold value of 3.7 as shown by the horizontal broken line in Figure 6-20. The reason for choosing three different threshold values arises due to the pattern observed for MD values for a healthy device (blue graph in Figure 6-20).

During MD analysis for device salt-0.125, the MD values are much higher than the MD threshold value of 2.0 (red graph in Figure 6-20) just before total failure of the device. Here while the Mahalanobis distance algorithm does detect anomalies present in the device, it does so too close to failure time. This can be explained by the possibility that the extra salt treatment administered to the device cause severe pitting corrosion, which lead to failure quickly.

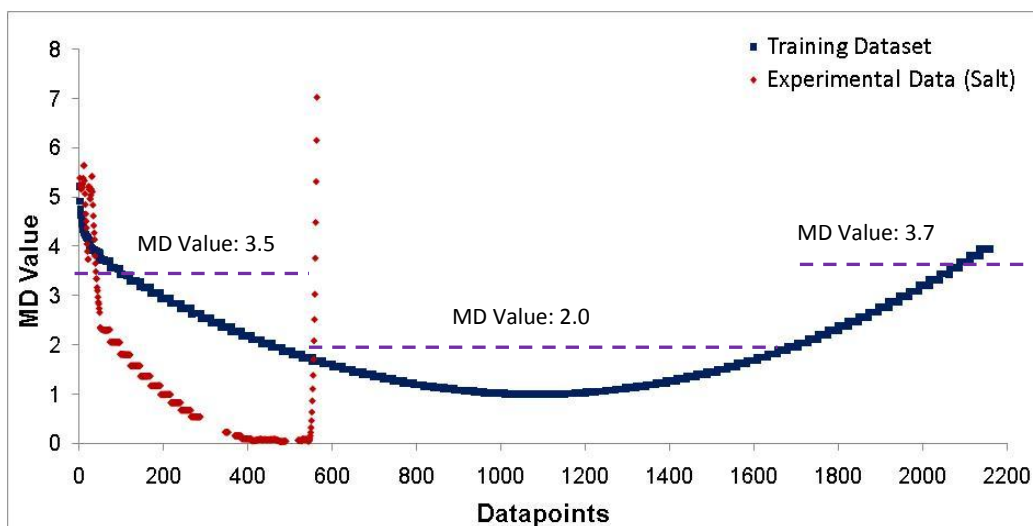


Figure 6-20: Comparing of MD values (0.125mm iron wire - salt) and threshold MD values

Figure 6-21 shows the MD value history for salt-0.25 device (red graph) and the MD value history for a similar healthy device (blue graph). Again, three different MD thresholds are applied: (i) MD threshold value of 3.8, (ii) MD threshold value of 2 and (iii) MD threshold value of 3.5 as shown by the horizontal broken line in Figure 6-21. Here, the observation is similar to that for device salt-0.125 where the MD values are much higher than the MD threshold value just before total failure of the device. Similarly, it seems that extra salt treatment administered to the device cause severe pitting corrosion, which leads to failure

quickly.

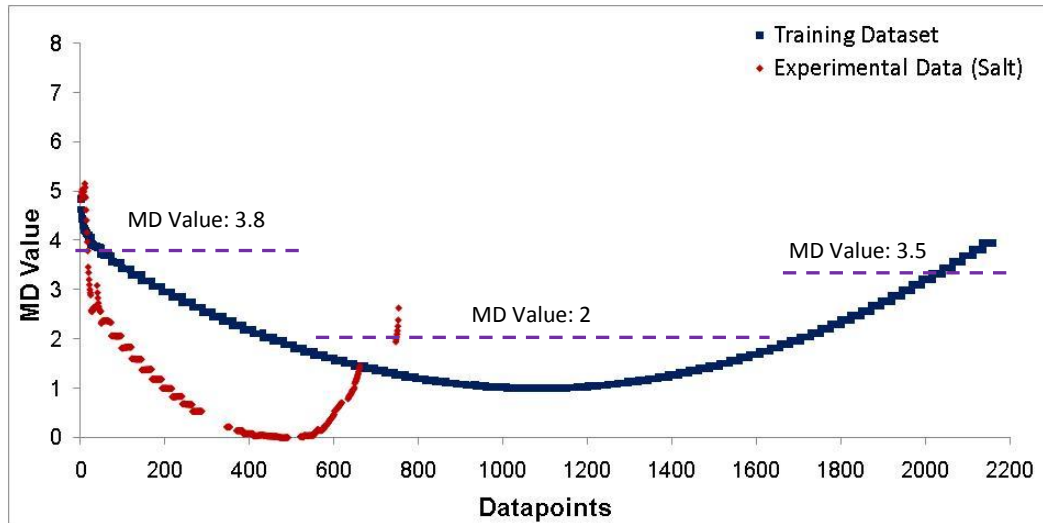


Figure 6-21: Comparing of MD values (0.25mm iron wire - salt) and threshold MD values

Figure 6-22 shows the MD value history for salt-0.5 device (red graph) and the MD value history for a similar healthy device (blue graph). Again, three different MD thresholds are applied: (i) MD threshold value of 3.7, (ii) MD threshold value of 2 and (iii) MD threshold value of 3.7 as shown by the horizontal broken line in Figure 6-22. Here, the observation is similar to that for device salt-0.125 where the MD values are much higher than the MD threshold value just before total failure of the device. Similarly, it seems that extra salt treatment administered to the device cause severe pitting corrosion, which leads to failure quickly.

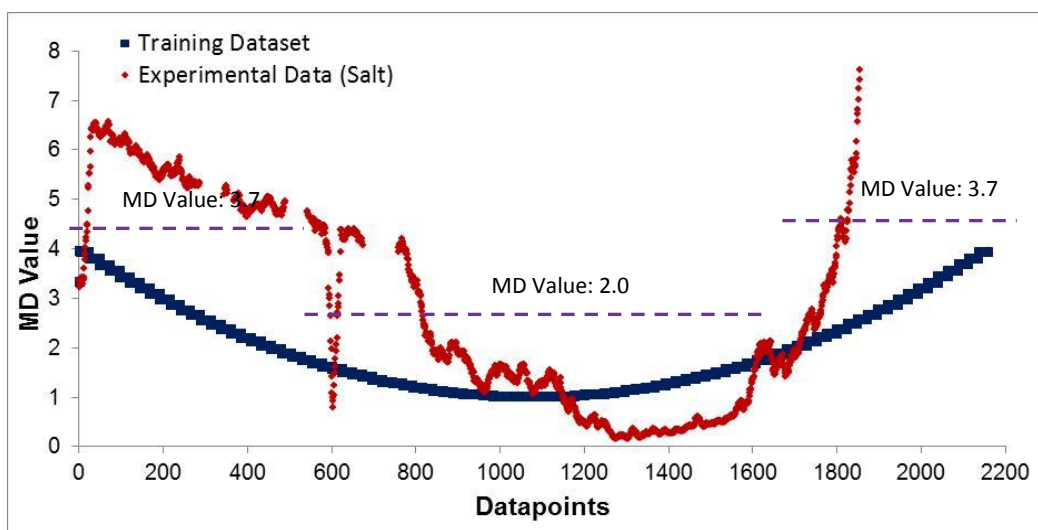


Figure 6-22: Comparing of MD values (0.5mm iron wire - salt) and threshold MD values

Comparing the healthy (blue) graphs against the test (red) graphs for the 3 salt devices, it is clear to see that a pattern forms after data point 360 (which approximately represents day 15), the time after which the devices were subjected to harsher salt treatments for the salt experiment. Thus, we observe that Mahalanobis distance analysis is useful in identifying anomalies or faulty behavior. However, the patterns generated need more analysis in order to identify anomalies earlier on (as soon as they start to develop rather than just before failure). It should be noted that the training dataset used for Mahalanobis Distance has been developed for uniform corrosion, while it appears that the failure on the salt devices were due to pitting corrosion.

In a similar manner, MD analysis is carried out on the devices for the dry and water environments. Figure 6-23 to Figure 6-25 show the MD value histories for devices, dry-0.125, dry-0.25 and dry-0.5, respectively. The MD threshold values for each device are displayed along with the graph of MD values for healthy devices (blue graphs). Here as expected, the MD values remain below the corresponding MD threshold values, as the three devices in the dry experiment do not experience much corrosion. The graphs for MD value histories for the devices of the water experiment are found in the appendix.

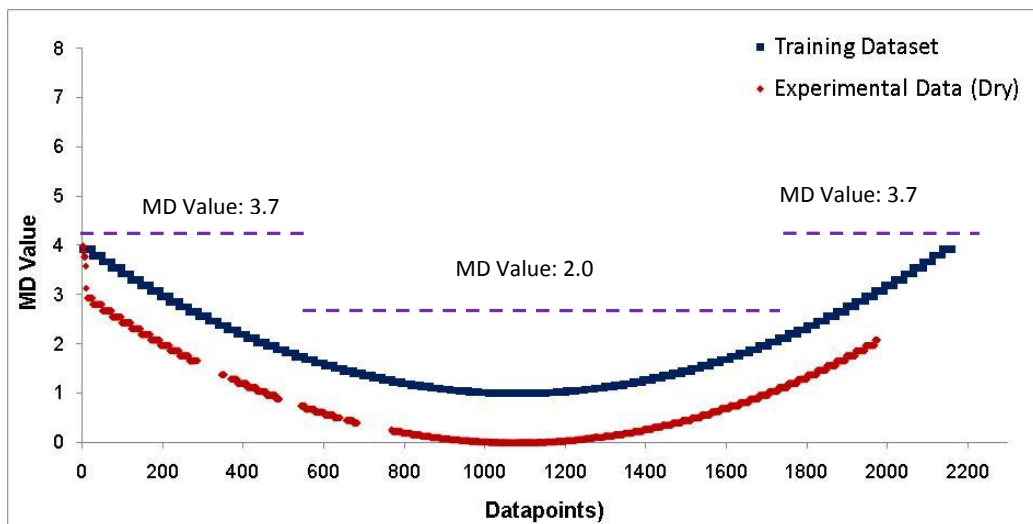


Figure 6-23: Comparing of MD values (0.125mm iron wire - dry) and threshold MD values

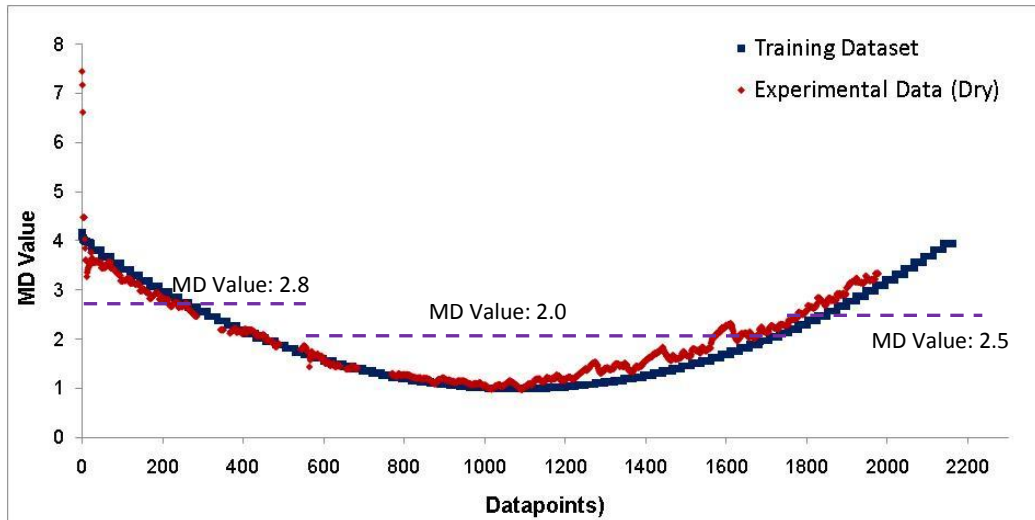


Figure 6-24: Comparing of MD values (0.25mm iron wire - dry) and threshold MD values

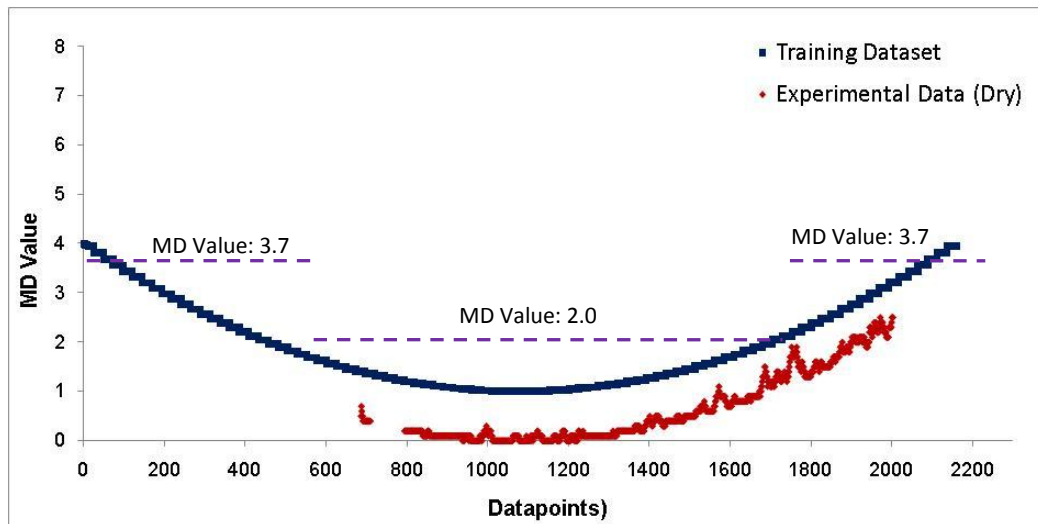


Figure 6-25: Comparing of MD values (0.5mm iron wire - dry) and threshold MD values

Thus comparing the healthy (blue) graphs against the test (red graphs) for the 3 dry devices, shows that MD analysis performs well as the MD values are at or below the MD threshold values which reflects what is expected for all 3 dry devices. Data from more experiments with better control on the environmental conditions and more experiments for monitoring different forms of corrosion would provide a comprehensive training dataset, which can then be used for MD analysis. The graphs showing the results of MD analysis for the 3 iron wires in water environment can be found in appendix section 9.3.4. The MD values for the iron wires in the water environment follow a similar trend to that of the iron wires in the dry environment.

6.2.4. Building the BN models for the Experimental trials

The Bayesian network model developed is again organised in a layered structure with the top layer representing the prediction of remaining life of the system under consideration, the middle layer representing the diagnosis and prognosis observations of the structure and the bottom layer representing usage and health observations with the nodes in the different layers connected by causal links. A Bayesian network model is built for each experiment environment: salt (Figure 6-26), dry (Figure 6-27) and water (Figure 6-28).

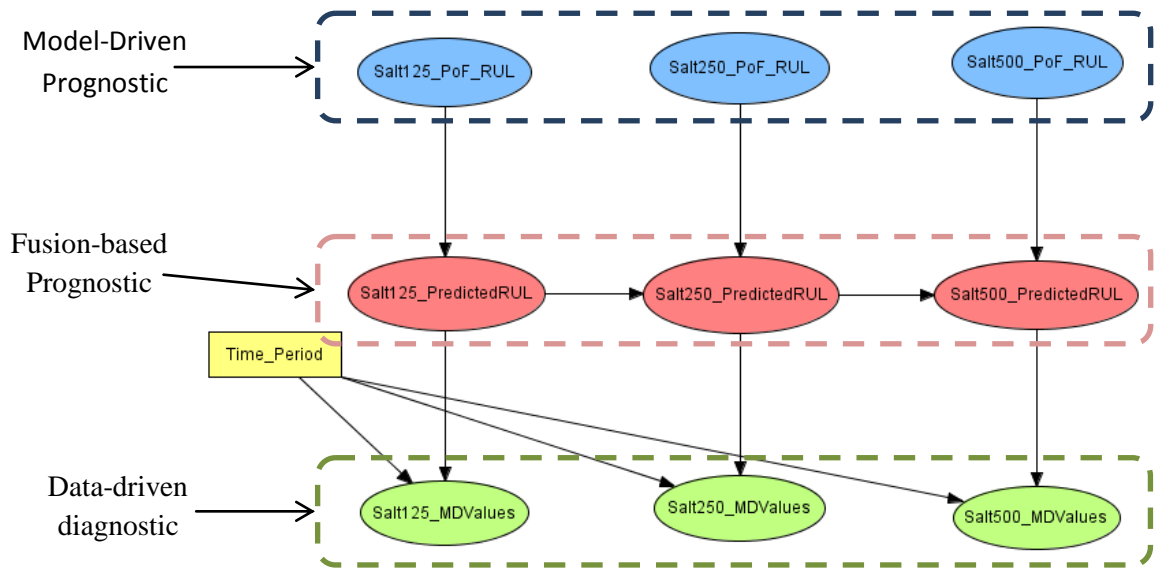


Figure 6-26: Network for Salt Environment Lab Experiments

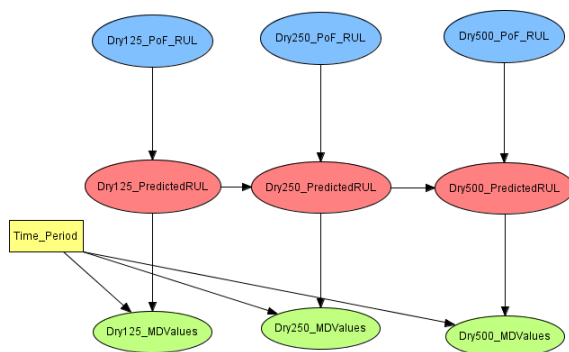


Figure 6-27: Network for Dry Environment Lab Experiments

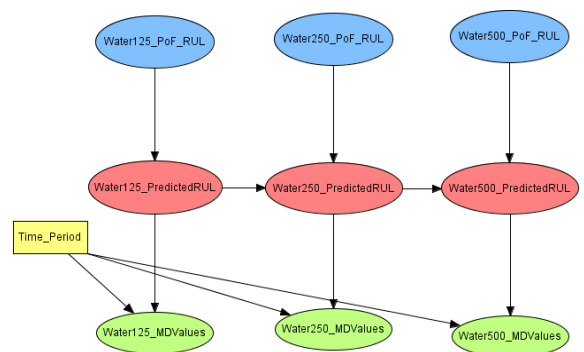


Figure 6-28: Network for Water Environment Lab Experiments

In Figure 6-26, remaining life predictions from PoF models for the 3 test devices (0.125mm, .25mm and 0.5mm) provide input for the top layer nodes: Salt125_PoF_RUL, Salt250_PoF_RUL and Salt500_PoF_RUL. The bottom layer nodes (Salt125_MDValues, Salt250_MDValues and Salt500_MDValues) represent the anomaly detection results for the three devices during the experiment. The nodes in the middle layer represent the diagnosis and prognosis for the three devices: Salt125_PredictedRUL, Salt250_PredictedRUL and Salt500_PredictedRUL. One additional node representing the time is included to account for the point in time at which the model is run (usually each time new input data for bottom layer nodes is available). Similar to the Bayesian network model for the demonstrator example, the nodes across the layers are linked together such that evidence recorded for one of the nodes will result in a belief updating of all the nodes connected to it.

The links between nodes 'Salt125_PoF_RUL' and 'Salt125_PredictedRUL' mean that the probability distribution of the predicted remaining life of the 0.125mm device using PoF models will affect the probability distribution of the updated predicted remaining life of the 0.125mm device. The links between nodes 'Salt125_PredictedRUL' and 'Salt125_MDValues' mean that the probability distribution of the updated predicted remaining life of the 0.125mm device in turn affects the probability distribution of MD values which is initially calculated from the MD analysis of failure precursors of that device. The node 'Salt125_PredictedRUL' links to node 'Salt250_PredictedRUL' that in turn links to node 'Salt500_PredictedRUL'. This is to represent the correlation between failure rates in all three devices under experimentation.

The next step was to build the Conditional Probability Tables (CPTs) associated with each node in the model. The initial set of probabilities values is based on measurements from the devices for the first 10 days. The details for populating the CPTs are provided below:

1. Salt125_PoF_RUL – the states for this variable are continuous and have been discretized into intervals ($-\infty - 500$, $500-1000$, ... , $3000 - \infty$) to represent the estimated lifetime of this device under healthy conditions. As this node is a root node, the probabilities of its states are defined by normal distribution based on mean values of PoF predicted remaining life for a healthy device from section 6.2.2 as shown in Table 6-3. The CPTs is populated as shown in Figure 6-29 .

Salt125_PoF_RUL	
Expression	Normal (2328, 145544)
-inf - 0	5.231E-10
0 - 500	8.268E-7
500 - 1000	2.49E-4
1000 - 1500	0.015
1500 - 2000	0.18
2000 - 2500	0.479
2500 - 3000	0.287
3000 - inf	0.039

Figure 6-29: CPT for Salt125_PoF_RUL Node in Hugin

2. Salt250_PoF_RUL – the states for this variable are also continuous and have been discretised into intervals ($-\infty - 500, 500-1000, \dots, 4500 - \infty$) to represent the estimated lifetime of this device under healthy conditions. Similar to node Salt125_PoF_RUL, the CPT for this node follows a normal distribution populated using mean values of PoF predicted remaining life for a healthy device as shown in Table 6-3.
3. Salt500_PoF_RUL – the states for this variable are continuous and have been discretised into intervals ($-\infty - 1000, 1000-2000, \dots, 8000 - \infty$). Similar to nodes Salt125_PoF_RUL and Salt250_PoF_RUL, the CPT for this node follows a normal distribution using mean values of PoF predicted remaining life for a healthy device as shown in Table 6-3.
4. Salt125_MDValues – The states here are continuous and have been discretised into intervals ($-\infty - 0, 0 - 1, \dots, 10 - \infty$) to represent the typical MD values expected during the experiment. This node has two parent nodes: Time_Period and Salt125_PredictedRUL. The probabilities of the states of this node are conditional on how the state of its parent nodes combine and follows a normal distribution based on MD threshold values. The CPT is populated using the Expression Builder feature in Hugin shown in Figure 6-30.

Salt125_MDValues		1st Part												Middle Part											
Time_Period																									
Salt125_Pr...	-inf - 0	0 - 500	500 - 1000	1000 - 1500	1500 - 2000	2000 - 2500	2500 - 3000	3000 - inf	-inf - 0	0 - 500	500 - 1000	1000 - 1500	1500 - 2000	2000 - 2500	2500 - 3000	3000 - inf									
Expression	0	Normal (3.47 * (1 + 4Normal (3.47 * (1 + 3Normal (3.47 * (1 + 2Normal (3.47 * (1 + 1Normal (3.47, 0.54) Normal (3.47 * (1 - 1 Normal (3.47 * (1 - 3												Normal (1.98 * (1 + 4Normal (1.98 * (1 + 3Normal (1.98 * (1 + 2											
Salt125_Pr...	-inf - 0	0 - 500	500 - 1000	1000 - 1500	1500 - 2000	2000 - 2500	2500 - 3000	3000 - inf	-inf - 0	0 - 500	500 - 1000	1000 - 1500	1500 - 2000	2000 - 2500	2500 - 3000	3000 - inf									
Time_Period	1st Part	Middle ...	3rd Part	1st Part	Middle ...	3rd Part	1st Part	Middle ...	3rd Part	1st Part	Middle ...	3rd Part	1st Part	Middle ...	3rd Part	1st Part	Middle ...	3rd Part							
-inf - 0	0	0	0	1.792E...	4.656E-8	1.342E...	7.066E...	1.49E-6	1.358E...	7.048E...	3.104E-5	5.663E-9	1.789E-9	4.23E-4	9.777E-7	1.167E-6	0.004	7.051E-5	0.009	0.091	0.029	0.119	0.252	0.171	
0 - 1	1	1	1	3.151E...	3.281E-5	2.246E...	2.549E...	4.425E-4	8.73E-9	5.254E-9	0.004	1.404E-6	2.788E-6	0.023	9.401E-5	3.868E-4	0.089	0.003	0.149	0.414	0.162	0.453	0.5	0.359	
1 - 2	0	0	0	8.932E...	0.004	1.34E-8	1.495E-8	0.024	2.012E-6	6.455E-6	0.091	1.259E-4	7.312E-4	0.238	0.003	0.022	0.418	0.037	0.482	0.408	0.369	0.367	0.227	0.335	
2 - 3	0	0	0	4.122E-8	0.094	2.869E-6	1.449E-5	0.241	1.677E-4	0.001	0.421	0.004	0.034	0.5	0.043	0.238	0.405	0.193	0.317	0.083	0.321	0.06	0.021	0.119	
3 - 4	0	0	0	3.152E-5	0.424	2.221E-4	0.002	0.499	0.005	0.049	0.401	0.05	0.289	0.22	0.21	0.503	0.081	0.384	0.042	0.003	0.106	0.002	3.649E-4	0.016	
4 - 5	0	0	0	0.004	0.398	0.006	0.07	0.216	0.058	0.34	0.079	0.227	0.493	0.02	0.388	0.217	0.003	0.29	0.001	2.464E-5	0.013	1.008E-5	1.144E-6	7.952E-4	
5 - 6	0	0	0	0.096	0.077	0.066	0.388	0.019	0.244	0.47	0.003	0.391	0.172	3.302E-4	0.274	0.018	2.326E-5	0.083	4.43E-6	3.202E-8	6.156E-4	9.348E-9	6.217E...	1.459E-5	
6 - 7	0	0	0	0.432	0.003	0.261	0.436	3.143E-4	0.392	0.132	2.195E-5	0.257	0.012	1.001E-6	0.073	2.87E-4	2.97E-8	0.009	3.239E-9	7.118E...	1.05E-5	1.43E-12	5.727E...	9.714E-8	
7 - 8	0	0	0	0.393	2.071E-5	0.391	0.099	9.364E-7	0.24	0.007	2.754E-8	0.064	1.452E-4	5.253E...	0.007	7.784E-7	6.485E...	3.631E-4	3.896E...	2.662E...	6.492E-8	3.552E...	8.828E...	2.326E...	
8 - 9	0	0	0	0.072	2.553E-8	0.223	0.004	4.828E...	0.056	7.121E-5	5.908E...	0.006	3.113E-7	4.67E-14	2.766E-4	3.534E...	2.382E...	5.348E-6	7.602E...	1.658E...	1.443E...	1.42E-22	2.258E...	1.99E-13	
9 - 10	0	0	0	0.003	5.38E-12	0.048	3.386E-5	4.216E...	0.005	1.206E-7	2.131E...	2.097E-4	1.113E...	6.945E...	3.787E-6	2.628E...	1.457E...	2.853E-8	2.384E...	1.708E...	1.145E...	9.076E...	9.536E...	6.045E...	
10 - inf	0	0	0	1.563E-5	1.907E...	0.004	4.53E-8	6.158E...	1.6E-4	3.396E...	1.281E...	2.68E-6	6.507E...	1.714E...	1.88E-8	3.162E...	1.475E...	5.468E...	1.195E...	2.901E...	3.228E...	9.237E...	6.62E...	6.502E...	

Figure 6-30: CPT for Salt125_MDValues in Hugin

5. Salt250_MDValues – the states are assigned the same as for the node Salt125_MDValues and the CPT is populated using the same procedure as for that node with marginal probabilities derived from Table 6-5.
6. Salt500_MDValues – the states are assigned the same as for the node Salt125_MDValues and Salt250_MDValues and the CPT is populated using the same procedure as for that node with marginal probabilities derived from Table 6-6.
7. Salt125_PredictedRUL – the states for these nodes are similar to that of node Salt125_PoF_RUL. However, this node one parent node, Salt125_PoF__RUL. The probability distribution of predicted remaining life from node Salt125_PoF_RUL is assumed to also represent the probability distribution of predicted remaining life from node Salt125_PredictedRUL. Thus, the probability distribution follows a normal distribution with the mean value being the current value of node Salt125_PoF_RUL Table 5-14: Input data for Canary Device from MD Analysis Results and is inputted in Hugin as shown in Figure 6-31.

Salt125_PredictedRUL							
Expression	Normal(Salt125_PoF_RUL, 145000)						
Salt125_Po...	-inf - 0	0 - 500	500 - 1000	1000 - 1500	1500 - 2000	2000 - 2500	
-inf - 0	0.501	0.27	0.033	0.001	7.088E-6	1.018E-8	2.1
0 - 500	0.405	0.46	0.237	0.032	0.001	7.078E-6	1.1
500 - 1000	0.09	0.237	0.46	0.237	0.032	0.001	7.1
1000 - 1500	0.004	0.032	0.237	0.46	0.237	0.032	0.1
1500 - 2000	4.036E-5	0.001	0.032	0.237	0.46	0.237	0.1
2000 - 2500	7.403E-8	7.078E-6	0.001	0.032	0.237	0.46	0.1
2500 - 3000	2.551E-11	1.018E-8	7.078E-6	0.001	0.032	0.237	0.1
3000 - inf	1.624E-15	2.87E-12	1.018E-8	7.088E-6	0.001	0.033	0.1

Figure 6-31: CPT for Salt125_PredictedRUL in Hugin

8. Salt250_PredictedRUL – the states for this node are similar to that of node Salt250_PoF_RUL and the CPT is similar to that of node Salt125_PredictedRUL. However, this node has three parent nodes instead of two: Time_Period, Salt250_PoF_RUL and Salt125_PredictedRUL. The probability distribution for this node is assigned in same manner as for node Salt125_PredictedRUL and is then adjusted to account for effect of node Salt125_PredictedRUL. After preliminary analysis, the correlation factor between predicted remaining lives of canary and parrot

devices is set at 0.2. Thus, mean for the normal distribution is adjusted using the expression builder in Hugin as shown Table in Figure 6-32.

Salt250_PredictedRUL	
Expression	Normal(Salt250_PoF_RUL + Salt125_PredictedRUL * 0.2, 280000)
Salt125_Pr...	-inf - 0
Salt250_Po...	-inf - 0 0 - 500 500 - 1... 1000 - ... 1500 - ... 2000 - ... 2500 - ... 3000 - ... 3500 - ... 4000 - ... 4500 - inf
-inf - 0	0.501 0.325 0.086 0.011 6.972E-4 1.941E-5 2.379E-7 1.262E-9 2.859E... 2.743E... 8.524E... 0.463 0.293 ... 1.423E... 4.174E... 0.389 0.233 ... 3.155E... 7.929E...
0 - 500	0.327 0.351 0.239 0.075 0.011 6.778E-4 1.918E-5 2.367E-7 1.259E-9 2.856E... 1.903E... 0.339 0.349 ... 1.585E... 9.959E... 0.357 0.339 ... 4.175E... 2.255E...
500 - 1000	0.143 0.239 0.351 0.239 0.075 0.011 6.778E-4 1.918E-5 2.367E-7 1.259E-9 1.764E... 0.161 0.257 ... 7.486E... 9.887E... 0.2 0.29 ... 2.339E... 2.667E...
1000 - 1500	0.027 0.074 0.239 0.351 0.239 0.075 0.011 6.778E-4 1.918E-5 2.367E-7 6.812E-9 0.033 0.087 ... 1.51E-7 4.098E-9 0.049 0.115 ... 5.59E-8 1.316E-9
1500 - 2000	0.002 0.011 0.074 0.239 0.351 0.239 0.075 0.011 6.778E-4 1.918E-5 1.101E-6 0.003 0.013 ... 1.314E-5 7.121E-7 0.005 0.021 ... 5.751E-6 2.72E-7
2000 - 2500	7.667E-5 6.761E-4 0.011 0.074 0.239 0.351 0.239 0.075 0.011 6.778E-4 7.489E-5 1.14E-4 9.377E-4 ... 4.997E-4 5.218E-5 2.343E-4 0.002 ... 2.578E-4 2.368E-5
2500 - 3000	1.133E-6 1.911E-5 6.761E-4 0.011 0.074 0.239 0.351 0.239 0.075 0.011 0.002 1.859E-6 2.906E-5 ... 0.008 0.002 4.536E-6 6.217E-5 ... 0.005 8.739E-4
3000 - 3500	7.05E-9 2.358E-7 1.911E-5 6.761E-4 0.011 0.074 0.239 0.351 0.239 0.075 0.027 1.28E-8 3.945E-7 ... 0.064 0.022 3.712E-8 9.964E-7 ... 0.045 0.014
3500 - 4000	1.835E... 1.253E-9 2.358E-7 1.911E-5 6.761E-4 0.011 0.074 0.239 0.351 0.239 0.141 3.698E... 2.315E-9 ... 0.22 0.124 1.277E... 6.922E-9 ... 0.183 0.094
4000 - 4500	1.99E-14 2.841E... 1.253E-9 2.358E-7 1.911E-5 6.761E-4 0.011 0.074 0.239 0.351 0.326 4.464E... 5.816E... ... 0.349 0.311 1.836E... 2.062E... ... 0.339 0.277
4500 - inf	8.966E... 2.726E... 2.844E... 1.256E-9 2.37E-7 1.935E-5 6.955E-4 0.011 0.086 0.324 0.503 2.244E... 6.204E... ... 0.358 0.541 1.1E-16 2.613E... ... 0.428 0.615

Figure 6-32: CPT for Salt250_PredictedRUL in Hugin

- Salt500_PredictedRUL – the states for this node are similar to that of node Salt500_PoF_RUL and the CPT is populated using the same procedure as for that node Salt250_PredictedRUL.
- Time_Period – the states of this variable are categorical (“1st part”, “Middle part”, “3rd Part”). They have been devised as such to represent the three different MD threshold values were assigned for any healthy device as described in section 6.2.3. For this experiment, the evidence is propagated in the network every day and depending on the period that particular day fall, the relevant stated is selected.

Salt125		Salt250		Salt500	
Mean(days)	Variance	Mean(days)	Variance	Mean(days)	Variance
2328	1445544	3222	278818	5959	953843

Table 6-3: PoF model-based input data

Time (days)	Mean MD Value	Standard Deviation	MD Threshold	Variance
1 st Part	2.73	0.96	0.54	3.47
Middle Part	1.24	0.74	0.55	1.98
Last Part	2.73	0.97	0.95	3.71

Table 6-4: Input data from MD Analysis Results for 0.125mm salt device

Time (days)	Mean MD Value	Standard Deviation	MD Threshold	Variance
1st Part	2.73	1.03	1.07	3.76
Middle Part	1.23	0.74	0.55	1.98
Last Part	2.44	1.06	1.12	3.50

Table 6-5: Input data from MD Analysis Results for 0.25mm salt device

Time (days)	Mean MD Value	Standard Deviation	MD Threshold	Variance
1st Part	2.72	0.97	0.93	3.69
Middle Part	1.24	0.74	0.55	1.98
Last Part	2.74	0.97	0.94	3.70

Table 6-6: Input data from MD Analysis Results for 0.5mm salt device

6.2.4.1. Running the Bayesian Network Model

With all the CPTs specified, the BN model is compiled and ‘run’. The predictions of the remaining life using the PoF models and the MD values from Mahalanobis Distance analysis are used as evidence input for nodes (Salt125_PoF_RUL, Salt250_PoF_RUL, Salt500_PoF_RUL, Salt125_MDValues, Salt250_MDValues and Salt500_MDValues). The state for the node Time_Period, representing time for the experiment is selected as appropriate. The reasoning engine (using Hugin) for this Bayesian network model then performs propagation of probabilities and the updated probability distributions for the 3 hypothesis nodes (Salt125_PredictedRUL, Salt250_PredictedRUL and Salt500_PredictedRUL) are obtained. The same procedure is repeated for the Bayesian network models for Dry and Water experiment using input data from Table 9-1 to Table 9-4 in appendix section 9.3.5.

6.2.4.2. Analysis of results

Table 6-7 provides a timeline of the main events occurring for the salt experiment. The last column ‘Prediction Time’ indicates the time at which evidence is propagated within the Bayesian network model to obtain updated probability distributions for predicted remaining life for all three salt devices. The BN model ran every day but the results in Table 6-8 only show updated predictions from approximately last 10 percent of the lifetime. A visual representation of the daily updated probability distribution graphs for the three iron wire

devices for all three experiments (salt, water and dry environments) can be found in appendix section 9.3.6.

Time (days)	Event	Description	Prediction Time (days)
1	A	Start of the experiment for all three environments	1
13	B	Salt Environment Experiment stopped and devices undergo treatment	11
15	C	Experiment for Salt environment is restarted	16
27	D	Salt-0.125 device fails	24
30	E	Salt-0.25 device fails	27
79	F	Salt-0.5 device fails	77
85	G	Experiment is stopped for remaining two environments	

Table 6-7: Experiment Timeline

The probability distribution graphs in Table 6-8 provide a numerical interpretation of the results of the salt experiment nodes Salt125_PredictedRUL, Salt250_PredictedRUL and Salt500_PredictedRUL. The state intervals are represented on the right hand side column within the nodes and the probability associated with each state interval is represented on the left hand side column as a percentage. At day 1, the probability distributions predict a remaining life in the range of 1500-2000 days for the Salt125_PredictedRUL node, 1000-2000 days for the Salt250_PredictedRUL node and 4000-6000 days for the Salt500_PredictedRUL node. The predicted remaining lives are shorter than the expected at this stage due to higher corrosion rates in the beginning. At day 11, just before the iron wire devices were subjected to further salt treatment, the probability distributions predict a remaining life in the range of range of 2500-3000 days for the Salt125_PredictedRUL node, 3000-3500 days for the Salt250_PredictedRUL node and 4000-5000 days for the Salt500_PredictedRUL node, which reflects healthy wires devices.

At day 16, one day after the additional salt treatment was administered to the three iron devices, the probability distributions predicted the same remaining lives as for at day 11. At day 24, three days before the Salt125 device fails, the probability distribution for the Salt125_PredictedRUL node shifts to the intervals (500 – 1500). At day 27, three days before the Salt250 device fails, the probability distribution for the Salt250_PredictedRUL node

remains similar to that as at day 11. At day 77, two days before the Salt500 device fails, the probability distribution for the Salt500_PredictedRUL remains similar to that as at day 11.

Time (days)	Salt125	Salt250	Salt500
1	<p>Salt125_PredictedRUL</p> <pre> 0.00 -inf - 0 5.3E-4 0 - 500 0.19 500 - 1000 9.42 1000 - 1500 56.96 1500 - 2000 32.43 2000 - 2500 1.00 2500 - 3000 1.4E-3 3000 - inf </pre>	<p>Salt250_PredictedRUL</p> <pre> 0.00 -inf - 0 1.19 0 - 500 12.97 500 - 1000 40.25 1000 - 1500 35.76 1500 - 2000 9.14 2000 - 2500 0.68 2500 - 3000 5.92E-3 3000 - 3500 1.18E-5 3500 - 4000 5.48E-9 4000 - 4500 1.51E-11 4500 - inf </pre>	<p>Salt500_PredictedRUL</p> <pre> 0.00 -inf - 0 1.49E-5 0 - 1000 5.47E-3 1000 - 2000 0.45 2000 - 3000 8.68 3000 - 4000 39.57 4000 - 5000 43.38 5000 - 6000 7.79 6000 - 7000 0.13 7000 - 8000 1.76E-5 8000 - inf </pre>
11	<p>Salt125_PredictedRUL</p> <pre> 56.30 -inf - 0 8.14E-4 0 - 500 0.09 500 - 1000 1.62 1000 - 1500 6.48 1500 - 2000 9.74 2000 - 2500 25.29 2500 - 3000 0.49 3000 - inf </pre>	<p>Salt250_PredictedRUL</p> <pre> 0.00 -inf - 0 2.27E-5 0 - 500 2.05E-3 500 - 1000 0.08 1000 - 1500 1.41 1500 - 2000 10.70 2000 - 2500 31.31 2500 - 3000 40.20 3000 - 3500 14.75 3500 - 4000 1.48 4000 - 4500 0.07 4500 - inf </pre>	<p>Salt500_PredictedRUL</p> <pre> 0.00 -inf - 0 0.12 0 - 1000 1.54 1000 - 2000 10.09 2000 - 3000 35.56 3000 - 4000 40.57 4000 - 5000 11.89 5000 - 6000 0.22 6000 - 7000 3.49E-4 7000 - 8000 1.31E-9 8000 - inf </pre>
16	<p>Salt125_PredictedRUL</p> <pre> 0.00 -inf - 0 0.03 0 - 500 1.29 500 - 1000 11.02 1000 - 1500 30.27 1500 - 2000 38.91 2000 - 2500 18.37 2500 - 3000 0.12 3000 - inf </pre>	<p>Salt250_PredictedRUL</p> <pre> 0.00 -inf - 0 4.74E-5 0 - 500 4.54E-3 500 - 1000 0.15 1000 - 1500 1.94 1500 - 2000 10.47 2000 - 2500 27.70 2500 - 3000 39.82 3000 - 3500 17.80 3500 - 4000 2.02 4000 - 4500 0.09 4500 - inf </pre>	<p>Salt500_PredictedRUL</p> <pre> 0.00 -inf - 0 0.34 0 - 1000 3.73 1000 - 2000 15.79 2000 - 3000 35.58 3000 - 4000 34.58 4000 - 5000 9.81 5000 - 6000 0.18 6000 - 7000 2.91E-4 7000 - 8000 1.12E-9 8000 - inf </pre>
24	<p>Salt125_PredictedRUL</p> <pre> 0.00 -inf - 0 3.84 0 - 500 32.93 500 - 1000 49.32 1000 - 1500 13.28 1500 - 2000 0.62 2000 - 2500 7.6E-4 2500 - 3000 5.61E-7 3000 - inf </pre>	<p>Salt250_PredictedRUL</p> <pre> 0.00 -inf - 0 5.02E-3 0 - 500 0.22 500 - 1000 3.46 1000 - 1500 19.43 1500 - 2000 39.68 2000 - 2500 29.68 2500 - 3000 6.99 3000 - 3500 0.52 3500 - 4000 0.01 4000 - 4500 2.21E-4 4500 - inf </pre>	<p>Salt500_PredictedRUL</p> <pre> 0.00 -inf - 0 0.21 0 - 1000 4.09 1000 - 2000 23.78 2000 - 3000 42.97 3000 - 4000 24.47 4000 - 5000 4.41 5000 - 6000 0.07 6000 - 7000 1.96E-4 7000 - 8000 8.17E-9 8000 - inf </pre>
27	<p>Salt250_PredictedRUL</p> <pre> 0.00 -inf - 0 3.65E-3 0 - 500 0.17 500 - 1000 2.90 1000 - 1500 17.58 1500 - 2000 38.89 2000 - 2500 31.64 2500 - 3000 8.13 3000 - 3500 0.66 3500 - 4000 0.02 4000 - 4500 3.35E-4 4500 - inf </pre>	<p>Salt500_PredictedRUL</p> <pre> 0.00 -inf - 0 2.52E-3 0 - 1000 0.17 1000 - 2000 3.38 2000 - 3000 21.39 3000 - 4000 43.15 4000 - 5000 28.03 5000 - 6000 3.78 6000 - 7000 0.10 7000 - 8000 1.31E-4 8000 - inf </pre>	

77	Salt500_PredictedRUL	
	0.00	-inf - 0
	3.81E-3	0 - 1000
	0.35	1000 - 2000
	7.38	2000 - 3000
	36.51	3000 - 4000
	43.22	4000 - 5000
	12.32	5000 - 6000
	0.22	6000 - 7000
	3.37E-4	7000 - 8000
1.23E-9	8000 - inf	

Table 6-8: Updated Probability Distributions for Predicted Remaining Life for all three salt devices.

The results for the analysis of the salt devices reveal that while the Bayesian network model can detect and predict that the Salt125 device will fail shortly, it fails to identify in time that the two devices Salt250 and Salt500 were about to fail. This could be accounted based on two factors. First, the discretisation of the nodes need to make use of smaller intervals thus representing the actual condition and behavior of the devices more accurately and the CPTs for those nodes need to be update accordingly. Secondly, it is suspected that the harsh salt treatment applied the second time on the devices triggered pitting corrosion, which is a failure mechanism that this Bayesian network model does not account for. Additionally, the accuracy of the prediction for the remaining life of the salt devices is not satisfactory and should be improved. However using the fusion based prognostic tool for remaining life prediction provides better results compared to using the model-driven prognostic tool as the fusion based prognostic tool incorporates data from the diagnostic tool when available to update the remaining life prediction.

6.3. Summary

This chapter describes the trial experiment carried out to test the diagnostic and prognostic tools developed. The experiment consisted of three sets of three different iron wire devices placed in three desiccators with varying relative humidity conditions (labelled: salt, water and dry). The three iron wire devices are initial versions of canary and parrot sensor devices with the thinner wire device representing a canary device and the thicker one representing a parrot device. The experiment was run until the three wire devices in the salt environment all failed. There was some measurement data loss due to the trial experiment being interrupted several times for various reasons. Additionally, the changes in room temperature proved to be high enough to affect the electrical resistance readings of the two thinnest iron wires. Thus, the noise due to temperature changes had to be removed from the electrical resistance readings before being used in the diagnostic and prognostic tools.

The predicted remaining life of the iron wire devices was calculated using the PoF model developed in chapter 4 based on the electrical resistance readings taken for the first ten days. Similarly, readings for the first ten days were used as training data for Mahalanobis distance analysis, which is used within the data-driven diagnostic tool. Diagnostics using Mahalanobis distance analysis was then performed on a daily basis. Finally, the fusion based prognostic tool implemented using Bayesian network model was used to provide probability distributions of predicted remaining life for the iron wire devices.

The results obtained using the model-driven prognostic tool using a PoF model, the data-driven diagnostic tool using Mahalanobis distance analysis and the fusion based prognostic tool are promising. The PoF model itself requires one year's worth of electrical resistance data before prediction can be made but was here adapted for the length of time the experiment ran and therefore could not be validated in a formal manner. The Mahalanobis distance analysis of the three iron wire devices in the salt environment detected deviations from normal/healthy behavior at the earliest time possible, although not all the graphs show this due to missing measurement data. The Bayesian network model needs optimization regarding the states and CPTs of the node as it is not sensitive enough to reflect the true effect of even small changes in predicted remaining life from PoF model and diagnostic information from Mahalanobis distance analysis.

The test results were very informative and revealed that the diagnostic and prognostic tools have low robustness when dealing with noisy and/or missing data. This trial experiment only investigated one possible design of canary/parrot devices. More designs of the devices need to be trialed in order to test and validate first whether the devices can monitor performance parameters that indicate particular failure mechanisms and second, whether the diagnostic and prognostic tools developed can provide results with accuracy.

7. Conclusion and Future Work

This thesis has focused on developing diagnostic and prognostic tools in order to predict remaining life of aged structures based on damage caused by corrosion and investigating the use of low-cost sensor devices to monitor aged iron structures. A summary of the research work is presented in section 7.1. The contributions to the field of diagnostics and prognostics in aged structures are discussed in section 7.2. Recommendations for diagnostic and prognostic tools for Cutty Sark iron structures are made in section 7.3. Finally, the way forward and possible directions for future research are outlined in the last section.

7.1. Summary of Research

The first part of this thesis described the deterioration problem that affects aged structures, especially corrosion damage in aged iron structures. The Cutty Sark is used as an example application for the diagnostic and prognostic tools developed for monitoring of aged structures. Background information is provided regarding monitoring of aged marine structures as well as the corrosion mechanisms that take place in such structures. A literature review of diagnostic and prognostics techniques follows describing the different types of models available and in development for monitoring of engineering structures and systems.

While there are many models and algorithms developed for diagnostic and prognostic purposes, currently diagnostic tools have enjoyed more success than prognostic tools in application in the real world. Multiple challenges remain in the application of diagnostic and prognostics to complex structures. These range from lack of appropriate sensors, little understanding of physical behavior of the structure, lack of historical data to the interdisciplinary effort required to integrate diverse systems together to develop robust tools. Added to this, problems often particular to monitoring of aged iron structures are that budgets are often limited regarding implementation of monitoring system. In addition, iron structures that have experience corrosion for over a century, usually have corrosion distributed unevenly across structure and can vary from one structure to another to due varying environmental conditions being subjected to.

The second part of thesis introduced the concept of novel sensors (canary and parrot devices) and presented the diagnostic and prognostic tools developed for monitoring corrosion damage

and predicting remaining life in aged iron structures. A Physics-of-Failure (PoF) model is developed based on the linear bi-logarithmic law for corrosion to predict remaining life of an iron structure as a model-driven prognostic tool. Currently the only influencing factor is time with this model representing the general rule that corrosion decreases with time due to protective layer buildup on the iron structure. The data-driven diagnostic tool developed uses Mahalanobis distance as the anomaly detection algorithm taking performance parameters as input. A fusion based prognostic tools is also developed using Bayesian networks where probability distributions of predictions of remaining life are processed by integrating predictions of remaining life (using PoF) with information of any anomaly detected in the structure(using MD analysis).

The tools developed were tested using a demonstration example based on simulation data (Chapter 5) and data obtained from a trial experiment (Chapter 6). While the PoF model performed reasonable well for both tests, a comprehensive PoF model for corrosion-based damage would involve other environmental variables. The same challenge applies for the MD analysis technique employed in the diagnostic tool. The more simulation and experimental data for different failure mechanisms and varying conditions, available for use in the training data set, the better the MD analysis will perform.

Using Bayesian networks as the fusion approach for the prognostic tool provides many advantages. While the accuracy of predictions is low due to lack of correlation information, experimental data and more expert knowledge, once more input is available, it can be added to the Bayesian network models developed so far with relative ease. Currently due to initial lack of information and knowledge regarding corrosion processes in iron structures, the Bayesian network model provides a good starting point to predict remaining life of a structure as one can choose to input as little or as much information available to them at one point into the Bayesian network model to obtain predictions of remaining life. Additionally, when more Physics-of-Failure models are built for other failure mechanisms, these data processed from these models can be incorporated relatively easily into the Bayesian network models thus further increasing the accuracy of the predictions of remaining life. The same applies for data processed from data-driven diagnostic tools that could implement other algorithms to detect anomalies.

7.2. Research Contributions and Impact

This thesis makes several contributions in the field of diagnostics and prognostics for aged structures and these are summarized as follows:

- Sensor monitoring system - A bespoke sensor monitoring system comprising of canary and parrot devices has been devised in order to acquire environmental and performance data for the iron structures around the ship. The use of canary and parrot devices provides a practical low-cost solution regarding the requirement that only non-destructive measuring techniques can be used for aged structures of great historical value. Currently temperature and relative humidity (environmental conditions) and electrical resistance (performance) are being measured using the sensor monitoring system and has demonstrated promising results. Additionally the information acquired from the sensor monitoring system will increase understanding of how corrosion forms and progresses enabling engineers and maintenance personnel to control and predict corrosion on structures better.
- Diagnostic Tools to detect damage in aged iron structures - A diagnostic tool is implemented to detect corrosion-related damage in aged iron structures using a distance measure technique called Mahalanobis distance. For the demonstration example and the trial experiment, electrical resistance was used as the performance parameter for corrosion related-damage. As more performance parameters are identified and monitored, the same distance measure technique can be used to detect anomalies and it has the added advantage of removing and correlation between performance parameters that might influence the damage detection.
- Model-driven prognostic tool to predict the remaining life of iron structures - A prognostic algorithm is developed using PoF approach based on the linear bi-logarithmic law for corrosion. After initial measurements of corrosion rate are acquired, the prognostic algorithm is used to predict remaining life of the structure. This prognostic algorithm is adapted into two slightly different versions for use on the demonstration example and the trial experiment. The prognostic algorithm can be run on a regular basis based on the frequency of corrosion rate measurements and the amount of history data to be incorporated.
- Fusion-based prognostic tool - A novel fusion approach using Bayesian networks is employed to develop to a prognostic tool that performs prediction of remaining life

with integrated uncertainty analysis. It incorporates the results from the diagnostic tool and the PoF-based prognostic tool and provides probability distributions of predicted remaining life. This is a first and an original application of the fusion technique for diagnostic and prognostic purposes for aged structures.

- Demonstrate PHM Framework - A notional example consisting of a canary and parrot device pair under the effect of various scenarios was presented. Using the diagnostic and prognostic tools developed, the prediction of remaining life was calculated and compared with expected values for each scenario. Additionally, the diagnostic and predictive capabilities of the tools developed were also put to test using experimental data.
- Publications – The tools developed and preliminary results from the research work have been disseminated in three international conferences and two journal papers.

7.3. Recommendations for Diagnostic and Prognostic tools for Cutty Sark iron structures

Based on the research work carried out so far on diagnostic and prognostic tools for aged iron structures, the following set of recommendations are proposed for the development of such tools for Cutty Sark ship:

- Instrumentation for Measurement - Once the parameters to be measured are known it is important to use instrumentation of the required accuracy for carrying out measurement on sensors and the appropriate data acquisition system.
- Sensor devices - Practical issues such as ease of installation, use and maintenance are as important as the accuracy and reliability of the measurements for low-cost sensor devices. In that respect, any new or adapted designs of the sensor devices should take into account the measurement equipment that will be integrated as well as the actual gathering and transfer of the data. Additionally, the relation between a canary sensor device, parrot sensor device and actual structure should be clear. Since the sensor devices are measuring corrosion processes (which is normally a slow and long-term deterioration mechanism), the sensor devices themselves need to have long remaining life and be able to maintain long-term reliability of the measurements.
- Consider all possible sources of noise - For example in the experiment carried out (as detailed in chapter 6), even slight changes in room temperature affected the electrical

resistance of iron wires and the measurement data had to be de-noised before being used for diagnostic and prognostic analysis.

- Operational and Environmental Conditions - As much as possible all the operation and environmental settings should be investigated such that the structure's behaviour can be understood from all perspectives.
- Training data - It is imperative to collect data from the actual structure and incorporate this data in the development of any diagnostic and prognostic tool, this is because simulated data cannot fully represent the conditions and behaviour of the actual structure and thus tools developed using solely simulation data will often provide poor results

7.4. Areas for Future Research

The diagnostic and prognostic tools developed for aged structures need further development in order to be able to deploy it as an application for real-world projects. There are several potential extensions to the work presented in this thesis and future research could expand along following areas:

- Further development of the sensor devices - While the sensor devices developed have been useful in terms of proof of concept for the sensor monitoring system, there is still much to be accomplished before they are operational. Currently the sensor devices developed are used for electrical resistance measurement only. Temperature and relative humidity sensors could be integrated into the canary/parrot sensor devices. More designs of the sensors need to be made to represent the different structures to be monitored. These sensors require testing under varying environmental and loading conditions in order to obtain robust correlations. Once sufficiently large set of data is obtained for the canary/parrot sensor devices as well as the actual structures being monitored if possible, the correlation factors can be determined more accurately.
- Extension of the PoF Models - The current PoF model used for remaining life prediction only uses time as the factor influencing the corrosion rate. With additional experiment trials studying the effect of other factors as sulphur concentration and chloride concentration, the PoF model could be extended to include them. Furthermore, PoF models for failure mechanisms other than corrosion should be investigated.

- Investigation of anomaly detection algorithms - The Mahalanobis distance analysis has been trained to detect one main form of failure, that is, uniform corrosion. Once other failure mechanisms are identified, the Mahalanobis distance analysis can also be trained to those failures. Apart from Mahalanobis Distance, other distance measures such as Euclidean Distance can be explored for use in simpler cases where no correlation of data is expected.
- Further Development of Bayesian Network models - Various improvements can be made on the Bayesian network models designed. Currently, discrete nodes are used to represent continuous variables, as they are more convenient to manipulate in Hugin tool. These nodes could be converted to continuous ones to better capture the original distributions and increase the precision of the variable values. The structure of the Bayesian network models can be extended to include other variables representing other types of measurements such as structural distortion, stress, etc.

The Bayesian network models developed so far are static Bayesian network models. That is, they do not intrinsically account for historical values of health observations and rely primarily on the PoF model to perform initial predictions. The models can be extended into temporal Bayesian network models where the models are structured temporally as well as organised into layers. In such a model, the transition function would be time-dependent.

The derivation of the CPTs of the Bayesian network models needs optimising through input from more experts as well as data gathered from further lab experiments. While in the beginning, it is acceptable to rely more on input from experts to derive CPTs, it is expected that once more data is acquired through experimental trials and from the sensor monitoring system, the CPTs should be revised accordingly. Thus, input bias that often results from elicitation of probabilities from experts is reduced.

- Simulation of failure data - Since the goal of maintenance is to prevent failure, allowing a structure to fail to obtain failure data can be expensive and in some cases impossible even (e.g. safety critical systems). As a result, it is hard to obtain failure data from real systems, which can be used to develop diagnostic and prognostic tools. Thus in order to obtain failure data, simulation needs to be carried out based on analytical models. The demonstrator example used in chapter 5 used simulation data based on corrosion rates obtained from literature. The simulation data can be further

enhanced by adding the influence of more factors on corrosion. Data can also be simulated for many more realistic scenarios (e.g. varying periods of time to which the structures is subjected to environmental conditions and other load conditions as well as varying the strengths of the environmental and load conditions).

- Validation of Models - The proposed diagnostic and prognostic tools have been validated using a demonstrator example and the preliminary experiment carried out. It is however necessary to test and validate the tools further using a real application. Once the sensor devices have been finalised, the tools developed need to be tested for accuracy and robustness through trial runs with the sensor devices placed within the actual structures being monitoring based on a formal validation and testing plan.

8. References

- ACHENBACH, J D. 2009. Structural Health Monitoring - What is the prescription? *Mechanics Research Communications.*, pp.137-142.
- AGENA. 2011. *Bayesian Network and Simulation Software for Risk Analysis and Decision Support.* [online]. [Accessed 25 May 2011]. Available from World Wide Web: <<http://www.agenarisk.com/>>
- AHMAD, Z. 2006. *Corrosion Engineering and Corrosion Control.* Oxford: Butterworth-Heinemann.
- AMARI, S. 2006. *A Novel Approach Developed by Relex Software.* [online]. [Accessed 02 October 2006]. Available from World Wide Web: <http://www.relex.com/resources/art/art_conditionmaint2.asp>
- ANASTASI, G., G. LO RE, and M. ORTOLANI. 2009. WSNs for Structural Health Monitoring of Historical Buildings. *In: 2nd Conference on Human System Interaction.* Catania, pp.571-576.
- AUWERAER, H. V.D. 2003. International Research Projects on Structural Health Monitoring: An Overview. *Structural Health Monitoring.*, pp.341-358.
- BALAGEAS, Daniel. 2010. *Introduction to Structural Health Monitoring.* [online]. [Accessed 22 Jul 2010]. Available from World Wide Web: <http://www.iste.co.uk/data/doc_xqjujdlhnfls.pdf>
- BARAJAS, Leandro G and Narayan SRINIVASA. 2008. Real-time diagnostics, prognostics & health management for large-scale manufacturing maintenance systems. Evanston, Illinois: Proceedings of the 2008 International Manufacturing Science and Engineering Conference.
- BARDAL, E. 2003. *Corrosion and Protection.* London: Springer.
- BAYESIA. *Bayesia - Make the Best Decisions.* [online]. [Accessed 25 May 2011]. Available from World Wide Web: <<http://www.bayesia.com/>>
- BLISCHKE, Wallace R and D.N. Prabhakar MURTHY. 2003. *Case Studies in Reliability and Maintenance.* Hoboken, New Jersey: John Wiley & Sons.
- BOGDAN, B A, A A MUFTI, and A BAGCHI. 2005. SHM data interpretation and structural condition assessment of the Manitoba Golden Boy. *In: NDE02/SPOE 2005 Conference.* San Diego, pp.213-224.
- BROMLEY, J, N A JACKSON, A M GIACOMELLO, and F V JENSEN. 2004. The use of Hugin to develop Bayesian network as an aid to integrated water resource planning. *Environmental Modelling and Software.*, pp.231-242.
- CAMPBELL, Sheelagh A, S P GILLARD, I B BEECH et al. 2005. The s.v. Cutty Sark: electrochemistry in conservation. *T. Inst.Met.Fin.*, pp.19-26.
- CHENG, Shunfeng and Michael PECHT. 2007. Multivariate State Estimation Technique for Remaining Useful Life Prediction of Electronic Products. *In: AAAI Fall Symposium on Artificial Intelligence for Prognostics.* Arlington, VA, pp.26-32.

- CHENG, Shunfeng and Michael PECHT. 2009. A Fusion Prognostics Method for Remaining Useful Life. *In: 5th Annual IEEE Conference on Automation Science and Engineering*. Bangalore.
- CHENG, Shunfeng and Michael PECHT. 2009. A Fusion Prognostics Method for Remaining Useful Life Prediction of Electronic Products. Bangalore: 5th Annual IEEE Conference on Automation Science and Engineering.
- COLE, I. 2008. Development of a Sensor-Based Learning Approach to Prognostics in Intelligent Vehicle Monitoring. *In: International Conference on Prognostics and Health Management*. Denver.
- CORVO, F., J. MINOTAS, J. DELGADO, and C. ARROYAVE. 2005. Changes in atmospheric corrosion rate caused by chloride ions depending on rain regime. *Corrosion Science.*, pp.883-892.
- CUDNEY, Elizabeth A, Jungeui HONG, Rajesh JUGULUM, and Kioumars PARYANI. 2007. An Evaluation of Mahalanobis-Taguchi System and Neural Network for Multivariate Pattern Recognition. *Journal of Industrial and Systems Engineering*. **1**(2), pp.139 - 150.
- CUDNEY, Elizabeth A, Kioumars PARYANI, and Kenneth M RAGSDALL. 2006. Applying the Mahalanobis-Taguchi System to Vehicle Handling. *Concurrent Engineering: Research and Application*. **14**(4), pp.343 - 354.
- DAWOTOLA, Alex W, T B TRAFALIS, Z MUSTAFFA et al. 2011. Data-driven Risk Based Maintenance Optimisation of Petroleum Pipelines Subject to Corrosion. *In: Twenty-first (2011) International Offshore and Polar Engineering Conference*. Maui, Hawaii.
- DECISION SYSTEMS LABORATORY. 2007. *GeNie & SMILE*. [online]. [Accessed 25 May 2001]. Available from World Wide Web: <<http://genie.sis.pitt.edu/about.html>>
- DHILLON, B. 2006. *CBM Methodology: Maintainability, Maintenance and Reliability for Engineers*. Boca Raton: Taylor & Francis Group.
- DHILLON, B S. 2006. *Maintainability, Maintenance and Reliability for Engineers*. Boca Raton: Taylor & Francis Group.
- DISSANAYAKE, P B and P A KARUNANANDA. 2008. Remaining Service Life Prediction of Riveted Wrought Iron Railway Bridges using System Reliability Approaching. *J. Natn. Sci. Foundation*. **36**(2), pp.151-156.
- D'SILVA, Siddharth H, Laci JALICS, and Mark KRAGE. 2007. *A Statistical Approach for Real-Time Prognosis of Safety-Critical Vehicle Systems*.
- ENGEL, S J, B J GILMARTIN, K BONPORT, and A HESS. 2000. Prognostics, the real issues involved with predicting life remaining. *In: IEEE Aerospace Conference*. Big Sky, MT, pp.457-469.
- ESRF. 2005. *Preserving the Mary Rose*. [online]. [Accessed 25 October 2010]. Available from World Wide Web: <<http://www.esrf.eu/files/press/MARYROSEENGLISH2609.pdf>>
- FLORES-QUINTANILLA, J L, R MORALES-MENENDEZ, R A RAMIREZ-MENDOZA et al. 2005. Towards a new fault diagnosis system for electric machines based on dynamic probabilistic models. *In: American Control Conference*. Portland, pp.2775-2780.

- GARNETT, E S. 2005. *Impedance-Based Structural Health Monitoring to detect Corrosion*.
- GARZIERA, R., M. AMABILI, and L. COLLINI. 2007. Structural Health Monitoring Techniques for Historical Buildings. *In: IV Conferencia Panamericana de END*. Buenos Aires, pp.CD-ROM.
- GASCOIGNE, A and D BOTTOMLEY. 1995. *Atmospheric Corrosion rates of Railway Bridge Structures*. Derby, UK: Scientifics.
- GLISIC, B. and AL. 2007. Monitoring of Heritage Structures and Historical Monuments Using Long-Gage Fibre Optic Interferometric Sensors - An Overview. *In: 3rd International Conference on Structural Health Monitoring of Intelligent Infrastructures*. Vancouver, pp.CD-ROM.
- GOEBEL, Kai and Piero BONISSONE. 2005. Prognostics Information Fusion for Constant Load Systems. 7th Annual Conference on Information Fusion, Fusion 2005, Vol 2., pp 1247-1255.
- GOEBEL, Kai, Neil EKLUND, and Pierino BONANNI. 2006. Fusing Competing Predictin Algorithms for Prognostics. Big Sky, MT: IEEE Aerospace Conference.
- GOEBEL, Kai, Neil EKLUND, and Piero BONANNI. 2007. Prognostic Fusion for Uncertainty Reduction. Rohnert Park, CA: AIAA Infotech@Aerospace Conference and Exhibit.
- GOH, K M, B TIAHJONO, T BAINES, and S SUBRAMANIAM. 2006. A Review of Research in Manufacturing. *In: IEEE International Conference on Industrial Informatics*. Singapore, pp.417-422.
- GONZALEZ, J E and et AL. 2003. The effect of environmental and meteorological variables on atmospheric corrosion of carbon steel, copper, zinc and aluminium in a limited geographic zone with different types of environments. *Corrosion Science.*, pp.799-815.
- GREITZER, F. and AL. 2001. Determining how to do prognostics, and then determining what to do with it. *In: AUTOTESTCON*. IEEE Systems Readiness Technology Conference, pp.780-792.
- GUPTA , K, R J STANLEY, M T GHASR et al. 2007. Fusion of Multimodal Data for Improved Corrosion Detection. *In: ICONIC 2007*. St Louis, MO.
- GU, Jinwei, Chien-I TU, Ravi RAMAMOORTHY et al. 2006. Time-Varying Surface Appearance: Acquisition, Modelling and Rendering. *ACM Transactions on Graphics - Proceedings of ACM SIGGRAPH 2006*. **25**(3).
- HADDEN, G D, P BERGSTROM, T SAMAD et al. 2000. Application Challenges: System Health Management for Complex Systems. *In: IPDPS 2000 Workshops on Parallel and Distributed Processing*. Cancun, pp.784-791.
- HALL, P L and J E STRUTT. 2003. Probabilistic physics of failure models for component reliabilities using Monte Carlo simulation and Weibull analysis: a parametric study. *Reliability Engineering and System Safety.*, pp.233-242.
- HERITAGE LOTTERY FUND. 2011. *Investing in Success*. [online]. [Accessed 14 September 2011]. Available from World Wide Web: <<http://www.hlf.org.uk/news/Pages/Investinginsuccess.aspx>>

- HESS, A., G CALVELLO, and P FRITH. 2005. Challenges, Issues and Lessons Learned Chasing the "Big P": Real Predictive Prognostics Part 1. *In: IEEE Aerospace Conference*. Big Sky, MT, pp.3610-3619.
- HESS, A, G CALVELLO, P FRITH et al. 2006. Challenges, Issues, and Lessons Learned Chasing the " Big P": Real Predictive Prognostics Part 2. *In: IEEE Aerospace Conference*. Big Sky, pp.1-19.
- HOLLAND, Steven W. 2008. Integrated Vehicle Health Management in the Auto Industry. *In: Electronics System-Technology Conference, ESTC*. Greenwich, pp.85-88.
- HUGIN. 2011. *Hugin Expert - Advanced Decision Support Using Bayesian Network and Influence Diagrams*. [online]. [Accessed 25 May 2011]. Available from World Wide Web: <http://www.hugin.com/>
- INAUDI, Daniele, Nicoletta CASANOVA, and Branko GLISIC. 2001. Long-term deformation monitoring of historical constructions with fibre optic sensors. *In: 3rd International Seminar on Structural Analysis of Historical Constructions*. Guimaraes.
- INAUDI, D and R WALDER. 2009. Integrated Structural Health Monitoring Systems for Buildings. *In: Seventh International workshop on Structural Health Monitoring*. Stanford, CA.
- JENKINS, T. 2007. *Corrosion Science and the application of the Butler-Volmer equation to measure the rate of corrosion*. [online]. [Accessed 29 January 2007]. Available from World Wide Web: <http://staff.bath.ac.uk/chsataj/lecture%2015%202005.pdf> >
- KACPRZYNSKI, G J, M J ROEMER, G MODGIL et al. 2002. Enhancement of Physics-of-Failure Prognostics Models with System Level Features. *In: IEEE Aerospace Conference Proceedings*.
- KO, J. M. and Y. Q. NI. 2005. Technology Developments in Structural Health Monitoring of Large-Scale Bridges. *Engineering Structures*., pp.1715-1725.
- KOTHAMASU, Ranganath, Samuel H HUANG, and William H VERDUIN. 2006. System health monitoring and prognostics - a review of current paradigms and practices. *International Journal Advance Manufacturing Technology*., pp.1012-1024.
- KUMAR, S, V SOTIRIS, and M PECHT. 2008. Health Assessment of Electronic Products using Mahalanobis Distance and Projection Pursuit. *International Journal of Computer, Information, Systems Science, and Engineering*., pp.242-250.
- KUMAR, Sachin, Myra TORRES, Y C CHAN, and Michael PECHT. 2008. A Hybrid Prognostics Methodology for Electronic Products. Hong Kong: IEEE World Congress on Computational Intelligence.
- LUBOWIECKA, Izabela, Julia ARMESTO, Pedro ARIAS, and Henrique LORENZO. 2009. Historic bridge modelling using laser scanning, ground penetrating radar and finite element methods in the context of structural dynamics. *Engineering Structures*., pp.2667-2676.
- LUMINA. 2011. *Analytica*. [online]. [Accessed 25 May 2011]. Available from World Wide Web: <http://www.lumina.com/>

- MANDENO, W. L. 2008. *Conservation of iron and steelwork in historic structures and machinery*. Wellington: Department of Conservation, New Zealand.
- MANDENO, W L. 2008. *Conservation of iron and steelwork in historic structures and machinery*. Wellington: New Zealand Department of Conservation.
- MATTHEW, S, D DAS, R ROSSENBERGER, and M PECHT. 2008. Failure mechanisms based prognostics. *In: International Conference on Prognostics and Health Management*. Denver, pp.1-6.
- MAYOL, Dottie E. 1996. *The Swedish ship Vasa's revival*. [online]. [Accessed 10 September 2010]. Available from World Wide Web: <<http://www.abc.se/~pa/publ/vasa.htm>>
- MELCHERS, R. E. 1999. Corrosion Uncertainty Modelling for Steel Structures. *Journal of Constructional Steel Research.*, pp.3-19.
- MELCHERS, R. E. and R. J. JEFFREY. 2008. Probabilistic Models for Steel Corrosion Loss and Pitting on Marine Infrastructure. *Reliability Engineering and System Safety.*, pp.423-432.
- MENGSHOEL, O. J., Adnan DARWICHE, and Serdar UCKUN. 2008. Sensor Validation using Bayesian Networks. *In: 9th International Symposium on Artificial Intelligence, Robotics and Automation in Space*. Los Angeles.
- MUFTI, A A. 2003. Restoration and Structural Health Monitoring of Manitoba's Golden Boy. *Can. J. Civ. Eng.*, pp.1123-1132.
- MUSTER, T, I COLE, W GANTHER et al. 2005. Establishing a physical basis for the in-situ monitoring of airframe corrosion using intelligent sensor networks. *In: 2005 Tri-Service Corrosion Conference*. Orlando.
- NIE, L, M AZARIAN, M KEIMASI, and M PECHT. 2007. Prognostics of ceramic capacitor temperature-humidity-bias reliability using Mahalanobis distance analysis. *Circuit World.*, pp.21-28.
- NIU, Gang, D ANAND, and M PECHT. 2010. Prognostics and health management for energetic material systems. *In: Prognostics and Health Management Conference*. Macau, pp.1-7.
- NORSYS SOFTWARE CORP. *Netica Bayesian Network Software from Norsys*. [online]. [Accessed 25 May 2011]. Available from World Wide Web: <<http://www.hugin.com/>>
- NPL. 2006. *Corrosion of Metals by Wood*. [online]. [Accessed 05 December 2006]. Available from World Wide Web: <http://www.npl.co.uk/lmm/docs/corrosion_of_metals_by_wood.pdf>
- O&M Best Practices Guide, Release 2.0*. [online]. [Accessed 15 June 2010]. Available from World Wide Web: <http://www1.eere.energy.gov/femp/pdfs/OM_5.pdf>
- ORSAGH, Rolf, Michael ROEMER, and Jeremy SHELDON. 2004. Comprehensive Prognostics Approach for Predicting Gas Turbine Engine Bearing Life. *In: IGTI Turbo Expo*. Vienna.
- ORSAGH, Rolf, Michael ROEMER, Jeremy SHELDON, and Christopher KLENKE. 2004. A Comprehensive Prognostics Approach for Predicting Gas Turbine Engine Bearing Life. Vienna, Austria: ASME Turbo Expo, Vol. 7, pp. 777-785.

- PAIK, J K and F BRENMAN. 2006. *Condition Assessment of Aged Ships*. Southampton, UK: 16th International Ship and Offshore Structures Congress.
- PATNAIK, A R, A NAYAK, V NARASIMHAN, and P PATNAIK. 2006. An Integrated PHM Approach for Gas Turbine Engines. *In: Canadian Conference on Electrical and Computer Engineering*. Ottawa, pp.2476-2479.
- PECHT, Michael. 2006. Prognostics and Health Management of Electronics. *In: International Conference on Electronic Materials and Packaging, 2006. EMAP 2006*. Kowloon, pp.1-10.
- PECHT, Michael G. 2008. *Prognostics and Health Management of Electronics*. Hoboken, New Jersey: John Wiley & Sons.
- PINJALA, K K, B C KIM, and P VARIYAM. 2003. Automatic Diagnostic Program Generation for Mixed Signal Load Board. *In: International Test Conference*. Charlotte,NC, pp.403-409.
- POURBAIX, M. 1982. *Atmospheric Corrosion*. New York: Wiley.
- Preservation and Research - The Vasa Museum*. 2010. [online]. [Accessed 10 September 2010]. Available from World Wide Web: <<http://www.vasamuseet.se/en/Preservation--Research/>>
- PRZYTULA, K W and A CHOI. 2007. Reasoning Framework for Diagnosis and Prognosis. *In: IEEE Aerospace Conference*. Big Sky.
- PRZYTULA, Wojtek and Arthur CHOI. 2007. *Reasoning Framework for Diagnosis and Prognosis*. Big Sky, MT: IEEE Aerospace Conference.
- PRZYTULA, Wojtek and Arthur CHOI. 2008. An Implementation of Prognosis with Dynamic Bayesian Networks. *In: 2008 IEEE Aerospace Conference*. Big Sky, MT, pp.1-8.
- PRZYTULA, Wojtek, Denver DASH, and Don THOMPSON. 2003. Evaluation of Bayesian Networks used for Diagnostics. *In: 2003 IEEE Aerospace Conference.*, pp.3177-3187.
- PRZYTULA, Wojtek and Don THOMPSON. 2000. *Constructions of Bayesian Networks for Diagnostics*. Big Sky, MT: IEEE Aerospace Conference.
- RAMAKRISHMAN, A and M PECHT. 2003. A Life Consumption Monitoring Methodology for Electronic Systems. *IEEE Transactions on Components and Packaging Technologies.*, pp.625-634.
- Resistivity and Temperature Coefficient*. 2011. [online]. [Accessed 20 January 2011]. Available from World Wide Web: <<http://hyperphysics.phy-astr.gsu.edu/hbase/tables/rstiv.html>>
- RIGETOP SEMICONDUCTOR-SENTINEL SILICON LIBRARY. 2004. *Hot Carrier (HC) Prognostic Cell*.
- ROBERGE, P R. 2000. *Handbook of Corrosion Engineering*. New York: McGraw-Hill.
- ROBERGE, P R, R D KLASSEN, and P W HABERECHE. 2002. Atmospheric corrosivity modelling - a review. *Materials and Design.*, pp.321-330.

ROTHWELL GP. 2006. *Corrosion Phenomena: An Introduction*. [online]. [Accessed 05 December 2006]. Available from World Wide Web:

<http://www.npl.co.uk/lmm/docs/introduction_to_corrosion_phenomena.pdf>

SADIQ, Rehan, Balvant RAJANI, and Yehuda KLEINER. 2004. Probabilistic risk analysis of corrosion associated failures in cast iron water mains. *Reliability Engineering and System Safety*., pp.1-10.

SADIQ, R, B RAJANI, and Y KLEINER. 2004. Probabilistic Risk Analysis of Corrosion Associated Failures in Cast Iron Water Mains. *Reliability Engineering and System Safety*. **86**(1), pp.1-10.

SALVINO, Liming W, Charles FARRAR, Jerome P LYNCH, and Thomas F BRADY. 2009. Multi-tiered Sensing and Data Processing for Monitoring Ship Structures. *In: High Performance Marine Vehicles Symposium*. Linthicum, MD.

SANDBORN, P. 2005. A Decision Support Model for Determining the Applicability of Prognostic Health Management (PHM) Approaches to Electronic Systems. *In: Reliability and Maintenance Symposium*., pp.422-427.

SCHWABACHER, Mark. 2005. A survey of data-driven prognostics. *In: AIAA Infotech@Aerospace Conference*. Reston, VA: American Institute for Aeronautics and Astronautics Inc.

SCHWABACHER, M and Kai GOEBEL. 2007. A Survey of Artificial Intelligence for Prognostics. *In: AAAI Fall Symposium on Artificial Intelligence for Prognostics*. Arlington.

SCHWEITZER, Philip A. 2007. *Fundamentals of Metallic Corrosion: Atmospheric and Media Corrosion of Metals*. Boca Raon: Taylor & Francis Group.

SMITH, R and K MOBLEY. 2006. *Fundamental Requirements of Effective Preventive/Predictive Maintenance*. [online]. Available from World Wide Web:

<<http://www.reliabilityweb.com/excerpts/excerpts/pm.htm>>

SMITHS AEROSPACE. 2004. *Intelligent Tools for Prognostics Health Management and its applications to Avionics*. CALCE.

SOARES, C G and et AL. 2008. Corrosion wastage model for ship crude oil tanks. *Corrosion Science*., pp.3095-3106.

SOARES, C. G. and et AL. 2008. Influence of environmental factors on corrosion of ship structures in marine atmosphere. *Corrosion Science*., pp.2014-2026.

SOLIS, M, A ROMERO, and P GALVIN. 2009. Monitoring the Mechanical Behaviour of the Weathervane Sculpture Mounted atop Seville Cathedral's Giralda Tower. *Structural Health Monitoring*., pp.41-57.

SPECKMANN, Holger and Henrik ROESNER. 2006. *Structural Health Monitoring: A Contribution to the Intelligent Aircraft Structure*.

STARR, a. and A. BALL. 2000. Systems Integration in Maintenance Engineering. *Proceedings of the Institution of Mechanical Engineers, Part E: Journal of Process Mechanical Engineering*., pp.79-85.

STRAUB, Daniel. 2004. *Generic approaches to risk based inspection planning for steel structures*. Zurich: Verlag der Fachvereine Hochschulverlag AG an der ETH Zurich.

SUN, Bo, Shengkui ZENG, Rui KANG, and Michael PECHT. 2010. Benefits Analysis of Prognostics in Systems. *In: Prognostics and Health Management Conference*. Macao, p.18.

TAGUCHI, Genichi, Subir CHOWDHURY, and Yuin WU. 2000. *The Mahalanobis-Taguchi System*. McGraw-Hill Professional.

The construction and salvage of the Vasa. [online]. [Accessed 10 September 2010]. Available from World Wide Web: <<http://www.mmk.su.se/~magnuss/hist.html>>

TRETHEWEY, K. and J. CHAMBERLAIN. 1995. *Corrosion for Science and Engineering*. Harlow: Longman Scientific & Technical.

TSE, C Y, W S LIU, E S YEUNG, and S W CHAN. 2010. An integrated structural health monitoring system for the preservation of the historic Fireboat Alexander Grantham. *In: Metal 2010 Conference*. Charleston.

TULLMIN, Martin and Pierre R. ROBERGE. 1995. Tutoria: Corrosion of Metallic Materials. *IEEE TRANSACTIONS ON RELIABILITY.*, p.Vol. 44 No.2.

VICHARE, N and M PECHT. 2006. *Enabling Electronic Prognostics Using Thermal Data*. Nice.

VICHARE, N and M PECHT. 2006. *Enabling Electronic Prognostics Using Thermal Data*. Nice.

VICHARE, N and M PECHT. 2006. Prognostics and Health Management of Electronics. *IEEE Transactions on Components and Packaging Technologies.*, p.Vol. 29 No. 1.

WANG, G and B BOON. 2009. *Condition Assessment of Aged Ships and Offshore Structures*. Seoul, South Korea: 17th International Ship and Offshore Structures Congress.

WATKINSON, David and Mark LEWIS. 2010. *Brunel's SS Great Britain*. [online]. [Accessed 26 July 2010]. Available from World Wide Web: <<http://www.ssgreatbritain.org/ArticlesandResearch.aspx>>

WATKINSON, David, Matthew TANNER, Robert TURNER, and Mark LEWIS. 2010. *ss Great Britain: teamwork as a platform for innovative conservation*. [online]. [Accessed 26 July 2010]. Available from World Wide Web: <<http://www.ssgreatbritain.org/ArticlesandResearch.aspx>>

WEATHER, BBC. 2006. *BBC Weather Centre - World Weather - Average Conditions - London*. [online]. [Accessed 10 July 2010]. Available from World Wide Web: <http://www.bbc.co.uk/weather/world/city_guides/results.shtml>

YANNIAN, Wang and Jiang ZHUANGDE. 2005. Decision fusion framework in diagnostic and prognostic assessment of long-distance oil pipeline leakage and damage based on Dempster-Shafer theory. 7th International Symposium Measurement Technology and Intelligent Instruments, 349-352.

YAN, Liu and Li SHI-QI. 2007. Decision Support for Maintenance Management using Bayesian Networks. *In: International Conference on Wireless Communications, Networking and Mobile Computing*. Shanghai, pp.5713-5716.

YUANTAI. 2008. Corrosion of low carbon steel in atmospheric environments of different chloride content. *Corrosion Science.*, pp.997-1006.

ZHANG, Huiguo, Rui KANG, and Michael PECHT. 2009. A hybrid prognostics and health management approach for condition-based maintenance. *In: IEEE International Conference on Industrial Engineering and Engineering Management.* Hong Kong, pp.1165-1169.

9. Appendix

9.1. Additional PHM Framework Information

9.1.1. Additional Parrot Device Designs

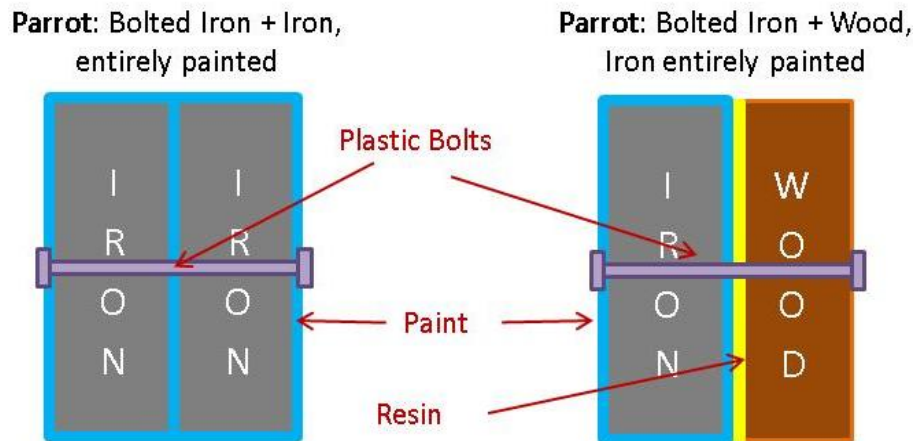


Figure 9-1: Parrot Device Designs (a)

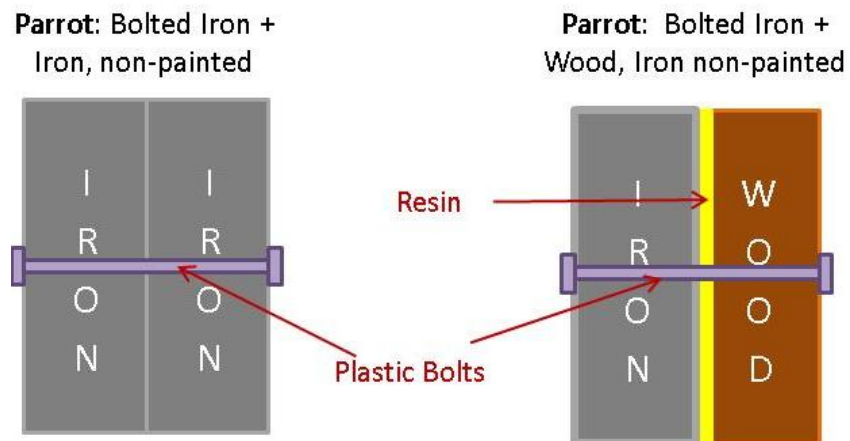


Figure 9-2: Parrot Device Designs (b)

9.1.2. Additional Canary Device Designs

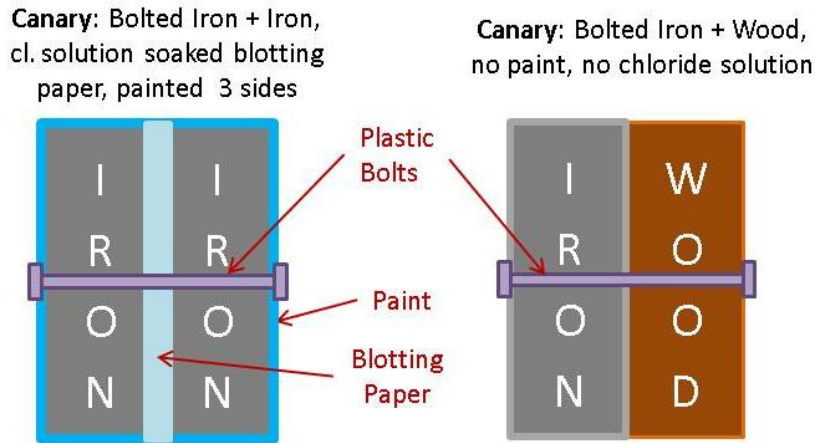


Figure 9-3: Canary Device Designs (a)

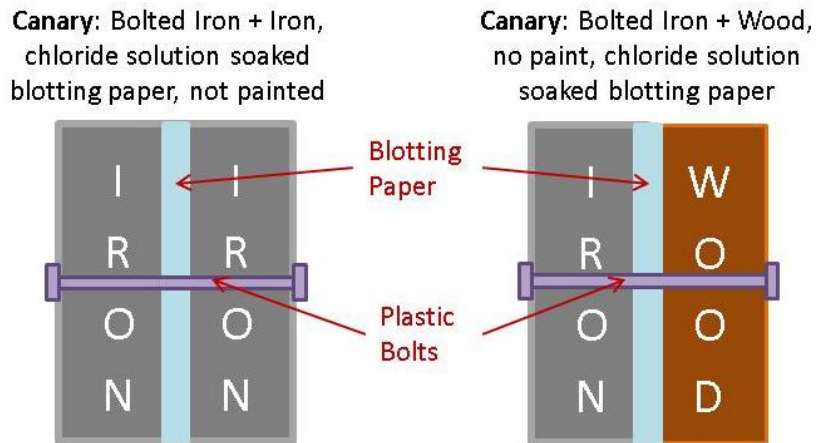


Figure 9-4: Canary Device Designs (b)

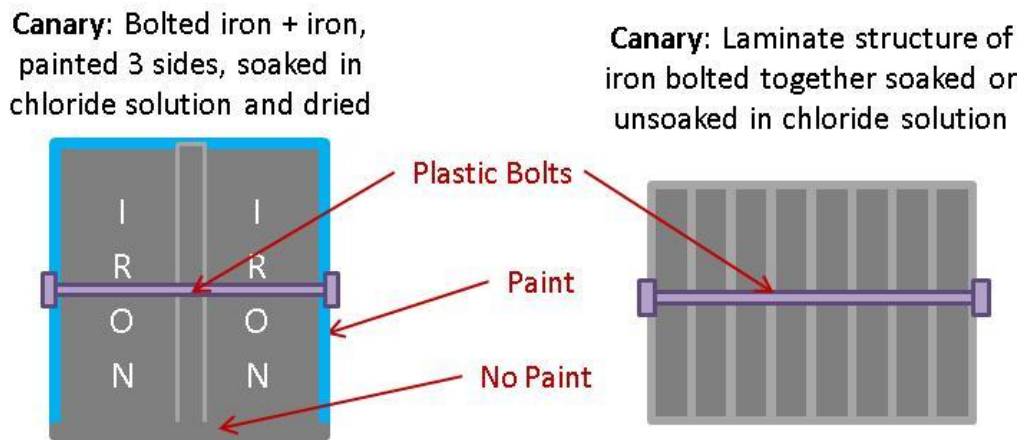


Figure 9-5: Canary Device Designs (c)

9.2. Demonstrator Example

9.2.1. MD Analysis of Canary and Parrot Devices

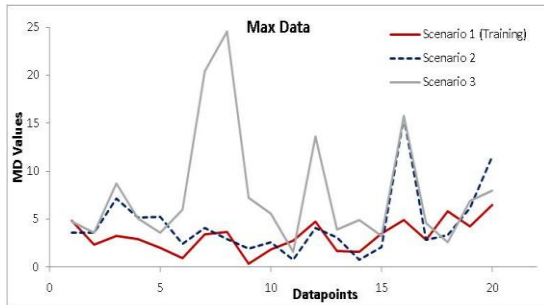


Figure 9-6: MD Analysis of Max Data for Scenarios 2 & 3 for Canary

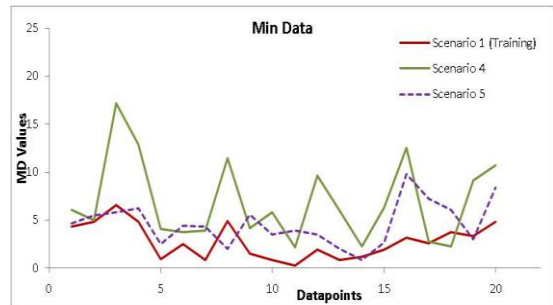


Figure 9-8: MD Analysis of Min Data for Scenarios 4 & 5 for Canary

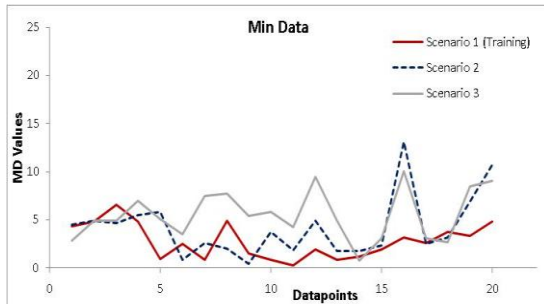


Figure 9-7: MD Analysis of Min Data for Scenarios 2 & 3 for Canary

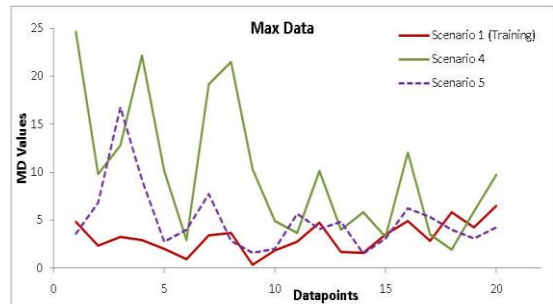


Figure 9-9: MD Analysis of Max Data for Scenarios 4 & 5 for Canary

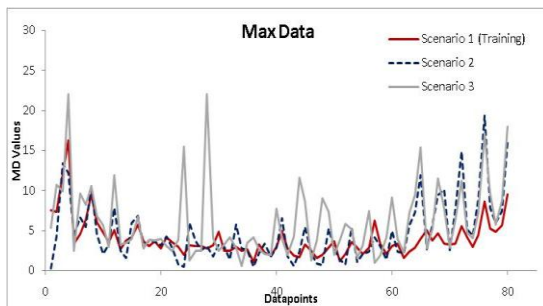


Figure 9-10: MD Analysis of Max Data for Scenarios 2 & 3 for Parrot

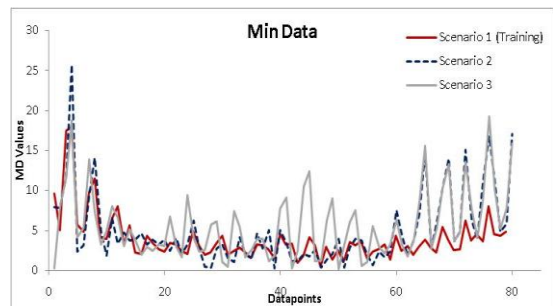


Figure 9-11: MD Analysis of Max Data for Scenarios 2 & 3 for Parrot

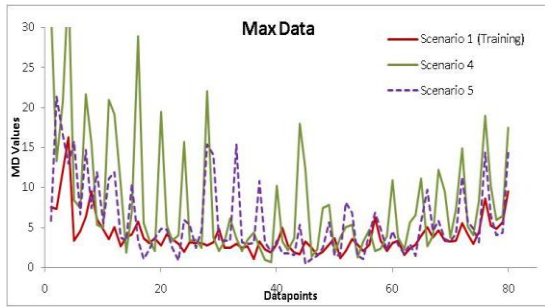


Figure 9-12: MD Analysis of Max Data for Scenarios 4 & 5 for Parrot

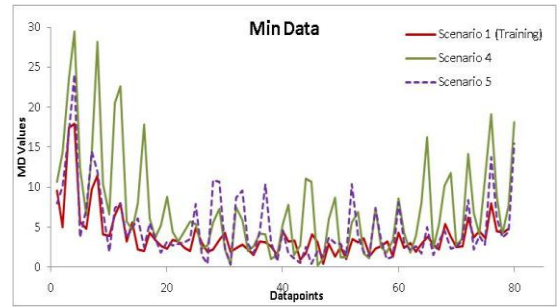


Figure 9-13: MD Analysis of Max Data for Scenarios 4 & 5 for Parrot

9.3. Additional Experimental Trials Information

9.3.1. Temperature and Relative Humidity

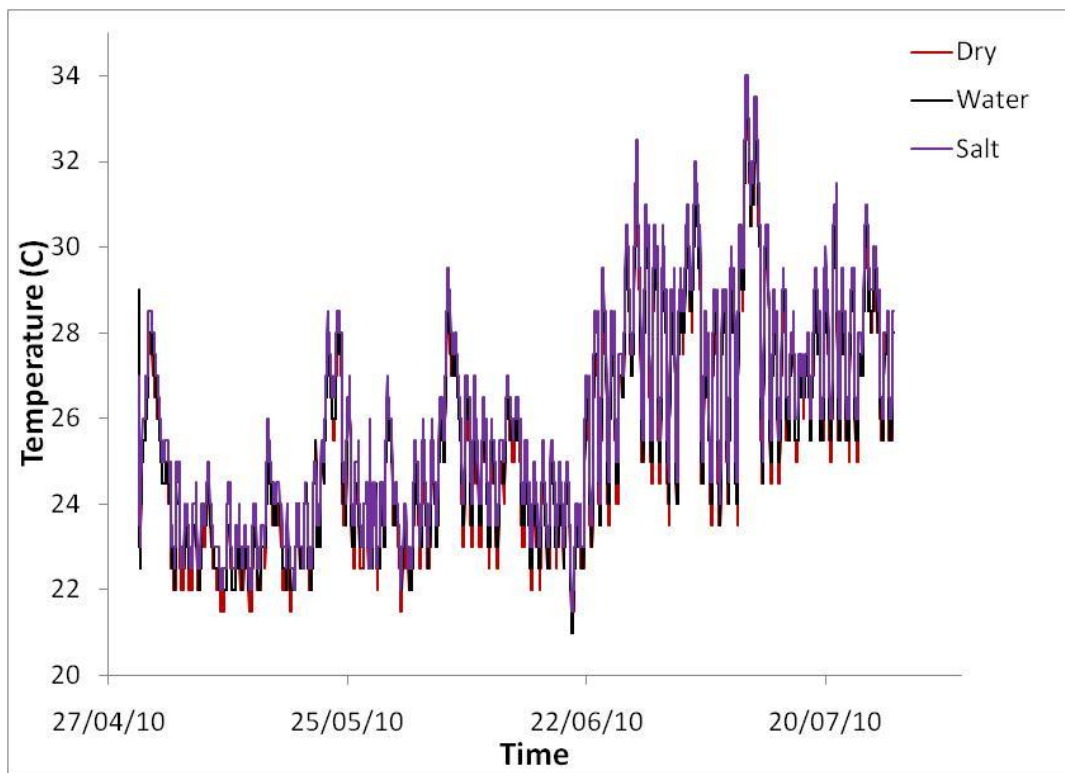


Figure 9-14: Temperature readings for experiment

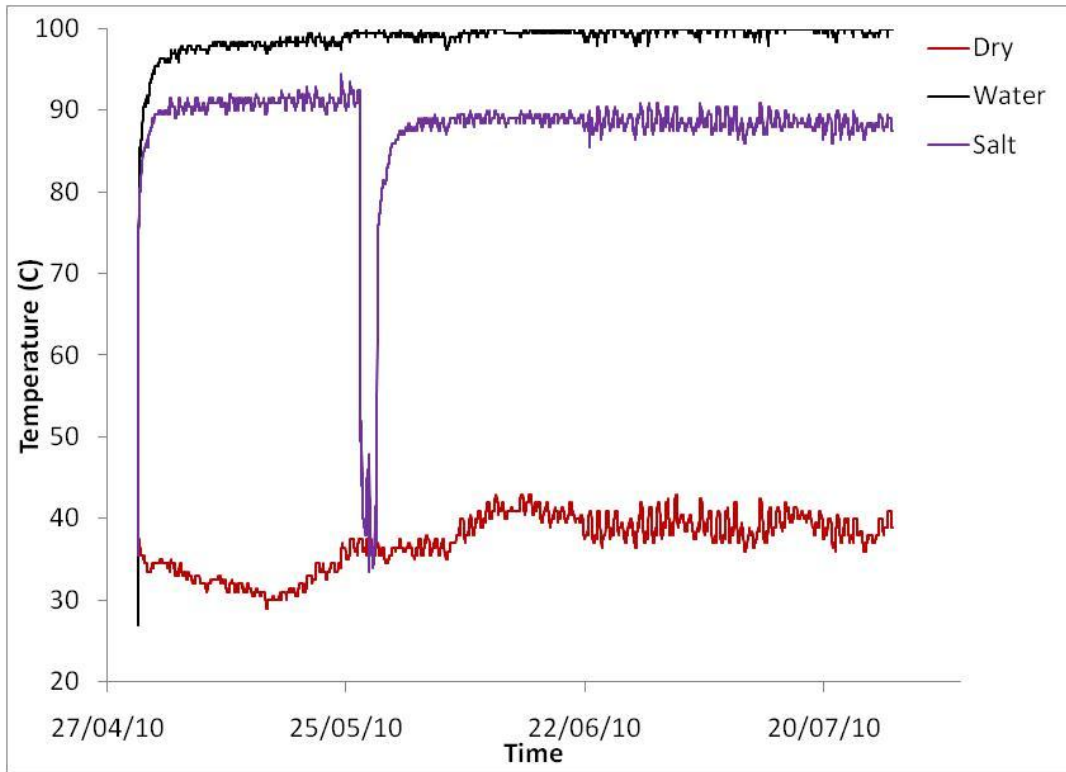


Figure 9-15: Relative Humidity readings for experiment.

9.3.2. Overlay Graphs of Temperature and Electrical Resistance for Dry and Water Environments

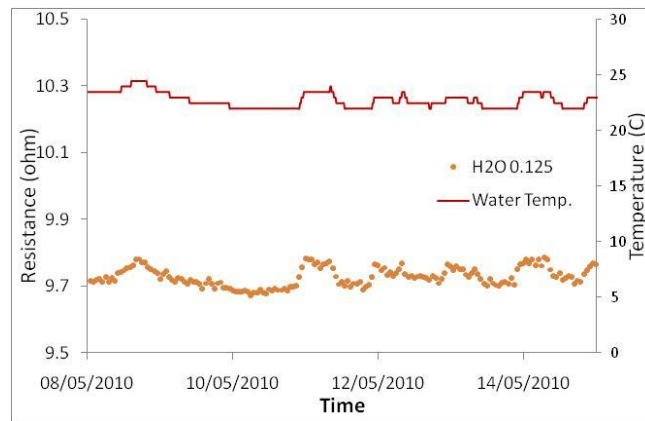


Figure 9-16: Overlay of Temperature and Resistance (0.125mm) -Water Environment

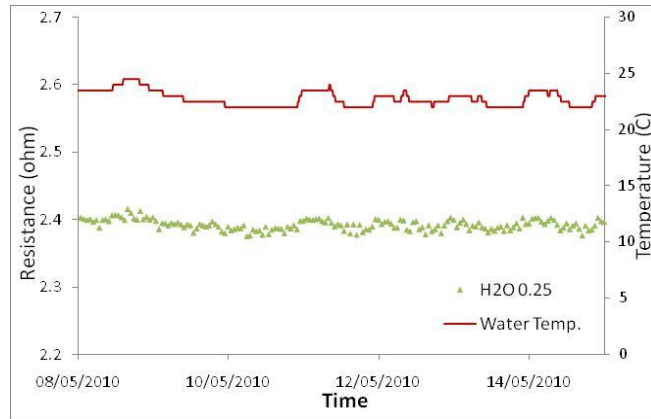


Figure 9-17: Overlay of Temperature and Resistance (0.25mm) -Water Environment

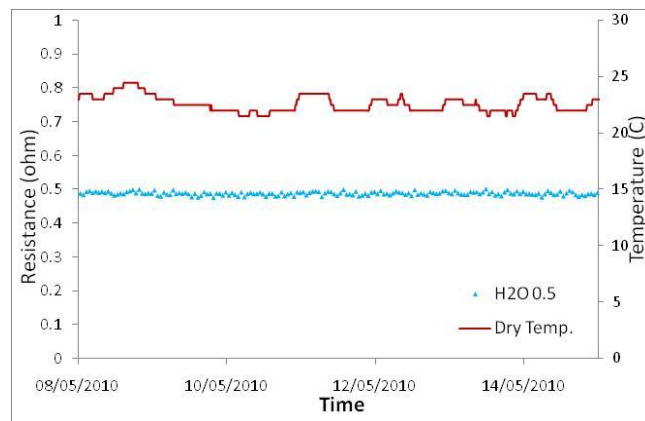


Figure 9-18: of Temperature and Resistance (0.5mm) -Water Environment

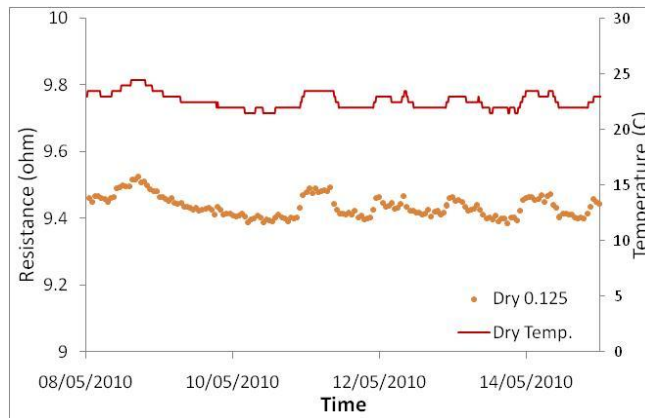


Figure 9-19: of Temperature and Resistance (0.125mm) -Dry Environment

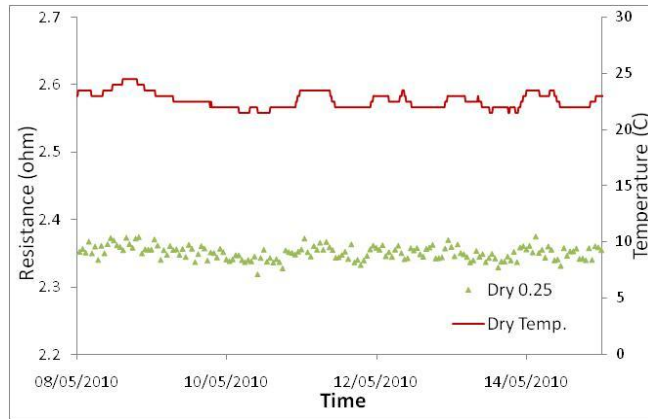


Figure 9-20: of Temperature and Resistance (0.25mm) -Dry Environment

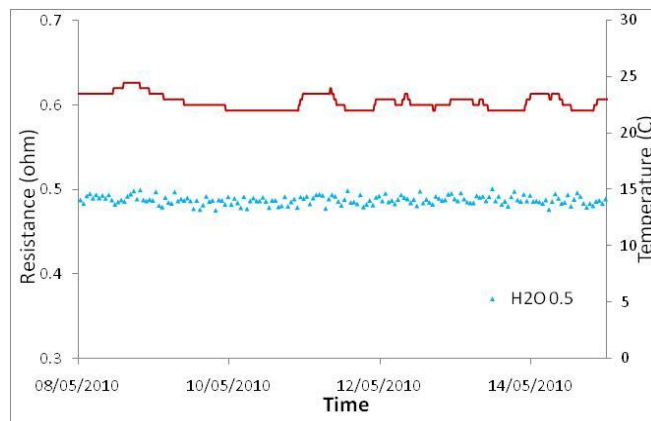


Figure 9-21: of Temperature and Resistance (0.5mm) -Dry Environment

9.3.3. Difference in electrical resistance before and after adjustment of temperature effect

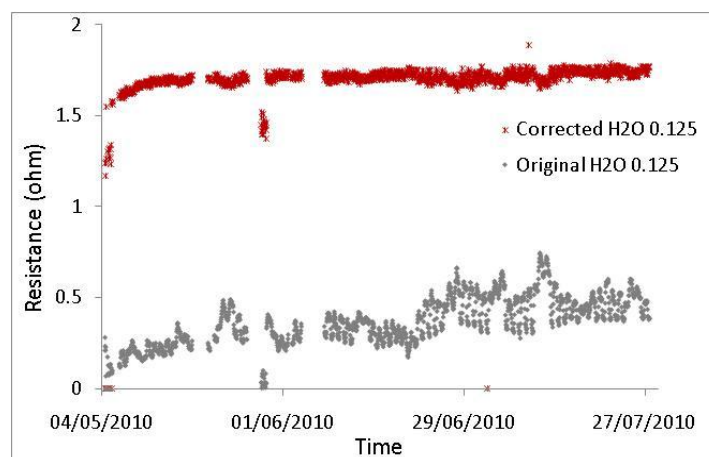


Figure 9-22: Resistance Difference before and after adjustment for temperature effect (0.125mm wire in water environment)

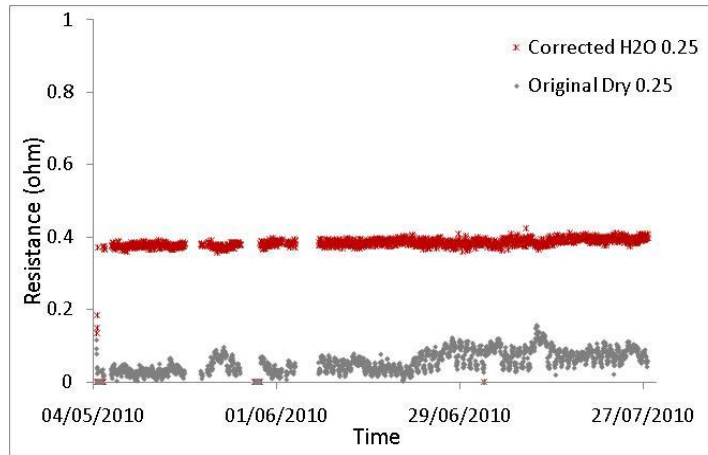


Figure 9-23: Resistance Difference before and after adjustment for temperature effect (0.25mm wire in water environment)

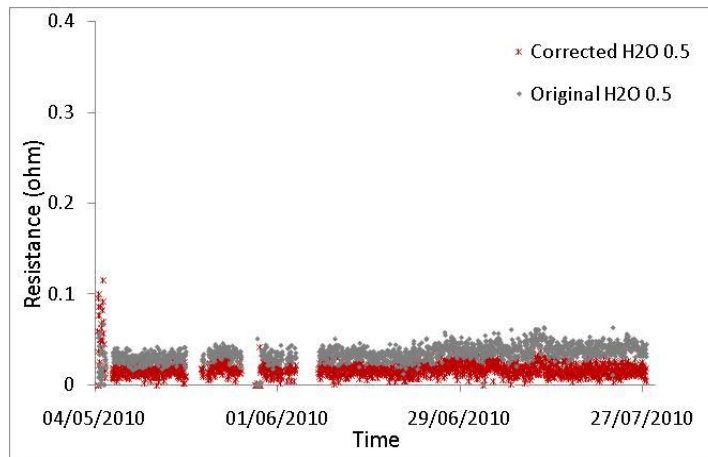


Figure 9-24: Resistance Difference before and after adjustment for temperature effect (0.5mm wire in water environment)

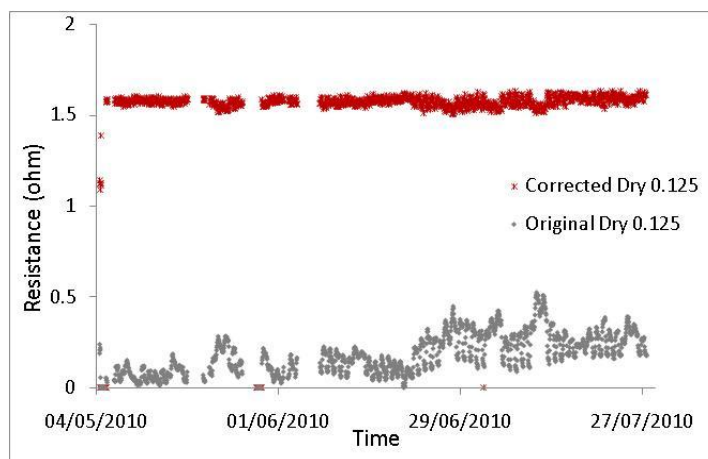


Figure 9-25: Resistance Difference before and after adjustment for temperature effect (0.125mm wire in dry environment)

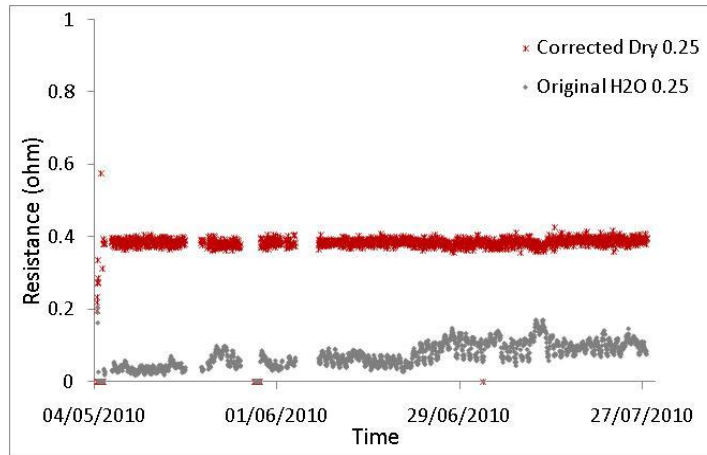


Figure 9-26: Resistance Difference before and after adjustment for temperature effect (0.25mm wire in dry environment)

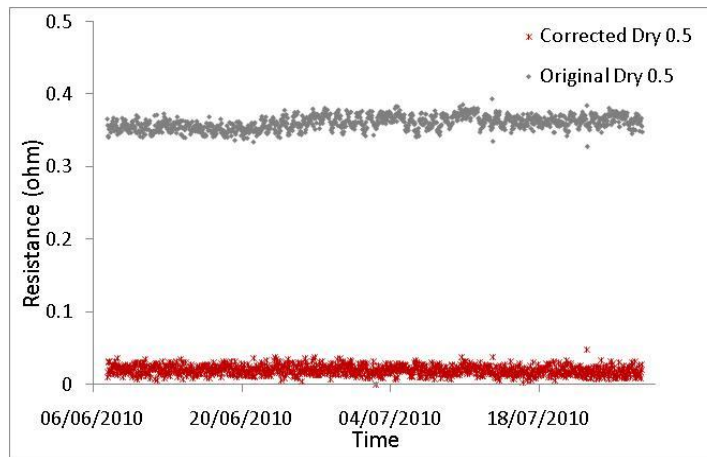


Figure 9-27: Resistance Difference before and after adjustment for temperature effect (0.5mm wire in dry environment)

9.3.4. MD values for Analysis of Water Environment

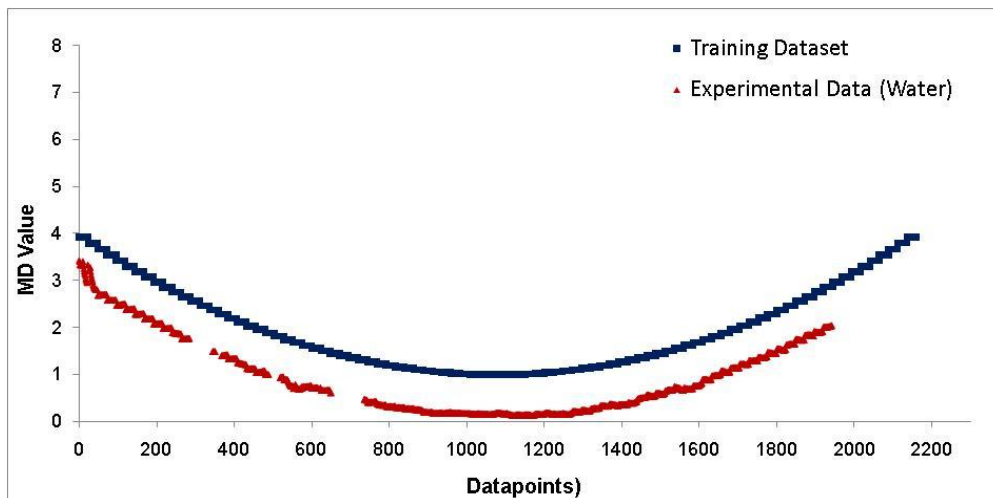


Figure 9-28: MD Values for experiment on Water - 0.125mm

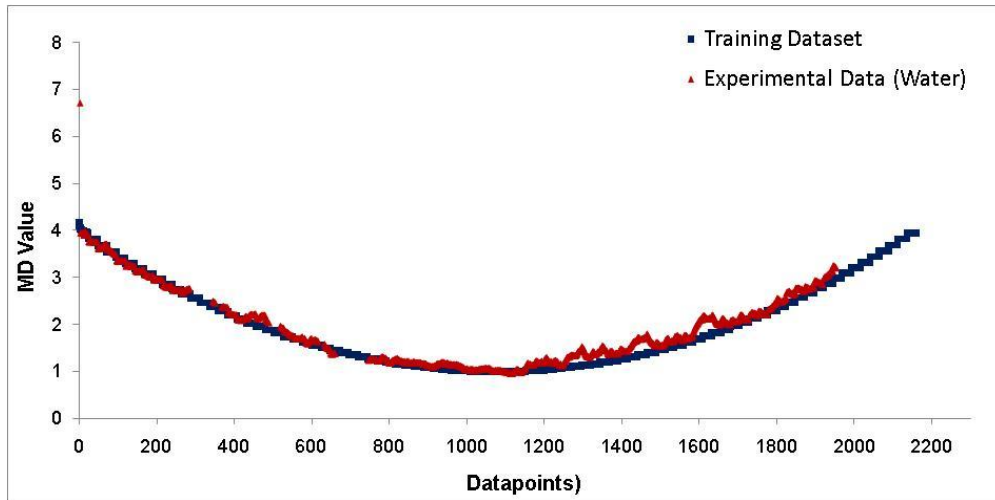


Figure 9-29: MD Values for experiment on Water - 0.25mm

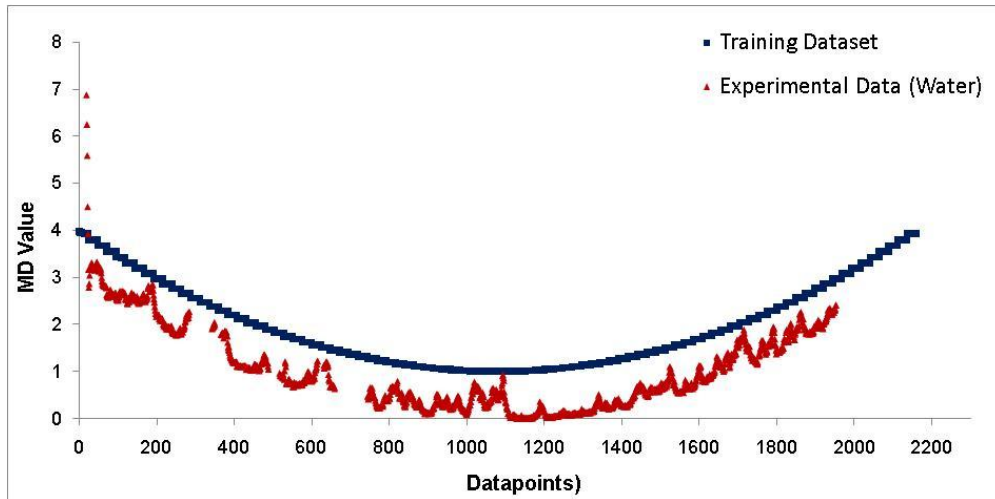


Figure 9-30: MD Values for experiment on Water - 0.5mm

9.3.5. Bayesian Network Preparation Tables for CPTs

Dry/Water125		Dry/Water250		Dry/Water500	
Mean(days)	Variance	Mean(days)	Variance	Mean(days)	Variance
1222	40131	1539	63588	42148	47722788

Table 9-1: PoF model-based input data

Time (days)	Dry/Water125			
	Mean MD Value	Standard Deviation	MD Threshold	Variance
1 st Part	2.73	0.97	0.93	3.69
Middle Part	1.24	0.74	0.55	1.98
Last Part	2.73	0.97	0.94	3.70

Table 9-2: Input data from MD Analysis Results

Time (days)	Dry/Water250			
	Mean MD Value	Standard Deviation	MD Threshold	Variance
1 st Part	2.72	0.05	0.00	2.77
Middle Part	1.24	0.74	0.55	1.98
Last Part	2.45	0.00	0.00	2.45

Table 9-3: Input data from MD Analysis Results

Time (days)	Dry/Water500			
	Mean MD Value	Standard Deviation	MD Threshold	Variance
1 st Part	2.73	0.97	0.94	3.70
Middle Part	1.23	0.74	0.54	1.96
Last Part	2.73	0.97	0.94	3.70

Table 9-4: Input data from MD Analysis Results

9.3.6. Visual Representation of Bayesian Network Analysis Results

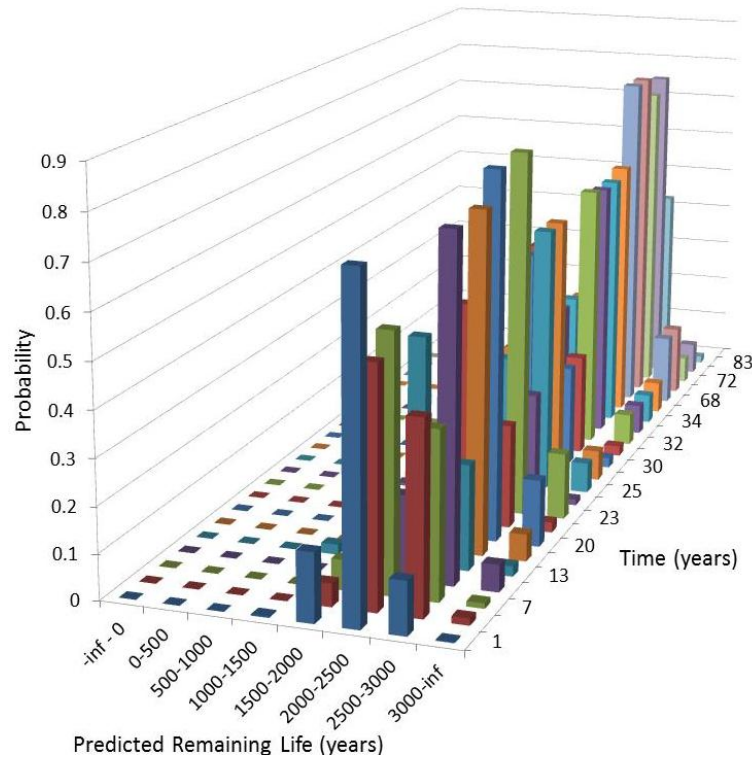


Figure 9-31: Probability Distributions of Predicted Remaining Life for Dry-0.125 device

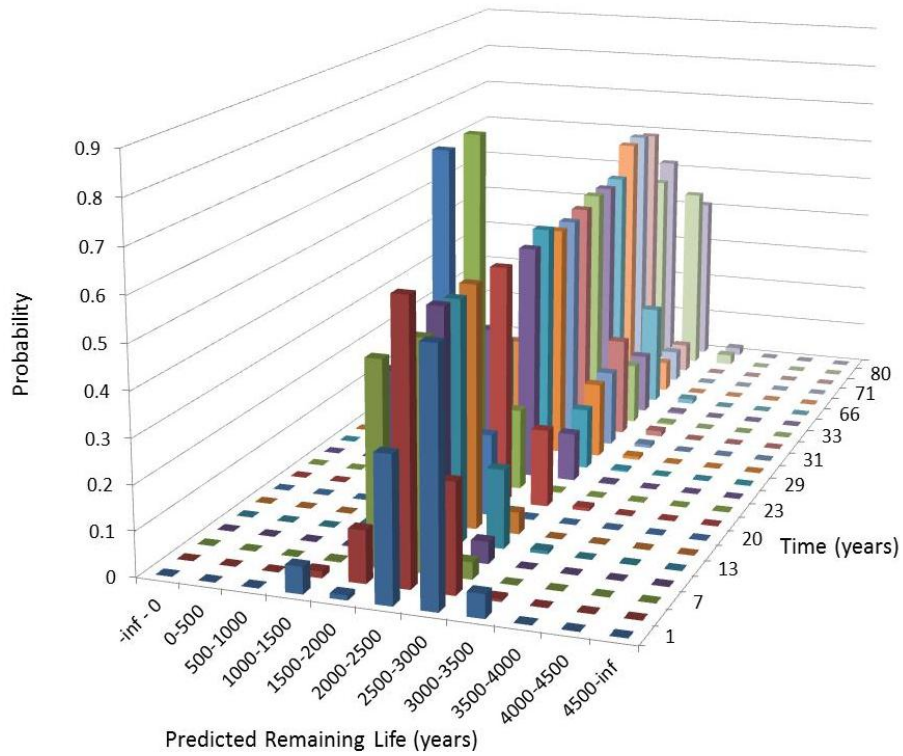


Figure 9-32: Probability Distributions of Predicted Remaining Life for Dry-0.25 device

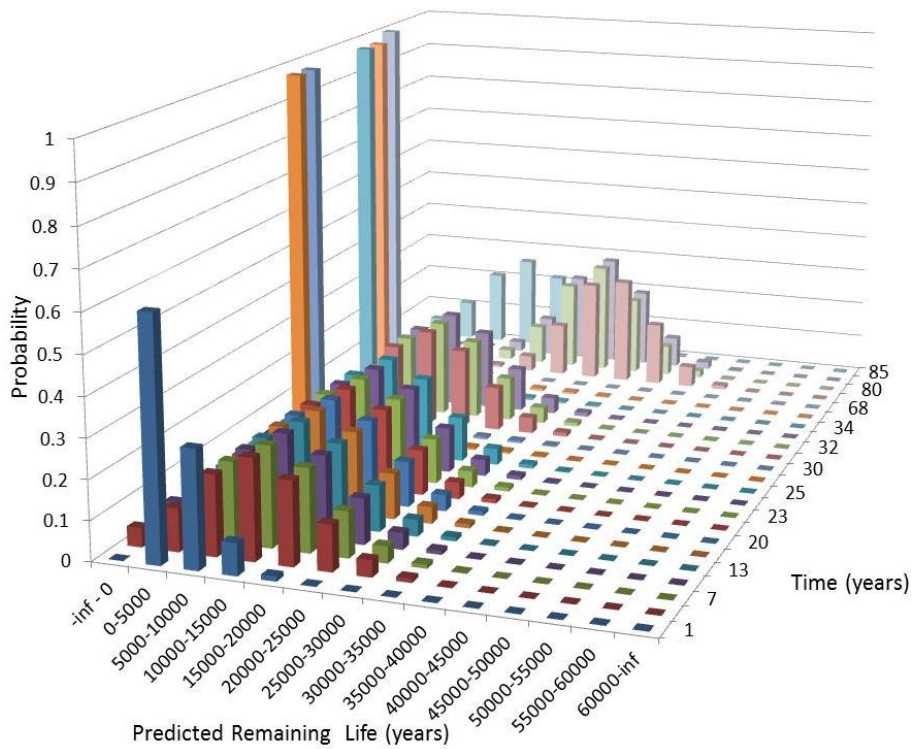


Figure 9-33: Probability Distributions of Predicted Remaining Life for Dry-0.5 device

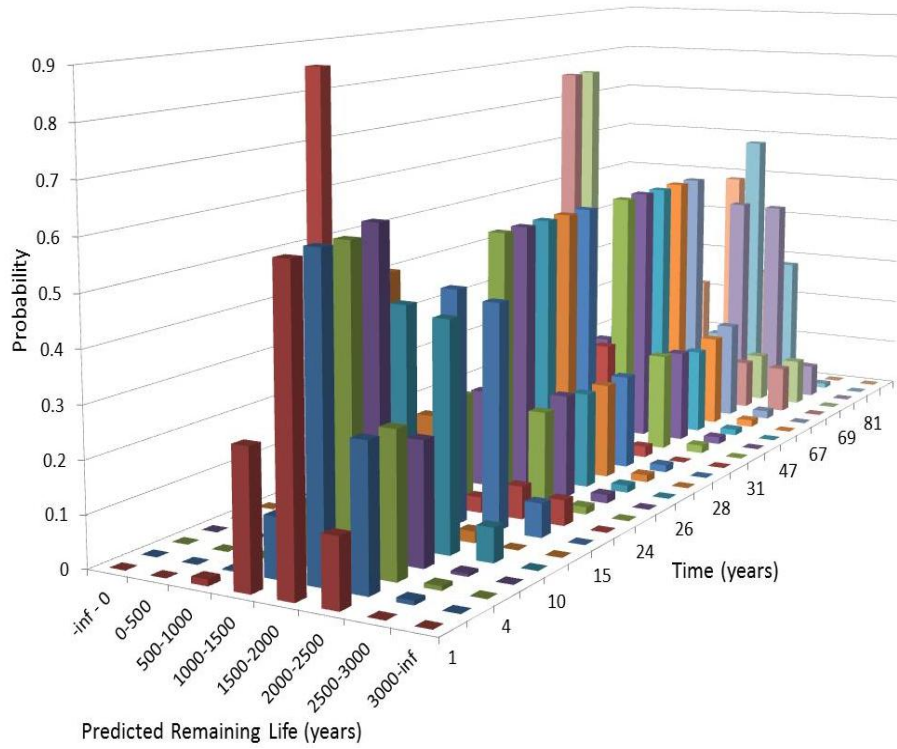


Figure 9-34: Probability Distributions of Predicted Remaining Life for Water-0.125 device

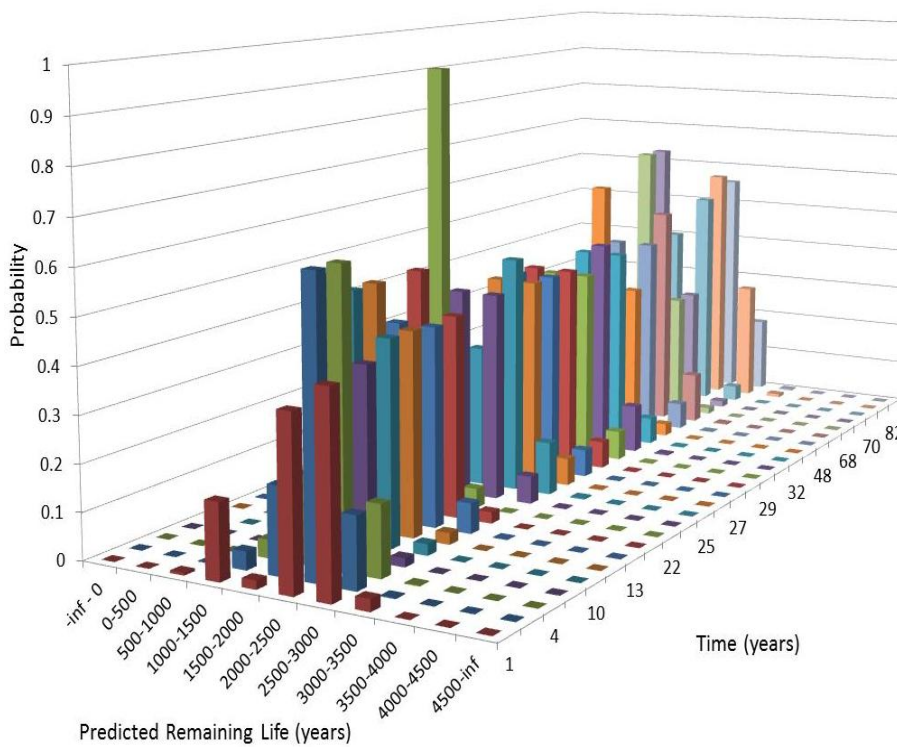


Figure 9-35: Probability Distributions of Predicted Remaining Life for Water-0.25 device

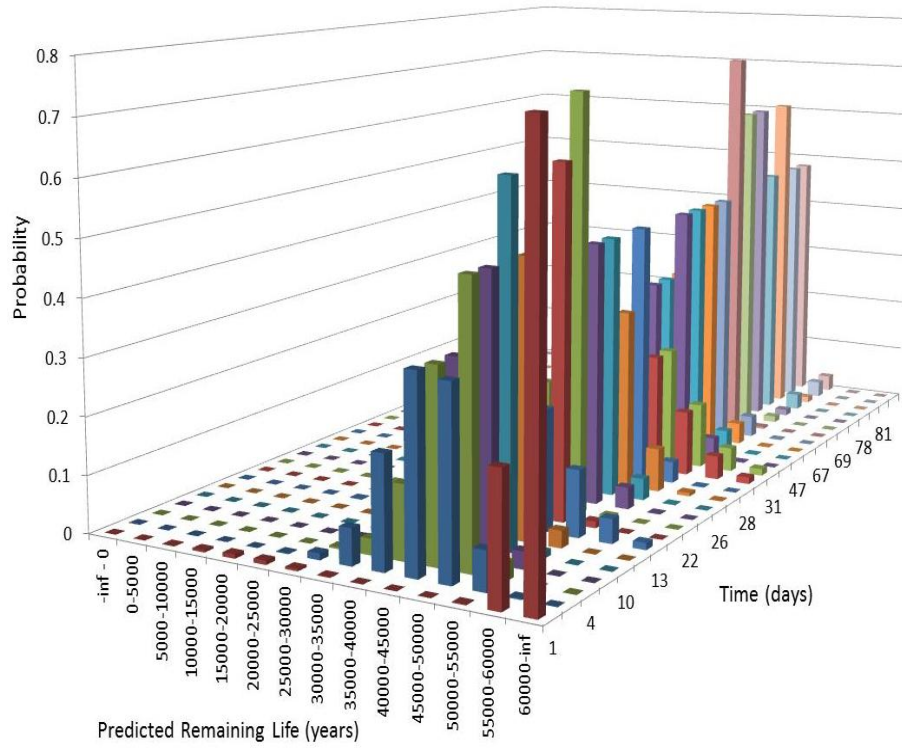


Figure 9-36: Probability Distributions of Predicted Remaining Life for Water-0.5 device

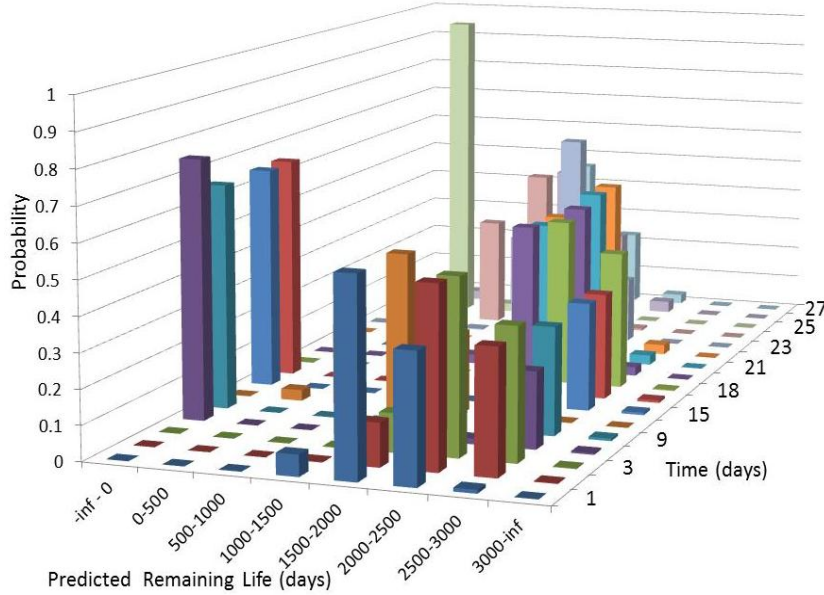


Figure 9-37: Probability Distributions of Predicted Remaining Life for Salt-0.125 device

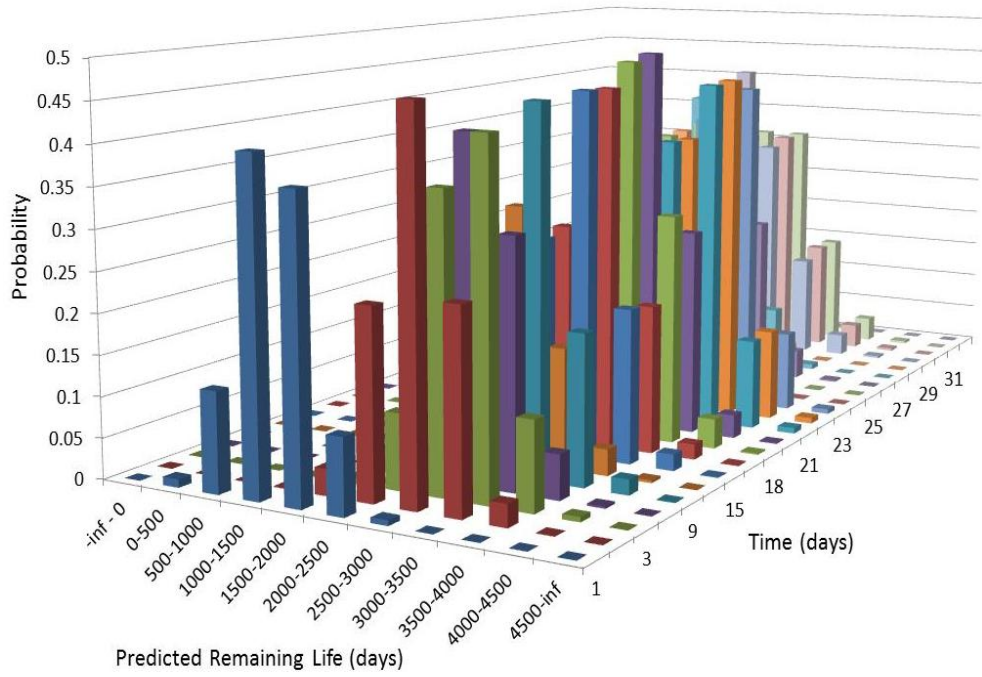


Figure 9-38: Probability Distributions of Predicted Remaining Life for Salt-0.25 device

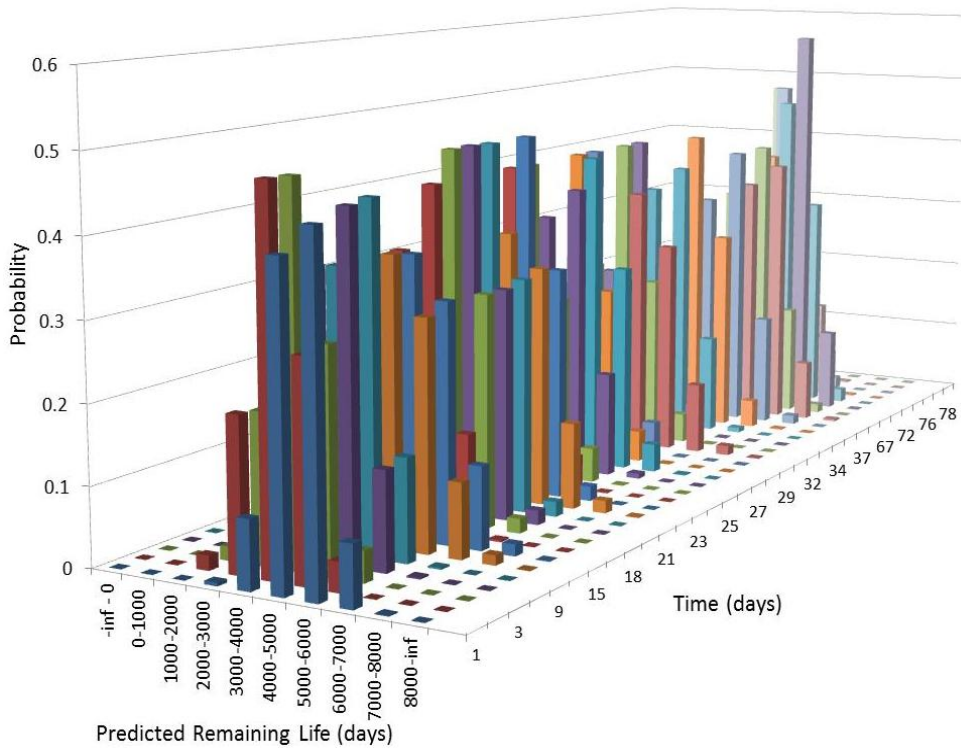


Figure 9-39: Probability Distributions of Predicted Remaining Life for Salt-0.5 device